

STAT

Page Denied

OSTOSLAVSKIY, I.V. AND KALACHEV, G.S.

LONGITUDINAL STABILITY AND CONTROLLABILITY
OF AN AIRCRAFT

Approved by the Ministry of Higher Education USSR
as a Textbook for Higher Educational Institutions
of Aviation

STATE PUBLISHING HOUSE FOR THE DEFENSE INDUSTRY

Moscow 1951

STAT

This book is a textbook for higher aviation institutes for the course on longitudinal stability and controllability of aircraft. It describes the methods of analyzing the questions of longitudinal stability and controllability of an aircraft and gives recommendations for the employment of these methods in designing an aircraft.

On the basis of the material presented in the book, the student will be able to make the necessary calculations of stability and controllability and rationally select the basic aerodynamic design parameters determining the longitudinal stability and controllability of an aircraft.

The book is written in connection with the syllabus of the course given at the Moscow Aviation Institute, and is intended for students at higher aviation institutes and for aircraft engineers.

50
52
54
56



Preface

(Translator's Note: The first two pages of the Preface are missing in original)



the problems of stability and controllability of an aircraft on the problems which are not connected among themselves, of static stability and dynamic stability, and to the conclusion that the whole problem must under all circumstances be coordinated.

The present work is an attempt at such a unified exposition of all the intimately interwoven questions of longitudinal stability and controllability of an aircraft.

The material of the book has been selected and arranged in accordance with the course of lectures delivered during the last few years at the Moscow Order of Lenin Aviation Institute imeni Ordzhonikidze.

Part of the material in this book is set in small type and is intended for readers who desire to familiarize themselves in greater detail with the questions under consideration.

In the desire not to overload the book, the authors were compelled to discuss certain questions which, in their opinion, are secondary in a hasty and summary style. However, the fundamental propositions, as for instance the influence of the compressibility of the air on the longitudinal moment, the analysis of the disturbed motion of an aircraft, the connection between maneuverability, controllability and stability, have been discussed in rather great detail. The course has been written by the authors under the assumption that the readers are familiar with theoretical and experimental aerodynamics and with aerodynamic computation.

The book is intended for students at higher aviation institutes and for engineers of designing offices, and may also be utilized by scientific workers in the field of aerodynamics, stress analysis, and problems of stability.

Recognizing the complexity of the task undertaken, the authors will be thankful to readers for any criticism; such remarks will be taken into consideration by them in their future work.

The authors express their thanks to Professor V.S.Pyshnov, Professor Ya.M.Kuritskes, and Professor A.K.Martynov, who read the manuscript and who have given a

number of valuable suggestions.

603330-C		2	OSI	REP	RE REQ NO.
LD					* with transmitted ATIC TRANS F-TS-8628/U
IA	ONE			OCI DIR	
IR	1 OIS	X			
B	BR	TSS			
	GR	OO/C	X		
	ICB	* 1(a) FD			
	RSB	FB			
	TR	SS			
	ML	COM			
	MON	LOG			
(S)	ORR	OBI			
ST	AR	NA	AI	Q	

FORM NO. 618
JAN 1964
USE PREVIOUS EDITIONS. DISSEMINATION LADDER (15)



STAT

SYMBOLS USED

- S - area of aircraft wings;
 l - span of wings;
 b - chord of wing;
 b_0 - root chord of wing (in plane of symmetry);
 b_1 - wing tip chord;
 b_m - mean geometric chord of wing;
 b_A - mean aerodynamic chord (MAC);
 $\lambda = \frac{l^2}{S}$ - aspect ratio of wing;
 $\tau = \frac{b_1}{b_0}$ - wing taper;
 $\bar{c} = \frac{c}{b}$ - relative profile thickness (greatest relative thickness of profile);
 $\bar{f} = \frac{f}{b}$ - relative camber of profile;
 S_{flap} - portion of wing area served by flaps;
 l_{flap} - span of flaps (distance between outer tips of flaps);
 $b_{A \text{ flap}}$ - mean aerodynamic chord of part of wing served by flaps;
 γ - angle of sweepback of wing (angle between transverse axis of aircraft OZ and projection of line of foci of wing onto the coordinate plane XOZ);
 ν - dihedral angle V of wing (angle between transverse axis of aircraft and plane of wing chord);
 L - length of aircraft;
 L_{fus} - length of fuselage;
 S_{fus} - area of rectangle described about horizontal projection of fuselage;
 $S_{h.t.}$ - area of horizontal tail surface;
 $b_{h.t.}$ - chord of horizontal tail surface;

v

STAT

S_{lev} - area of elevator;

b_a - chord of elevator;

$S_{h.t.} = \frac{S_{h.t.}}{S}$ - relative area of horizontal tail surface;

$S_a = \frac{S_a}{S_{h.t.}}$ - relative area of elevator;

$l_{h.t.}$ - arm of horizontal tail surface (distance between center of gravity of aircraft and hinge axis of elevator);

$l_{h.t.} = \frac{l_{h.t.}}{b_A}$ - relative arm of horizontal tail surface;

$A = \frac{S_{h.t.} l_{h.t.}}{S b_A}$ - relative statical moment of area of horizontal tail surface;

V - speed of flight or speed of air stream relative to aircraft;

V_i - indicated airspeed;

a - velocity of propagation of sound in air;

$M = \frac{V}{a}$ - ratio of flying speed (stream) to speed of sound (criterion of similitude with respect to compressibility of air);

$R = \frac{Vb}{\nu}$ - criterion of similitude with respect to viscosity of air (b is a characteristic length, for which the length of the MAC for the wing is usually taken);

ν - kinematic coefficient of viscosity of air;

H - flight altitude;

T - absolute temperature of air;

ρ - mass density of air;

ρ_0 - mass density of air at the ground (under standard atmospheric conditions $\rho_0 = 0.125 \text{ kg sec}^2/\text{m}^4$);

$\Delta = \frac{\rho}{\rho_0}$ - relative density of air;

$q = \frac{\rho V^2}{2}$ - velocity head of air stream;

p - air pressure;

p_0 - air pressure at point where $V = 0$;

- P_{∞} - air pressure far upstream of the aircraft (atmospheric pressure);
- $\bar{p} = \frac{P - P_{\infty}}{q}$ - coefficient of pressure;
- $V_{h.t.}$ - flow velocity at horizontal tail surface
- $k = \frac{V_{h.t.}^2}{V^2}$ - coefficient of deceleration of stream in zone of horizontal tail surface;
- θ - flight path angle (angle between tangent to trajectory of center of gravity of aircraft and the horizontal plane);
- θ - angle of pitch (angle between longitudinal axis of aircraft and horizontal plane);
- α - angle of attack;
- α_0 - angle of zero lift (value of α at which $c_y = 0$);
- $\omega_z = \frac{d\theta}{dt}$ - angular velocity of rotation of aircraft with respect to transverse axis of aircraft OZ (angular velocity of pitch);
- $\dot{\alpha} = \frac{d\alpha}{dt}$ - derivative of angle of attack with respect to time;
- φ - angle of setting of stabilizer with respect to mean aerodynamic wing chord;
- δ - angle of deflection of elevator;
- τ - angle of deflection of elevator trimmer;
- $\alpha_{h.t.}$ - angle of attack of horizontal tail surface;
- ϵ - downwash angle at tail;
- Y - lift;
- $c_y = \frac{Y}{Sq}$ - coefficient of lift;
- Q - drag;
- Y_1 - normal force (aerodynamic force directed along normal axis of aircraft OY);
- X_1 - tangent force (aerodynamic force directed along longitudinal axis of aircraft OX);

STAT

- c_{yl}, c_{xl} - coefficients of normal and tangent force of aircraft;
- x_p - coordinate of center of pressure of aerodynamic forces on profile with respect to its nose;
- $\bar{x}_p = \frac{x_p}{b}$ - relative coordinate of center of pressure;
- x_f - coordinate of focus with respect to nose of profile chord (or beginning of MAB);
- $\bar{x}_f = \frac{x_f}{b} = \frac{\partial c_m}{\partial c_y}$ - relative coordinate of focus;
- M_z - moment of aerodynamic forces with respect to the transverse axis of aircraft OA (pitching moments);
- $m_z = \frac{M_z}{SbAq}$ - coefficient of moment;
- m_{z0} - coefficient of moment at $c_y = 0$;
- c_m - coefficient of aerodynamic moment of profile with respect to nose;
- c_{m0} - coefficient of moment of profile at c_y of profile equal to zero;
- $m_z^c = \frac{dm_z}{dc_y}$ and
- $m_z^d = \frac{\partial m_z}{\partial \alpha}$ - coefficient of longitudinal static stability (on overload);
- $m_z^\delta = \frac{\partial m_z}{\partial \delta}$ - coefficient of effectiveness of elevator;
- $\frac{dm_z}{dc_y}$ - coefficient of longitudinal static stability (with respect to air speed);
- m_z^w - coefficient of damping of aerodynamic moment;
- m_z^a - coefficient of moment due to lag of downwash at tail;
- F - propulsive force;
- y_p - arm of propulsive force with respect to center of gravity of aircraft;
- $a = \frac{\partial c_y}{\partial \alpha} = c_y^a$ - slope of curve $c_y = f(\alpha)$ at constant value of Mach number;
- $\frac{\partial c_{y_{h.t.}}}{\partial \delta}$ - partial derivative of lift coefficient of tail with respect to angle of deflection of elevator;



- $\frac{\partial c_{y \text{ h.t.}}}{\partial \delta}$ - relative coefficient of effectiveness of elevator;
- $\frac{\partial c_{y \text{ h.t.}}}{\partial \alpha_{\text{h.t.}}}$ - hinge moment of elevator with respect to its axis of rotation;
- M_h - hinge moment of elevator with respect to its axis of rotation;
- $m_h = \frac{M_h}{S_b b_A q k}$ - coefficient of hinge moment of elevator;
- $m_h^\alpha, m_h^\delta, m_h^\tau$ - derivatives of coefficient of hinge moment of elevator with respect to angle of attack of horizontal tail surface, angle of deflection of elevator and angle of deflection of trimmer;
- F - force applied by pilot to control stick;
- $k_h = \frac{1}{57.3} \frac{d\delta^\circ}{dx_F}$ - transmission ratio from elevator to control stick;
- x_p - linear displacement of elevator control lever (reckoned at point of application of force by pilot to lever);
- G - weight of aircraft;
- m - mass of aircraft;
- $I_z = m r_z^2$ - moment of inertia of aircraft with respect to transverse axis directed along span;
- $r_z = \sqrt{\frac{I_z}{m}}$ - radius of inertia of aircraft with respect to transverse axis;
- $\bar{r}_z = \frac{r_z}{b_A}$ - relative radius of inertia;
- $n = \frac{Y}{G}$ - overload of aircraft;
- $\rho = \frac{2m}{\rho S b_A}$ - coefficient of relative density of aircraft;
- $\tau = \frac{2m}{\rho S V}$ - unit time in reducing the general equations of motion of the aircraft to the dimensionless form;
- $\bar{t} = \frac{t}{\tau}$ - dimensionless time;
- T - period of vibrations;
- $\bar{T} = \frac{T}{\tau}$ - period of vibrations in dimensionless form;

x_T - coordinate of center of gravity of aircraft along MAC with respect to its nose;

$\bar{x}_T = \frac{x_T}{b_A}$ - relative coordinate of center of gravity of aircraft;

y_T - coordinate of center of gravity along normal to MAC;

$\bar{y}_T = \frac{y_T}{b_A}$ - relative coordinate of center of gravity of aircraft;

F_b - force on stick due to weight unbalance of longitudinal control, including the elevator;

F_{spr} - force on stick due to the springs in the system of elevator control.



x

STAT

INTRODUCTION

In the course of aerodynamic calculation, the aircraft is considered as a material point with a mass equal to the mass of the aircraft moving under the action of aerodynamic forces, the propulsive force of the engine, and the force of gravity. It is assumed that all these forces are in equilibrium, which is maintained by the pilot controlling the aircraft.

In reality, the aircraft represents a body having a definite extension, i.e.,

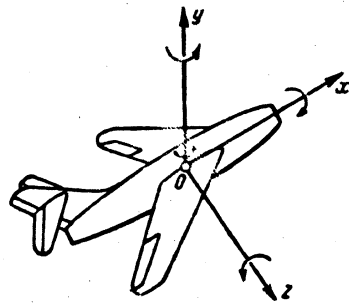
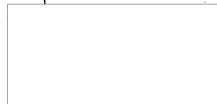


Fig.0.1 - Three Axes with Respect to which Rotary Motions of the Aircraft are Possible

a system of material points: the forces acting on the aircraft are, in general, not applied to its center of gravity. The pilot must continuously control the aircraft which control is more or less difficult, depending on the degree of stability of the aircraft. The flight of the aircraft is essentially a continuous chain of unstable motions so that, maintaining the required flight path, the

pilot must intervene in the control of the aircraft.

The actual motion of the aircraft, in the general case, may be represented as the sum of three rotational motions about the three axes of the coordinate system, with the origin of coordinates located at the center of gravity of the aircraft, and of three translational motions of the center of gravity of the aircraft in three



coordinate planes (Fig.0.1).

The sum of the rotational motion about the axis OZ and the translational motion of the center of gravity of the aircraft in the plane XOY gives the so-called longitudinal motion of the aircraft, the study of which is found to be most important for practice. With respect to this motion we may speak of longitudinal stability and controllability of the aircraft.

In exactly the same way we may speak of the lateral stability of motion consisting of the sum of the three remaining components of motion. In the present course we shall confine ourselves to the considerations of the questions connected with the longitudinal stability and controllability of an aircraft, characterizing the motion in the plane of symmetry of the aircraft.

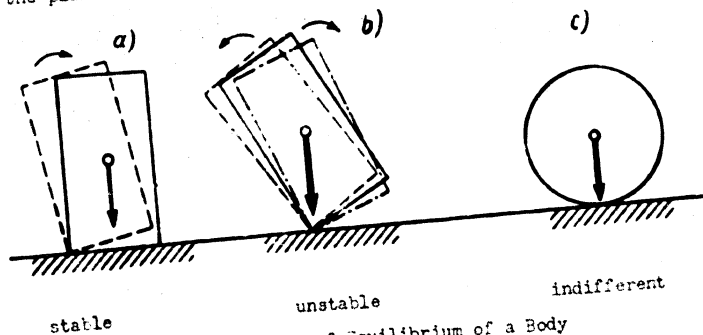


Fig.0.2 - Forms of Equilibrium of a Body

The concept to the stability of an aircraft is closely connected with the concept of its equilibrium.

It is well known from mechanics that three forms of equilibrium of a solid body may exist: stable, unstable, and indifferent. The simplest example of a stable position of equilibrium of a body, is a parallelepiped standing on its base (Fig.0.2a). At a slight deviation from the state of equilibrium, the parallelepiped will tend to return to its original position of equilibrium. At a sufficiently great deviation from the equilibrium position, the parallelepiped will not return

to its original position, but instead will fall over. If we displace a parallelepiped from its equilibrium position and then give it a sufficiently strong push in the direction of the original position, the parallelepiped, moving from the deflected position, will pass through the original position of stable equilibrium and, continuing to move further, will overturn on the opposite lateral edge. In this way the state of equilibrium of one and the same body under certain conditions (depending on the value and character of the disturbance) may prove to be either stable or unstable. A parallelepiped placed on its edge (Fig.0.2b) will be in a position of unstable equilibrium. In such an equilibrium, any disturbance, no matter how small, will bring the body out of the position of equilibrium. Finally, a sphere on a surface (Fig.0.2e) will be in a state of indifferent equilibrium, since any position occupied by it, on interruption of the action of the disturbance, will be an equilibrium position.

The examples we have considered above relate to the case when the body is at rest in its initial position. However, the same arguments are also applicable to the case when the body is in motion. The difference is only that, in the case when the body, before being exposed to the disturbance, occupies a definite position in space, the criterion of stability is the return of the body to the initial position on interruption of the action of the disturbance; however, in the case when the body, before the disturbance, was moving in space in a definite way (along a definite trajectory with a definite law of variation of velocity with time, etc.), the criterion of stability will be the return of the body to the initial motion on interruption of the action of the disturbance.

The motion of a ball along the runway of a bowling alley may serve as an example of stable motion. Under the influence of disturbances (for example, roughness in the walls of the groove of the alley), the ball will be somewhat deflected from the original motion imparted to it by the bowler. However, as soon as the action of the disturbance stops, the ball returns to its original motion.

If we hold onto the seat of a bicycle and attempt to roll it in a straight line, we will note that it is necessary to intervene continuously in the motion of the bicycle, by correcting its random deflections from a rectilinear trajectory which are due to the roughness of the roadway. The bicycle exhibits an unstable motion.

The stability of a moving body is the designation given its property, in the presence of disturbances, of resuming its original motion after the action of the disturbance has ended. Passing to the study of the problem of aircraft stability, we must primarily consider the possible equilibrium positions of an aircraft and the possible types of disturbances that will deflect it from the equilibrium position.

On considering this question of the stability of a body we may speak either of its stability in the broad sense of the word, with any perturbation removing the body from its state of equilibrium, or of stability in the special sense, i.e., with the perturbations bounded by certain limits. In most technical problems we have to do with the second concept of stability, when the deflections of the body from the equilibrium position are small. In solving problems of aircraft stability we will, in the following, consider the disturbances small.

The following forces act on an aircraft in flight: the force of gravity, the aerodynamic forces applied to the wings, fuselage, empennage, etc., and the traction of the engine installed on the aircraft. It is obvious that, in equilibrium, the sum of all forces acting on the aircraft must be zero, and the vector of resultant aerodynamic forces and traction must pass through the center of gravity of the aircraft. It follows from this that the equilibrium of the aircraft during different states of flight may be attained either by displacement of the vectors of the aerodynamic forces and traction in such a way that the vector of their resultant passes through an invariant center of gravity of the aircraft, or by a corresponding displacement of the center of the aircraft in such a way that the resultant of the vectors of all the aerodynamic forces and traction passes through the center of gravity; in this case, the resultant of the aerodynamic forces, the traction, and

the force of gravity must be equal to zero, for which purpose the angle of attack of the wings and the operating conditions of the engine must be varied in an appropriate manner.

It is obvious from general considerations that the former method of control of an aircraft, for the accomplishment of which an empennage is necessary, is the more perfect. It is precisely this method of control that was used by the noted inventor



Fig.0.3 - A.F.Mozhayskiy's Airplane Model

of the airplane, the Russian seaman A.F.Mozhayskiy, whose airplane (Fig.0.3) about 70 years ago, made the first flight in the world. On this aircraft Mozhayskiy placed a "tail, which may be raised and lowered and which serves to vary the direction of flight upward and downward and, by means of the vertical area, moving it to the right or left to obtain lateral control of the apparatus" (Bibl.1). In this way, about 70 years ago, Mozhayskiy gave the correct solution of the problem of controlling an aircraft. It was only inertness of the Tsarist Government of Russia that hindered subsequent development and application of the brilliant creative ideas and designs of A.F.Mozhayskiy.

It is interesting to note that, when the first flights were made abroad, several decades after the flight of the Mozhayskiy aircraft, a second method of controlling the aircraft was used. O.Lilienthal controlled his glider by shifting his own body with respect to the glider in such a way that the center of gravity of the glider was displaced, in accordance with the displacement of the point of application of

the aerodynamic forces acting on the glider. Such gliders were called balancing gliders. On the aircraft of the Wright Brothers, a twist of the wing tip was used, leading to the corresponding displacement of the point of application of the aerodynamic forces. The birds, who show no apparent special organs of control, such as the rudder of a modern aircraft, control their flight in about the same way. Thus both Lilienthal and the Wright Brothers took the path of blind imitation of nature, although such imitation is far from always preferable. For example, most machines made by man use the rocking motion and the wheel, but neither rocking nor any organ similar to the wheel is encountered among living beings. It is clear that methods of controlling an aircraft as used on the apparatus of Lilienthal and the Wright Brothers, which are still suitable at low speeds of flight and at small aircraft dimensions when the value of the moment acting on the aircraft is varied by simple displacement of the pilot's body or by twisting of the wings, may become entirely unsuitable when the speed of flight and the size of the aircraft are increased. For this reason, in its subsequent development, aviation proceeded along the path indicated by Mozhayskiy. Thus the principle of aircraft control, used in modern designs throughout the entire world, was first worked out in Russia.

Most Russian aircraft designers used Mozhayskiy's principle of control in their designs. Thus, the Russian inventor A.V. Shiukov in 1909 built a glider with ailerons and a tail, which was a great step forward by comparison with the balancing glider of Lilienthal. The elevators and ailerons on this glider were controlled by a single lever in the same way as is done on modern aircraft. In its test flights, the Shiukov glider proved to be stable and controllable.

The talented Russian designer and scientist S.S. Mezhdanovskiy, as early as the 1890's, investigated the glider, using an empennage, like A.F. Mozhayskiy, to ensure its stability. Thus already at the very beginning of the birth of aviation, the progressive scientists of our country, correctly defined the method for ensuring stability and controllability of the aircraft, although the general knowledge in

this field at that time was naturally in an embryonic state. The insufficient knowledge of the laws of stability at that time lead to frequent accidents with flying machines.

This is explained by the fact that engineers at that time had only a vague idea of the law of change in the forces acting on aircraft in flight, and did not understand the immense importance of the mutual position of the center of gravity of the aircraft and the point of application of the resultant aerodynamic force. At that time, the existence of the downwash in the region of the tail, caused by the wing lift, was also unknown, although this is a factor of exceptional significance in stability calculations; however, by that time the famous Russian scientist S.A.Chaplygin had already laid down the general principles of the theory of inductive resistance based precisely on the downwash beyond the wings of an aircraft.

The general development of aviation and its scientific foundation, aerodynamics, led to substantial expansion of the theoretical and experimental knowledge on stability allowing at the present time the construction of a well-organized and rather complete theory of stability, as well as the development of the engineering methods of calculating the stability and controllability of the aircraft. An outstanding and honorable merit in this field belongs to the scientists of our country, who worked out and solved a number of problems in this field.

Without dwelling on the general investigations of the stability of motion of a body, conducted by the famous Russian scientists Academicians L.Euler (1749) and Ye.Kotel'nikov (1774), Professor N.Ye.Zhukovskiy (1822) A.M.Lyapunov (1892), and others, we shall confine ourselves here merely to a short survey of the work on aircraft stability.

The great Russian scientist, founder of aerodynamic science, the "Father of Russian Aviation" N.Ye.Zhukovskiy, began in 1909 to deliver a course "Theoretical Principles of Aeronautics" in which, together with other questions, he considered the problem of aircraft stability. This course was the first systematic course on

the theory of flight to be given in the world. In it Zhukovskiy analyzed the moments of the forces acting on the aircraft in flight, and the measures necessary to ensure stable flight of the aircraft. Academician S.S.Chaplygin investigated the moments acting on the aircraft wing, using the concept of the "metacentric curve", which is a curve representing an envelope along which there slide the ends of the vector of the aerodynamic forces acting on the wing.

The work on aircraft stability underwent a brilliant development after the October Revolution, which released science and scientists in the USSR. During the years of Soviet power, Professors V.P.Vetchinkin, A.F.Zhuravchenko, V.S.Nedrov, V.S.Pyshnov, V.M.Matveyev, Ya.M.Kuritskes, and others did much in the field of practical application of theory to the development of engineering methods of calculating aircraft stability, and also in the conduct of experimental studies on questions of stability.

V.P.Vetchinkin, scientist and successor of N.Ye.Zhukovskiy, since the First World War studied the field of the dynamics of flight and stability; the results of these studies were published in 1918 in separate publications. His major work, "Dinamika poletov" (Dynamics of Flight) which appeared in 1927 was long a vademecum for aviation engineers.

B.N.Yur'yev in his noted work "Induktivnoye soprotivleniye" (Inductive Resistance) published in 1922, described methods of determining the downwash beyond the wings of the aircraft and methods of calculating the longitudinal stability of aircraft.

B.T.Goroshchenko in 1929-1930 published a series of papers on aircraft stability in which he emphasized the immense influence of the position of the center of gravity of an aircraft on its stability. In 1932 the course on the longitudinal stability of aircraft written by Ya.M.Kuritskes was published, containing a systematic exposition of the methods of calculating stability. In 1935 V.S.Pyshnov published his course "Aerodinamika samoleta" (Aerodynamics of the Aircraft) in

which he considered, in particular, questions of stability.

Recently Professor K.A. Moiseyev, together with his associates, is working out the theory of the so-called "technical stability" the characteristic features of which are the estimation of the finiteness and continuity of the acting disturbing forces, in distinction to the theory of A.M. Lyapunov, who postulated the disturbances to be infinitesimal and did not take account of the continuity of the acting forces.

As in all fields of aerodynamics, the methods of experimental study of the forces and moments acting on the wing and on the other parts of the aircraft occupy an important position in the solution of problems of stability. The organization in the USSR in 1918, on the initiative of N.Ye. Zhukovskiy, of the Central Aerodynamic Institute (TsAGI) played an immense role in this, and the theoretical and experimental work of most of our aviation scientists is connected with the name of that institute. The tests performed in the wind tunnels of the TsAGI allowed a number of laws governing the behavior of aircraft in flight to be discovered and studied. The theoretical studies of the TsAGI led to the development of rational engineering methods of calculating the stability and controllability of aircraft. As a result of the work of the TsAGI and of other aviation research institutes and academic institutions, it became possible to explain the cause of many phenomena in flight that had not been previously understood, and to prevent many accidents.

The aerodynamic studies of the questions of stability were performed not only in wind tunnels but also in flight, since, by means of wind tunnels alone, it is impossible to study the problems of stability in all their multiplicity. A considerable number of such problems are connected with the unstable motion of the aircraft, which cannot always be successfully modeled in the wind tunnel. The methods of experimental study in flight, where special instrumentation permits determining the kinematic and aerodynamic parameters of the unstable motion of aircraft, proved to be very fruitful.

In the Soviet and foreign literature on stability, numerous concepts and terms

became established, often arbitrary, and sometimes even hindering comprehension of the essence of the question. Thus there are various existing concepts on "static" and "dynamic" stability. These terms may give the idea that in fact two somehow differing aircraft stabilities exist. In reality, of course, only a single stability of the aircraft exists, which has been defined above as the ability of the aircraft to return, after termination of the disturbance, to its original motion or, as they say, to maintain the original state of flight. Professor V.S.Vedrov in his book "dinamicheskaya ustoychivost' samoleta" (Dynamic Stability of Aircraft), one of the major works on stability, writes as follows:

"There exists neither static nor dynamic stability of an aircraft. There exists only a single stability, and this stability, because of a historic misunderstanding, is called dynamic stability".

However, the concepts of "static stability" and "dynamic stability", although they are perhaps not completely successful as far as terminology goes, have firmly embedded themselves in aircraft construction routine, and have a certain practical meaning. To elucidate this meaning, let us return to the above-presented example of the parallelepiped standing on a plane. Let us incline the parallelepiped, bringing it out of the equilibrium position, and then let us leave it to itself. If the deviation is not too great, the parallelepiped will begin to tilt back toward the equilibrium position. The moment of weight of the parallelepiped with respect to the edge on which it rests, causes, immediately after the disturbance, a motion of the parallelepiped toward its original position of equilibrium.

If the parallelepiped, in its original position, stands on edge, then any deviation from its original equilibrium position results in a tendency of the parallelepiped to deviate still further from its original position.

The concept of "static stability" was introduced to evaluate the character of the motion of the body in the first instant after the disturbance. In the former case, the parallelepiped may be termed statically stable, in the second case static-

ally unstable. These conventional definitions must be understood in the sense that, in the former case, the initial motion of the parallelepiped after its deviation will take place in the direction of a return to the original equilibrium position, and in the latter case, in the direction of further increase of the deviation from the initial equilibrium position.

An aircraft is termed "statically stable" in the case when the moment of the aerodynamic forces, generated on a deviation of the aircraft from the equilibrium position, is such that the rotation of the aircraft caused by it during the first instant of time takes place in the direction of the original equilibrium position. The moment of aerodynamic forces in the case of a "statically unstable" aircraft is such that the resultant rotation of the aircraft is directed toward a further increase of the initial deviation from the equilibrium position*.

Thus we do not have to do here with the stability of the aircraft but with the character of the motion of the aircraft in the first instant after the aircraft deviates from the equilibrium position.

It is clear from the above that the so-called "static stability" of an aircraft is a necessary condition for its actual or, as it is sometimes called, its "dynamic" stability.

An actual judgment as to the stability of an aircraft can be reached only by studying the entire process of motion of the aircraft after the disturbance or, in conventional terms, after the "disturbed motion" of the aircraft. In the process of disturbed motion of the aircraft, the factor of static stability, as will become

*The direction of motion of an aircraft in the first instant after the interruption of the action of a disturbance still constitutes no guarantee that the aircraft will in fact return to the initial equilibrium position. One might, for example, imagine that the aircraft will oscillate about the initial equilibrium position and that these oscillations will increase in amplitude with time.

clear from the following, plays a substantial role.

The task of the present course is the study of questions connected with the stability of the aircraft, and familiarization with the existing engineering methods of assuring the proper stability. Since the flight of an aircraft in motion is controlled by the pilot, the second problem of the course, namely the study of the questions of controllability of the aircraft, is intimately related to its stability.

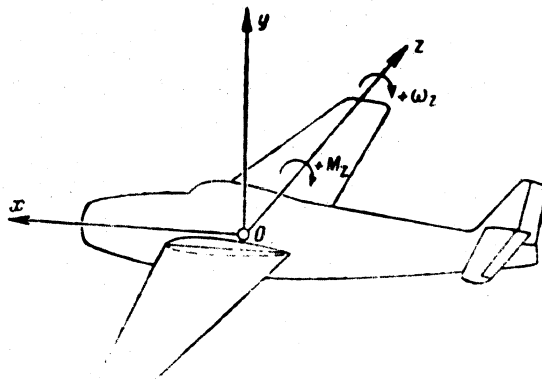


Fig.0.4 - System of Axes Connected with the Aircraft

In studying the moments acting on the aircraft we shall use a system of axes of coordinates connected with the aircraft (Fig.0.4). The origin of coordinates of this system is located at the center of gravity of the aircraft. The axis ox is directed parallel to the wing chord forward in the direction of flight, the oy axis is lying in the vertical plane of symmetry of the aircraft and is directed upward, while the oz axis is perpendicular to the first two axes and is directed along the right wing.

Accordingly, the moments with respect to the oz axis and the angular velocity will be positive if they tend to increase the angle of attack of the wing, and negative if they tend to decrease the angle of attack (Fig.0.4).

For example, if a positive lift acts on the horizontal tail surfaces, the moment of this lift with respect to the ox axis will be negative; when the aircraft comes out of the dive, the angular velocity ω_z will be positive, etc.

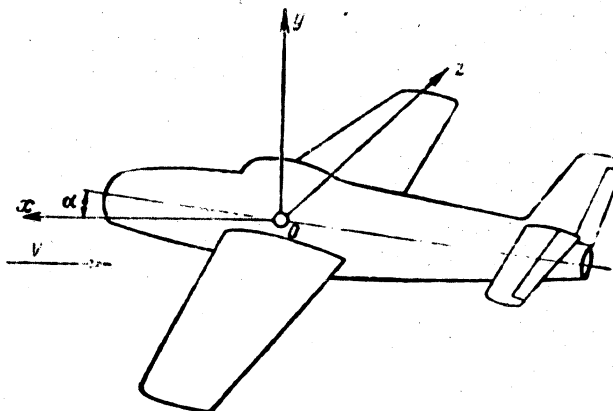


Fig.0.5 - Semiconnected System of Axes

In studying the motion of the center of gravity of the aircraft in the vertical plane, we shall use the system of axes that is said to be semi-connected with the aircraft (Fig.0.5) in which the origin of coordinates is likewise located at the



Fig.0.6 - Relation between the Angle α , θ and ϕ .

center of gravity of the aircraft. The ox axis is directed along the velocity of flight, the oy axis lies in the plane of symmetry of the aircraft and is directed



upwards and the oz axis is directed in the same way as in the connected system of axes. In this way, this system is different from the preceding one in that the ox and oy axes of the second system are rotated by the angle of attack with respect to the corresponding axes of the first system.

Besides the angle of inclination of the trajectory to the horizon, θ , and the angle of attack α , we shall also use the concept of the angle of pitch ϕ . The angle between the direction of the wing chord and the horizon is called the angle of pitch (Fig.0.6).



CHAPTER I

CONCEPT OF THE STABILITY AND CONTROLLABILITY OF THE AIRCRAFT.

Piloting and Motion of the Aircraft

Stability has been defined above as the property of an aircraft without the intervention of the pilot to maintain the character of the motion given it by the pilot. Let us see how such motion of the aircraft assigned by the pilot is effected in practice. With this object let us briefly consider several characteristic maneuvers and regimes of flight of the aircraft. This will give an idea of the role of stability of the aircraft and will give a more distinct picture of the phenomena taking place during flight.

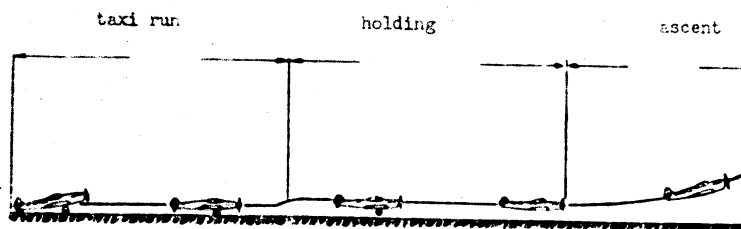


Fig.1.1 - Classical Scheme of Aircraft Takeoff

The main object of the takeoff is to give the aircraft a definite speed so that it may break away from the ground and commence flight. The takeoff may be schematically divided into three stages: the taxi run on the ground, holding above the ground to gain speed, and, finally the ascent (Fig.1.1). There are naturally transitional stages between the individual stages*.

*The scheme given in Fig.1.1 shows the classical takeoff adopted for instruction in flying schools. In practice, pilots often deviate from the scheme and gain speed at the same time that they gain altitude.

The control of the aircraft during the take-off reduces, on the whole, to the following operations: The pilot pushes forward the gas lever to put the engine to full power. The aircraft moves from its position and runs along the ground on three wheels. In order to reduce the drag of the aircraft during the take-off run, the pilot, as he gains speed, desiring to produce a moment for depressing the aircraft nose, smoothly pushes the control lever of the elevator forward, thereby lifting the tail of the aircraft off the ground, which reduces the angle of attack of the wing.

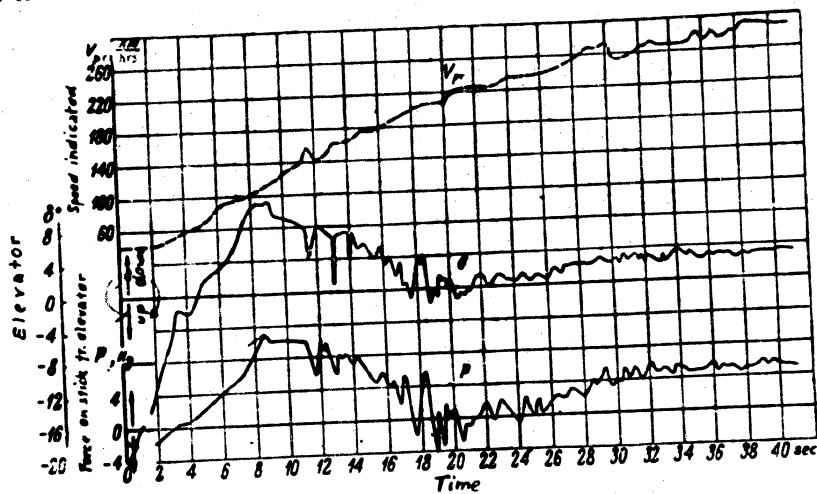


Fig.1.2 - Example of Variation of Velocity of Motion, Angle of Deflection of the Elevator and Force Applied to the Stick by the Pilot During the Flight of a Fighter with Landing Gear and Tail Wheel.

At about 1/3 or 1/4 the length of the take-off run, the aircraft tail is raised into the required position, and the pilot holds it in this position until the instant of breakaway from the ground. As the speed increases, the angle of deflection of the elevator necessary to maintain the take-off angle of pitch decreases. By the moment of breakaway, the position of the elevator is closer to neutral. After the break-

away, the speed of the aircraft continues to increase, but the elevator gradually, but very slightly, is deflected downward. Usually the pilot brings up the landing gear of the aircraft already during the holding period.

In connection with these operations of the pilot, the speed of motion of the aircraft increases with time, as will be seen from Fig.1.2.

Figure 1.2 gives the records of variation with time of the speed V , the angle of deflection of the elevator, and the force P on the stick from the elevator during the take-off of a fighter having a landing gear equipped with a tail wheel.

These records were obtained by means of recording instruments installed on the aircraft.

The motion of the elevator in general takes place in accordance with the above-described operations of the pilot*.

However, as will be seen from Fig.1.2, there are additional moments always superimposed on the fundamental type of motion. These motions are due to random disturbances during the take-off process (gusts of wind, roughness of the ground, errors in motions of the pilot, etc.). To all these disturbances the pilot, often unconsciously, reacts by the appropriate deflections of the elevator. As a result of this, the curves shown in Fig.1.2 were uneven and irregular.

In this way, besides piloting the aircraft in accordance with the fundamental task of take-off, to gain the necessary speed, the pilot must also expend energy for correcting random and unforeseen motions of the aircraft. The more stable the aircraft is, the less will be these unproductive expenditures of energy by the pilot, since the aircraft will return of its own accord to the original motion, and the

*The take-off in an aircraft with a landing gear and nose wheel differs somewhat from the above pattern, but only in the region of the take-off run. In this case, after the first section of the run, the pilot slightly raises the nose wheel above the ground and continues the run on two wheels.

smoother therefore will be the curves analogous to those given in Fig.1.2.

flying on Course. The basic state of flight, in which the aircraft spends the greater part of its time in the air, is the state of rectilinear flight on a definite course. Even for fighter aircraft, rectilinear flight occupies not less than about 70% of the total flying time.

The term rectilinear flight does not characterize the actual motion of the aircraft with complete accuracy. This term indicates rather the pilot's endeavor to maintain a rectilinear flight. In reality, the motion of the aircraft as a result of atmospheric disturbances, random deflections of the rudders, irregular operation of the engines, etc. has the character of larger or smaller fluctuations with respect to a center line, which only in small segments can be considered as a straight line.

Let us consider in somewhat greater detail the motion of the aircraft and its control in rectilinear flight under the conditions of the action of atmospheric disturbances on it, or, as they say, in "bumpy air" (Fig.1.3).

On a stable aircraft the pilot does not respond by a conscious motion by the elevator to each shock of a "bump" but usually automatically maintains his habitual average pressure on the stick or control wheel. For this reason the angle of deflection of the elevator, the pressure on the stick, the airspeed, etc. are all constantly varied.

Only in cases where the airspeed or position of the aircraft with respect to the horizon, as a result of the action of disturbances, become markedly different from the values during the initial regime of flight, does the pilot intervene in the control. In this case he does not restore the original regime of flight by the corresponding movements of the rudder, but, by carrying out by a definite deflection of the rudder from the wanted direction, he restores the aircraft to the original regime of flight and, after a certain length of time, verifies the airspeed or the position of the aircraft. The intervals between these conscious motion manipula-

tions of the stick or wheel to deflect the elevator, vary on the average, according to the estimates of various pilots, from 5 sec. to 1 min.

The frequent correction of the aircraft motion requires an additional expenditure of energy by the pilot and distracts his attention from the fulfillment of the

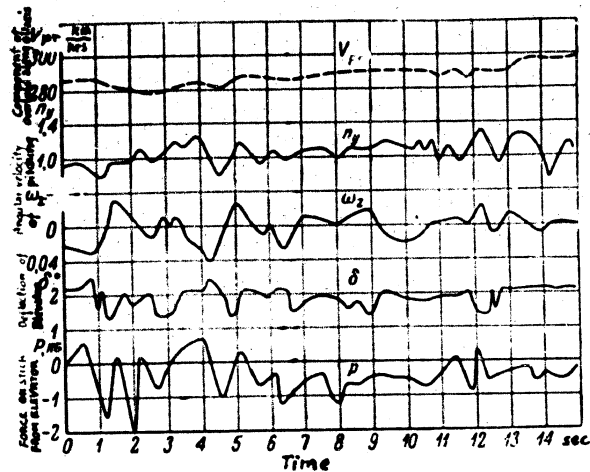


Fig.1.3 - Records of Variation of Speed (by instrument) in Flight of a Fighter through Bumpy Air, and Variations of Overload $n_y = Y/G$ (Y: lift; G: weight of aircraft); of the angular velocity of pitch ω_p , the deflection of the elevator δ and the force on the stick P.

primary task (for example, from observation of the enemy). In flight on an aircraft with a high degree of longitudinal stability, the piloting is simpler. The pilot may completely abstain from intervention in the control of the aircraft and even leave the control stick alone for a certain length of time.

The instrument records shown in Fig.1.3 were obtained on a flight in bumpy air on a fighter with normal stability characteristics. On larger aircraft and on aircraft with inadequate stability, the deflections of the rudder and the force

applied by the pilot to the control stick may be considerably greater. In addition, the pilot is more often forced to move the control stick on an unstable aircraft.

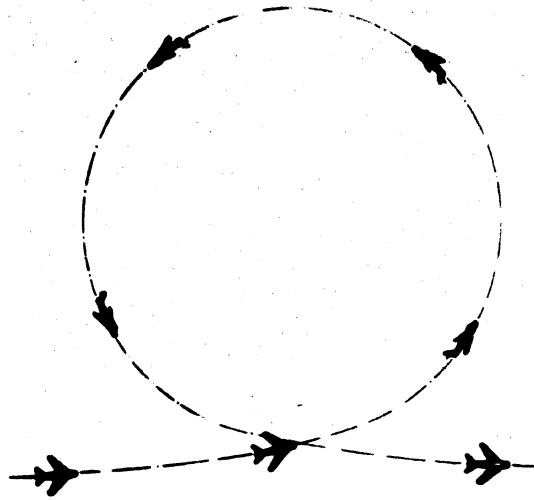


Fig.1.4 - Plan View of Trajectory of a Turn.

The turn. Let us consider one of the figures of the so-called "stunt flying" a regular turn (i.e. a slip-free turn) which is used for turning the aircraft in a horizontal plane (Fig.1.4).

The regular turn is one of the most complex in the execution of maneuvers. In the regular execution of a turn, the pilot must simultaneously keep track of the variation in flying height, of the position of the aircraft with respect to the horizon, of the bank indicator, i.e. of the indicator of deviation of the velocity vector of the motion of the aircraft with respect to the air from the aircraft plane of symmetry. The motions of the rudder in making a turn must be exactly coordinated, that is, they must continuously follow a definite sequence and the deflections of the rudder must continuously be commensurable.

As an example, Fig.1.5 gives the records of a few parameters relating to the turn of one aircraft: the speed along the trajectory, component of angular velocity of rotation of the aircraft about the transverse axis, and the component of overload with respect to the normal axis of the aircraft, n_y , and the records of the deflections of the elevator and of the forces from the elevator on the control stick.

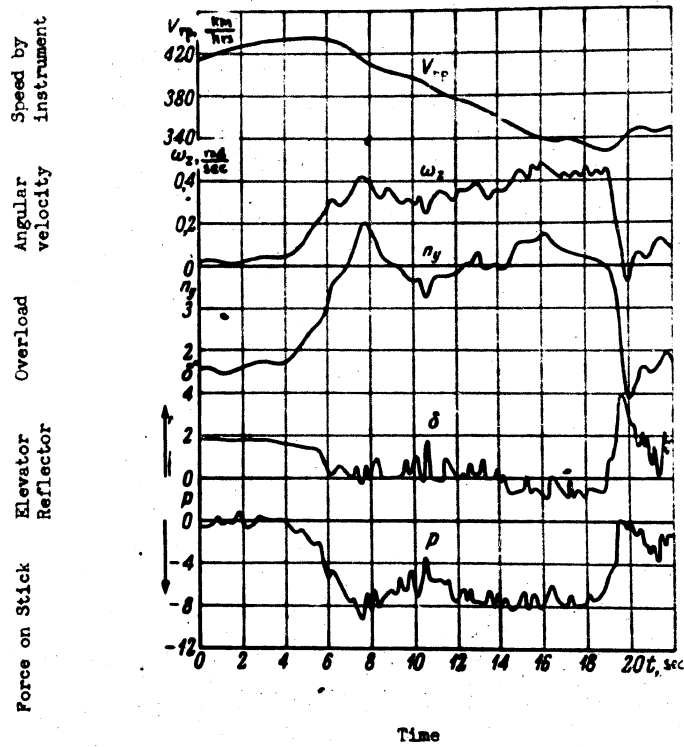


Fig.1.5 - Instrument Records in Making a Turn on One of our Fighters.

As we see, in making a turn as well, additional motions caused by random disturbances are also superimposed on the fundamental motion of the aircraft. The



pilot is continuously compensating the deviations of the aircraft from its basic motion by means of small deflections of the rudder, so as not to allow the aircraft to deviate from its assigned motion, or, as they say, its regime of flight.

It is obvious that an aircraft which, after the rudders are set in a definite position necessary for making a turn will automatically cancel the random deviations from that state, without requiring the pilot's intervention, i.e., an aircraft possessing stability, will be the best aircraft from the point of view of control.

Motions of Aircraft with Long and Short Periods

From the above diagrams of the motion of an aircraft it will be seen that these motions of the aircraft and actions of the pilot may in general be divided into the two types schematically shown in Fig.1.6.

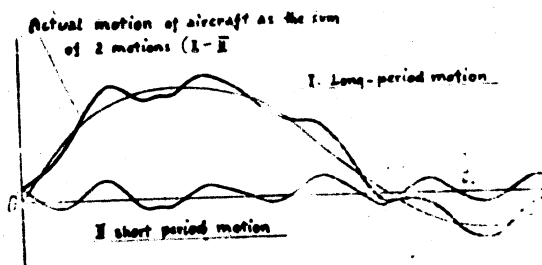


Fig.1.6 - Schematic Representation of Motion of Aircraft in the Form of the Sum of Two Partial Motions of Long and Short Periods

On the one hand, the aircraft and its rudders perform slow and major motions with a period of 10 sec or more; on the other hand they also make smaller motions that are smaller but sharper, with a period of about 1 sec and for the deflections of the rudders, even less than 1 sec. By means of slow and large motions of the rudders the pilot assures the main motion of the aircraft (take-off, rectilinear flight, turn, etc.), while by smaller movements of the rudders, as already



indicated, he continuously compensates the deviations of the aircraft from its fundamental motion, counteracting the random disturbances, and maintaining the required flight path.

A more detailed analysis of the causes of these small movements will be given in Chapter X.

Maneuverability

The motion of the aircraft in the air and on the ground consists of a large number of maneuvers and attitudes. The actions of the pilot necessary for controlling the aircraft are likewise numerous and varied in character. For this reason, in studying the whole complex group of questions connected with stability, controllability, and maneuverability of an aircraft, it is primarily necessary to agree on the concepts and terms to be used in the future.

The object of a maneuver executed by the pilot is to put the aircraft into a definite position in space. For example, in executing a maneuver in aerial combat, the pilot has the object of putting the aircraft in the most advantageous position with respect to the enemy aircraft. The ability of an aircraft to vary, in a definite time interval, its speed, altitude, and direction of flight, will be denoted as its maneuverability.

Accordingly, the maneuverability of an aircraft will be characterized by the rapidity of changes in the parameters of motion and in the aircraft position in space.

The parameters of motion of the center of gravity of an aircraft are the flying speed and altitude, the angles of inclination of the trajectory with respect to the ground axes of coordinates, and the curvature of the trajectory, or the angular velocity of rotation of the trajectory.

The position of the aircraft center of gravity in space may be determined if three coordinates of the center of gravity with respect to a system of axes of coordinates fixed with respect to the ground, are given or determined.

Indexes of Maneuverability

There are many indexes of aircraft maneuverability, and it is practically impossible to consider them all. In accordance with the definition adopted above let us consider, as typical examples, a few individual indexes of aircraft maneuverability.

The flying speed is a very important parameter of the aircraft motion. The indexes of aircraft maneuverability connected with the speed, will be the following quantities: V_{\min} = minimum possible speed of steady flight; V_{\max} = maximum horizontal speed in flight at full throttle; V_{\lim} = limiting flying speed allowable under the conditions of mechanical strength of the aircraft or of its controllability. The quantities V_{\min} , V_{\max} , and V_{\lim} may differ at various altitudes. For this reason it is impossible in a given case, when characterizing the maneuverability of an aircraft, to confine the calculation to three values of these quantities; their variation with the altitude must be taken into consideration. Further indexes of aircraft maneuverability, with respect to speed, may be considered: V_{land} = minimum possible landing speed and maximum speed with extended flaps and landing gear at minimum and maximum aircraft weight, etc. As an index of aircraft maneuverability the following ratios are used:

$$\frac{V_{\max}}{V_{\text{stab}}}; \quad \frac{V_{\text{rp}}}{V_{\text{stab}}}$$

The rate of change in flying speed is also an important index of aircraft maneuverability. In operating an aircraft, particularly in combat, it is of extraordinary and vital importance to be able as rapidly as possible to increase or decrease the flying speed of the aircraft. In other words, the values of the possible tangential accelerations and retardations of the aircraft are indexes of maneuverability. To increase the aircraft maneuverability in this respect, special

brakes are often used (for example, in diving) and so-called accelerators (for example, in take-off).

The following may serve as indexes of aircraft maneuverability in the vertical plane: rate of climb, ceiling, maximum and minimum rate of descent of an aircraft.

The elevation over an enemy at the beginning of an aerial combat is a very important factor, since it allows the utilization of an additional reserve of potential energy determined by the altitude of flight required for execution of maneuvers in approaching and destroying the enemy.

The curvature of the trajectory and the angles of its inclination with respect to a system of coordinate axes, fixed relative to the ground, is likewise an important factor in the evaluation of aircraft maneuverability. The following may serve as indexes of aircraft maneuverability in this respect: radius and time of execution of a steady horizontal turn, time of executing stunt figures, loss or gain of height and speed in stunt flying. In view of the fact that, in aerial combat, the motion of the aircraft is very complex, these indexes consist of various combinations of parts of individual figures. The rapidity with which the aircraft can pass from one attitude to another is also a rather important index of maneuverability.

Finally the characteristics of aircraft motion on the ground are indexes of its maneuverability: length of time of taxi and take-off run and possible radii of turn in ground run with the engines running.

It will be clear from the above that it is extremely difficult to work out a single generalized index of maneuverability whose numerical value would serve for evaluating these properties of an aircraft as a whole. The maneuverability must be evaluated in each specific case with respect to specific conditions. For example, a fighter which is more rapidly able to assume a more advantageous position for the beginning of a combat, but also more rapidly to reach its objective, or to reach the most advantageous position with respect to its objectives or with respect to

1 the enemy for a position most advantageous for the utilization of its available
2 means of defeating the enemy with a minimum danger to itself, will be the more
4 maneuverable fighter.

6 Controllability of an Aircraft

8 The controllability of an aircraft is usually taken to mean its ability to re-
10 spond by the corresponding motions to the actions of the pilot by means of elevator,
12 ailerons, and rudder. For example, the ability of an aircraft to vary its position
14 in space as a result of rotation about the three axes of coordinates and to change
16 from one state of flight to the other at the will of the pilot, is often called the
18 controllability of an aircraft.

20 Pilots say of a well controllable aircraft that it "answers the stick well".
22 This means that, to execute the maneuvers required of the aircraft, the pilot must
24 make motions which are simple, in the nature of deflecting the stick, and must apply
26 efforts that are small in magnitude but distinct, to which the aircraft responds by
28 a corresponding change in its position in space without unnecessary delay.

30 This definition, born of flying practice, is sufficiently exact and convenient
32 from the viewpoint of aviation engineering. We will, therefore, term the control-
34 lability of an aircraft its ability to respond to efforts applied by the pilot and
36 to displacements of the control levers of the rudders by corresponding displace-
38 ments in space, or the ability of the aircraft to "follow the rudders" as pilots
40 usually express it.

42 It is obvious enough that the quality of an aircraft, with respect to its con-
44 trollability, strongly influences the possible maneuverability in operation as well
46 as in assuring flight safety.

48 Indicators of Controllability. The pilot judges the controllability of an air-
50 craft by the displacements (deflections) of the rudder control levers and by the
52 force applied by him to the levers in maintaining a definite state of flight and
54 in executing maneuvers.
56

By means of the control stick the pilot deflects the rudder; the deflection of the rudder produces a corresponding aerodynamic moment which begins to rotate the aircraft with respect to its center of gravity at an angular velocity varying with time. The existence of an angular velocity leads to the appearance of what is known as the damping moment, which is due to the fact that the angle of contact between airstream and individual part of the aircraft varies as it rotates. In this case, aerodynamic moments connected with the angular velocity are generated, which tend to prevent the rotation of the aircraft. Finally, the rotation of the aircraft causes a change in angle of attack, leading to the generation of additional dynamic moments.

Depending on the combination of the values of these moments, the motion of the rudder and the corresponding motion of the stick required for a definite maneuver will vary with time. The manipulation may become simpler or more complicated. The lag in response of the aircraft to the deflection of the rudder will likewise vary. For example, in large and heavy aircraft with high moments of inertia, other conditions being equal, the lag in response of the aircraft to the action of the pilot will be considerable.

Flying experience has shown that the force applied for displacing the levers must not be so great as to unnecessarily fatigue the pilot, and must not be so small as to hamper the coordination and compatibility or "metering" of the deflection of the control levers, required for execution of a maneuver.

This means that certain limits exist, within which the values of the force applied to the stick and the magnitude of displacement of the stick must be held.

The work expended by the pilot on the deflection of the control surfaces is only a part of the total work expended by him in controlling the aircraft. On this basis, the engineer and pilot N.V.Adamovich (Bibl.2) proposed a broader interpretation of the concept of controllability, stating that it must be evaluated by the total physiological work expended by the pilot in controlling the aircraft.

The physiological work of the pilot comprises the expenditure of physical, i.e., muscular energy, and the expenditure of nervous energy. From this point of view, freeing the pilot from any operation in the control of the aircraft, for example, by the use of various types of automatic devices for control of engine speed, propeller operation, and of other units, leads to an improvement in controllability, not only as a result of the reduced expenditure of physical work by the pilot but also as a result of relieving the pilot from observation of the corresponding aircraft instruments. Enlargement of the field of view of the pilot by increasing the cabin area and wider window space also improve the controllability of the aircraft. With a good view the strain on the pilot is lessened, increasing the accuracy of manipulation of the rudders. In an aircraft with a good view the pilot makes fewer mistakes and need not deflect the rudders additionally to correct his errors. In this way, the improvement in view not only reduces the expenditure of nervous energy, but also lowers the expenditure of muscular energy. Analogous statements apply to the quality of the indicating instruments and their arrangement on the instrument panel.

The use of various types of signal devices or automatic devices to prevent the pilot from bringing the aircraft close to states of flight that are dangerous for any reason, substantially influences the aircraft controllability. For example, a light or acoustic signal emitted on entry of the aircraft into critical angles of attack, on approach to the critical Mach number, on approach to impermissible speeds, on critical reduction in the fuel reserve, etc. will improve the controllability of the aircraft by freeing the pilot from the necessity of observing the corresponding instruments; this results in facilitating the control of the aircraft in general. The factors affecting the controllability of an aircraft, in the above broader sense, may include arrangement and shape of the control levers, convenience of landing, comfortable position of the pilot in his seat, etc. An improper arrangement of the control levers and their unsatisfactory shape or color might not only result in additional physical work for the pilot in the control of the air-

craft but might even cause accidents. For example, if the pilot, in flight near ground level, confuses the levers controlling the landing gear and the flaps, a crackup may occur.

At present, the methods of quantitative evaluation of controllability are not sufficiently worked out in the above broader sense. In the following, aircraft controllability will be considered only from the point of view of the response of the aircraft to the displacement of the stick and to the force applied to it by the pilot for deflecting the elevator. In the following Chapters we will discuss the modern methods of a quantitative analysis of aircraft controllability.

Flight Conditions. In order to define the concepts of stability, used in the rest of this book, agreement as to the concept of a steady state of aircraft flight and of aircraft equilibrium in this state must be reached.

A steady motion of the aircraft, during which the parameters of motion of the center of gravity and the position of the aircraft axes relative to the vertical (for longitudinal motion) remain invariant through time, will be called a steady state of flight.

Let us clarify these definitions. For this purpose, as parameters characterizing the motion of the center of the aircraft, we will use the speed, the angle of inclination of the flight path to the horizon, and the radius of curvature of that path. As parameters defining the position of the aircraft relative to the vertical, let us take the angles between the vertical and the coordinate axes of the aircraft. In that case, the conditions of steady motion will be satisfied only by rectilinear horizontal flight, climb or descent at constant speed, and regular horizontal turns at constant velocity, constant angle of bank, and constant angle of pitch. These conditions of steady motion, as shown by an analysis of the equations of steady motion (Bibl.3), require a constant weight of the aircraft throughout the time under consideration. In practice, this condition cannot be satisfied, since the weight of the aircraft is constantly decreasing because of the consump-

tion of fuel. Thus the aircraft has no steady states of flight in the above sense. It follows that, on closer analysis, we may speak of steady motion only with respect to one of the parameters of motion or with respect to some definite combinations of these parameters. For example, we may speak of a gliding dive of the aircraft at a speed that is steady relative to the air, when the velocity head $q = \frac{\rho V^2}{2}$, the angle of attack, and other parameters vary continuously with any change in altitude. We may speak of a glide that is steady relative to the velocity head when the actual speed is continuously varying.

In addition to the influence of the variation of weight of the aircraft during flight, the actual motion of the aircraft, as mentioned above, is not strictly steady for still another reason, namely the fact that the aircraft is constantly subjected to various types of minor perturbations in the form, for example, of irregularities (cyclic nature) of engine operation, atmospheric fluctuations, air currents, irregularities (periodicities) of the vortices shed by the various parts of the aircraft, etc. The deviations of the parameters of aircraft motion, due to these causes, may be practically imperceptible to the pilot, but their existence does not allow us, strictly speaking, to consider this motion as being a steady state of flight of the aircraft. For this reason, from the viewpoint of a correct interpretation of actual conditions the state of flight must be defined as a motion such that its parameters remain within assigned narrow limits. Such a state, for example, is horizontal rectilinear or curvilinear flight at constant speed within the limits of accuracy of its determination or within the limits of predetermined deviations. Conditions of flight may likewise include steady gliding as well as the descent of an aircraft at a practically constant indicated air speed or at practically constant Mach number.

In the theoretical consideration of the motion of an aircraft and its stability, assumptions that schematize the phenomenon and simplify the analysis are usually made. For example, in most problems the weight of the aircraft and the

density of the air are considered constant within the limits of the time interval under consideration. This procedure will be used in the context. Theoretical conclusions, under these assumptions, yield valuable practical results.

Balancing of the Aircraft. In considering the stability of an aircraft the expressions "state of balancing the aircraft", "the aircraft is dynamically balanced at the initial condition of flight", "balancing curves" are often used. In this case, the balancing of an aircraft means the equilibrium of moments in the initial steady state of flight, obtained by deflecting the control surfaces.

Balancing curves is the term used for the curves indicating the variation in the deflections of the control surfaces, the control stick, or the forces required for balancing the aircraft at various attitudes, plotted as functions of some parameter characterizing the state of flight. In this case it is usually assumed that the state of flight varies only as a result of the variation in the position of the control surfaces, at constant position of the engine control levers, the flap and landing-gear levers, the control used for the rudder tabs, etc.

Stability

At some instant of time, let an external influence (gust of wind, gunfire, random deflection of the control surfaces, engine failure, etc.) cause the aircraft to deviate from the steady state of flight, and then let the action of this cause (disturbance) cease. Despite the fact that the action of the perturbation has ceased, the motion of the aircraft (at least for a certain length of time) will differ from its motion during the initial state. The unsteady motion of the aircraft after start of a disturbance is called disturbed motion, in differentiation from the basic or initial motion (before start of the disturbance).

The actual motion of an aircraft consists of a continuous chain of disturbed motions, since there are almost always disturbances in the atmosphere. This is demonstrated, for example, in Fig.1.3 which shows the parameters of motion in flight along a given course.

We will adopt the following formulation of the concept of aircraft stability: we will understand the stability of an aircraft to mean its ability to maintain a given attitude and return to it after cessation of various kinds of perturbations.

From the point of view of evaluating the airworthiness of an aircraft with respect to its stability and controllability, the fact whether the aircraft does or does not return to the original attitude after cessation of a perturbation is not the only important point. Others include: the rate at which this return takes place, the manner in which the motion of the aircraft varies under the influence of a definite disturbance at the first instant of time and the nature of the disturbed motion. In studying the stability of an aircraft, it is therefore advisable to consider the whole question of disturbed motion instead of merely its final results. The above definition of aircraft stability relates to the actual or - as it is often called - the dynamic stability of the aircraft. In addition to the dynamic stability, as stated in the Introduction, there also exists the concept of static stability, the meaning of which will be considered in detail later in the text.

We mentioned above that, in practice, the pilot is continuously operating the control surfaces by applying variable forces to the control stick. For simplifying the theory, it is convenient to consider the extreme cases of connection of the pilot with the control elements: the case of fixed stick and the case of free stick.

Accordingly we may speak of the stability of an aircraft in these two extreme cases. Let us imagine that the pilot, having established a certain state of flight, fixes the control surfaces in positions corresponding to this attitude. Let a certain disturbance begin to act on the aircraft. Let us assume that during the time of action of the disturbance and during the time of the subsequent motion of the aircraft the control surfaces remain fixed. Such a motion will be termed flight with fixed controls.

Let us assume that the pilot, by means of the trimming tabs, has balanced the

aircraft in flight under the initial conditions in such a way that the force exerted on the control levers, at a position of the control surfaces corresponding to the given attitude is zero. Then the flier will be able to remove his hands and feet from the control levers, i.e., to release the controls. In this case the aircraft will continue its flight at the preceding attitude until some disturbance begins to act on it.

In disturbed motion of an aircraft with free control surfaces, there will no longer remain motionless. They will be deflected as a function of the variations in the forces and moments acting on the control surfaces themselves and on the control cables. The deflections of the control surfaces will cause additional aerodynamic moments relative to the center of gravity of the aircraft. At one and the same initial attitude, the disturbed motion of the aircraft with free control surfaces will, in the general case, differ from the disturbed motion of the aircraft with fixed controls. In order to characterize the stability of the initial state of flight of an aircraft with free control surfaces, we will introduce the concept of stability with free controls. If the pilot, after balancing the aircraft in the initial state of flight, fixes the control levers in an unchanging position, the stability of an aircraft with fixed controls will be in question*.

Static Stability of Aircraft

We have already briefly considered, above, the physical meaning of the concept of static stability and have given its definition. This concept may also be considered from the point of view of aeromechanics.

If we consider an aircraft with fixed control surfaces as an absolutely rigid body, such an aircraft will have six degrees of freedom. However, if we take into

*In our further discussion, everywhere except in Chapter XI, we will consider the aircraft (and in particular, the control drive) as absolutely rigid. In this way, a fixed stick will correspond to a fixed control surface.

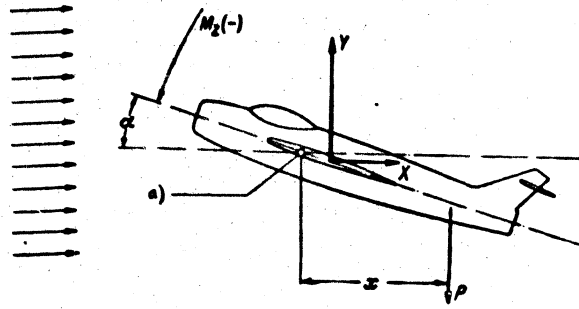
account possible deformations of the aircraft and deflections of the control surfaces in flight, the number of degrees of freedom will be considerably greater. In constructing and solving the equations of aircraft motion we must take as the independent variables, certain parameters of motion whose number must be equal to the number of degrees of freedom. The setting up of the equations of motion and the solutions of these equations is not a convenient method for solving practical problems in aircraft design offices, laboratories, or flight testing of aircraft. For routine work in designing and testing, simplified although less refined methods of solution are required. The characteristic of the static stability of an aircraft is of substantial importance in this connection.

Role of Static Stability. Before passing to the definition of this term, let us recall that static stability is far from characteristic for the actual stability of an aircraft, although it is one of its necessary conditions. The characteristics of static stability are very important for the rating of an aircraft, but their influence on disturbed motions is manifested only in combination with other aircraft parameters which are likewise of substantial importance in design. An advantage of the characteristics of static stability over the other parameters, as will be seen from what follows, lies in the fact that it is simplest for the designer to vary the static stability so as to influence the behavior of the aircraft in the air in the desired direction i.e., act on its actual (dynamic) stability and controllability.

To define the essential nature of static stability, let us imagine an aircraft with one degree of freedom of motion, namely an aircraft able to rotate about the transverse axis passing through the center of gravity of the aircraft. In practice, this condition can be realized in a wind tunnel if the transverse axis of the aircraft is fixed (Fig.1.7). Let the aircraft be in the air stream of constant velocity. Then, the condition of equilibrium of the aerodynamic moment ($\sum M_z = 0$) will correspond to one or more angles of attack at constant angle of deflection of the elevator. At some angles of attack the equilibrium may be stable, at others,

unstable.

If the rotation of the aircraft is restrained, at various angles of attack, then, for each angle of attack, an aerodynamic moment of definite value and sign will act on the aircraft and can be balanced by the external force P applied on a



a) Axis of Rotation

Fig.1.7 - Diagram of Forces and Moments Acting on the Aircraft in Wind-Tunnel Tests

definite arm x . By plotting the force P and the arm x against various angles of attack we can construct a diagram of the moments $M_z = P x$ acting on the aircraft at a constant angle of deflection of the elevator and various angles of attack (Fig.1.8).

To the equilibrium positions ($M_z = 0$) will correspond the points 1, 2, and 3 of the intersection of the curves of the moments with the abscissa. In accordance with the generally adopted rule of signs, a moment tending to increase the angle of attack will be considered positive. A moment tending to decrease the angle of attack will be considered negative.

Let us see what states of equilibrium of the aircraft (points 1, 2, and 3) will be stable, and what states will be unstable. Let us take the equilibrium position at point 1. Let the aircraft be deflected from this position of equilibrium, reducing the angle of attack by applying the corresponding moment. As indicated in Fig.1.8, a positive moment, tending to increase the angle of attack, will begin to

act on the aircraft. If the aircraft is released by removing the external force P, it will begin to increase the angle of attack and, after a certain time, will set

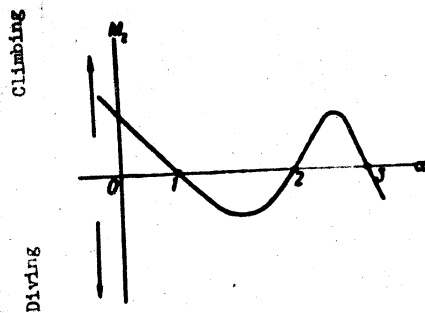


Fig.1.8 - Diagram of the Aerodynamic Moments Acting on the Aircraft with Respect to its Transverse Axis z.

itself at the angle of attack corresponding to the initial state of equilibrium at point 1. This means that the condition of equilibrium at point 1 will be stable. By similar reasoning we can prove that the state of equilibrium at point 1 will also be stable. Conversely, the state of equilibrium at point 2 will be unstable. In fact, if the aircraft is deflected from its position at point 2 to a somewhat smaller angle of attack, differing very slightly from the initial angle of attack at point 2, then a negative moment, tending to turn the aircraft

toward still smaller angles of attack will begin to act on the aircraft. When the aircraft is removed from the influence of the external force P, the angle of attack will decrease until the aircraft enters the region of the equilibrium state corresponding to point 1. Here the aircraft, after performing a few oscillations (usually damped) will set itself at the angle of attack α_1 .

The stability of the aircraft in such motion, artificially reproduced in the wind tunnel or conventionally in flight, with restricted degrees of freedom, is conventionally termed static.

The existence of static stability in flight, at the initial instant of disturbed motion, results in a rotation of the aircraft in the direction of the original attitude of flight.

Conditions of Static Stability. As follows from the above reasoning, the con-

dition for the existence of static equilibrium in an aircraft with the generally adopted rule of signs, will be the negative slope of the tangent to the curve $M_z = f(\alpha)$ at the point of balancing of the aircraft ($M_z = 0$).

Analytically, the condition of static equilibrium will be expressed by the inequation

$$\frac{\partial M_z}{\partial \alpha} < 0.$$

The condition of static instability will be expressed by the inequation

$$\frac{\partial M_z}{\partial \alpha} > 0.$$

The condition of neutrality of the aircraft with respect to static equilibrium will be expressed by the equation

$$\frac{\partial M_z}{\partial \alpha} = 0.$$

Coefficients of Longitudinal Static Stability. For a qualitative and quantitative evaluation of static stability it is in practice more convenient to deal not with the moment itself but with the dimensionless coefficient of this moment. The coefficient of the longitudinal moment m_z is defined by the relation

$$m_z = \frac{M_z}{qSb},$$

where S is the wing area of the aircraft; b , a certain arbitrarily selected linear quantity for which the wing chord is usually taken; and $q = \frac{\rho v^2}{2}$, the velocity head. Further, in considering the stability of the aircraft in the range where the dependence of C_l on α is linear, it is in practice more convenient to use the relation of the coefficient m_z not with the angle of attack, but with the coefficient

of lift of the aircraft C_L , which is uniquely* connected with the angle of attack. In the graphic representation of this relation, curves similar to those shown in Fig.1.9 are constructed.

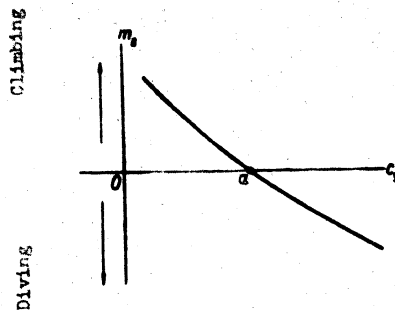


Fig.1.9 - Curve of the Coefficient of Longitudinal Moment (Pitching Moment) m_z as a Function of the Coefficient of Lift C_L .

The curve $m_z = f(C_L)$, given in Fig.1.9, may be obtained in wind-tunnel tests of the aircraft or its model and corresponds to the constant value of the Mach number and the constant value of the angle of rudder deflection δ . From the curve $m_z = f(C_L)$ we can estimate the value and sign of the static longitudinal stability. For this purpose, the derivative $\frac{\partial m_z}{\partial C_L} = m_z'$ is used, taken at the point of balancing ($m_z = 0$). The derivative m_z' is termed the coefficient of longitudinal

static stability of an aircraft.

It is obvious that, by the same reasoning as with respect to the curve $M_x = f(\alpha)$, the existence of static stability of the aircraft is determined by the inequation

$$m_z' < 0.$$

*A single-valued relationship between C_L and α is also obtained if we neglect the influence of the compressibility of the air; the influence of compressibility will be discussed in later Chapters of this book.

**The partial derivative is used, since in the general case, the coefficient m_z may be a function of the Mach number or the flying speed, besides being a function of C_L .



The absolute value of the derivative m_z^{c1} characterizes the degree of static stability - or instability - of the aircraft.

Stability, Controllability, and Safety of Flight

To ensure safety of flight, the pilot must be able to detect the instant at which the aircraft goes into angles of attack, overloads, or speeds that are dangerous from the point of view of strength or controllability. An involuntary transition to these dangerous states must be avoided. In the absence of automatic signals on the aircraft, preventing the pilot from bringing the aircraft close to dangerous attitudes and situations, the role of an "alarm" is largely taken over by the forces and deflection of the control levers for the control surfaces. In this case, the forces rather than the deflection play the major role. The requirements for a system of control developed by flight practice consist in making the force necessary for producing a destructive overload or for bringing the aircraft into high and low speeds, sufficiently noticeable for the pilot. The necessity of sufficiently great forces to bring the airplane into such critical states of flight makes certain demands on both the stability of the aircraft and the magnitude of the hinge moments of the control surfaces.

To summarize the above statements, we may note that longitudinal stability, controllability, and flight safety are intimately correlated. It cannot be said that high stability adversely affects the controllability and safety of an aircraft. On the other hand a high stability, at proper selection of the size of the control surfaces and their aerodynamic compensation, improves the controllability of the aircraft and the safety of flight. However, these conclusions are not invariably valid. A change in the conditions of utilization of the aircraft and future investigations may necessitate certain modifications in these concepts.

It must be remembered that flight with an unstable aircraft is possible; however, such flights are unpleasant for the pilot or dangerous and, therefore,

inadmissible. However, flights with an uncontrollable aircraft are entirely impossible.

In an uncontrollable aircraft it is impossible for the pilot to perform conscious motions, and the behavior of such an aircraft does not depend on the actions of the pilot. Flight on an uncontrollable aircraft must inevitably end in catastrophe. For this reason, controllability is the decisive factor for the very possibility of flight.

For a mathematical analysis of questions connected with stability and controllability of aircraft, a determination of the forces and the moments of these forces acting on the aircraft under various conditions is a prime requisite.

In the following Chapters we will discuss the basic methods of determining the moments acting on the aircraft in steady and unsteady flight.

CHAPTER II

FORCES AND MOMENTS ACTING ON AN AIRCRAFT WITHOUT TAIL SURFACES IN
STEADY RECTILINEAR FLIGHT

The moment coefficient of an aircraft without horizontal tail surfaces in steady rectilinear flight, like the moment coefficient of any aircraft, can be most reliably determined by model tests in a wind tunnel. In the absence of such facilities, the coefficient of moment may be approximately found by calculating the moments of the individual elements: wing, fuselage, engine nacelles, etc. The methods of such calculations are given below.

Moment of Wing with Constant Chord

Let us write the expression for the longitudinal moment acting on a wing with constant chord with respect to an axis lying in the plane of the chord at a certain distance from the leading edge of the wing (Fig.2.1). In this case it is convenient to use the components of the total aerodynamic force acting on the wing, taken in the system of fixed axes, in which the line of the chord is taken as the abscissa and the perpendicular to the chord, directed upward, is taken as the ordinate. Let

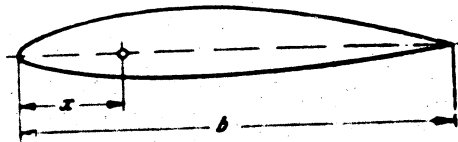


Fig.2.1 - Position of the Axes of Moments

us place the origin of coordinates on the leading edge of the wing. Let the coefficients of the components of the total aerodynamic force be C_{L1} , C_{D1} . We will

consider the moment positive if it tends to increase the angle of attack of the wing, and negative in the opposite case. It is not hard to see that the coefficients C_{L1} , C_{D1} are interconnected by a polar relationship analogous to the ordinary polar of the wing. This polar relationship, i.e., the curve $C_{D1} = f(C_{L1})$, is termed a polar of the second kind in contrast to the ordinary polar of the first kind. The relation between the coefficients of these polars is given by formulas whose derivation is elementary:

$$\left. \begin{aligned} C_{L1} &= C_L \cos \alpha + C_D \sin \alpha \\ C_{D1} &= C_D \cos \alpha - C_L \sin \alpha \end{aligned} \right\} \quad (2.1)$$

Since in practice, the angles of attack α are small, we may, without considerable error, take $\cos \alpha \approx 1$ and $\sin \alpha \approx \alpha$ where α is expressed in radians.

In this case, eq.(2.1) may be simplified and written in the form

$$\left. \begin{aligned} C_{L1} &\approx C_L + C_D \alpha; \\ C_{D1} &\approx C_D - C_L \alpha. \end{aligned} \right\}$$

The value of the derivative C_{D1} is considerably less than C_{L1} . For this reason and for further simplification, we may take

$$\left. \begin{aligned} C_{L1} &\approx C_L \\ C_{D1} &\approx C_D - C_L \alpha \end{aligned} \right\} \quad (2.1')$$

It is the latter formulas that are generally used in practice. Since C_{D1} is represented in the form of the two terms in a certain combination, it will be found that $C_{D1} < 0$, while $C_{D1} > 0$ is always the case. Figure 2.2 shows a typical polar of the second kind.

As stated above, on the basis of the theory of similitude the wing moment may be represented in the form

$$M_x = m_x S b^2 \frac{V^3}{2} = m_x S b q.$$

The coefficient m_x is termed the coefficient of longitudinal wing moment.

Since the quantities S , b , and q are always known, m_z must be defined for determining the wing moment.

If \bar{x}_p is the distance to the center of pressure (the points of application of the aerodynamic force) from the leading edge of the wing, related to the chord,

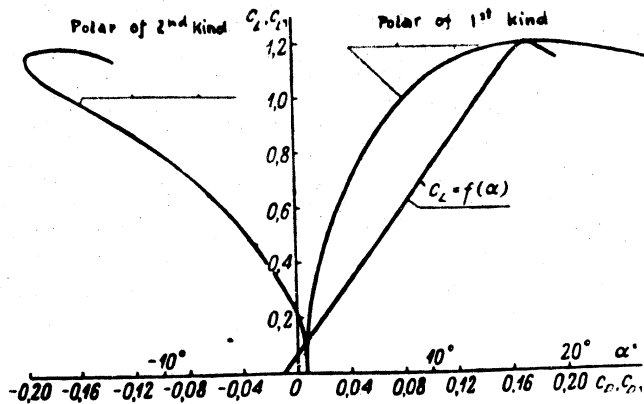


Fig.2.2 - Polars of First and Second Kinds in a Special Case

then, for the coefficient of moment with respect to the axis selected, located at the distance $x_T = \bar{x}_T b$ from the leading edge, we will have one of the following

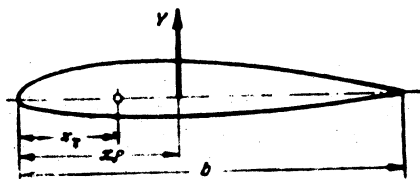


Fig.2.3 - Determination of Wing Moment; the Axis of Moments Lies in the Plane of the Chord

expressions (Fig.2.3):

$$m_z = -(\bar{x}_p - \bar{x}_T) c_y = c_m + c_L \bar{x}_T \quad (2.2)$$

where c_m is the moment coefficient of the wing with respect to the axis passing through its leading edge. The former expression is obtained by direct calculation of the moment with respect to the axis selected, while the latter is obtained if we first determine the moment with respect to the axis passing through the leading edge of the wing, and then, by the general rules of mechanics, passing through the axis selected. On the linear part of the curve $c_L = f(d)$, as is commonly known, the

$$c_m = c_{m0} + \frac{dc_m}{dc_L} c_L, \quad (2.3)$$

relation is obtained so that eq.(2.2), taking account of the approximate formula (2.1'), will yield

$$-\bar{x}_p c_L = c_{m0} + \frac{dc_m}{dc_L} c_L, \quad (2.4)$$

whence
$$\bar{x}_p = -\frac{c_{m0}}{c_L} - \frac{dc_m}{dc_L}.$$

We have obtained a certain expression for the center of pressure of the wing, from which it will be seen that, for the so-called "moment" profile of the wing in which $c_{m0} \neq 0$, the center of pressure is displaced along the chord, and, in particular, at $c_v = 0$, it approaches $\bar{x}_p = \infty$.

On the other hand, the second part of the same expression (2.2) furnishes

$$m_p = c_{m0} + \frac{dc_m}{dc_L} c_L + \bar{x}_p c_L = c_{m0} + \left(\frac{dc_m}{dc_L} + \bar{x}_p \right) c_L. \quad (2.5)$$

It is obvious that, on the chord of the profile, we can always select such a position of the axis

$$\bar{x}_p = \bar{x}_p = -\frac{dc_m}{dc_L}, \quad (2.6)$$

that the sum within the brackets of eq.(2.5) vanishes. The coefficient of moment with respect to the axis passing at the distance \bar{x}_p from the leading edge of the

wing (as will be clear from the above) will not depend on C_L and, consequently, also not on the angle of attack

$$m_p = c_{m0} + f(\alpha)$$

Aerodynamic Center

That point on the wing chord with respect to which the moment coefficient does not depend on the angle of attack nor on C_L , is termed the aerodynamic center. The line passing through the profile foci forming the wing is called the line of action. In modern wing profiles, the aerodynamic center is located at 20 - 24% of the chord in the leading edge.

As we have seen, the concepts of aerodynamic center and center of pressure do not coincide. We call an aerodynamic center that point of the profile with respect to which the moment coefficient does not depend on the angle of attack; while the center of pressure is the term for the point of intersection between wing chord and the vector of the aerodynamic force acting on the wing. Aerodynamic center and center of pressure coincide only in the special case of a symmetrical or so-called "S-shaped" profile. In such a profile $C_{m0} = 0$ and eqs. (2.4) and (2.6) give identical results for this case.

The concept of aerodynamic center is very convenient in the analysis of stability problems, since the position of the center does not depend* on the angle of attack nor on coefficient C_L and depends only on the geometrical shape of the wing profile.

*It will be clear from the following that the compressibility of the air affects the position of the aerodynamic center; however, for the time being we will consider the air to be an incompressible fluid.

The Influence of the Position of the Center of Gravity of the Aircraft
on the Wing Moment

By introducing the quantity \bar{x}_F , according to eq.(2.6), in eq.(2.5), we obtain the moment coefficient of the wing with respect to the axis located in the plane of the chord at the arbitrary distance \bar{x}_1 from the leading edge

$$m_z = c_{m0} - (\bar{x}_F - \bar{x}_1) c_L \quad (2.7)$$

As will be clear, in this special case the coefficient of the wing moment is a linear function of the coefficient of lift. Consequently, in an arrangement in which the center of gravity of the aircraft is located in the plane of the wing chord, m_z of the wing will be a linear function of C_L .

In the case when the center of gravity of the aircraft is not located in the plane of the wing chord, the expression for the coefficient of wing moment with

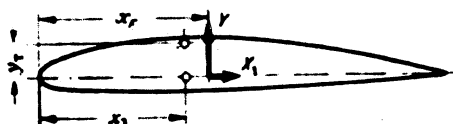


Fig.2.4 - Determination of the Wing Moment; the Axis of Moments does not Lie in the Plane of the Chord

respect to the axis passing through the center of gravity takes a somewhat more complex form (Fig.2.4)

$$m_z = c_{m0} - (\bar{x}_F - \bar{x}_1) c_L - y c_D$$

or, bearing in mind eq.(2.1'),

$$m_z = c_{m0} - (\bar{x}_F - \bar{x}_1) c_L - y c_D + y c_L \alpha = c_{m0} - (\bar{x}_F - \bar{x}_1 - y \alpha) c_L - y c_D \quad (2.8)$$



We see that the displacement of the center of gravity of the aircraft with respect to the wing, in elevation, impairs the linearity of the expression $m_z = f(C_L)$ the more strongly, the greater the angle of the attack of the wing, since C_D and C_L are not linear functions of C_L . Let us evaluate the value of the curvature of the relation $m_z = f(C_L)$.

As an example, let $c_{m0} = 0$; $x_f = 0,20$; $x_r = 0,25$ and let us take the relation for $C_L = f(\alpha)$ and $C_x = f(C_L)$ in the form

$$C_L = 5,8\alpha; \quad C_D = 0,007 + 0,07C_L^2.$$

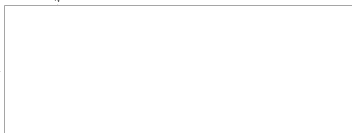
Then, depending on the coordinates of the center of gravity in elevation, we will have the following Table:

\bar{y}_r	c_L	0	0.1	0.2	0.3	0.4	0.5	0.6	0.7	0.8
0	m_z	0	0,0050	0,0100	0,0150	0,0200	0,0250	0,0300	0,0350	0,0400
-0,1	m_z	0,0007	0,0056	0,0103	0,0148	0,0191	0,0231	0,0270	0,0307	0,0342
+0,1	m_z	-0,0007	0,0044	0,0097	0,0152	0,0209	0,0269	0,0330	0,0393	0,0458

Thus, in a high-wing monoplane, when the center of gravity of the aircraft is below the wing ($\bar{y}_r < 0$), the coefficient of wing moment increases more slowly with increasing ($\bar{y}_r > 0$) while in the scheme of the low-wing monoplane ($\bar{y}_r = 0$), it increases faster than in the case when the center of gravity lies in the plane of the chords ($\bar{y}_r = 0$).

The nonlinearity of the function $m_z = f(C_L)$, due to the displacement of the center of gravity of the aircraft in elevation with respect to the wing, begins to manifest itself markedly only at sufficiently large values of C_L . For this reason, in a number of cases in studying questions of stability, we may use the simpler although less exact expression given by eq.(2.7) for the coefficient of wing moment.

A very great displacement of the center of gravity of the aircraft with



respect to the wing, in elevation, may change even the very character of the wing camber. As an example, Fig.2.5 gives the curves $m_z = f(C_L)$ for various values of \bar{y}_T , constructed under the above assumptions. It will be clear, at $\bar{y}_T = 1.0$, for $C_L > 0.1$, the derivative of the curve $m_z = f(C_L)$ changes its sign. This fact is sometimes used by designers to improve the longitudinal stability of an aircraft at high angles of attack, but this method has not taken hold. In modern aircraft design, the vertical displacement of the center of gravity rarely exceeds 10% of the chord, which fact also explains the remark made above as to the possibility of using eq.(2.7).

The position of the center of gravity of the aircraft with respect to the chord has an extremely great influence on the wing moment. By varying \bar{x}_T , the value of the derivative $\frac{dm_z}{dC_L}$ and its sign can be varied within wide limits. As will be seen from eq.(2.7), by locating the center of gravity of the aircraft ahead of the aero-

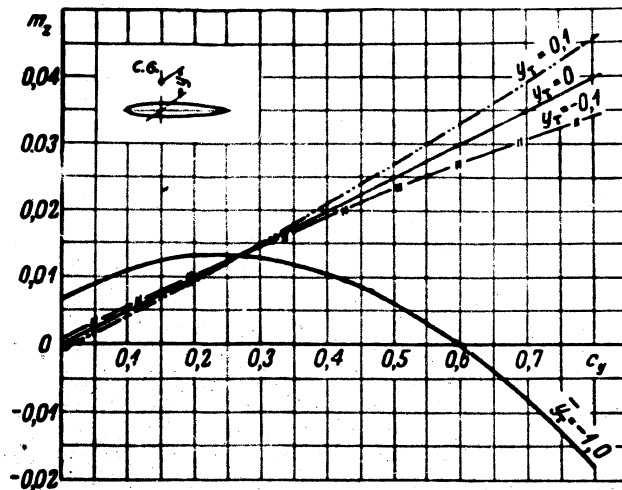


Fig.2.5 - Influence of the Position of the Center of Gravity in Elevation on the Wing Moment

dynamic center, we obtain a negative derivative $\frac{\partial m_z}{\partial C_L}$; by placing the center of gravity at the aerodynamic center, we have $\frac{\partial m_z}{\partial C_L} = 0$; by placing the center of gravity behind the aerodynamic center, $\frac{\partial m_z}{\partial C_L}$ will be positive.

In this way, by displacing the center of gravity along the wing chord, we may substantially influence the sign and value of the moment of the aerodynamic forces on the wing at any sudden change in angle of attack and at constant flying speed. For this reason, as will be shown below, the position of the center of gravity or, as it is also called, the "centering" of the aircraft is an extremely important factor influencing the stability of the aircraft.

The Moment of a Wing of Arbitrary Horizontal Contour

In the preceding arguments, the wing was assumed to be of rectangular planform, with a constant profile along the span. Such wing shapes are met only rarely today, owing to their unrational utilization of material (high design weight), especially in cases of cantilever wings. The wings used today have a nonequilateral trapezoid planform. The wing profile with respect to the wing span is often taken as variable. Wings of such shape, which have a number of aerodynamic advantages, have a mechanical strength approaching that of a body of equal resistance, and are considerably lighter in weight than rectangular wings.

Let us consider how the moment of a wing of arbitrary shape is expressed with respect to the center of gravity of the aircraft. We remark as a preliminary that, instead of seeking an expression for the moment with respect to the axis passing through the center of gravity of the aircraft we may determine the moment with respect to any other axis and then, using the well-known rules of mechanics, define the axis passing through the center of gravity.

Let us set up the expression for the moment of a wing of arbitrary planform but of a shape in which the line connecting the foci of the sections (the line of foci), is perpendicular to the plane of symmetry of the aircraft (Fig.2.6) with respect to the line of foci. For each elementary wing strip of a width d_z and an

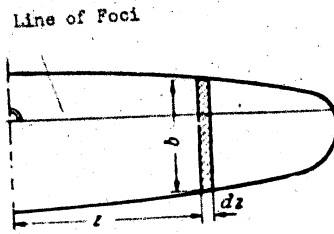


Fig.2.6 - For Determining the Moment of a Wing of Arbitrary Planform

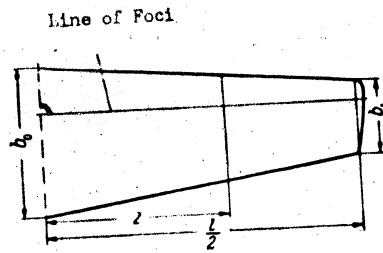


Fig.2.7 - For Determining the Moment of a Trapezoidal Wing

area bdz , the moment with respect to the axis will not, by definition, depend on the coefficient of lift. Consequently, we will have for the moment of the whole wing:

$$M_{z, KP} = 2q \int_0^{\frac{l}{2}} c_{mo} b^2 dz. \quad (2.9)$$

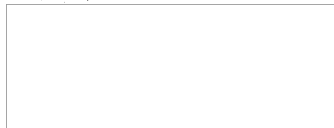
where KP denotes the wing.

In the wing assemblies encountered in practice, within the limits of smooth flow around the wing, the aerodynamic coefficients depend only slightly on the position of the section with respect to the span*. For this reason, it may be assumed that $c_{mo} = \text{const}$ in first approximation, on integration. We then have

$$M_{z, KP} = 2qc_{mo} \int_0^{\frac{l}{2}} b^2 dz. \quad (2.10)$$

If we confine the investigation to the class of trapezoidal wings, since it is precisely such wings that are most often used in practice, we may write (Fig.2.7)

*In particular, for flat wings with a constant spanwise profile, c_{mo} will be the same for all wing sections ($c_{mo} = id$).



$$b = b_0 - (b_0 - b_1) 2 \frac{z}{l} = b_0 \left[1 - \left(1 - \frac{1}{\eta} \right) \bar{z} \right] = b_0 \left(1 - \frac{\eta - 1}{\eta} \bar{z} \right), \quad (2.11)$$

where $\eta = \frac{b_0}{b_1}$ is the coefficient of wing taper or, as it is often called, the taper, and $\bar{z} = 2 \frac{z}{l}$. On introducing eq.(2.11) in eq.(2.10) and integrating, we obtain

$$M_{z, \text{tr}} = 2q c_{m0} b_0^2 \frac{l}{2} \left[1 - \frac{\eta - 1}{\eta} + \frac{(\eta - 1)^2}{3\eta} \right] = c_{m0} q b_0^2 \frac{\eta^2 + \eta + 1}{3\eta}. \quad (2.12)$$

The wing area is equal to

$$S = \frac{b_0 + b_1}{2} l = b_0 \frac{\eta + 1}{2\eta}. \quad (2.13)$$

The mean geometric wing chord is

$$b_{\text{tr}} = \frac{S}{l} = b_0 \frac{\eta + 1}{2\eta}. \quad (2.14)$$

Thus, the product $b_0^2 l$ may be represented in the form

$$b_0^2 l = S b_{\text{tr}} \left(\frac{2\eta}{\eta + 1} \right)^2. \quad (2.15)$$

On substituting this expression in eq.(2.12), we have

$$M_{z, \text{tr}} = c_{m0} q S b_{\text{tr}} \frac{4}{3} \frac{\eta^2 + \eta + 1}{(\eta + 1)^2}. \quad (2.16)$$

on representing M_z in the form

$$M_z = m_z S b_{\text{tr}} q,$$

we obtain

$$m_z = m_{z0} = c_{m0} \frac{4}{3} \left[1 - \frac{\eta}{(\eta + 1)^2} \right]. \quad (2.17)$$

Depending on the taper, the factor for C_{m0} varies within the limits from 1 at $\eta = 1$ to $4/3$ at $\eta = \infty$ (triangular wing).

Thus the moment coefficient of a trapezoidal wing, whose aerodynamic center is



perpendicular to the plane of symmetry of the aircraft relative to the wing area and to the mean geometric chord, is equal to the moment coefficient at $C_{L_1} = 0$ and is always greater than the moment coefficient at $C_{L_1} = 0$ of the profile of which the wing is formed. The degree of excess increases with the taper.

The Influence of Sweepback on the Wing Moment

Let us now assume that the wing is given a certain sweepback in planform so that the line of foci forms the angle χ with the line parallel to the wing span. (Fig.2.8).

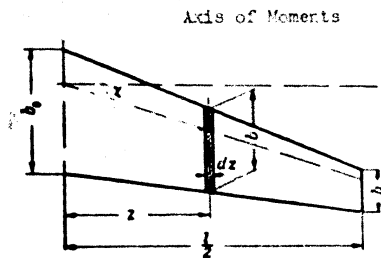


Fig.2.8 - For Determining the Moment of a Trapezoidal Wing with Sweepback

Let us determine the moment with respect to an axis passing through the aerodynamic center of a central wing section. In this case we shall consider the wing to be plane, i.e., not having a lateral dihedral nor a twist of the sections relative to the central section of the wing. For an elementary wing strip of a width dz , located at a distance z from the plane of symmetry of the wing, we will

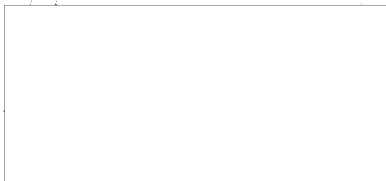
have

$$dM_z = (c_{m0} b dz b - c_y b dz x) q,$$

and, as will be clear from Fig.2.8, $x = z \tan \chi$. Integrating over the entire wing area, we obtain

$$M_z = 2q \left[\int_0^{\frac{l}{2}} c_{m0} b^2 dz - \int_0^{\frac{l}{2}} c_y b z \tan \chi dz \right]. \quad (2.18)$$

The first term of this expression is identical with that already considered; let us, therefore turn to the second term



$$I = 2q \int_0^{\frac{l}{2}} c_l b z \operatorname{tg} \chi dz. \quad (2.19)$$

As shown by special investigations, sweepback affects the distribution of C_l over the span; in this case it has been found that the integral cannot be taken analytically. Confining ourselves merely to a qualitative evaluation and assuming as before that C_l varies only slightly along the span, the integral may still be calculated analytically. By integrating, we have

$$\begin{aligned} I &= 2q c_l \operatorname{tg} \chi \int_0^{\frac{l}{2}} b z dz = 2q c_l \operatorname{tg} \chi b_0 \frac{l^2}{4} \int_0^1 \left(1 - \frac{\eta-1}{\eta} z\right) z dz = \\ &= q c_l \operatorname{tg} \chi \frac{b_0 l^2}{2} \frac{\eta+2}{6\eta}. \end{aligned}$$

On the basis of eqs. (2.13)-(2.15), we have

$$b_0 l^2 = S b_{cp} \lambda \frac{2\eta}{\eta+1},$$

so that

$$I = q c_l \operatorname{tg} \chi S b_{cp} \lambda \frac{\eta+2}{6(\eta+1)}. \quad (2.20)$$

In this way, in the general case, the total coefficient of longitudinal wing moment relative to an axis passing through the aerodynamic center of a central section related to the wing area, the mean geometric chord, and the velocity head, is equal to

$$m_x = c_{m0} \frac{1}{3} \left[1 - \frac{\eta}{(\eta+1)^2}\right] - c_l \operatorname{tg} \chi \frac{\eta+2}{6(\eta+1)}. \quad (2.21)$$

The moment with respect to a certain parallel axis, located at the distance from the aerodynamic center of the central section, will be equal to

STAT

$$m_x = m_x + \frac{\Delta x_r}{b_{ac}} c_l = m_x + \Delta x_r c_l = c_{ac} \frac{b}{3} \left[1 - \frac{\eta}{(\eta+1)^2} \right] - \left[\left(\lambda \eta \lambda \frac{\eta+2}{6(\eta+1)} + \bar{x}_r \right) - \bar{x}_c \right] c_l = m_{ac} - (\bar{x}_{r_{ac}} - \bar{x}_c) c_l$$

where x_p and x_T are relative (in fractions of the mean chord) coordinates of the aerodynamic center and of the center of gravity of the aircraft, respectively.

It follows from the resultant expressions that, in the case of a sweptback wing, measured along the line of foci, the aerodynamic center is displaced relative to the aerodynamic center of a central section in the direction of the sweepback, by the quantity

$$\Delta \bar{x}_r = \lambda \eta \lambda \frac{\eta+2}{6(\eta+1)}$$

It is obvious that this displacement, other conditions being equal, will be greater at greater sweepback, greater elongation of the wing and smaller wing taper.

Like the position of the center of gravity of the aircraft relative to the chord, the wing sweepback has a great influence on the wing moment. At positive sweepback (the wing tips being curved backward) and at constant position of the center of gravity, we obtain an increase in static stability (reduction of the derivative $\frac{\partial m_x}{\partial c_l}$); at negative sweepback (the wing tips being curved forward) the opposite is true.

The Mean Aerodynamic Wing Chord

Let us now attempt to select an equivalent rectangular wing such that its moment characteristics and forces Y_1, X_1 are identical with the moment characteristics and forces Y_1, X_1 of a wing of arbitrary planform. In this case, the area of the actual and equivalent wings must be the same.

The moment relative to the axis passing through the leading edge of the central section of arbitrary shape, having (in the most general case) a certain

lateral dihedral, is expressed by the formula (Fig.2.9)

$$M_z = 2q \left[\int_0^{\frac{l}{2}} c_{m \text{ sec}} b^2 dz - \int_0^{\frac{l}{2}} c_{l \text{ sec}} b x dz + \int_0^{\frac{l}{2}} c_{d1 \text{ sec}} b y dz \right] \quad (2.22)$$

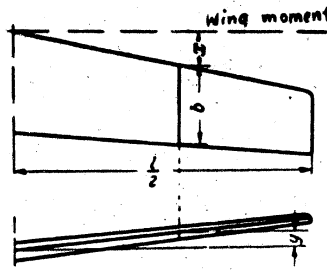


Fig.2.9 - For Determining the Wing Moment in the General Case
The moment of the equivalent rectangular wing is equal to

$$M_0 = c_m q S b_A - c_l q S x_A + c_{d1} q S y_A \quad (2.23)$$

where \$b_A\$ is the chord of the equivalent wing;

\$x_A, y_A\$ are the coordinates of the leading edge of the equivalent wing with respect to the point of intersection of the chord of a central wing section with the plane containing the selected axis of moments.

By hypothesis, the moment of the equivalent wing must be equal to the moment of the actual wing. For this reason, by equating eqs.(2.22) and 2.23) term by term, we have

$$c_m S b_A = 2 \int_0^{\frac{l}{2}} c_{m \text{ sec}} b^2 dz;$$

$$c_l S x_A = 2 \int_0^{\frac{l}{2}} c_{l \text{ sec}} b x dz;$$

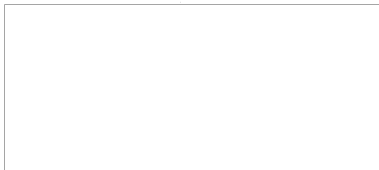
$$c_{d1} S y_A = 2 \int_0^{\frac{l}{2}} c_{d1 \text{ sec}} b y dz;$$

whence

$$\left. \begin{aligned} b_A &= 2 \int_0^1 \frac{c_{m \text{ sec}} ds}{c_D} \\ x_A &= 2 \int_0^1 \frac{c_{x \text{ sec}} ds}{c_D} \\ y_A &= 2 \int_0^1 \frac{c_{y \text{ sec}} ds}{c_D} \end{aligned} \right\} (2.24)$$

From eq.(2.24) we may find the chord of the equivalent wing and select the coordinates of its leading edge with respect to the coordinate axes. For the calculation, in addition to the geometric characteristics of the wing, we must also know the spanwise distribution of the aerodynamic coefficients. This distribution may be found by conventional methods, using the theory of inductive resistance. As mentioned above, however, for practical wings these aerodynamic coefficients show only a minor variation along the span so that it is permissible, in first approximation, to assume these coefficients as constant in the integration, i.e., to put $c_{m \text{ sec}} = c_m$, $c_{x \text{ sec}} = c_x$, $c_{y \text{ sec}} = c_y$; in this case eq.(2.24) may be replaced by the simpler expressions

$$\left. \begin{aligned} b_A &= 2 \frac{\int_0^1 c_m ds}{c_D} \\ x_A &= 2 \frac{\int_0^1 c_x ds}{c_D} \\ y_A &= 2 \frac{\int_0^1 c_y ds}{c_D} \end{aligned} \right\} (2.25)$$



For trapezoidal wings, the integrals may be determined analytically, since for such wings the following expressions will hold:

$$b = b_0 \left(1 - \frac{\eta-1}{\eta} \bar{z} \right);$$

$$x = x_{p0} + z \lg \lambda - x_p = \bar{x}_p b_0 \frac{\eta-1}{\eta} \bar{z} + \frac{l}{2} z \lg \lambda;$$

$$y = \frac{l}{2} \bar{z} \lg \psi,$$

where x_{p0} and x_p are, respectively, the coordinates of the aerodynamic center of the central section of the wing with respect to its leading edge, and the current section with respect to its nose; η is the angle of sweepback; and ψ the angle of lateral dihedral of the wing.

On introducing these expressions into eq. (2.25), bearing in mind eqs. (2.13)–(2.15), and performing integration, we obtain* an expression for the chord of the equivalent wing. It is obvious that the aerodynamic center of a wing of arbitrary shape will coincide with the aerodynamic center of a profile whose chord is equal to the chord of the equivalent wing. On performing these calculations, we obtain

$$b_A = \frac{S}{l} \frac{4}{3} \left[1 - \frac{\eta}{(\eta+1)^2} \right] = b_0 \frac{4}{3} \left[1 - \frac{\eta}{(\eta+1)^2} \right] \quad (2.26)$$

$$x_A = \frac{l}{3} \frac{1}{3} \frac{\eta+2}{\eta+1} \left(4 \frac{\bar{x}_p}{l} \frac{\eta-1}{\eta+1} + \lg \lambda \right) \quad (2.27)$$

$$y_A = \frac{l}{3} \frac{1}{3} \frac{\eta+2}{\eta+1} \lg \psi = \frac{l}{3} \frac{1}{3} \frac{\eta+2}{\eta+1} \psi. \quad (2.28)$$

Equation (2.26) shows that the chord of the equivalent wing, in the general case, is not equal to the mean geometrical chord of the actual wing: the chord of the

*In the subsequent discussion, we will neglect the influence of wing sweepback on the distribution of the circulation along the span.

equivalent wing is called the mean aerodynamic chord (MAC). Since the areas of both wings are equal by hypothesis, the span of the equivalent wing, in the general case, is not equal to the span of the actual wing; for this reason the wings will not be equivalent in their other aerodynamic characteristics, for example, in their inductive resistance. We now give an example for using the concept of MAC.

Let it be required to determine the angle of sweepback of a trapezoidal wing in such a way that the center of gravity lies at the aerodynamic center. Initial data: $S = 16 \text{ m}^2$; $L = 10 \text{ m}$; $\lambda = 6.25$; $\eta = 2.5$; $x_T = 1.0 \text{ m}$. The aerodynamic center profiles of which the wing is comprised is $x_p = 0.22$. The sweepback sought is obviously found from the condition

$$x_A + 0.22b_A = 1.0.$$

We determine the quantities

$$b_A = \frac{16}{10} \frac{4}{3} \left[1 - \frac{2.5}{3.5^2} \right] = 1.7 \text{ m};$$

$$x_A = \frac{10}{2} \frac{1}{3} \frac{4.5}{3.5} \left(4 \frac{0.22 \cdot 1.5}{6.25 \cdot 3.5} + \text{tg } \chi \right) = 2.14 (0.0604 + \text{tg } \chi).$$

The value of $\text{tg } \chi$ is determined from the equation

$$2.14 (0.0604 + \text{tg } \chi) + 0.22 \cdot 1.7 = 1.0,$$

whence

$$\text{tg } \chi = \frac{0.497}{2.14} = 0.232; \quad \chi \approx 13^\circ.$$

Hereafter, we will relate all moment coefficients to b_A instead of to b mean.

Moment of a Wing with Deflected Flaps or Slots

The wings of modern aircraft are usually provided with slots or flaps serving primarily to increase the lift during flight. Usually slots or flaps are used in

take-off and landing, but sometimes also for other flight conditions.

The camber of the wing profile is increased when the flap is extended (Fig. 2.10); the increase in the coefficient c_{mo} corresponds to this. In addition, a detailed analysis of wind-tunnel tests on wings with deflected flaps (or slots) shows that the aerodynamic center of the profile is somewhat displaced in the case of deflected wing flaps or slots. If the slots or flaps were installed over the entire

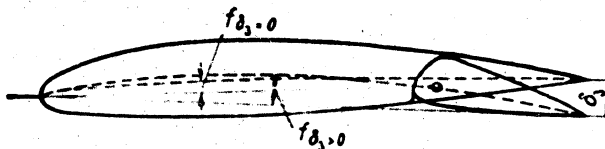


Fig.2.10 - Influence of Extension of Flap on the Camber of the Wing

wing span, then there would be no need for special calculations of the mean aerodynamic chord and the moment characteristics of a wing with deflected flaps. In this case, it would be sufficient, in eqs.(2.17) to (2.21), to take the values of c_{mo} and the aerodynamic center corresponding to the deflected flaps.

However, flaps are usually installed only on the inner part of the wing as far as the ailerons. In this way C_L , c_{mo} and the aerodynamic center of the profile varies over the wing span, so that corrections must be applied to the calculation scheme above presented.

Let us denote the aerodynamic coefficient of the wing sections which are applicable in the zone of the arrangement of opened slots or flaps by

Then, neglecting the moment from the tangential forces, we shall have, on the basis of eq.(2.22), for the moment of a wing with extended flaps (Fig.2.11)

$$M_z^A = 2q \left\{ \int_0^{l/2} c_{m0} b^2 dz + \int_0^{l/2} \Delta c_{m0}^{\delta} b^2 ds - \int_0^{l/2} \bar{x} \bar{\mu} c_{l_i}^{\delta} b^2 ds - \int_0^{l/2} c_{l_i}^{\delta} b x dz \right\} \quad (2.29)$$



in which fl indicates the distance between the ends of the slots or flaps (span of slots).

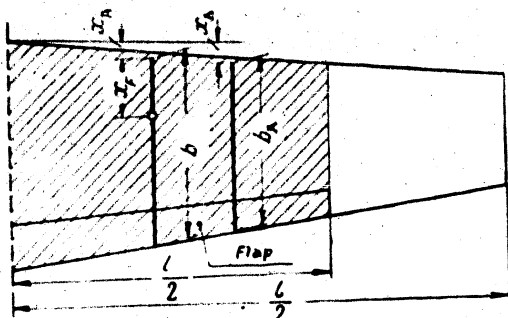


Fig.2.11 - For Determining the Moment of the Wing with Extended Slots
(The Hatched Part is the Wing Area Served by the Flaps)

By comparing the above expression with eq.(2.24), we arrive at the conclusion that the first integral within the braces, is equal to

$$\int_0^{l/2} c_{m0} b^2 dz = \frac{1}{2} m_{z0} S b_A$$

In exactly the same way,

$$\int_0^{l/2} \Delta c'_{m0} b^2 dz = \frac{1}{2} \Delta m'_{z0} S_{fl} b_{A,fl}$$

where S_{fl} and $b_{A,fl}$ denote, respectively, the part of the wing area served by the slots and the mean aerodynamic chord of this part of the area (cf. Fig.2.11). To elucidate the meaning of the two remaining integrals entering into eq.(2.29), let us rewrite them in a somewhat different form*.

* For simplicity, we will assume in the following that the aerodynamic characteristics vary in the given case only within the limits of the part of the wing area served by the slots.



$$\int_0^1 \bar{x}_p c_i'' \theta'' ds + \int_0^1 c_i'' b x ds - \int_0^1 \bar{x}_p c_i'' \theta'' ds +$$

$$+ \int_0^1 \Delta \bar{x}_p c_i'' \theta'' ds + \int_0^1 \bar{x}_p \Delta c_i'' \theta'' ds + \int_0^1 c_i'' \theta'' ds + \int_0^1 \Delta c_i'' \theta'' ds.$$

By analogous reasoning, we conclude that

$$\int_0^1 \bar{x}_p c_i'' \theta'' ds = \frac{1}{2} \bar{x}_p c_i'' S \theta_{A_i}$$

$$\int_0^1 c_i'' b x ds = \frac{1}{2} c_i'' S \theta_{A_i}$$

The third integral $\int_0^1 \bar{x}_p \Delta c_i'' \theta'' ds$, may be represented in the form

$$\int_0^1 \bar{x}_p \Delta c_i'' \theta'' ds = \frac{1}{2} \bar{x}_p \Delta c_i'' S \theta_{A_i}$$

In exactly the same way

$$\int_0^1 \Delta c_i'' \theta'' ds = \frac{1}{2} \Delta c_i'' S \theta_{A_i}$$

where x_A fl is the distance between the leading edge of the mean aerodynamic chord b_A fl of the wing section served by the slots and the leading edge of the chord of the center section related to b_A fl. The value of $\Delta \bar{x}_p$ is very small and may be, in practice, disregarded. Then, bearing in mind the remarks made and the expres-



sions obtained, eq. (2.29) may be rewritten in the following form:

$$M_y^{fl} = S b_A q \left\{ m_{00} + \Delta m_{00}^{fl} \frac{S_{fl} b_{A, fl}}{S b_A} \bar{x}_P c_l + x_A c_l - \bar{x}_P \frac{S_{fl} b_{A, fl}}{S b_A} \Delta c_l^{fl} - \bar{x}_{A, fl} \frac{S_{fl} b_{A, fl}}{S b_A} \Delta c_l^{fl} \right\}$$

On passing to the moment coefficient of a wing with extended flaps, we will have

$$m_y^{fl} = m_{00} + \Delta m_{00}^{fl} - (\bar{x}_P + \bar{x}_A) c_l - (\bar{x}_P' + \bar{x}_A') \frac{S_{fl} b_{A, fl}}{S b_A} \Delta c_l^{fl} \quad (2.30)$$

As will be clear from Fig. 2.11,

$$(\bar{x}_P' + \bar{x}_A') b_{A, fl} = (\bar{x}_A + \bar{x}_{P, fl}) b_A$$

where $x_{P, fl}$ is the distance from the aerodynamic center of the part of the wing area served by the slots to the leading edge of the mean aerodynamic chord of the whole wing, expressed in fractions of the mean aerodynamic chord of the wing.

Moreover, it is obvious that

$$\Delta c_l^{fl} \frac{S_{fl}}{S} = \Delta c_l^{fl} \frac{S_{fl} b_{A, fl}}{S b_A} = \Delta m_{00}^{fl}$$

where $\Delta C_{L_{KP}}^{fl}$ and Δm_{00}^{fl} are the increments in the coefficients of lift and in zero moment of the whole wing with extended flaps. In this way, the moment coefficient of a wing with extended flaps, relative to an axis passing through the leading edge of the center section, is expressed by the formula

$$m_y^{fl} = m_{00} + \Delta m_{00}^{fl} - (\bar{x}_P + \bar{x}_A) c_l - (\bar{x}_A + \bar{x}_{P, fl}) \Delta c_l^{fl} \quad (2.31)$$

The moment coefficient of a wing with respect to the center of gravity of the aircraft, located at the distance $(x_A + x_Y) b_A$ from an axis passing through the leading edge of the central cross section, will be equal to



$$m_{20}^{\text{fl}} = m_{20} + \Delta m_{20}^{\text{fl}} - (\bar{x}_p - \bar{x}_0) c_i - (\bar{x}_{pA} - \bar{x}_0) \Delta c_i^{\text{fl}} \quad (2.32)$$

where, for brevity, the subscript "KP" (wing) of the coefficients has been omitted. In order to use eq.(2.32) we must know the values of $\Delta m_{20}^{\text{fl}}$, x_p^{fl} , and ΔC_L^{fl} . These values are obtained by statistical processing of the experimental data.

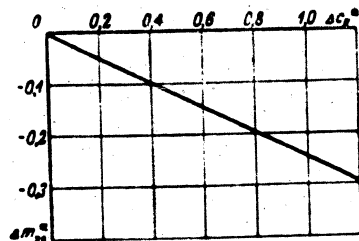


Fig.2.12 - Graph for the Approximate Determination of the Coefficient $\Delta m_{20}^{\text{fl}}$

The values of $\Delta m_{20}^{\text{fl}}$ may be determined approximately from the graph of Fig.2.12 of the function of ΔC_L^{fl} .

The value of x_p^{fl} may be determined (Fig.2.12) by the formula

$$\bar{x}_{pA} = \frac{b_{\lambda, \kappa}}{b_{\lambda}} (0.23 + \bar{x}^{\kappa}) - x_{\lambda} \quad (2.33)$$

where, as already mentioned,

$$b_{\lambda, \kappa} = \frac{2}{S_{\kappa}} \int_0^{1/S_{\kappa}} b^{\kappa} dz.$$

The value of ΔC_L^{fl} is determined by the empirical formula

$$\Delta c_i^{\kappa} = \left(\frac{\Delta c_j}{\Delta x_{\kappa}} \right) \Delta a_{\kappa}^i k_{sL} \quad (2.34)$$

STAT

where $k_{sl} = 1 - 0.75 \frac{l_{sl}}{l}$ allows for the influence of the slit in the center of the flap.

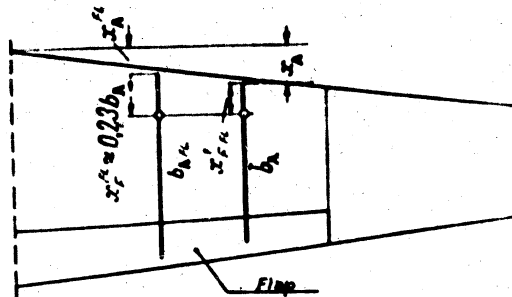


Fig.2.13 - Determination of the Aerodynamic Center of the Part of the Wing Area Served by the Flaps

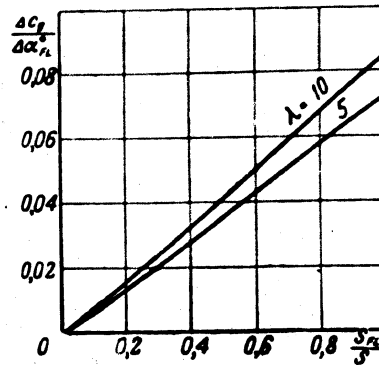


Fig.2.14 - Relation of $\frac{\Delta C_L}{\Delta \alpha_{fl}^k}$ to the ratio $\frac{S_{fl}}{S}$

The relationship of the ratio $\frac{\Delta C_L}{\Delta \alpha_{fl}^k}$ to $\frac{S_{fl}}{S}$ is shown in Fig.2.14 for two values of the wing aspect ratio $\lambda = 5$ and $\lambda = 10$. For the other values of λ , interpolation must be used. For trapezoidal wings the ratio $\frac{S_{fl}}{S}$ may be calculated



by the formula

$$\frac{S_{fl}}{S} = \frac{2\eta - \frac{l_{fl}}{l}(\eta - 1)}{\eta + 1} \frac{l_{fl}}{l}, \quad (2.35)$$

where l_{fl} is the distance between the external tips of the flaps;

$\eta = \frac{b_0}{b_1}$ is the coefficient of wing taper.

The displacement of $\Delta\alpha_{fl}$ of the angle of zero lift on any deviation with extended flaps, relative to the angle of extension of the flaps and their relative chord $\bar{b}_{fl} = \frac{b_{fl}}{b}$ is shown in Fig.2.15.

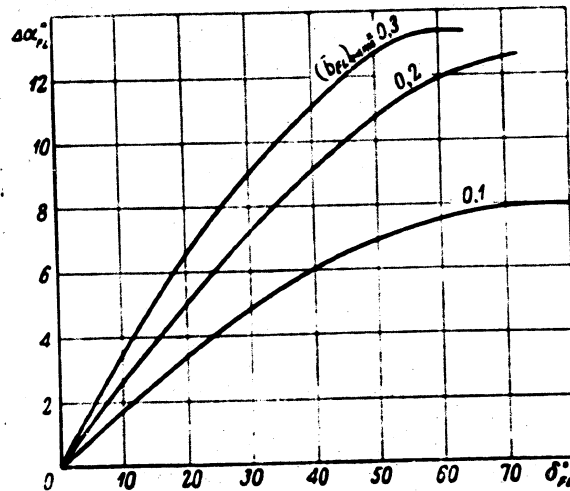


Fig.2.15 - Displacement of the Angle of Zero Lift with Extended Slots.

Wing Moment at High Angles of Attack

The expression for the wing moment with respect to its leading edge

$$c_m = c_{m0} + \frac{dc_m}{dc_L} c_L$$

STAT

which we have used until now, as already stated, is valid only within the range of angles of attack within which a smooth flow of air around the wing is assured. On approaching the critical angle of attack, corresponding to $C_{l \text{ max}}$, and on exceeding this angle of attack, the smoothness of the flow around the wing is impaired due to detachment of the flow, and the linear representation of $c_m = f(C_l)$ is no longer possible. In this case, the results of wind-tunnel tests of a model must be used directly to determine the wing moment. As an example, Fig. 2.16 gives the curve of variation of the moment coefficient along the leading edge, and the polar of the second kind for a rectangular wing. Obviously, as the critical angle of attack is approached, the curve $c_m = f(C_l)$ begins to deviate more and more from a straight line and, at $C_l > C_{l \text{ max}}$, it sharply changes its original slope. As a result of the increase in C_D at large angles of attack and of the retardation in the increase of C_l , followed by its interruption on further increase of C_{l1} , the values of $m_z = f(C_l)$ vary markedly at angles of attack near the critical values. All this, taken together, leads to a substantial change in the character of the curves $m_z = f(C_l)$ or $m_z = f(\alpha)$ at large angles of attack. The basic cause is the detachment of the boundary layer from the upper surface of the profile and the variation in the distribution of pressure resulting from this detachment.

At increasing angles of attack in the region where the linearity of the functions $c_m = f(C_l)$ and $C_l = f(\alpha)$ is already impaired, the coefficient c_m with respect to the leading edge usually continues to increase in absolute value, while C_l drops. As shown in eq. (2.2), this causes a sharp increase in the static stability contributed by the wing. In the diagram of $m_z = f(\alpha)$, obtained in wind-tunnel tests, a "wall" m_z often appears; the curve shows a sharp bend downward and is characterized by negative derivatives.

Since the above phenomena are connected with viscosity, while the Reynolds number is the fundamental criterion of similitude with respect to viscosity, the result of wind-tunnel tests at large angles of attack must be used with extreme

caution if the Reynolds number of the test does not correspond to the Reynolds number of the actual wing. If the similitude is not maintained in Reynolds numbers, then, on passage to the actual aircraft the value of the angle of attack at which the "wall" of moments begins may change and the whole character of this "wall" may become different.

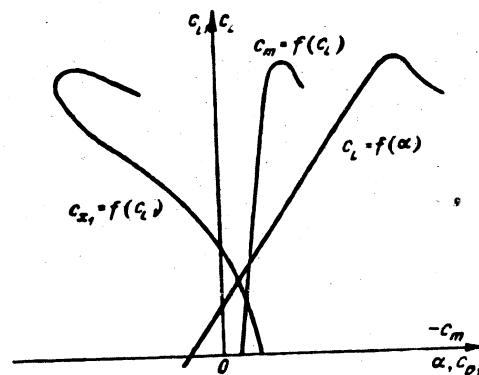


Fig.2.16 - Approximate Form of the Curves $c_m = f(C_L)$, $C_L = f(\alpha)$ and of the Polar of the Second Kind

Moment of a Sweptback Wing at Large Angles of Attack

Let us now see how the coefficient of longitudinal moment of a sweptback wing behaves as it approaches the critical angle of attack.

It is well known that, in a wing with a positive sweepback, flow separation occurs near the wing tips, while in a wing with negative sweepback a region of detachment of flow appears near the central part of a wing (Fig.2.17).

This takes place as a result of the increased thickness of the boundary layer in these zones of sweptback wings. This thickening causes separation at lower values of the pressure gradient $\frac{dp}{dx}$ over the profile contour. If we resolve the vector of total flow velocity into a perpendicular component and a component

parallel to the leading edge of the wing, we will find that the component perpendicular to the leading edge has a direct influence on the distribution of pressure

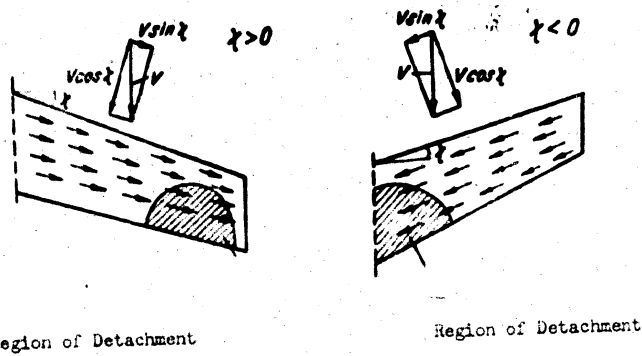


Fig.2.17 - Flow in the Boundary Layer on Sweptback Wings

along the wing sections, while the component parallel to the leading edge causes a displacement of the boundary layer.

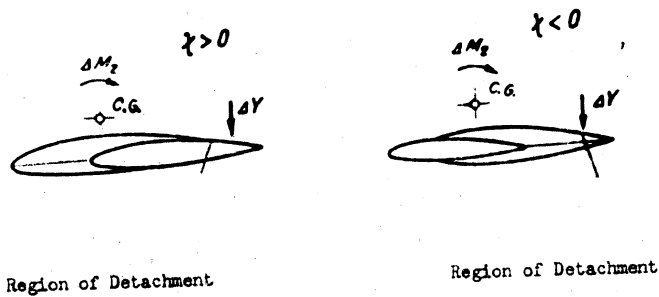


Fig.2.18 - Influence of Flow Separation Along a Sweptback Wing on its Moment with Respect to the Center of Gravity of the Aircraft

As will be seen from Fig.2.18, the boundary layer on the upper surface of a wing with positive sweepback becomes thicker in the direction toward the wing tips, while in wings with negative sweepback this occurs in the direction toward the center of the wing.



In both these cases, a flow separation results beyond the center of gravity (cf. Fig. 2.19). In this case the local values of the coefficient C_L of the sections located in the zone of separation are decreased, thereby creating a pitching moment, i.e., the appearance of a certain $\Delta m_z > 0$. In this case, the contributions of the wing to the static stability is reduced. This phenomenon takes place no matter whether the aircraft is of the mid-wing, high-wing or low-wing type.

This unpleasant phenomenon can be controlled by using, in the region of probably detachment on a sweptback wing, special profiles with higher values of $C_{L \max}$ than displayed by the profile in the rest of the wing, or some other means of preventing the thickening of the boundary layer in these zones of sweptback wings. It is obvious that larger values of $C_{L \max}$ of the sections, for example, at the tips of a wing with positive sweepback, will result from a premature flow separation in this region.

It must be borne in mind that the above remark, as to the influence of the Reynolds number on the slope of the curve $m_z = f(\alpha)$ at large angles of attack, is completely applicable to sweptback wings.

The calculation of the moments at large angles of attack is not reliable enough, owing to the complexity of the phenomenon. For this region of angles of attack it is better to use the results of wind-tunnel tests on aircraft models.

Influence of the Compressibility of Air on the Wing Moments

We have assumed above that the coefficients of the aerodynamic forces acting on a wing of given geometric dimensions are a function only of the angles of attack

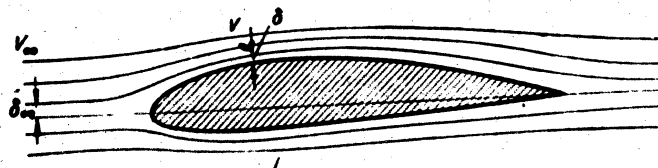


Fig. 2.19 - Schematic Representation of the Flow Around the Wing

of the wings. This assumption is sufficiently correct only at small Mach numbers, when the compressibility of air may be neglected in first approximation. As the Mach numbers increase, the assumption that the aerodynamic characteristics are independent of the Mach number becomes more and more inaccurate, and, after the local velocity at any point of the wing becomes equal to the speed of sound, this assumption sharply contradicts the actual situation.

Before speaking of the influence of the compressibility of the air on the wing moment, let us briefly recall the physics of the phenomena that take place in the flow around a wing.

As the Mach number increases, the local velocities and the decompression on the wing contour also increase, and they increase faster than the Mach number of the oncoming flow. According to this, the pressures acting on the wing contour decrease.

If for simplicity, we assume that the configuration of the streamlines around the wing do not vary with the Mach number, then at some arbitrarily selected but definite point on the wing contour the condition (Fig.2.19)

$$\rho V \delta = \rho_{\infty} V_{\infty} \delta_{\infty}$$

must be satisfied, so that

$$\frac{\rho}{\rho_{\infty}} \frac{V}{V_{\infty}} = \frac{\delta_{\infty}}{\delta} = \text{const.}$$

At the same time, in a compressible fluid, the density of the air is expressed by the formula

$$\rho = \rho_{\infty} \left[1 - \frac{\theta - 1}{2} M^2 \left(\frac{V^2}{V_{\infty}^2} - 1 \right) \right]^{\frac{1}{\theta - 1}}$$

where k is the adiabatic index.

The preceding condition may thus be written in the form

$$\frac{V}{V_{\infty}} \left[1 - \frac{\theta - 1}{2} M^2 \left(\frac{V^2}{V_{\infty}^2} - 1 \right) \right]^{\frac{1}{\theta - 1}} = \text{const.}$$

It is clear from this expression that when the Mach number increases, the ratio V/V_∞ also increases. In reality, when the Mach increases, the configuration of the streamlines does not remain unchanged, and the phenomenon proves to be far more complex, but the ratio V/V_∞ and, consequently, the decompression as well, do increase with increasing Mach. This means that at one and the same angle of attack, and with increasing Mach number, the coefficients C_L and c_m of the profile increase.

In the 1930's an approximate theory of a wing in a circulating flow of compressible fluid was developed. It is possible to use this theory, but only while the local velocity at any point of the wing is not yet equal to the speed of sound. According to this approximate theory, at increasing Mach numbers, the pressure at all points of the wing varies inversely proportionally to $\sqrt{1-M^2}$. The Soviet scientist S.A. Khristianovich, considering this problem, came to the conclusion that in a more accurate solution, the pressures at different points of the wing vary in different ratios with any variation in the Mach number: the decompression increases more strongly the greater the initial decompression at the corresponding points of the profile at $M = 0$, i.e., in an incompressible fluid.

It has been found that, at subcritical Mach numbers, the coefficient of lift of the wing profile increases with M approximately by the law:

$$c_l \approx \frac{c_{l0} M^2}{\sqrt{1-M^2}} \quad (2.36)$$

In about this same ratio the moment coefficient of the profile also varies, so that the aerodynamic center $x_F = \frac{\partial c_m}{\partial C_L}$ in the subcritical region of Mach numbers, varies only slightly. The moment coefficient at $C_L = 0$ increases approximately in the proportion

$$c_{m0} \approx \frac{c_{m0} M^2}{\sqrt{1-M^2}} \quad (2.37)$$

The variations in C_L and c_{m0} with the Mach number are rather substantial. Thus,

STAT

at $M = 0.6$, the coefficients C_L and c_{mo} increase by about 25% over their values in an incompressible fluid.

At $M = M_{kp}$, the point of the profile contour at which the decompression in an incompressible fluid would be greatest, the local velocity becomes equal to the speed of sound. When the Mach number increases further, a more or less large zone of supersonic velocities appears on the profile contour. In this zone, pressures less than the critical pressure act on the profile, i.e., pressures of the point of the profile at which the local velocity is equal to the speed of sound. This critical pressure, as is commonly known, is determined by the expression

$$p_{cp} = 0.527 p_0 \quad (2.38)$$

where p_0 is the pressure at that point of the profile at which $V = 0$

$$p_0 = p_\infty \left(1 + \frac{\gamma-1}{2} M_\infty^2\right)^{\frac{\gamma}{\gamma-1}} = p_\infty \left(1 + \frac{\gamma-1}{2} M_\infty^2\right)^{3.5} \quad (2.39)$$

The Wing Moment at Mach Numbers Exceeding the Critical

If the Mach number of the relative flow is higher than the critical value ($M > M_{kp}$) then the velocities will be supersonic in a certain region of the flow in the neighborhood of the wing, while the pressures will be lower than atmospheric pressure and lower than $p_{kp} = 0.527 p_0$. This supersonic zone of flow terminates in a pressure discontinuity in the same way as that observed in a de Laval nozzle. As the Mach number increases, the supersonic zone broadens, while the pressure discontinuity is shifted in direction of the trailing edge of the profile. At $M \approx 1$, the pressure discontinuity is located close to the trailing edge of the profile.

Experiment has shown that, after formation of a supersonic zone, the relative pressures $\frac{p}{p_0}$ in the entire forward part of the profile, up to the compression discontinuity vary relatively little with increasing Mach number, while in the trailing part of the profile, beyond the compression discontinuity, they continue to drop sharply. In this case, in the leading part of the profile the relative decompression $\bar{p} = \frac{p - p_\infty}{q_\infty}$ begins to decrease, as will be seen from Fig. 2.20, while in the trailing part it continues to increase.

Thus, as the Mach number increases in the region $M_{kr} < M < 1$, the decompression zone of the profile increases and gradually shifts toward the trailing edge of the profile.

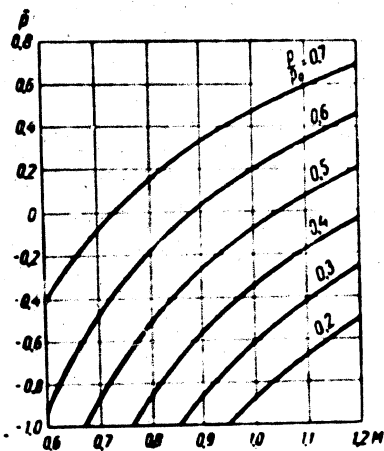


Fig. 2.20 - Coefficient of Pressure versus Mach Number and Ratio

This phenomenon at $C_l \neq 0$ is usually observed first on the upper wing surface and appears on the underside of the wing only at further increase of the Mach number. As a result, the coefficient of wing drag increases sharply, the coefficient of lift at first continues to increase and then decreases after the decompression jump appears on the lower wing surface. The coefficient of longitudinal moment increases in absolute value, since the redistribution of pressure leads to the appearance of a moment tending to reduce the angle of attack. All this is illustrated in Fig. 2.21, which gives

experimental data for the NACA 4412 profile.

Obviously, the variations in the aerodynamic coefficient of the wing are substantial; for this reason and because of the influence of the compressibility of the air, the wing moment relative to the center of gravity of the aircraft may vary appreciably. Figure 2.22 gives the curves $m_x = f(C_l)$ at various Mach numbers, corresponding to the wing whose characteristics for $\alpha = -0.15^\circ$ are shown in Fig. 2.21, and to the coordinates of the center of gravity of the aircraft

$$\bar{x}_T = 0.22, \bar{y}_T = -0.06.$$

It should be added that large positive pressure gradients occur behind the



STAT

decompression jump, possibly leading to a flow separation at the wing surface and thus further complicate an already complex phenomenon.

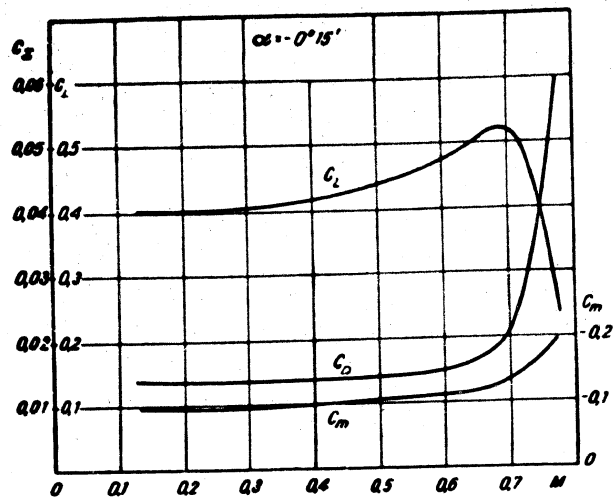


Fig.2.21 - Relation of Aerodynamic Coefficients of the Profile and Mach Number, from Experiments

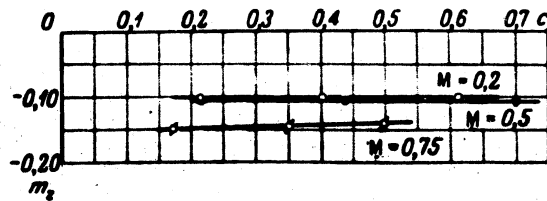


Fig.2.22 - Wing Moment Relative to the Center of Gravity of the Aircraft at Various Mach Numbers

STAT

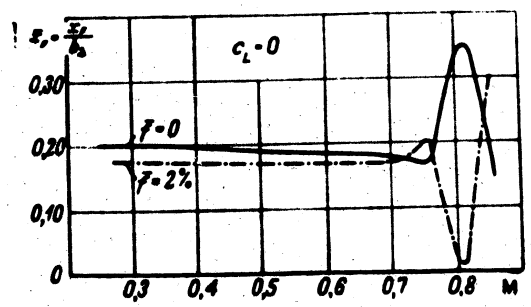
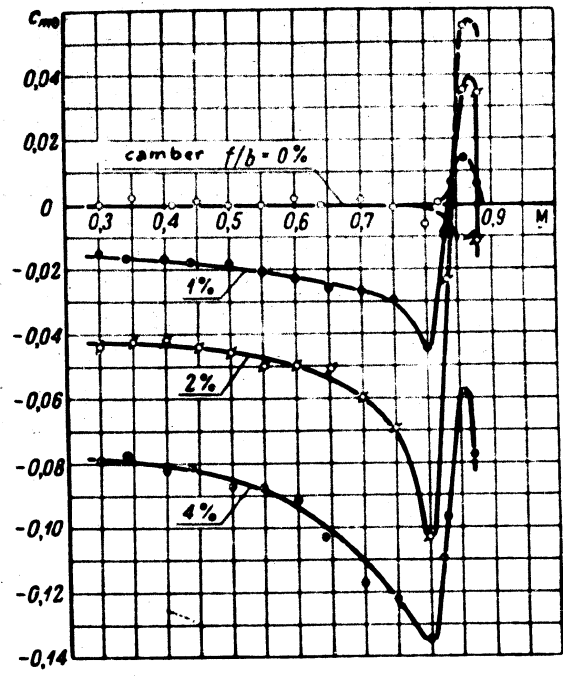


Fig. 2.23 - Relation of m_{20} and x_f to M for Two Profiles

Figure 2.23a shows the curves of c_{mo} and Fig. 2.23b, the curves \bar{x}_F , both as functions of the Mach number. As will be seen, for different profiles, curves of different character are obtained, and no universal relationship seems to exist between these coefficients and the Mach number.

Thus, for aircraft flying at supercritical Mach numbers, the moment coefficient of the wing must be taken on the basis of wind-tunnel tests of a model of the given aircraft.

Wing Moment at Supersonic Speeds

Let us discuss the determination of the wing moment coefficient in flight at supersonic speed, i.e., at $M > 1$. In this case, it will be considered that the local velocities at all points of the wing profile are greater than the speed of sound. It is well known that the pressure at any point of the profile, at an assigned $M > 1$, is determined approximately from the magnitude of the velocity head of an undisturbed flow and from the magnitude of the angle between the tangent to the contour of the profile at the given point, as well as from the direction of the undisturbed flow. In the so-called "linearized" wing theory in supersonic flow, it is proved that in first approximation the dimensionless coefficient of pressure

$\bar{p} = \frac{p - p_\infty}{q_\infty}$ is equal to

$$\bar{p} = -2 \lg A \theta = -\frac{2}{\sqrt{M^2 - 1}} \theta, \quad (2.40)$$

where θ is the angle between the tangent to the profile contour and the direction of the undisturbed flow; the sign of this angle is determined by the rule of signs for the angle of attack (Fig. 2.24).

Let us confine ourselves to a consideration of thin wing profiles, which are of interest for supersonic flying speeds. For such profiles we may put $\cos \theta \approx 1$ and $\sin \theta \approx \theta$. The expressions for the aerodynamic coefficient of such a profile may be presented in the following form:

$$\left. \begin{aligned} c_x &= \int (\bar{p}_u - \bar{p}_l) dx \\ c_o &= \int (\bar{p}_u \theta_u - \bar{p}_l \theta_l) dx \\ m_x &= \int (\bar{p}_u - \bar{p}_l) x dx \end{aligned} \right\} (2.41)$$

In these formulas, \bar{p}_H and \bar{p}_B are the dimensionless coefficients of pressure for corresponding points on the lower and upper profile surfaces, while θ_H and θ_B are the corresponding angles between the tangents and the direction of the undisturbed flow.

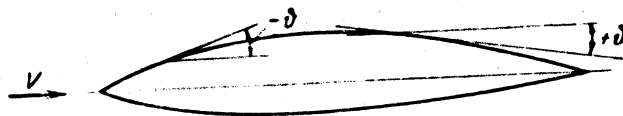


Fig.2.24 - Determination of the Angle θ at Supersonic Flow Around the Profile

The integrals (2.41) can be calculated if the geometric characteristics of the profile are known. Such calculations have been made by A.A.Levadev (Bibl.4) who obtained the following expressions

$$\left. \begin{aligned} c_x &= \frac{4}{\sqrt{M^2-1}} (\alpha - \alpha_0) \\ \alpha_0 &= b_0 \bar{c} F_1(M) \\ c_o &= \frac{20}{\sqrt{M^2-1}} \left(\frac{\bar{c}^3}{2} + 2\bar{c}^2 \right) + \frac{4}{\sqrt{M^2-1}} \left(\alpha - \frac{3}{2} \alpha_0 \right) + c_{o0} \\ \bar{x}_r &= \frac{1}{2} (1 - b_0 \bar{c} F_1(M)) \\ c_{m0} &= (\bar{x}_r b_0 2\bar{c}^2 + b_0 \bar{c}^3) F_1(M) - \frac{20}{\sqrt{M^2-1}} \bar{c} \end{aligned} \right\} (2.42)$$

where α is the angle of attack of the profile at $C_L = 0$;

\bar{c} is the relative thickness of the profile;

$\bar{\Gamma}$ is the camber of the profile:

$$F_1(M) = \frac{(M^2 - 2\gamma + 0.7M^2)}{4(M^2 - 1)^{1.5}};$$

$$F_2(M) = \frac{(M^2 - 2\gamma + 0.7M^2)}{2(M^2 - 1)^2};$$

C_D is the coefficient of drag due to friction;

k_1, k_2, k_3 are certain numerical coefficients depending on the shape of the profile.

The values of these coefficients for a few profiles are presented in the following Table.

Profiles	k_1	k_2	k_3
Rhomboid	4	1	4
Formed by two sinusoids	$\frac{\pi^2}{2}$	$\frac{4}{\pi}$	$\frac{\pi^2}{2}$
Formed by two arcs of a circle	$\frac{16}{3}$	$\frac{4}{3}$	$\frac{16}{3}$

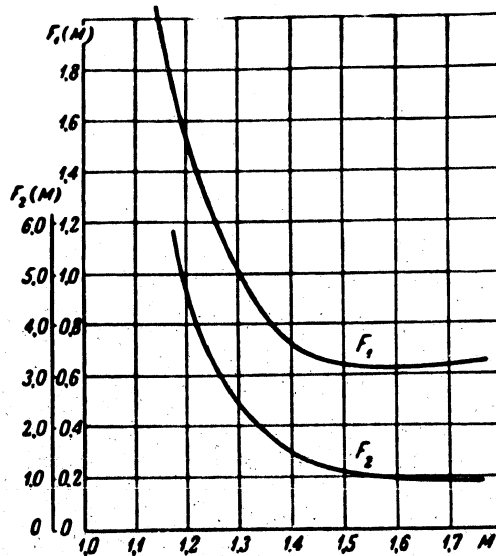


Fig. 2.25 - Graph of Functions $F_1(M)$ and $F_2(M)$

STAT

Figure 2.25 gives the functions $F_1(M)$ and $F_2(M)$.

For a symmetric profile, the expression (2.42) is simplified and takes the following form:

$$\left. \begin{aligned} c_l &= \frac{4}{\sqrt{M^2-1}} \alpha, \\ c_D &= \frac{k_1 \bar{c}^2}{\sqrt{M^2-1}} + \frac{4}{\sqrt{M^2-1}} \alpha^2 + c_{l\text{ TP}} = \frac{k_1 \bar{c}^2}{\sqrt{M^2-1}} + \\ &+ \frac{\sqrt{M^2-1}}{4} c_D^2 + c_{l\text{ TP}}, \\ \bar{x}_F &= 0,5 [1 - k_1 \bar{c} F_1(M)] \\ c_{m0} &= 0. \end{aligned} \right\} \quad (2.43)$$

The coefficient of drag due to friction C_{DTP} plays a minor role in stability calculations and may, in first approximation, be taken as equal to the coefficient for subsonic Mach numbers.

These expressions were derived under the assumption that the viscosity of the air is zero. Here, in the leading part of the profile we obtain $\bar{p} < 0$, but in the trailing part $\bar{p} > 0$, which is responsible for the existence of a wave drag even at $C_L = 0$. As indicated in eq.(2.40), the quantity \bar{p} is directly proportional to the angle θ ; for this reason, the variation in the angles θ substantially affects the aerodynamic characteristics of the profile.

As a result of the viscosity of the air, a boundary layer is formed near the wing surface, whose thickness increases in the direction of the trailing edge of the profile. In this case, the internal flow circulates around a profile having the characteristics of a slightly deformed actual profile, in view of the fact that the thickness of the actual profile is increased by the so-called thickness of displacement* of the boundary layer (Fig.2.26). As a result of the viscosity of the air,

*The concept of "thickness of displacement" is considered and applied in the course on theoretical aerodynamics.

the values θ of the thickened profile in the trailing part of the profile are less than the values of θ of the actual profile. The values of θ obtained in the trailing part of the profile are also smaller.

Equation (2.41) indicates that, as a result of the influence of viscosity, the value of C_l is somewhat reduced at a given angle of attack while C_D and m_2 decrease even more.

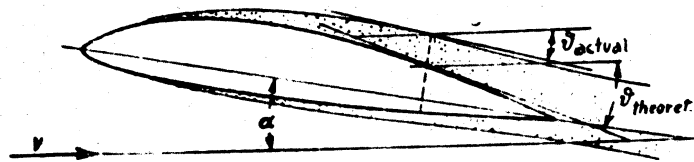


Fig.2.26 - Influence of the Viscosity of Air on the Angles θ

The theoretical solution of the problem of the flow of a compressible viscous gas around the wing is very complex. For this reason, the calculations can be based on eq.(2.43), obtained without allowing for viscosity, and take the above remarks on the character of the influence of viscosity into consideration. As an illustration, Fig.2.27 gives the experimental data and computational curves constructed by eq.(2.43). As will be seen, the discrepancy between the experimental data and the calculated values may amount to 2 - 3% for the moment characteristics, which are of greatest interest to us.

Let us write the expression for the moment coefficient of a symmetric profile with respect to the center of gravity located on the profile chord at a distance of \bar{x}_r from its leading edge. As before, we have

$$m_2 = (\bar{x}_r - \bar{x}_f) C_l.$$

Let us find the position of the aerodynamic center at $M > 1$. For a symmetric

arc profile with a relative thickness, for example of $\bar{c} = 0.08$ at $M = 2$, we have

$$\bar{x}_F = 0.5 (1 - \sqrt{1 - 0.08 \times 0.732}) \approx 0.46$$

As stated previously, at subsonic Mach numbers, the aerodynamic center ordinarily lies within the limits of $0.2 < \bar{x}_F < 0.24$. Consequently, at supersonic flying speeds, the aerodynamic center shifts considerably in the direction of the trailing edge of the wing profile. This produces a noticeable increase in the contribution of the wing to the static stability of the aircraft. If, for example, in

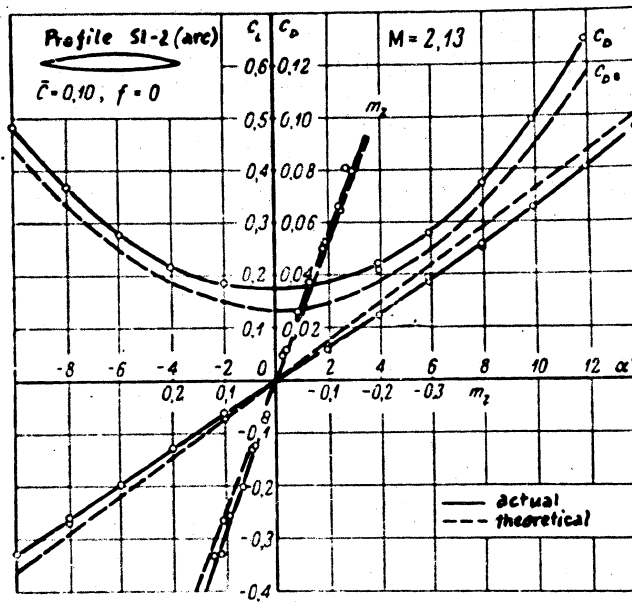


Fig. 2.27 - Experimental and Calculated Data for Profile

an airplane with the center of gravity located at 22% of the chord, $\bar{x}_F = 0.23$ at subsonic flying speeds, then on passage from small Mach numbers to $M = 2$ for the example taken, the absolute value of the derivative $\frac{\partial m_z}{\partial C_L}$ will increase from the value $\frac{\partial m_z}{\partial C_L} = -0.01$ to $\frac{\partial m_z}{\partial C_L} = -0.24$. This fact, in conjunction with certain other

peculiarities of the aerodynamic characteristics at $M > 1$, makes it difficult to design an aircraft having a satisfactory degree of stability at both subsonic and supersonic Mach numbers.

It is clear from eq.(2.42) that at $M = 1$, the expressions for C_L , C_D and \bar{x}_F become infinite. At Mach numbers close to $M = 1$, however, these expressions cease to be correct, since the velocities obtained on part of the profile contour are subsonic, and the theory is thus inapplicable.

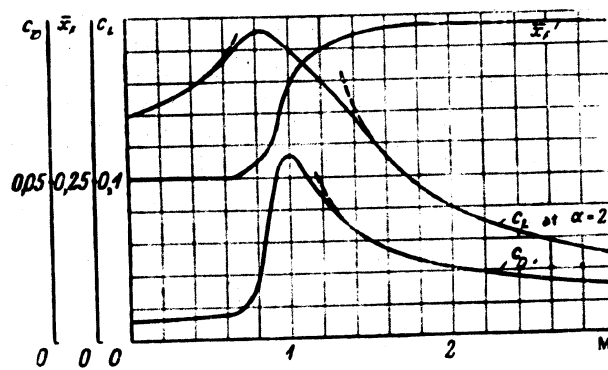


Fig.2.28 - Approximate Variation of Aerodynamic Characteristics of a Profile as a Function of the Mach Number

For a region of mixed subsonic and supersonic flows, as already stated, no theoretical solutions exist for the problem of flow around the body, so that the very scanty experimental data must be used. Figure 2.28 shows the approximate slope of the curves for the aerodynamic coefficients of the wing, plotted against the Mach number. The character of the slope of these curves in the region of mixed flow (ranging approximately from $M \approx 0.8$ to $M \approx 1.3$) depends on a number of individual features of the profile and is different for different profiles.

STAT

Peculiarities of the Calculations of the Moment of Sweptback

Wings at Large Mach Numbers

Sweptback wings, especially in recent times, have begun to be used more and more, in connection with the fact that, over a certain range of Mach numbers, sweepback attenuates the influence of the compressibility of air on the aerodynamic characteristics of a wing.

Let us imagine a wing of infinite span and constant chord, around which a stream of air flows perpendicular to the wing span. As a result of the fact that the wing profile has a certain thickness, varying along the chord, the local velocities in the neighborhood of the chord of the wing will differ from the velocity of the oncoming stream, and the pressure acting on the wing surface will differ from the atmospheric pressure.

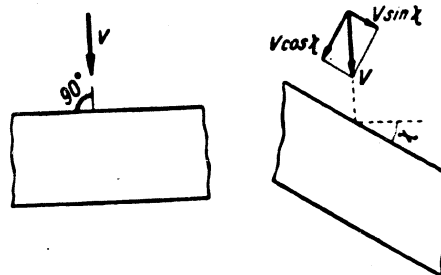


Fig.2.29 - Flow Around a Wing, Slip-free and with Slip

Let us now consider the same wing, but with an air stream directed along the wing span, flowing around it. In this case, as a result of the fact that the wing span is assumed to be infinitely great, and the thickness of the wing is constant in each section parallel to the span, the local velocities will be equal to the velocities of the oncoming stream, while the pressures will be equal to the atmospheric pressures. The existence of a velocity of flow directed along the span of an

infinitely long wing of constant chord, will not lead to the appearance of aerodynamic forces*.

Let us further imagine this same wing in a circulating flow at a certain slip angle χ (Fig.2.29). By resolving the velocity vector of the flow V into $V \cos \chi$ and $V \sin \chi$, we come to the conclusion that the second component, in the analysis of the pressure forces acting on the wing may be rejected, and that the pressures will be determined not by the total value of the velocity V , but by its component $V \cos \chi$, which may be termed the "effective" velocity V_e .

$$V_e = V \cos \chi.$$

Accordingly, the effective Mach number in this case will be

$$M_e = M \cos \chi.$$

For this reason, in a wing exposed to a circulating flow with slip phenomena connected with a shock wave occur at a larger Mach number than in a wing about which the stream flows perpendicular to the leading edge. This allows the aircraft designer to advance into the region of rather high Mach numbers, almost without encountering the unpleasant influence of the compressibility of the air. The difference in the critical Mach numbers at high slip angles may reach a considerable value. For example, if a straight wing of infinite span has $M_{kp} = 0.7$, then the critical Mach number at a slip angle $\chi = 45^\circ$, increases to

$$M_{kp} = \frac{0.7}{\cos 45^\circ} = 1.0.$$

Sweptback wings may be considered, with a certain approximation, as wings without sweepback but located in a circulating flow at angles of slip equal to the sweepback angle χ . In this case, however, the slip effect will be decreased at the

* Except for the forces of friction, which do not concern us in this case.

center and at the tips of a sweptback wing, because of the three-dimensional nature of the flow in these places, which does not permit the above-discussed resolution of velocity. This is due to the fact that the sweptback wing does not accurately reproduce the effect of a slipping wing of infinite span. Nevertheless, giving a wing sweepback is one of the most effective means of penetrating into the region of high Mach numbers.

Since, in a slipping wing of infinite span, the distribution of pressures along a section perpendicular to the leading edge is determined by the value of the velocity $V_e = V \cos \chi$, while, in calculating these coefficients, we relate all the forces and moments to the square of the total velocity of the oncoming flow, the coefficients of the forces due to the pressures acting on the wing must vary in the ratio

$$\left(\frac{V_e}{V}\right)^2 = \cos^2 \chi. \quad (2.44)$$

In the calculation it is necessary to take into consideration the fact that, together with the actual Mach number, the effective Mach number

$$M_e = M \cos \chi. \quad (2.45)$$

must also enter the formula. In addition, it must be borne in mind that the angle of attack of a section perpendicular to the leading edge will not be equal to the angle of attack of the wing measured in the vertical plane containing the velocity vector of the oncoming flow (cf. Fig.2.29) as well as the fact that the drag likewise does not lie in the plane.

If all this is borne in mind, it will be found that, for the subsonic region of Mach numbers, the aerodynamic center of a sweptback wing, in first approximation, does not depend on the sweepback angles, that the moment coefficient at $C_L = 9$ increases somewhat less with increasing Mach numbers than in a straight wing, and that the derivative of the coefficient of lift with respect to the angle of attack like-

wise increases somewhat less with increasing Mach numbers than in a straight wing. For this region of Mach numbers, in first approximation, the expressions are true.

$$\left. \begin{aligned} c_{m0} &= \frac{c_{m0\ MRA}}{\sqrt{1 - M^2 \cos^2 \chi}} \\ \bar{x}_p &\approx \bar{x}_{p\ MRA} \\ \frac{dc_L}{d\alpha} &\approx \left(\frac{dc_L}{d\alpha} \right)_{MRA} \frac{1}{\sqrt{1 - M^2 \cos^2 \chi}} \end{aligned} \right\} (2.26)$$

These formulas are true so long as a shock wave does not occur on the sweptback wing, i.e., only in that part of the wing which may be considered as a slipping wing, i.e., if they are inapplicable to the wing center and to its tips.

For the supersonic region of Mach numbers, we will have the following expressions*:

$$\left. \begin{aligned} c_n &= \frac{c}{\cos \chi} \\ c_e &= \frac{\bar{c}}{\cos \chi} \\ c_i &= \frac{4 \cos \chi}{\sqrt{M^2 \cos^2 \chi - 1}} \alpha \\ c_L &= \frac{4 \alpha^2 \cos \chi}{\sqrt{M^2 \cos^2 \chi - 1}} + \frac{\sqrt{M^2 \cos^2 \chi - 1}}{4} \cos \chi c_n^2 + c_{p, \eta} \\ \bar{x}_p &= 0.5 \left[1 - k_2 \frac{\bar{c}}{\cos \chi} \frac{(M^2 \cos^2 \chi - 2)^2 + 0.7 M^2 \cos^2 \chi}{4 (M^2 \cos^2 \chi - 1)^{1.5}} \right] \end{aligned} \right\} (2.27)$$

The value and position of the mean aerodynamic chord of a sweptback wing, will be determined, as before, from eqs.(2.26) to (2.28).

*For simplicity of discussion we confine ourselves to the case of a symmetric profile, although the derivation of analogous expressions for an asymmetric profile involves no fundamental difficulties.



Figure 2.30 shows the influence of sweepback on the aerodynamic coefficients of a wing of infinite span, formed by two arcs of a circle with a relative thickness, taken along the relative flow, $\bar{c} = 0.08$ for $M = 2$.

As will be clear, when the angle of sweepback increases, the lift properties of the wing are improved, the aerodynamic center is shifted somewhat forward, while the rate of such shift increases with increasing sweepback. The coefficient of wave drag, for small values of γ , first declines slightly and then increases. It must be borne in mind that, at large angles of sweepback, when the product $M \cos \xi$ approaches unity, eq.2.47 become unsuitable, since local subsonic velocity zones appear on the profile.

It must be noted that the change in the longitudinal moment, on transition from subsonic to supersonic flying speeds is less in sweptback wings than in straight wings. This fact may be of advantage in designing aircraft for supersonic flying speeds.

The Fuselage Moment

The moment coefficient of the fuselage with respect to the center of gravity of the aircraft, by analogy with the moment coefficient of the wing, may be represented by the following expression (Fig.2.31):

$$m_{z_f} = (c_{m_f} + \bar{x}_f c_{y_f}) \frac{S_f l_f}{S b_A} \quad (2.48)$$

where c_{m_f} is the moment coefficient of the fuselage relative to an axis passing through its leading edge;

c_{L_f} is the coefficient of lift of the fuselage;

$\bar{x}_f = \frac{x_f}{l_f}$ is the dimensionless coordinate of the center of gravity of the aircraft relative to the nose of the fuselage;

S_f is the area of the rectangle described about the

horizontal projection of the fuselage* ; the coefficients c_{mf} and c_{y_f} are referred to this area ;
 l is the length of the fuselage, with which the coefficient c_{mf} is related.

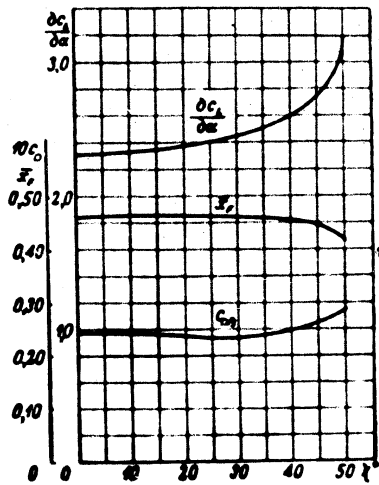


Fig. 2.30 - Influence of Sweepback on the Aerodynamic Characteristics of a Wing at $M = 2$

Experiment has shown that the coefficients C_{L_f} and c_{mf} are strongly dependent on the shape of the fuselage. As an example, Fig. 3.32 gives the values of C_{L_f} and c_{mf} obtained in experiments with two models of a fuselage of different form, but closely resembling each other. As is clear, even a relatively small difference in the shape of the fuselage leads to a marked difference in the aerodynamic characteristics. For this reason, it is preferable, in determining the moment coefficient of the fuselage, to use experimental data, the more so since the interference of fuselage and wing still more complicates the determination of

the moment characteristics.

*This area is selected conditionally. It is possible to select instead, for example, the area of the center section of the fuselage. Then, the coefficients C_{L_f} and c_{mf} would change in magnitude and the center section of the fuselage would enter into the equation.

On analyzing the results of the tests shown in Fig.2.32, it will be seen that fuselage No.1, where the flow around the transverse section is better at small

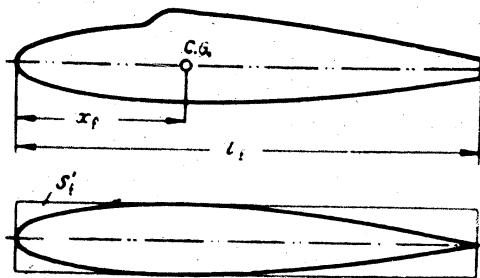


Fig.2.31 - For Determining the Moment of the Fuselage

angles of attack than in the fuselage No.2, has a smaller coefficient of lift than fuselage No.2, at one and the same angle of attack. This is natural enough, since the poorer the flow around the transverse section of the fuselage, the greater will be the resistance to the oncoming stream in the presence of an angle of attack, and, consequently, the greater will be its lift. It is also clear that, at the same coefficient of lift, the moment coefficient of the fuselage No.1 is greater than the moment coefficient of the fuselage No.2.

The calculation of the moment coefficients of the fuselage is somewhat facilitated by the fact that the fuselages of modern aircraft differ only slightly in form from that of bodies of revolution. For this reason, in first approximation, these peculiarities of the geometric form of the fuselage may be reflected in the form of one characteristic parameter for which the aspect ratio $\lambda_f = \frac{f}{b_f}$ may be taken, where b_f is the maximum width of the fuselage in planform.

The estimation of the moment due to the fuselage may be reduced to a determination of the additional moment coefficient Δm_{zof} (additional to that produced by the wing at $C_L = 0$) and to a determination of the shift in the aerodynamic center $\Delta \bar{x}_{Ff}$ due to the influence of the fuselage. Such an approach assumes the fuselage moment

to be small in comparison with the wing moment so that the error in estimating the fuselage moment thus has no substantial influence on the moment of the whole aircraft. This assumption is closer to the actual situation, the smaller the area of

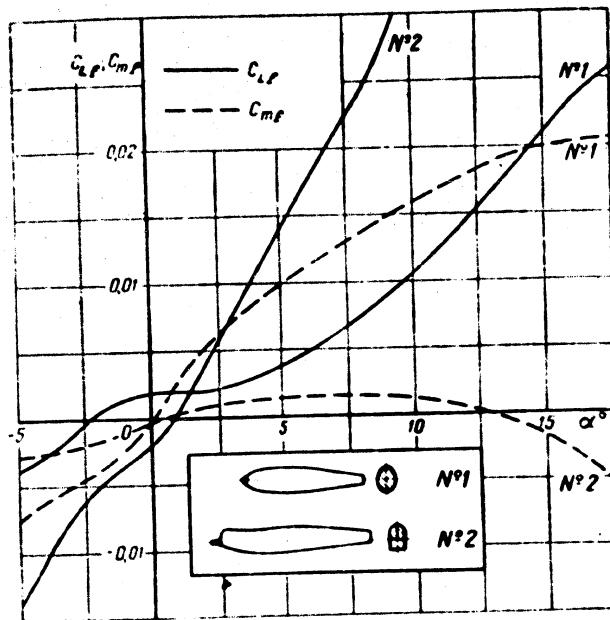


Fig.2.32 - Results of Tests of Two Fuselage Models

the fuselage projection is by comparison with the wing area. As the area of the wings decreases, this assumption becomes less and less correct.

The shift of the aerodynamic center due to the influence of the fuselage may be calculated, if we start from the following considerations.

The moment coefficient acting on the wing and fuselage is obviously equal to

$$m_z = m_{z, w} + m_{z, f} = m_{z, w} - (\bar{x}_f - \bar{x}_1) c_l + (c_{m, f} + \bar{x}_f c_{l, f}) \frac{S_f l_f}{S_b \lambda}$$

If \bar{x}_{f1} denotes the relative coordinate of the aerodynamic center and fuselage, then

the coefficient m_z may be presented in the form

$$m_z = m_{z0} - (\bar{x}_{r1} - \bar{x}_r) c_L.$$

By equating these two expressions and taking the derivative with respect to C_{L_f} , we will have

$$-(\bar{x}_{r1} - \bar{x}_r) = -(\bar{x}_f - \bar{x}_r) + \left(\frac{\partial c_{mf}}{\partial c_{L_f}} \frac{dc_{L_f}}{d\alpha} + \bar{x}_f \frac{dc_{L_f}}{d\alpha} \right) \frac{S_f l_f}{S b_A}.$$

On determining, from this expression, the shift of the aerodynamic center due to the influence of the fuselage, we have

$$\Delta \bar{x}_{r0} = \bar{x}_{r1} - \bar{x}_f = - \left(\frac{\partial c_{mf}}{\partial c_{L_f}} + \bar{x}_f \right) \frac{dc_{L_f}}{d\alpha} \frac{S_f l_f}{S b_A}. \quad (2.49)$$

The ratio $\frac{\partial c_{mf}}{\partial c_{L_f}}$ is nothing other than the dimensionless distance of the aerodynamic center of the fuselage from its leading edge, taking it with reversed sign, i.e., $-\bar{x}_{pf}$.

The lift coefficient of the fuselage C_{L_f} may be considered linearly dependent on the angle of attack α , so that

$$\frac{dc_{L_f}}{d\alpha} = k \frac{d\alpha}{d\alpha} = \frac{k}{\alpha}.$$

where the coefficient k must be a function of the elongation of the fuselage. In this way we have the right to propose a relation of the form

$$\Delta \bar{x}_{r1} = -k_f \frac{1}{\alpha} \frac{S_f l_f}{S b_A}, \quad (2.50)$$

for the shift $\Delta \bar{x}_{r1}$ of the aerodynamic center due to the influence of the fuselage; where k_f is a certain generalized function of x_f and $\lambda_f = \frac{l_f}{b_f}$. The value of k_f as

a result of processing data of wind-tunnel experiments, are shown in Fig.2.33.

As an example, let us determine the shift of the aerodynamic center due to the

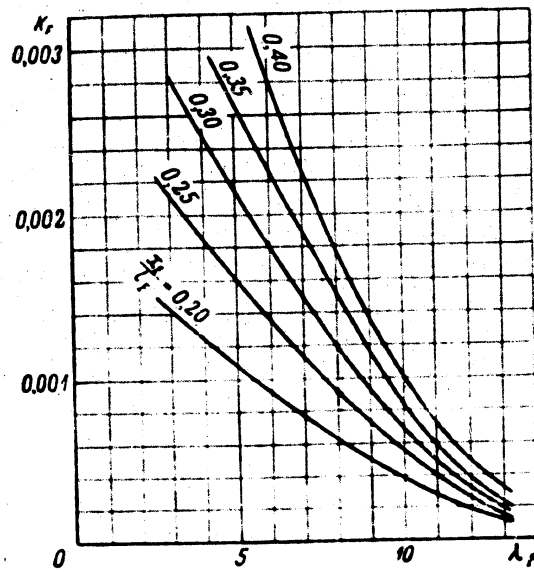


Fig.2.33 - Graph for Determining the Coefficient k_f

fuselage moment, assuming that the wing area $S = 16 \text{ m}^2$, the mean chord $b_A = 1.6 \text{ m}$, the fuselage length $l_f = 9 \text{ m}$, and the width of the fuselage $b_f = 0.9 \text{ m}$. The center of gravity of the aircraft is located at 30% of the fuselage length from its nose.

The derivative is

$$\frac{dc_f}{d\lambda_f} = a = 0,07.$$

$$S_f = 0,9 \cdot 9 = 8,1 \text{ m}^2;$$

$$\lambda_f = \frac{9}{0,9} = 10;$$

$$\bar{x}_f = 0,3.$$

We determine

From Fig.2.33 we find

$$k_f = 0,00066.$$

Equation (2.50) furnishes

$$\Delta \bar{x}_{fz} = 0,00066 \frac{8,19 - 1}{1 - 1,60,07} \approx -0,027$$

In our example, the aerodynamic center was shifted forward by 2.7% MAC; in other cases the shift of the aerodynamic center may be as much as 5% of the MAC and more.

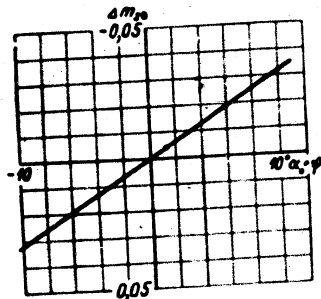


Fig.2.34 - Graph to Determine Δm_{zof} Due to the Influence of the Fuselage

The variation in the coefficient m_z , due to the influence of the fuselage, may be determined from experimental data in first approximation by Fig.2.34. It is found that this variation may be considered to be approximately a function only of $(\alpha_0 + \varphi)$ where α_0 is the angle of attack at $C_L = 0$, and φ is the angle of setting with respect to the axis of the fuselage.

The above calculation of the fuselage moment should be regarded merely as a rough calculation in first approximation,

and, as already stated, the results of model wind-tunnel tests should be used as far as possible for more accurate calculations. This is particularly necessary for high-speed aircraft, since the influence of the compressibility of the air on the fuselage moment has never been thoroughly investigated and since it is at present difficult to propose even approximate formulas for its estimation.

Moment of the Engine Nacelles

In cases where the engines are installed on the aircraft wing, the calculations must take into consideration the moment produced by the engine nacelles. These nacelles usually occupy a certain part of the wing area, and this makes it difficult to segregate the moment due to the engine nacelles. It is simpler to estimate the moment due to the engine nacelles by determining the corresponding shift of the aerodynamic center in the direction of its nose.

For determining the shift in the aerodynamic center due to the influence of the engine nacelles, the following empirical formula obtained by working up experimental data, may be used:

$$\Delta \bar{x}_{F_{em}} = -i \left(\frac{\Delta x}{b} \right) \frac{b}{b_A} \frac{S_1}{S} k_{en} \quad (2.51)$$

where i is the number of engine nacelles on the wing;

$\frac{\Delta x}{b}$ is the local shift of the aerodynamic center on the parts of the wing where the engine nacelles are placed;

b is the local wing chord measured along the axis of the engine nacelles (Fig.2.35);

$S_1 = bc_{en}$ is the area of the rectangle described about that part of the wing area occupied by the engine nacelles;

k_{en} is a certain empirical coefficient depending on the form of the nacelles.

The values of $\Delta x/b$, as a function of $\frac{c_{en}}{b}$ (cf. Fig.2.35) obtained by working up experimental data, are given in Fig.2.36. The coefficient k_{en} , as a function of the aspect ratio of the engine nacelles is determined from Fig.2.37, which is likewise constructed from experimental data.

The work-up of the experimental results shows that the influence of the engine nacelles on the moment coefficient is small at $C_L = 0$ and may be neglected, reducing

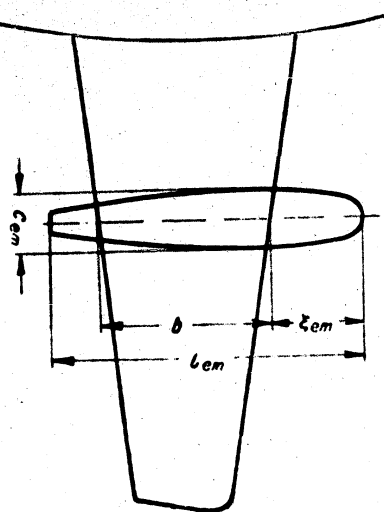


Fig.2.35 - For Determining the Moment of the Engine Nacelles

the influence of the engine nacelles only to the shift of the aerodynamic center.

If, for example, on a two-engine aircraft, the engine nacelles are characterized by the dimensions $\frac{z_{en}}{b} = 0.6$; $\lambda_{en} = 5$; $b/b_A = 1.2$; $\frac{S_1}{S} = 0.8$ we obtained

$$\frac{\Delta x}{b} = 0.245 \text{ and } k_{en} = 0.87.$$

From eq.(2.51) we have

$$F_{en} = -2 \times 0.245 \times 1.2 \times 0.08 \times 0.87 = -0.041$$

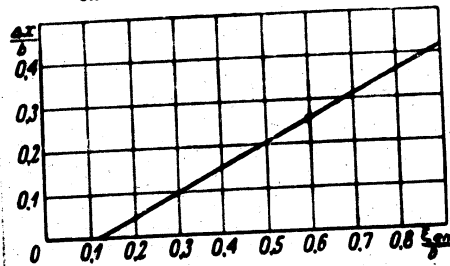


Fig.2.36 - Shift of the Aerodynamic Center Due to the

Influence of the Engine Nacelles

Thus, in the example selected by us, the aerodynamic center is shifted forward by 4.1% MAC, due to the influence of the engine nacelles; in some cases, the shift

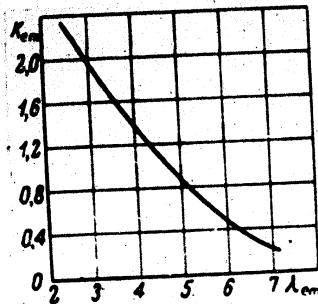


Fig. 2.37 - Values of the Coefficient k_{en} Form Experimental Data

may be even greater. The above data do not allow for the influence of the compressibility of the air. However, even the few available experimental data, show that, at Mach numbers exceeding the critical value, the compressibility of air may have a substantial influence on the moment due to the engine nacelles.

For this reason, in calculating fast aircraft, the results of model wind-tunnel tests must be used.

Moment of Thrust of Propeller and Jet Engine

In the general case, the engine axis does not pass through the center of gravity of the aircraft. For this reason, a moment due to thrust acts on the aircraft. It is usually assumed that the direction of the thrust coincides with the direction of the engine axis. In that case, the moment of thrust is equal to

$$M_p = -Fy_p$$

where y_p is the arm of the force of thrust with respect to the center of gravity of the aircraft (Fig. 2.38).

The moment coefficient of thrust is equal to

$$m_p = -\frac{Fy_p}{Sb\Delta q} \quad (2.52)$$

The thrust of a propeller, as generally known, may be presented in the form

$$P = iBFq, \tag{2.53}$$

where i is the number of engines;

B is the load factor on the propeller area;

$F = \frac{\pi D^2}{4}$ is the area of the propeller.

On substituting eq.(2.53) in eq.(2.53) we have

$$m_{zp} = -i \frac{F y_p}{S b_A} B. \tag{2.54}$$

In steady horizontal flight, the propeller thrust is equal to the drag of the aircraft

$$P = C_D S_q$$

so that, in this case,

$$m_{zp} = - \frac{y_p}{b_A} C_D \tag{2.54'}$$

In the so-called oblique slipstream of the propeller, i.e., in flight at an angle of attack relative to the propeller other than zero, a transverse force,

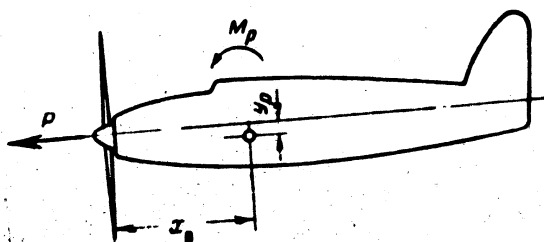


Fig.2.38 - For Determining the Moment of Thrust

additional to the thrust, acts on the propeller blade in the plane of rotation of the propeller (Fig.2.39). This force yields a certain moment tending to increase the angle of attack. The moment coefficient of this lateral force may be determined

by the approximate empirical formula

$$m'_{zp} = 0,05 \frac{x_B}{b_A} \frac{1D^2}{S} c_L, \quad (2.55)$$

where x_B is the distance between the center of gravity of the aircraft and the plane of rotation of the propeller (cf. Fig. 2.38).

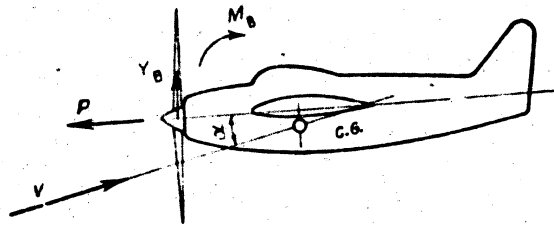


Fig. 2.39 - Transverse Force Acting on the Propeller

The coefficients ϵ_{zp} and m'_{zp} are relatively small. Thus, for a fighter with $S = 14 \text{ m}^2$, $D = 3.1 \text{ m}$, $x_B / b_A = 1$ and $y_B / b_A = 0.1$, in the state of gaining altitude ($C_L \approx 0.3$; $B = 0.5$), we have

$$m_{zp} \approx -0.027; \quad m'_{zp} \approx 0.010$$

In view of the fact that m'_{zp} is less than m_{zp} , the moment of the transverse force acting on the propeller is sometimes neglected in calculation.

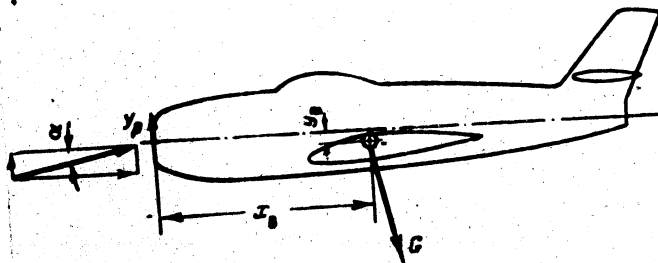


Fig. 2.40 - Transverse Force in the Case of a Turbojet Engine

STAT

In an aircraft with a turbojet engine, in flight at a certain angle of attack with respect to the axis of the engine, a transverse force yielding a moment tending to increase the angle of attack also appears. This is explained by the fact that, in this case, at the engine intake the component of the momentum per second of the mass of air entering the engine, perpendicular to the engine axis, is lost (Fig. 2.40). The resultant transverse force is equal to the momentum lost

$$Y_p = mV \sin \alpha \approx mVa,$$

where m is the mass of air entering the engine per second and $\sin \alpha$, in view of its smallness, is replaced by α .

Since the thrust

$$P \approx m(W - V),$$

where W is the velocity of the gas jet at the engine exhaust, it follows that

$$Y_p = P \frac{\alpha}{\frac{W}{V} - 1}$$

and that the moment coefficient of this force with respect to the center of gravity of the aircraft is

$$m'_{sp} = \frac{P}{3q} \frac{x_B}{b_A} \frac{\alpha}{\frac{W}{V} - 1}, \quad (2.56)$$

where q is the velocity head.

This coefficient is likewise small and can, in most cases, be neglected. For example, at $P = 2500$ kg; $S = 20$ m²; $q = 5000$ kg-m²; $W/V = 2$; $\alpha = 3^\circ$; $x_B / b_A = 1.0$;

$y_B / b_A = 0.1$, we have $m'_{sp} = -0.0025$; $m'_{sp} = 0.0012$.

As the flying speed decreases, the load factor on the propeller disk increases.

In this case, the moment coefficient of thrust also increases. Figure 2.41 shows roughly the variation of the coefficient of propeller thrust with flying speed.

The thrust of a liquid-jet (rocket) engine, in first approximation, does not

depend on the speed or altitude of flight. For this reason, with declining flying speed, the moment coefficient of thrust in aircraft with rocket engines increases

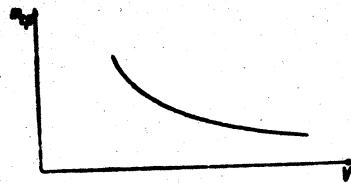


Fig.2.41 - Coefficient of Moment of Propeller Thrust

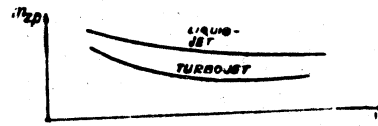


Fig.2.42 - Moment Coefficient of Thrust for Turbojet and Liquid-Jet Engines

more slowly than in aircraft with piston or turboprop engines (Fig.2.41). The thrust of a turbojet engine, decreases slightly at first with increasing flying speed and then also increases. The curve of the moment coefficient of thrust of a turbojet engine, as a function of speed, has a corresponding slope (Fig.2.42).

Moment Coefficient of an Aircraft without Horizontal Tail Surfaces

Summing the moments of all forces acting on the aircraft except those acting on the horizontal tail surface will give the resultant moment of the aircraft except for the moment of the horizontal tail surface, or, as it is usually expressed, the moment of an aircraft without horizontal tail surfaces, will be

$$M_{z, a. t.} = M_{z, sp} + M_{z, f} + M_{z, en} + M_{z, p} + M_{z, r}$$

On substituting in this expression the values of m_z kp, m_z f, and m_z en, eqs.(2.8) or (2.32), (2.50), (2.51), (2.52), (2.54) and (2.55) will yield, at undeflected flaps and operating engine,



$$m_{g.b.h.t} = m_{g0} - (\bar{x}_p - \bar{x}_1) c_L - \bar{y}_1 (c_D - c_{L\alpha}) + \Delta m_{g0p} + \quad (2.57)$$

$$+ k_p \frac{\partial \alpha}{\partial c_L} \frac{S_1 l_f}{S b_A} c_L + i \left(\frac{\Delta x}{b} \right) \frac{b}{b_A} \frac{S_1}{S} k_{cm} + m_{g0} + m_{g0}^*$$

By grouping similar terms, we rewrite this expression in the form

$$m_{g.b.h.t} = m_{g0} + \Delta m_{g0cm} - \left[\left(\bar{x}_p - k_p \frac{\partial \alpha}{\partial c_L} \frac{S_1 l_f}{S b_A} - i \frac{\Delta x}{b} \frac{b}{b_A} \frac{S_1}{S} k_{cm} \right) - \bar{x}_1 \right] c_L + \bar{y}_1 c_L \alpha - \bar{y}_1 c_D + m_{g0} + m_{g0}^*$$

When landing with deflected flaps, and in the absence of thrust, we will have

$$m_{g.b.h.t} = m_{g0} + \Delta m_{g0p} + \Delta m_{g0}^{fl} - \left[\left(\bar{x}_p - k_p \frac{\partial \alpha}{\partial c_L} \frac{S_1 l_f}{S b_A} - i \frac{\Delta x}{b} \frac{b}{b_A} \frac{S_1}{S} k_{cm} \right) - \bar{x}_1 \right] c_L - (\bar{x}_{pfl} - \bar{x}_1) \Delta c_L^{fl} + \bar{y}_1 (c_{L\alpha} - c_D). \quad (2.57^*)$$

On subtracting from eq.(2.57) and eq.(2.57*) the terms $\bar{x}_1 c_L - \bar{y}_1 (c_D - c_{L\alpha})$ and then taking the derivatives with respect to C_L , of the expressions so obtained, we obtain expressions for the aerodynamic center of the aircraft without horizontal tail surfaces, with operating engines* and on landing with inoperative engines and with deflected flaps

$$\bar{x}_{FB.h.t} = - \frac{\partial (m_{g.b.h.t} - \bar{x}_1 c_L + \bar{y}_1 (c_D - c_{L\alpha}))}{\partial c_L} = \bar{x}_p - k_p \frac{\partial \alpha}{\partial c_L} \frac{S_1 l_f}{S b_A} - i \frac{\Delta x}{b} \frac{b}{b_A} \frac{S_1}{S} k_{cm} \quad (2.58)$$

* It is assumed here that the moment coefficient of thrust does not depend on the angle of attack nor on the coefficient C_L .

$$\bar{x}_{Fb.A.C.} = \bar{x}_P - h_P \frac{\partial \alpha}{\partial c_L} \frac{S_f l_f}{S b_A} - i \frac{\Delta x}{b} \frac{b}{b_A} \frac{S_1}{S} h_{cov} \quad (2.58')$$

It follows from these expressions that the aerodynamic center of an aircraft without horizontal tail surfaces is closer to the nose of the MAC than the wing aerodynamic center. In individual cases the shift of the aerodynamic center may be 8 - 10% MAC or more.

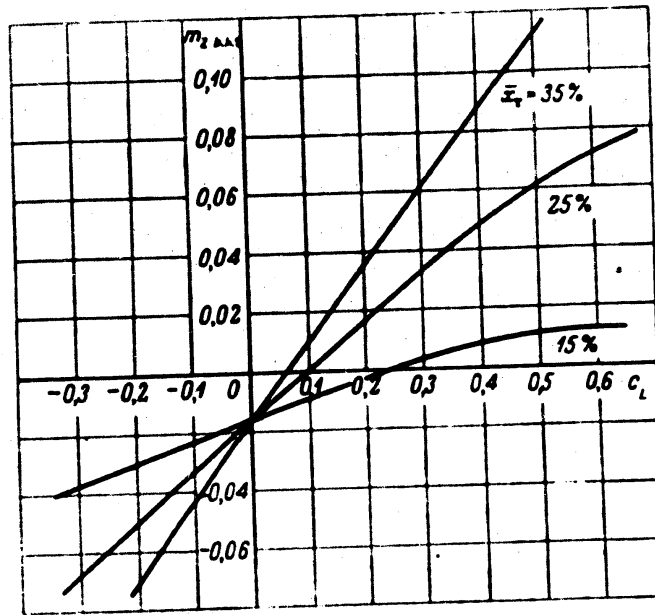
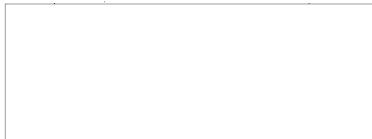


Fig.2.43 - Curves of m_{zht} . for Various Positions of the Center of Gravity of the Aircraft

By making use of eq.(2.58) and eq.(2.58') with $\bar{y}_T = m_{zp} = m'_{zp} \approx 0$, we may rewrite eqs.(2.57) and (2.57') in the form

$$m_{z.b.h.t} = m_{z0.b.h.t} - (x_{Fb.h.t} - \bar{x}_T) c_L, \quad (2.59)$$



where

$$m_{z0 h.t.f} = m_{z0} + \Delta m_{z0f} \quad (2.60)$$

for the case of flight with undeflected flaps, and

$$m_{z0 h.t.f} = m_{z0} + \Delta m_{z0f} + \Delta m_{z0}^{\overline{m}} \quad (2.60^*)$$

for the case of landing with deflected flaps.

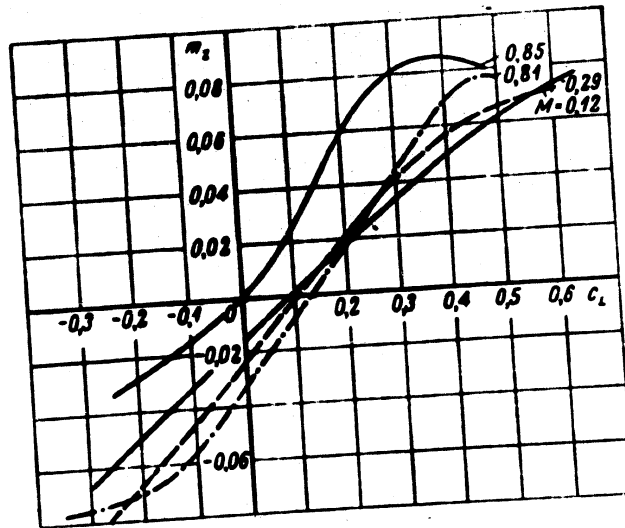


Fig.2.44 - Influence of the Compressibility of Air on the Moment Coefficient of the Aircraft without Horizontal Tail Surfaces

Figure 2.43 shows the slope of the curves of m_z h.t. as a function of C_L in horizontal flight for various positions of the center of gravity of the aircraft relative to the mean aerodynamic chord for a two-engine aircraft. As indicated in this graph, it is possible, by selecting a sufficiently forward centering, to have m_z h.t. = $f(C_L)$ decrease with increasing C_L , i.e., the negative derivative $\frac{\partial m_z \text{ h.t.}}{\partial C_L}$.

will be ensured.

Figure 2.44 shows the approximate curves of $m_{\dot{z}} \text{ h.t.} = f(C_L)$ for various Mach numbers. It is clear that the character of the slope of the curves, as a function of the Mach number, may vary considerably. As will be demonstrated later in this book, these variations may complicate the realization of the proper stability and controllability of aircraft at high flying speeds.

CHAPTER III

MOMENT OF HORIZONTAL TAIL SURFACES IN STEADY FLIGHT

Purpose of the Horizontal Tail Surfaces

It has been shown in Chapter II that, by varying the abscissa of the center of gravity of the aircraft measured along the wing chord, it is possible to vary substantially the value of the moment coefficient of an aircraft without horizontal tail surfaces at a given angle of attack at the wing, and also to vary the character of the curve slope for $m_{z \text{ h.t.}}$ versus α° or versus C_L .

Let us see whether it is not possible to realize the equilibrium of an aircraft at various attitudes without the aid of the horizontal stabilizer and elevator, merely by shifting the center of gravity.

In the simplest case of $\bar{y}_T = y_p = 0$ the moment coefficient of an aircraft without elevator unit, in accordance with eq.(2.59) of Chapter II, is equal to

$$m_{z0 \text{ h.t.}} = m_{z0b \text{ h.t.}} - (\bar{x}_P \text{ h.t.} - \bar{x}_T) C_L$$

In order to ensure the equilibrium of an aircraft at any attitude without a tail surface, it is necessary that $m_{z \text{ h.t.}}$ vanishes at the corresponding values of C_L .

$$m_{z0 \text{ h.t.}} = m_{z0b \text{ h.t.}} - (\bar{x}_P \text{ h.t.} - \bar{x}_T) C_L = 0 \quad (3.1)$$

By determining the value of \bar{x}_T , we then obtain

$$\bar{x}_T = - \frac{m_{z0b \text{ h.t.}}}{C_L} + \bar{x}_P \text{ h.t.} \quad (3.2)$$

The coefficient $m_{z0b \text{ h.t.}}$ is usually negative - unless special measures are taken. For this reason, as obvious from the above expression, control of an aircraft by shifting the center of gravity, requires for all positive C_L :

$$\bar{x}_T > \bar{x}_P \text{ h.t.}$$

Thus the difference $(\bar{x}_P \text{ h.t.} - \bar{x}_T)$ is negative and, consequently,

$$\frac{d\bar{m}_z}{dx_1} = -(\bar{x}_{p.h.t.} - \bar{x}_1) > 0.$$

It will be seen from this that an aircraft controlled by shifting the center of gravity is statically unstable, the degree of instability increasing with the flying speed (with decreasing C_L). Flight on such an aircraft requires tense attention and constant intervention of the pilot.

Such a "balancing" method of control, which was used in some aircraft types in the earliest stages of aviation, is applicable, with considerable allowances, to small machines flying at low speed, but is completely inapplicable to large aircraft with high flying speed. Even at the beginning of aviation, progressive designers did not consider it possible to use the balancing control. In particular, A.F. Mozhayskiy in his world's first aircraft, already mentioned, used both horizontal and vertical tail surfaces.

The Possibility of Realizing a Tailless Aircraft

Equilibrium of a flying machine without horizontal tail surfaces under various flight conditions is possible even without having to shift the center of gravity. For this purpose, as will be clear from eq.(3.1), it is necessary to vary the moment coefficient in flight at $C_L = 0$.

Since, in the case of equilibrium, $m_{zob \text{ h.t.}} = 0$, then, if we determine $m_{z0 \text{ h.t.}}$ from eq.(3.1), we get

$$m_{z0 \text{ h.t.}} = (\bar{x}_{p.h.t.} - \bar{x}_1) C_L. \quad (3.3)$$

As we see, if for any assigned C_L we know how to assure a value of $m_{z0 \text{ h.t.}}$ satisfying the condition (3.3), then we will also know how to realize the equilibrium of the aircraft at any assigned flying speed within the flying range.

It is possible to vary the value of $m_{zob \text{ h.t.}}$ by, for example, varying the camber of the wing profile by the deflection of flaps.

If an aircraft is to have a definite degree of longitudinal static stability, i.e., if the inequality:

$$\frac{\partial m_{z, b.a.c.}}{\partial \alpha} < 0 \quad \text{b.a.c.} \quad \bar{x}_{p, b.a.c.} - \bar{x}_r > 0.$$

is to be valid, then eq.(3.3) indicates that, for all positive values of C_L it is necessary that the inequality

$$m_{z, \text{rob. n.t.}} > 0$$

is satisfied; however, this means that the flaps must be deflected upward.

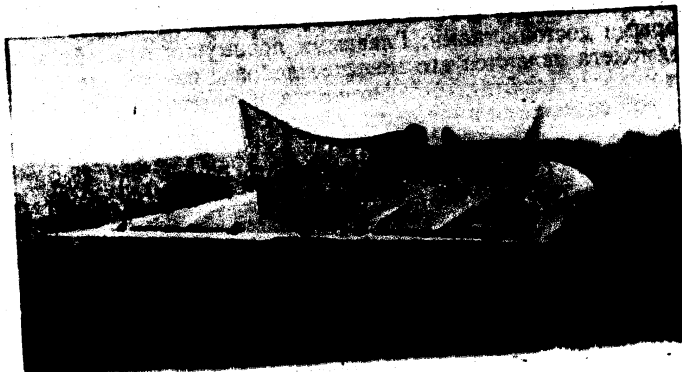


Fig.3.1 - B.I.Chernovskiy's Tailless Parabolic Aircraft

Thus a statically stable and controllable aircraft without horizontal tail surfaces is possible, the so-called "tailless aircraft". The designer B.I.Chernovskiy built one of the first tailless aircraft in the USSR (Fig.3.1).

A shortcoming of the tailless aircraft is the necessity of obtaining equilibrium by deflecting the flaps upward. In this case, the greater the angle of attack at which equilibrium must be obtained, the greater will be the angle by which the flaps must be deflected upward. This leads to a reduction of the lift coefficient of the wing, since the negative angles of deflection of the flaps reduce the lift

coefficient (Fig.3.2). It is very difficult to mechanize the wing of a tailless aircraft to increase the $C_{L \max}$ on landing, since, for example, a downward deflection

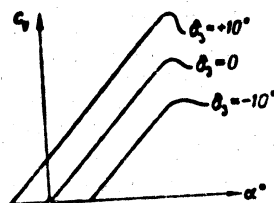


Fig.3.2 - Effect of Flap Deflection on the Coefficient of Wing Lift

of the slot or flaps would result in the appearance of negative m_{z0} , while $m_z > 0$ is required for equilibrium. In this way, in designing tailless aircraft, the smaller values of $C_{L \max}$ make it necessary to adopt a reduced load per square meter of wing area to obtain an acceptable landing speed; however, this reduces the maximum speed of the craft. Another drawback of the tailless aircraft is its reduced damping power (cf. infra, Chapter V) compared to an

aircraft with a tail.

It is true that tailless aircraft also have certain virtues besides these disadvantages. The major advantage of the tailless aircraft is its drag, due to the absence of a regular fuselage and to the less pronounced influence of the compressibility of air on such an aircraft (cf. later in the text).

The Moment of the Horizontal Tail Surfaces

Let us assume that, at a certain distance from wings of an aircraft, there is another wing of smaller size, a horizontal tail surface. This may be located upstream or downstream of the wings (Fig.3.3).

In order to realize equilibrium of the aircraft at a certain flight condition, the moment of the aircraft without horizontal tail surfaces, under this condition, must be balanced. This may be done by producing a lift of the necessary sign on the tail surface by a corresponding deflection of the entire tail unit or a certain part of it, the elevator. The greater the distance from the center of gravity of

the aircraft to the tail unit, the smaller will be the lift of the tail surfaces required for obtaining a moment of some definite value. At a sufficiently long arm of the tail-surface relative to the center of gravity of the aircraft, the component of the tail-surface lift in the total lift of the aircraft will be small. This explains the fact that the aerodynamic calculation of an aircraft is possible without allowing for the lift of the tail-surface.

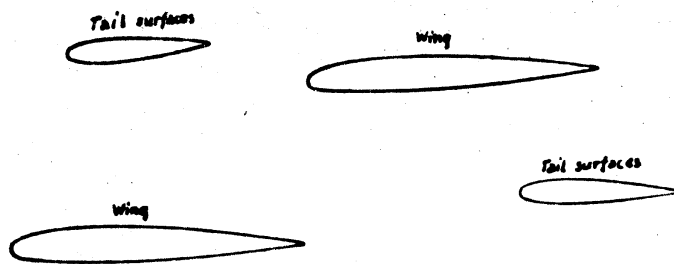


Fig.3.3 - Possible Arrangements of Mutual Positions of Horizontal Tail Surfaces

This possibility of controlling an aircraft with a relatively small force applied to the long arm (and thus without change in the practical balance of the forces acting on the aircraft) constitutes the basic idea of installing a tail surface on an aircraft.

As already mentioned, the horizontal tail surface may be located either behind the wing or in front of it. In the former case we have an aircraft of conventional design (Fig.3.4), in the latter case the so-called duck design* (Fig.3.5).

Without interpreting its meaning, let us denote the absolute value of the moment coefficient of the horizontal tail surface, by $m_{zh.t.}$. The coefficient of

* From the resemblance of such an aircraft to a duck in flight, when observed from the ground.

the total moment acting on the aircraft is represented by the algebraic sum of $m_{bh.t.}$ and $m_{h.t.}$. When the aircraft is in equilibrium, we have

$$m_{bh.t.} - (x_{Fbh.t.} - x_T) C_L + m_{h.t.} = 0,$$

whence

$$m_{h.t.} = -m_{bh.t.} + (x_{Fbh.t.} - x_T) C_L. \quad (3.4)$$



Fig.3.4 - The Yakovlev Aircraft

The moment of the horizontal tail surface is proportional to the lift acting on it, while the moment coefficient is proportional to the coefficient of lift of the horizontal tail surface. It is therefore possible, considering eq.(3.4), to draw the following conclusion:

For an aircraft of conventional design, the greater the term $(\bar{x}_{Fbh.t.} - \bar{x}_T) C_L$, the higher will be the values of $m_{bh.t.}$ necessary for equilibrium, and, consequently, the greater will be the negative lift to be created on the tail surface to ensure equilibrium at values of $C_L > 0$. For an aircraft of the duck design, the

greater the term $(\bar{x}_{fhh.t.} - \bar{x}_T) C_L$, the greater will be the positive lift that must be created on the tail surface for equilibrium. Although, as already stated, the



Fig.3.5 - The Duck Aircraft Design by A.I.Mikoyan and M.I.Gurevich

lift of the tail surface is small by comparison with the lift of the wing, a positive lift of the tail surface is still desirable, in order to improve the lift characteristics of the aircraft. This partly explains the fact that an aircraft of conventional design is usually constructed in such a way that it is statically unstable without the moment of the horizontal tail, while a "duck" aircraft is statically stable without tail unit.

We will discuss the features of aircraft of the "duck" or "tailless" type in more detail below.

Operating Conditions of the Horizontal Tail Surface

Let us consider first a horizontal tail surface installed beyond the aircraft wing (Fig.3.6).

The chord of the horizontal tail surface, in the general case, makes a definite angle φ with the wing chord, which is termed the angle of setting or dihedral of the tail surface.

The wings of an aircraft produce lift by hurling the air downward (more exactly, in a plane perpendicular to the direction of the flying speed) while the momentum per second of the air displaced downward is equal to the lifting force of the wings. For this reason, downstream of the wings and particularly in the region of the horizontal tail surface, the velocity vectors do not coincide with the direction of the relative flow on the aircraft, i.e., with the velocity vector of flight (cf. Fig. 3.6). Thus the tail surface operates in a downwash, whose value increases with the coefficient of wing lift. The fuselage likewise creates a downwash which, in the general case, affects the direction of the flow in the region of the tail surface.

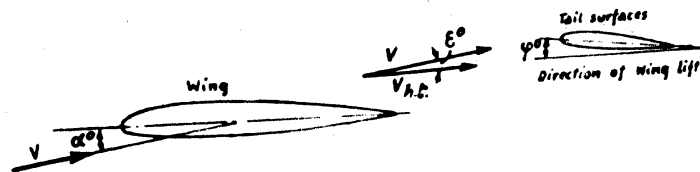


Fig. 3.6 - Conditions of Operations of Horizontal Tail Surface
Mounted Behind the Wing

It is assumed in hydrodynamics that the lift is completely determined by the velocity circulation, and is independent of the viscosity. On the other hand, the profile drag as well as the parasite drag due to friction and vortex formation, exist only in a viscous fluid, such as air. As a result of the profile drag of the wing, the momentum per second in a horizontal direction decreases by comparison with the momentum of the relative flow, i.e., the velocity component of the flow beyond the wing, taken in the direction of the velocity of the relative flow, is less than the flying speed.

Thus, if we disregard the influence of the slipstream on the tail, the velocity of flow in the region of the tail will be less than the flying speed, as a result of

deceleration.

The horizontal tail surface of modern aircraft consists of a fixed part[†], the stabiliser, and of a movable part, the elevator. By deflecting the elevator, the pilot changes the camber of the profile of the horizontal tail surface and thus its lift.

In calculating the moment of the horizontal tail surface, the difference in the angles of attack of the wing and the tail unit must be taken into consideration, as well as the variation in velocity of the relative flow on the tail unit as compared with the flying speed and the angle of deflection of the elevator.

When the pilot pulls the control stick (Fig.3.7), the elevator is deflected upward ($\delta < 0$), and a force directed downward is produced on the tail surface. In this case, a moment tending to increase the angle of attack ($M_z > 0$) is produced. When the pilot pushes the control stick (cf. Fig.3.7), the elevator is deflected downward ($\delta > 0$) and an additional lift (directed upward) is produced on the tail unit, creating a moment that tends to reduce the angle of attack ($M_z < 0$).

In a "duck" aircraft, there is no deceleration of the velocity in the region of the tail unit, since the wake (region of decelerated flow) is far behind the tail. In this case there is practically no downwash at the tail unit, since the vortex system produced by the wing is downstream of the tail unit and, in addition, the attached and detached vortices of the produced downwash have different signs (cf. Fig.3.8). When the control stick is pulled toward the pilot, the elevator is deflected downward in a duck aircraft while, when the stick is pushed away from the pilot, the elevator is deflected upward.

[†]The term "fixed" part of the tail is arbitrary. In some aircraft the pilot has a special handwheel for changing the angle of setting of the stabiliser with respect to the wing.

Downwash at the Tail

As established by the Russian scientists N.Ye.Zhukovskiy (Joukowski) and S.A.Chaplygin, the formation of a lift on the wing is connected with the creation of a vortex system. In first approximation, it may be considered that this vortex system consists of an attached vortex, whose axis is directed along the wing span,

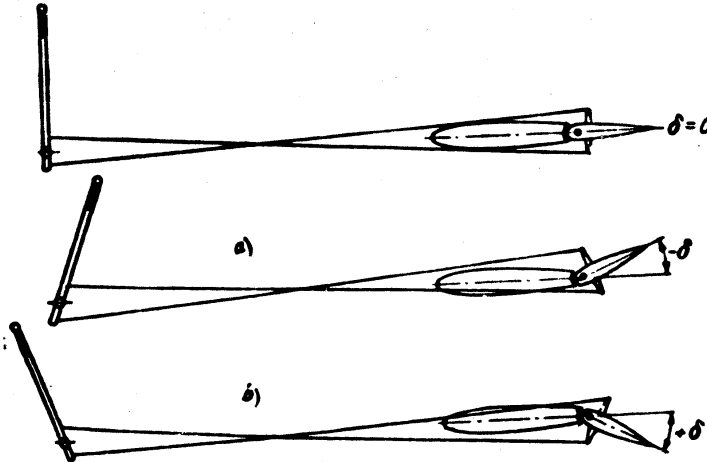


Fig.3.7 - Scheme for Manipulating Rudder

a) elevator raised "up"; b) elevator deflected "down"

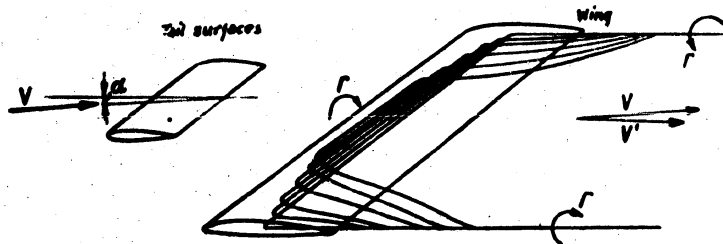


Fig.3.8 - Trailing Edge of Wing and Tail Unit

and of detached vortices running from the wing along its entire span and having axes directed along the velocity of the relative flow. The vortex sheet formed by the detached vortices is unstable, and at some distance from the wing it separates into two filaments spaced by a distance shorter than the wing span (Fig.3.9).

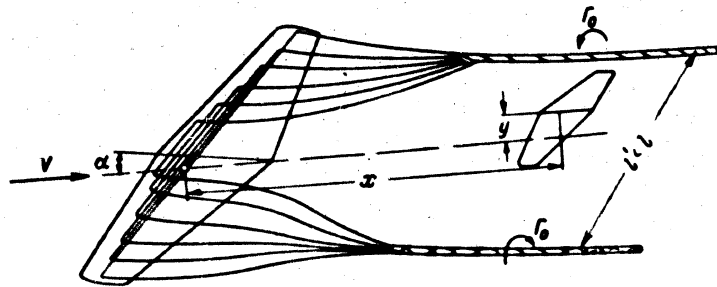


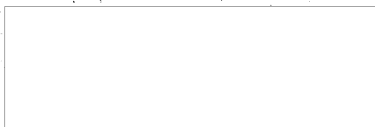
Fig.3.9 - Vortex System of the Wing

All these vortices induce certain velocities in space, which do not coincide in direction with the velocity of the relative flow. The resultant vector of velocity, representing the sum of the vectors of the inductive velocity and the velocity of the relative flow, make a certain angle ϵ of downwash with that flow.

With an approximation sufficiently accurate for practice, the actual system of vortices may be replaced in the calculation of the downwash at the tail surface by a simpler though arbitrary system (Bibl.5 and Fig.3.10) consisting of bound vortices, of a circulation varying along the wing span, and of two free vortices of a circulation equal to the bound vortices, in the plane of symmetry of the wing. The distance between the vortices may be determined on the basis of Joukowski's theorem. The wing lift according to his theorem is equal to

$$\gamma = \rho V \int_{-\frac{l}{2}}^{+\frac{l}{2}} \Gamma dz. \quad (3.5)$$

At the same time, sufficiently far downstream of the wing, where the influence of



the bound vortices can be neglected and where the wing may be replaced by a Π -shaped vortex, this same theorem will yield

$$Y = \rho V l_0 l', \quad (3.6)$$

where Γ is the circulation in the plane of symmetry of the wing and where l' is the distance between the free vortices.

By equating eqs.(3.5) and (3.6), we

find

$$l' = \frac{\int_{-\frac{l}{2}}^{+\frac{l}{2}} \Gamma dz}{\Gamma_0} \quad (3.7)$$

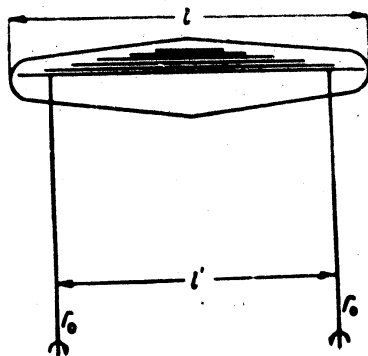


Fig.3.10 - Calculation Scheme for Vortices Downstream of the Wing

The greater the distance between the free vortices l' , the less will be the wake formed by these vortices. Consequently, if we consider two curves of circulation distribution with the same area $\int_{-\frac{l}{2}}^{+\frac{l}{2}} \Gamma dz$ but with different ordinates Γ_0 (Fig.3.11),

then a smaller wake of the free vortices will be created for the smaller ordinate Γ_0 .

This fact is particularly important in cases where a shock wave is formed at the center section of the wing, due to the influence of the compressibility of air, while the wing tips operate at subcritical Mach numbers. Because of the decrease in Γ_0 in this case, l' increases and the downwash at the tail decreases.

Let us derive the expression for the distance between the free vortices: For this purpose, let us use the approximate expression for the circulation of a trapezoidal wing.



$$\Gamma = 0.5\Gamma_0 \left[\sqrt{1-s^2} + 1 - \frac{\eta-1}{\eta} s \right]. \quad (3.8)$$

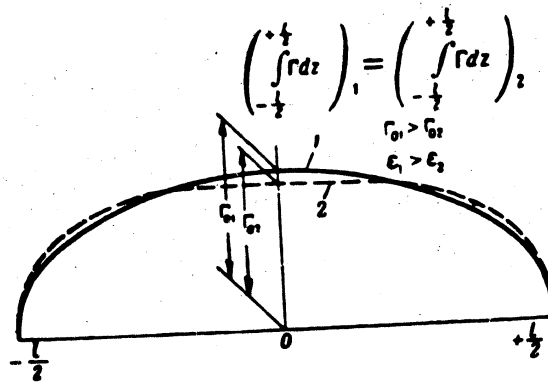


Fig.3.11 - Curves of Circulation with the Same Area but Different Values of Γ_0

where $\eta = \frac{b_0}{b_1}$ is the wing taper and $z = \frac{l}{2}$.

On substituting this expression in eq.(3.5) and integrating, we get

$$Y = 0.5\rho V\Gamma_0 l \left(\frac{\pi}{4} + 1 - \frac{\eta-1}{2\eta} \right) = 0.5\rho V\Gamma_0 l \left(1.285 + \frac{1}{2\eta} \right). \quad (3.9)$$

Replacing Y by its ordinary expression $Y = C_L S \frac{\rho V^2}{2}$ we find the expression for in terms of the C_L of the wing and its geometric characteristic.

$$\Gamma_0 = c_v \frac{S}{l} V \frac{\eta}{1.285\eta + 0.5}. \quad (3.10)$$

where η is the wing taper.

From eq.(3.5) we have

$$\int_{-\frac{l}{2}}^{+\frac{l}{2}} \Gamma dz = \frac{c_v S V}{2}. \quad (3.11)$$

On introducing eqs.(3.10) and (3.11) in eq.(3.7), we have

$$v = \frac{c_v SV}{2} \frac{1,285\eta + 0,5}{\eta} - l \frac{1,285\eta + 0,5}{2\eta}$$

or

$$\frac{v}{l} = \frac{1,285\eta + 0,5}{2\eta} - \frac{1,285\eta + 0,5}{2\eta} \quad (3.12)$$

where

$$\frac{1,285\eta + 0,5}{2\eta} = 0,64 + \frac{0,25}{\eta}$$

It is clear from eq.(3.12) that, with increasing wing taper, the coefficient v declines, i.e., the free vortices trailing from the wing approach the tail, so that, other conditions being equal, the downwash increases.

For the downwash at the tail surface, in the plane of symmetry of the aircraft, theory leads to the following expression:

$$\alpha = \frac{3}{\sqrt{3}} \kappa \quad (3.13)$$

where κ is a certain function of the coordinates of the tail unit with respect to the wing, related to the semispan of the wing and to the wing taper.

Equation (3.13), obtained theoretically, determines the angle of downwash in the plane of symmetry of the tail. At other points along the tail span, the downwash angle will differ from that calculated by eq.(3.13). In calculating the moment of the horizontal tail, we will be interested in the mean value of the downwash angle over the entire tail span. Allowance for the transition from the local angle of downwash in the plane of symmetry of the tail surface to the mean angle of

STAT

downwash over the span of the tail surface, and likewise for the general closeness to the theory, can be made by applying an empirical correction to eq.(3.13).

In first approximation, the value of the deceleration factor of the velocity k may be taken as constant for all cases. Moreover, for convenience in using eq.(3.13), the function κ , as shown by calculations, may be represented in the form of the derivative of three functions χ_1, χ_2, χ_3 with χ_1 allowing only for the influence of the wing span χ_2 (more accurately, the influence of the law of distribution of circulation along the wing span); χ_2 takes into consideration only the influence of the coordinates $\bar{x} = \frac{x}{l}$ of the tail unit with respect to the wing, while χ_3 allows for the influence of the coordinate $\bar{y} = \frac{y}{l}$ of the tail unit with respect to the wing (cf.Fig.3.9).

Thus, the following semi-empirical formula may be used* in the calculation:

$$\epsilon^\circ = \frac{46.2}{\lambda} \chi_1 \chi_2 \chi_3 C_L \quad (3.14)$$

where ϵ° is expressed in degrees. As will be seen, the angle of downwash is inversely proportional to the aspect ratio of the wing λ and directly proportional to the lift coefficient C_L .

Figures 2.12 to 3.14 give plots of the functions χ_1, χ_2, χ_3 .

In considering these diagrams, it will be noted that the functions χ_1, χ_2, χ_3 decline and that, consequently, the downwash decreases with increasing \bar{x}, \bar{y} and with increasing taper η .

The question as to the effect of the deflection of the slots or flaps on the downwash at the tail will be considered later in the text, together with the question as to the effect of the closeness of the ground on the downwash.

* Equation (3.14) has been derived for straight wings without sweepback. It may, however, be assumed that it can also be used without great error for the case of sweptback wings.

Since we have assumed the coordinates of the tail to be located in the velocity system of axes, while the coordinates of the tail relative to the wing are fixed in the system of bound aircraft axes, \bar{x} and \bar{y} will depend on the angle of attack of the wing.

If \bar{x}_0 and \bar{y}_0 denote the relative coordinates of the tail assembly in the special case where $\alpha = 0$, then

$$\left. \begin{aligned} \bar{x} &= \bar{x}_0 + 0,0174\bar{y}_0\alpha^2 \\ \bar{y} &= \bar{y}_0 - 0,0174\bar{x}_0\alpha^2 \end{aligned} \right\} \quad (3.15)$$

At the values of \bar{y}_0 met in practice in the flying range of angles of attack, \bar{x} differs very slightly from \bar{x}_0 . The values of \bar{y} depend on the angles of attack to a greater extent than the values of \bar{x} . It is therefore allowable, in first approximation, to calculate the angle of downwash for certain mean values \bar{x} mean, \bar{y} mean.

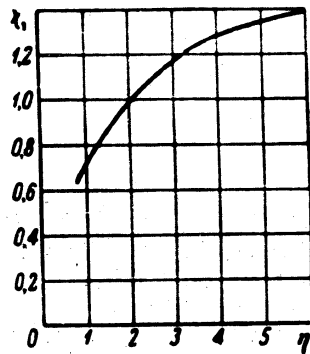


Fig.3.12 - Plot of the Function χ_1 for Calculating the Downwash

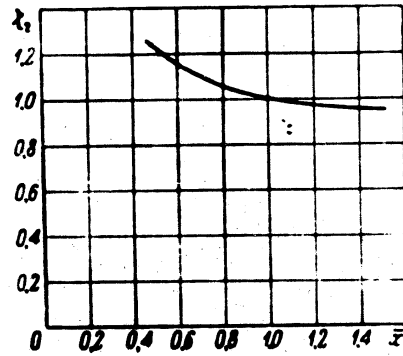
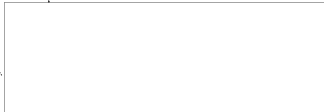


Fig.3.13 - Plot of the Function χ_2 for Calculating the Downwash

The values calculated from eq.(3.15) for a certain mean angle of attack $\alpha_{mean} \approx 4^\circ$, may be taken as these mean values.



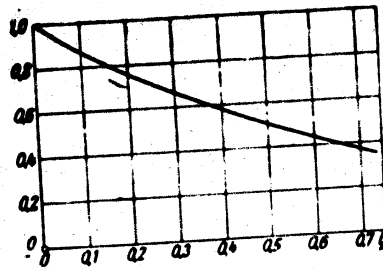


Fig.3.14 - Plot of the Function X_3
for Calculating the
Downwash

Influence of the Propeller and Fuselage on the Downwash
at the Tail Surface

In calculating aircraft with piston or turboprop engines, allowance must be made for the additional downwash due to the operating propeller.

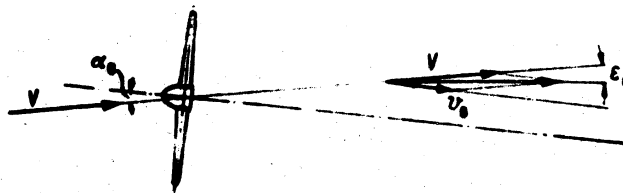


Fig.3.15 - Downwash from Propeller

With a certain assumption, it may be considered that the velocity of the slipstream is directed along the propeller axis which, in the general case, makes a certain angle with the direction of velocity of the relative flow. Consequently, some additional downwash due to the propeller will always exist (Fig.3.15). In addition, in aircraft with tractor propellers the air stream thrown back by the



propellers washes the wing before reaching the tail, thus varying the circulation of velocity around the wing and also varying its spanwise distribution. It is clear from what has been said in the preceding Section that the redistribution of the circulation will cause a variation in the downwash generated by the wing.

We have to do here with a very complex phenomenon, which is made still more complex by the fact that the velocities induced by the propeller are distributed nonuniformly along the radius of the propeller and likewise by the fact that the slipstream cut by the wing acquires a complex configuration (Fig.3.16) when it approaches the tail.

Theoretical studies on the downwash from the propeller are in existence, which throw considerable light on the qualitative aspects of this question (Bibl.6). They lead, however, to rather complex expressions and, in addition, do not in all cases ensure a qualitative agreement with experiment. For this reason, we will present only the empirical method of estimating the downwash from an operating propeller, a method generally adopted at present.

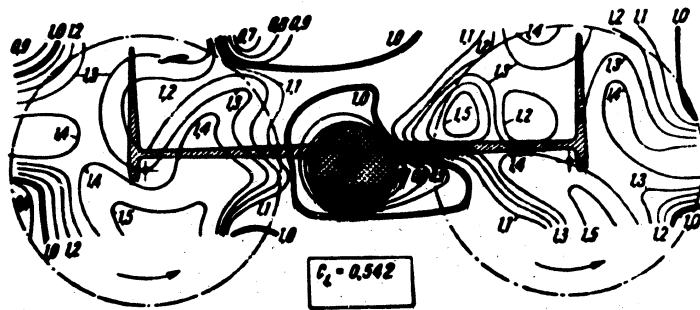
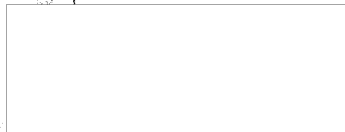


Fig.3.16 - Lines of Equal Velocity of Flow in the Region of the Tail Surface with an Operating Propeller

In this method, the value of the angle of downwash from the wing, determined from eq.(3.14), must be supplemented by the following quantity:



Single-engine
aircraft

Twin-engine
aircraft

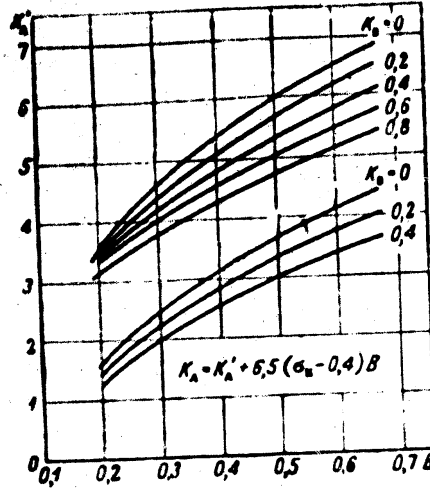


Fig.3.17 - Graph for Determining the Coefficient k_A

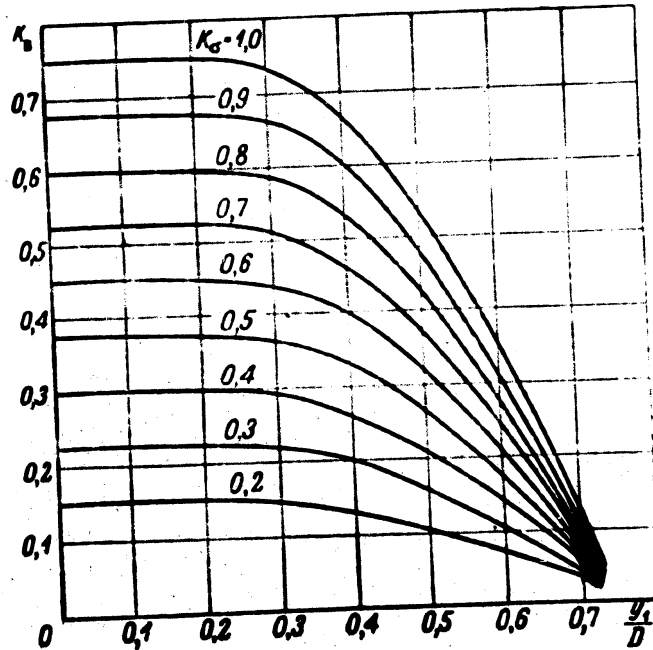


Fig.3.18 - Graph for Determining the Coefficient k_B



$$\epsilon_s = [k_A + 6,5(\sigma_k - 0,4)B]c_L, \quad (3.16)$$

where the coefficient k_A is determined from the graph in Fig.3.17 constructed from experimental data, depending on the load factor on the area B , delimited by the propeller, and on the coefficient k_B evaluating the nonuniformity of the downwash along the tail span. In eq.(3.16), $\sigma_k = \frac{S_{obz}}{S}$ is the relative value of the area of the wing exposed to the flow. The quantity σ_k is determined under the assumption that the slipstream generated by the propeller is a cylinder of a diameter equal to the diameter of the propeller D , and with an axis coinciding with the propeller axis.

The value $B = \frac{P}{Fq}$ of the load factor on the area defined by the propeller can be taken from aerodynamic calculation. The coefficient k_B , giving the intensity of the propeller slipstream striking the tail surface, is determined from Fig.3.18 in accordance with the ratio $\frac{y_1}{D}$ (where y_1 is the distance from the tail surface to the axis of the propeller in elevation) and from the coefficient k , which allows for the relative dimensions of propeller and tail surface. For single-engine aircraft

$$k_s = \frac{D}{l_{h.t.}};$$

for twin-engine aircraft

$$k_s = 1 - \frac{2a}{l_{h.t.}} + \frac{D}{l_{h.t.}},$$

where $l_{h.t.}$ is the span of the horizontal wing, while a is the distance from the plane of symmetry of the aircraft to the propeller axis.

In addition to the wing and propeller, the downwash in the region of the horizontal tail surfaces is also due to the fuselage, since this also possesses a lift. Besides this, the fuselage may be considered a kind of guiding apparatus. For this reason, if the horizontal tail surfaces are located on the fuselage or near it (Fig.3.19), then additional local downwashes are obtained from the flow around the

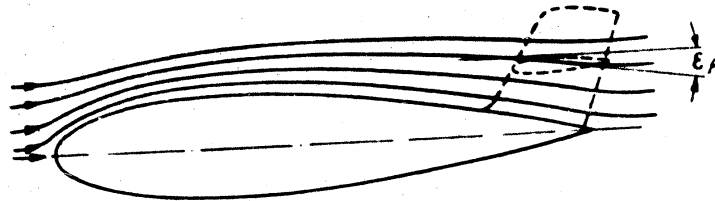


Fig.3.19 - Effect of the Fuselage on the
Downwash at the Tail Surface

trailing portion of the fuselage.

Experiment has shown that, ordinarily, the downwash due to the influence of the fuselage is small and, in first approximation, may be taken as constant. For all cases where the horizontal tail surfaces are close to the fuselage, we may take

$$\epsilon_f \approx 1^\circ \div 1,5^\circ \quad (3.17)$$

If the horizontal tail surfaces are located on the keel of the aircraft, the angle of downwash from the fuselage will be smaller so that, in the calculation for this case, the following value may be taken

$$\epsilon_f \approx 0,5^\circ \div 1,0^\circ \quad (3.17')$$

Influence of the Compressibility of Air on the Downwash

It has been stated in Chapter II that, at subsonic flying speeds and a given angle of attack, the coefficient C_L varies with increasing Mach numbers in first approximation by the law

$$C_L = \frac{C_{L_0}}{\sqrt{1 - M^2}}$$

This variation will apply approximately to all the wing sections along the span so that the character of the distribution of the wing circulation along the span will remain invariant. For this reason the downwash, at unchanged C_L of the wing does not vary either. It follows that, at subcritical Mach numbers, eq.(3.14) remains valid for determining the downwash. It must merely be borne in mind that to one and the same value of C_L there correspond various angles of attack of the wing at different values of the Mach number.

The picture is different at Mach numbers exceeding M_c . In this case a shock wave forms on part of the wing, and as a result the velocity circulation Γ around this region of the wing decreases, while Γ on the remainder of the wing continues to increase with increasing Mach numbers.

Usually the shock wave takes place earliest on the center section of the wing as a result of the mutual interference of wing and fuselage. For this reason, beyond the critical Mach numbers, the circulation is redistributed along the wing

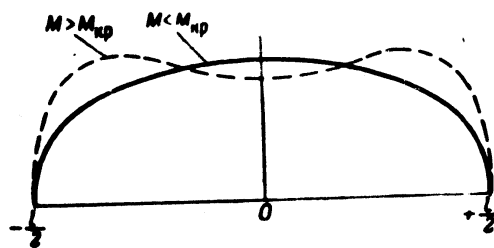


Fig.3.20 - Redistribution of the Circulation along the Span at $M > M_{kp}$

span, approximately as indicated in Fig.3.20. The reduction of the circulation in the plane of symmetry of the wing leads to an increase in the distance between the free vortices, and to a reduction in the downwash. This reduction of downwash may reach a considerable value, as shown in Fig.3.21, which gives the results

of the determination of downwash in a high-velocity wind tunnel for models of one aircraft. We see further that the decrease in the downwash is one of the causes of the so-called "being drawn into a dive" which is sometimes observed in flights at Mach numbers exceeding the critical.

STAT

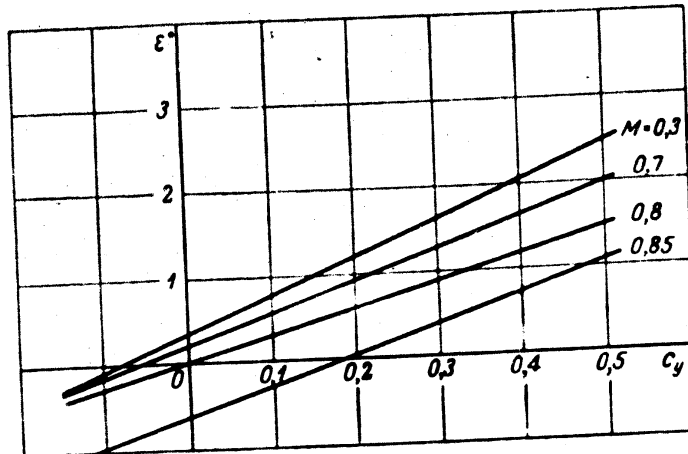


Fig.3.21 - Variation of Downwash as a Function of M
from Experimental Data

If we knew the region of the wing on which there is a drop in Γ owing to a shock wave, and if we knew the nature of this drop, we could calculate the value of the downwash by using the same reasoning that was used in determining the downwash beyond the wing at small Mach numbers. However, no such data are available at present so that, for estimating the influence of the compressibility of air on the downwash, we must use the data of aircraft model tests in the high-velocity wind tunnel.

The Downwash at Supersonic Flying Speeds

At supersonic flying speeds, that is, at $M > 1$, the disturbances of flow in an ideal gas produced by any source, are propagated only within a certain angle where

$$\sin \beta = \frac{1}{M}.$$

The region of propagation of the disturbances that arise when a stream of

compressible nonviscous gas flows around a wing of sufficiently great span (theoretically, infinite span) at Mach numbers over 1, is bounded by two lines radiating from the leading and trailing edges of the wing (Fig.3.22). In addition, the disturbance may also be propagated within cones having their vertices at the wing tips and an angle at the vertex equal to $2 \sin^{-1} \frac{1}{M}$.

Outside the zone hatched in Fig.3.22 and the cones originating at the wing tips, the flow theoretically remains undisturbed. If the horizontal tail surfaces are so placed that they do not enter this zone at all, they will operate as an isolated unit not subject to the disturbing influence of the wing. In this case there will be no downwash and no deceleration of the velocity in the region of the tail surface*.

The curve of variation in angle of downwash as a function of the Mach number at a constant value of C_L , will have the form schematically shown in Fig.3.23. The angle of downwash at first remains practically constant, beginning to decline at

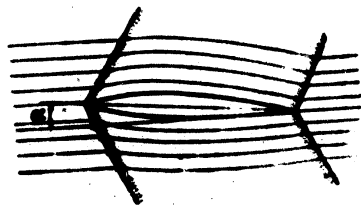


Fig.3.22 - Region of Propagation of Disturbances at $M > 1$

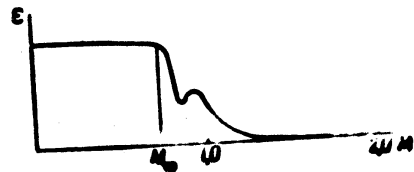


Fig.3.23 - Schematic Representation of the Relation $\epsilon = f(M)$ at $C_L = \text{const.}$

*It must be borne in mind that, in the case of a sweptback wing, with an angle of sweepback χ , the downwash will theoretically be zero at $M \cos \chi > 1$, since the effective Mach number $M = M \cos \chi$ (cf. Chapter II) must be used into the calculation in this case.

$M > M_{crit}$ and finally reaching a certain minimum. At a value of M at which the character of the distribution of the circulation along the wing span is approximately restored, the downwash again increases and, finally, at high Mach numbers drops to zero.

The Actual Angle of Attack of the Horizontal Tail Surface

If the angle of setting of the horizontal tail surface relative to the wing chord (dihedral) is equal to φ' , then the apparent or geometric angle of attack of the tail unit is equal to

$$(\alpha_{ht}^{\circ}) = \alpha^{\circ} + \varphi'$$

The actual angle of attack of the tail unit will be less than the apparent angle of attack by the value of the angle of downwash

$$\alpha_{ht}^{\circ} = (\alpha_{ht}^{\circ}) - \epsilon^{\circ} = \alpha^{\circ} + \varphi' - \epsilon^{\circ} \quad (3.18)$$

The angle of downwash at the tail surface, due to the wings of the aircraft, is equal to

$$\epsilon^{\circ} = \frac{46.2}{\lambda} X_1 X_2 X_3 = D \epsilon_1 \quad (3.18')$$

where, for brevity, we put $\frac{46.2}{\lambda} X_1 X_2 X_3 = D$, so that eq.(3.18) may be rewritten in the form

$$\alpha_{ht}^{\circ} = \alpha^{\circ} + \varphi' - \epsilon^{\circ} = \alpha^{\circ} + \varphi' - D \epsilon_1 \quad (3.19)$$

Let us take the derivative of eq.(3.19) with respect to α° . Neglecting the dependence of D on α° in the differentiation, we obtain

$$\frac{d\alpha_{ht}^{\circ}}{d\alpha^{\circ}} = 1 - D \frac{d\epsilon_1}{d\alpha^{\circ}}$$



STAT

Since the subtrahend in this expression is always positive, it follows that always $\frac{\partial \alpha_{h.t.}}{\partial \alpha} < 1$ i.e., the angle of attack of the horizontal tail surface increases more slowly than the angle of attack of the wings.

For modern aircraft $\lambda \approx 5$; $\frac{\partial C_L}{\partial \alpha} \approx 0.065$; $X_1 X_2 X_3 \approx 0.95$. On substituting these figures in the preceding expression we obtain

$$\frac{\partial \alpha_{h.t.}}{\partial \alpha} \approx 0.43$$

Thus in its lifting power, the horizontal tail is found to be about only half as efficient as the wing. In other words, the effective area of a horizontal tail surface (if the lift properties of a wing are ascribed to it) is approximately half of that belonging to its geometric area.

At high supersonic flying speeds, the downwash is absent, and at these speeds the effective tail area increases and becomes equal to its geometric area. The latter fact leads to certain difficulties in the design of high-speed aircraft, since it must fly equally well at subcritical and supersonic speeds. When the aircraft exceeds $M = 1$, the resultant effect is as though the tail area were suddenly doubled. From this point of view, the design of the "tailless aircraft" has a certain interest, since it has no horizontal tail surfaces so that the above-mentioned variations in its operating conditions cannot take place.

Influence of the Proximity of the Ground and of the Deflection of the Flaps on the Downwash at the Tail Surface

During take-off and landing of an aircraft, it flies for a certain time in the immediate proximity of the surface of the airfield (Fig.3.24). At the surface of the ground, the full velocity vector of the flow is parallel to the ground, and during horizontal flights of the aircraft very near the ground the inductive velocity must be zero.

It is obvious that the closeness of the ground also influences the inductive

velocities in the region of the tail unit.

An idea of the mechanism of the influence of the proximity of the ground on the

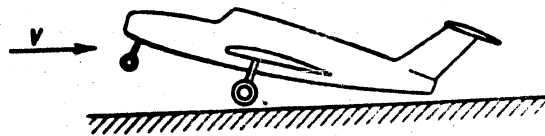


Fig.3.24 - Position of the Aircraft Shortly after Take-off
or During Landing

downwash at the tail surface can be obtained by using the method of conformal mapping, often used in hydrodynamics. The actual phenomenon may be placed by the diagram given in Fig.3.25. In this diagram, the downwash at the tail surface is

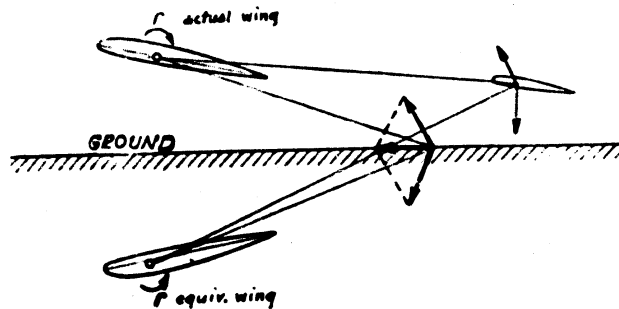


Fig.3.25 - Diagram for Determining the Downwash
Near the Ground

created by an actual flat wing and a virtual airplane wing representing the mirror image of the actual wing. The downwash from the equivalent wing is less than the downwash from the actual wing and has the opposite sign, so that the resultant downwash during flight close to the ground is less than in the case of a flight high above the ground.



During take-off and landing of an aircraft, the slots or flaps are usually deflected, so that the angle of downwash in this case can no longer be determined by eq.(3.14). With the deflected flaps occupying in the general case only the center section of the wing, the character of the distribution of circulation over the span

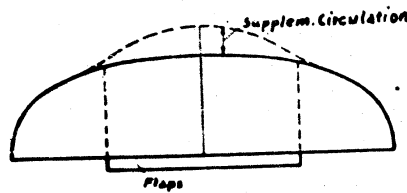


Fig.3.26 - Supplementary Circulation on Deflection of Flaps

is no longer what it was with undeflected flaps. The original curve of circulation is superposed by an additional curve of circulation due to the flaps (Fig.3.26). In this case it is as though the downwash were induced by two systems of vortices: a main system corresponding to the wing with undeflected flaps, and a supplementary

system corresponding to the deflection of the flaps. At one and the same value of C_L , the downwash will be greater with deflected flaps than with undeflected flaps.

Thus, on landing and during take-off, the downwash will decrease due to the nearness of the ground, and will increase due to deflection of the flaps. Without analyzing of this problem further, we confine the calculation to presenting a first semi-empirical formula which may be used for calculating the downwash of a wing on flight near the ground with deflected flaps.

$$\epsilon_{L, \text{down}} \approx \sqrt{\frac{h}{l} \left[\frac{35}{\lambda} \chi_1 \chi_2 C_L + \frac{32}{\lambda_{FL}} \Delta C_L \right]}. \quad (3.20)$$

Here the following symbols are used:

h is the distance from flaps to the ground, determined by Fig.3.27:

$h = h_{f1} + h'$ where h' is the distance from the lower edge of the wheels to the ground; h_{f1} is determined as shown in Fig.3.27;

C_L is taken for the wing with undeflected flaps;

ΔC_L is the increment of the coefficient C_L due to deflection of the flaps;

$\lambda_{fl} = \frac{l_{fl}^2}{S_{fl}}$ is the aspect ratio of the part of the wing area served by the slot or flaps (Fig.3.28);

l is the wing span;

the coefficients X_1 and X_2 have their previous meaning.

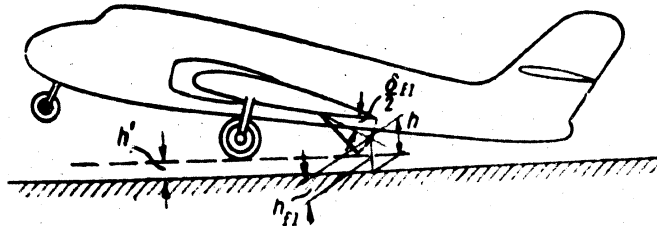


Fig.3.27 - For Determining the Value of h_m

Usually, in calculating the allowable forward centering (cf. infra, Chapter IV) h' is taken as equal to $0.2b_A$. The reduction in the downwash due to the influence of the ground is very substantial. For example, let the following data be given:

wing taper $\eta = 2$;

wing aspect ratio $\lambda = 5$;

wing span $l = 10$ m;

mean aerodynamic chord $b_A = 2$ m;

aspect ratio of part of wing area served by the flaps, $\lambda_{fl} = 3$;

coordinates of tail surface:

height of flaps above the ground $h = 1.0$ m;

coefficient $C_L = 1.2$, $\Delta C_L = 0.6$.

From the graphs in Figs.3.12 and 3.13 we find $x_1 = 0.99$; $x_2 = 1.0$.

From eq.(3.20) we calculate

$$\phi_{i,av} = \sqrt{\frac{1}{10} \left[\frac{35}{5} \cdot 0.99 \cdot 1.0 \cdot 1.2 + \frac{32}{3} \cdot 0.6 \right]} = 4.65^\circ$$

STAT

Far from the ground at $C_L = 1.2$ (without deflection of the flaps) we would have, according to eq.(3.18') and bearing in mind that $\lambda_3 = 0.76$:

$$z = \frac{46.2}{5} (0.99 \cdot 1.0 \cdot 0.76 \cdot 1.2) \approx 8.4^{\circ}$$

Thus, in spite of the substantial increase in C_L on deflection of the flaps, the downwash near the ground not only fails to increase but even decreases almost to half its value. This fact, as shown later, is very important for determining the permissible forward centering of an aircraft.

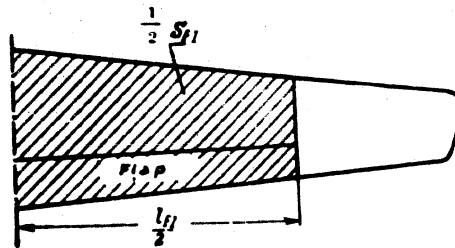


Fig.3.28 - For Determining λ_{f1}

Deceleration of Velocity in the Region of the Tail Assembly

As mentioned at the beginning of this Chapter, the velocity of flow in the region of the tail unit is not equal to the velocity of the relative flow (flying speed V). Above we denoted the velocity of flow in the region of the tail unit by

$$V_{h.t.} = \sqrt{k} V$$

The coefficient k is called the coefficient of deceleration of velocity at the tail unit, due mainly to the drag of the wings and fuselage.

Downstream of a body in a circulating flow of viscous fluid a trail (wake) is formed within which the velocities are lower than the velocity of the relative flow. The dimensions of the wake and the value by which the velocities are reduced within

within it depend on the configuration of the body and on its drag. In addition, as shown later in the text, the Mach number has a substantial influence on the dimensions of the wake.

If we knew the dimensions of the wake, then the mean value of the deceleration in it could be found by using the Bernoulli theorem on sections located far upstream of the aircraft and far downstream. Assume, for example, that the dimensions of the wake are limited in length by the wing span, and in height by 20% of the mean wing chord. Then assuming that the air pressure in the region of the tail unit is equal to the pressure far in front of the aircraft, we have

$$p_0 + \frac{\rho V^2}{2} = p_0 + \frac{\rho V_{A.T.}^2}{2} + \frac{1}{1-0.2^2} \rho S \frac{D^2}{2}$$

whence

$$\left(\frac{V_{A.T.}}{V}\right)^2 = 1 - \frac{D}{S}$$

At a value for the whole aircraft $C_L = 0.02$, we would have

$$D = 0.02 S$$

In reality, of course, the dimensions of the wake cannot be determined so simply as we have done in this example. For this reason, it is difficult to obtain a general expression connecting the coefficient of deceleration and the coefficient of drag of an aircraft. Here we are helped by the fact that the coefficients of drag of modern aircraft lie within relatively narrow limits, just as the dimensions of the wake, expressed in fractions of the chord or the wing span. It has been found that a fuselage with a tail in its rear section has a great influence on the coefficient of deceleration.

For the relatively narrow range of angles of attack at which normal flight

takes place and for subcritical Mach numbers, the universal relation of the coefficient k and the ratio $\frac{S_{h.t.}^f}{S_{h.t.}}$ given in Fig.3.29 may be adopted on the basis of experimental data. In this formula, $S_{h.t.}^f$ is the part of the area of the horizontal tail surface occupied by the fuselage, while $S_{h.t.}$ is the total area of the horizontal tail surface (including the part under the fuselage). The curve given in Fig.3.29

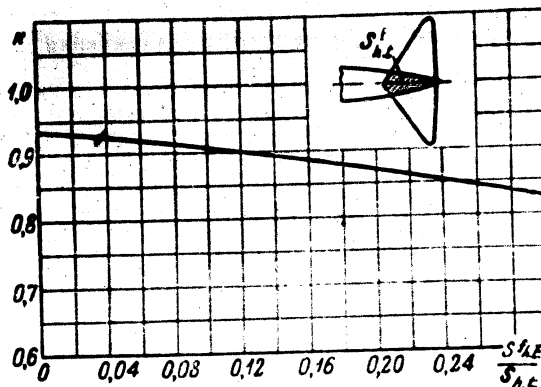


Fig.3.29 - Relation between the Coefficient of Retardation and $\frac{S_{h.t.}^f}{S_{h.t.}}$

relates to the case when the horizontal tail surface is located on the fuselage. If the tail surface is located on the vertical fin of the aircraft above the fuselage, as is the case in modern jet aircraft, or in the twin-tail design (Fig.3.30) higher values must be taken for k , for example, $k = 0.95$, which corresponds to $\frac{S_{h.t.}^f}{S} = 0$.

At subcritical Mach numbers in usual cases, the width of the wake amounts to 15-25% of the wing chord. At trans-critical Mach numbers, with a developing shock wave, the width of the wake may increase greatly, reaching 100% of the chord or more. As an example, Fig.3.31 shows the distribution of losses of the velocity head beyond the wing at various Mach numbers (the critical Mach number in this was equal to $M_{kp} = 0.65$) from the data of wind-tunnel tests. Obviously, the difference in the losses on transition from small Mach numbers to large ones is substantial.

As a result of such widening of the wake at $M > M_{kp}$, the designers often attempt to place the horizontal tail surfaces on high-speed aircraft as high as possible with respect to the wing in order to avoid shadowing of the tail surface by the wing and the creation of vibrations in the tail unit at high Mach numbers. It is considered that the distance from the horizontal tail surfaces to the plane of the wing chord in elevation should not be less than $0.4 b_{root} - 0.5 b_{root}$, where b_{root} is the root chord of the wing.

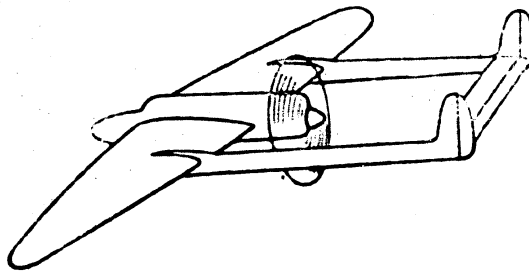


Fig.3.30 - Scheme of Twin-Tail Aircraft

At high (landing) angles of attack, and with deflected flaps or slots, the width of the wake zone likewise increases, together with the deceleration. Figure 3.32 gives experimental data on the additional coefficient of deceleration k_{land} (additional to its value at small angles of attack) for the case of deflected flaps and large angles of attack, so that the total coefficient of deceleration in this case is equal to $k_{total} = k + k_{land}$. The ratio $\frac{x_{h.t.}}{b_{root}}$ is plotted on the abscissa in this diagram, with $x_{h.t.}$ being the chordwise distance from the trailing edge of the root profile to the tail. The quantity $\frac{y_{h.t.}}{b_{root}}$ where $y_{h.t.}$ is the distance in elevation from the tail to the axial line of the wake, is plotted on the ordinate. In first approximation, $y_{h.t.}$ may be determined by the formula

$$y_{h.t.} = h + x_{h.t.}^2 \cdot \text{land}$$

where h is the elevation of the tail above the plane of the wing chord at $\alpha = 0$;
 ϵ_{land} is the angle of downwash (in radians) at landing.

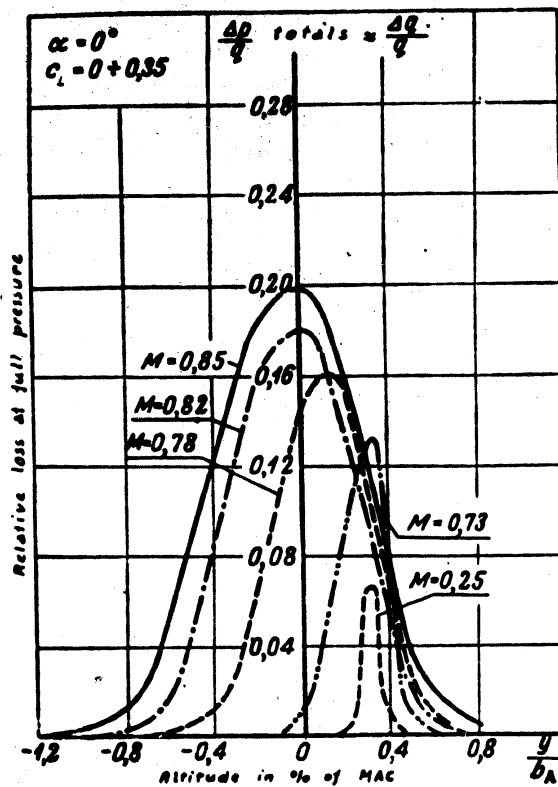


Fig.3.31 - Deceleration of Velocity at Various Mach Numbers

Influence of the Operating Propeller on the Flow Velocity at the Tail Surface

It is known from the theory of the ideal propeller that the velocity in the slipstream far from the propeller disk is equal to

$$V_2 = V \sqrt{1+B} \tag{3.21}$$

STAT

With an operating propeller, when the tail is located entirely within the slipstream, the effective coefficient of deceleration must theoretically be equal to

$$k_0 = k(1+B).$$

In reality, the velocity distribution along the propeller radius differs somewhat from that obtained by the theory of the ideal propeller. In addition, the tail is

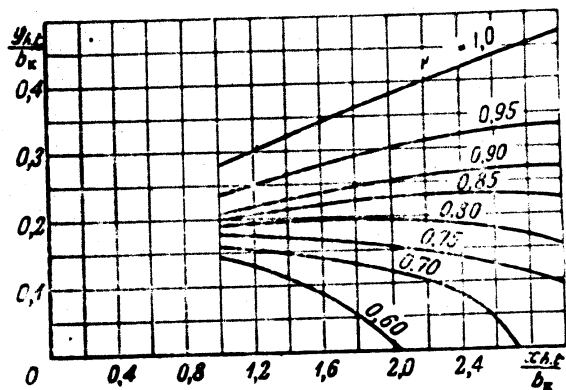


Fig.3.32 - Supplementary Coefficient of Deceleration of Velocity During Landing

usually not entirely within the slipstream. For this reason a correction, which may be obtained from experimental data, must be applied to the preceding expression. The final expression for k_0 takes the form

$$k_0 = k(1+k_0B). \quad (3.22)$$

The coefficient k_0 , allowing for the nonuniformity of the velocity distribution along the tail span should be taken from Fig.3.18.

STAT

Influence of Elevator Deflection on the Tail Moment

By deflecting the elevator upward or downward, the pilot changes the camber of the profile of the horizontal tail surfaces. The variation of the profile camber leads to a variation in the tail lift, causing an additional force on the tail, directed downward or upward, as the case may be.

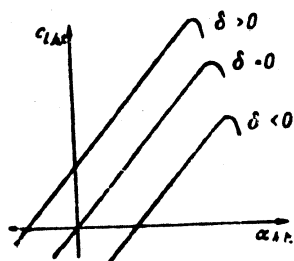


Fig.3.33 - The Curves of C_L of the Horizontal Tail Surfaces at Various Angles of Deflection of the Elevator

When the elevator is deflected, the curve $C_{Lh.t.} = f(\alpha_{h.t.})$ of the horizontal tail surfaces is displaced, within the limits of the linear dependence of C_L on α , equidistantly to the right or left (Fig.3.33) by a value proportional to the angle of deflection of the elevator. This fact substantially facilitates the analytical calculation of the tail moment, allowing use of the linear relationship $C_{Lh.t.} = f(\alpha_{h.t.}, \delta B)$. This relationship may be written in the form

$$C_{Lh.t.} = a_{h.t.} (\alpha_{h.t.} + n\delta) \quad (3.23)$$

where $a_{h.t.} = \frac{\partial C_{Lh.t.}}{\partial \alpha_{h.t.}}$ is the derivative of the curve $C_{Lh.t.} = f(\alpha_{h.t.})$ and n is the so-called "coefficient of elevator efficiency". To determine the coefficient n , we may use the empirical formula

$$n = \sqrt{\frac{S_0}{S_{h.t.}} \left(1 - \frac{S_{ax.c.}}{S_0}\right)} \approx 0,9 \sqrt{\frac{S_0}{S_{h.t.}}} \quad (3.24)$$



where S_B is the area of the elevator;

$S_{h.t.}$ = the area of the horizontal tail surfaces;

$S_{ax.c.}$ is the area of the so-called axial compensation*,

i.e., that part of the elevator area located in front of the axis of rotation (Fig.3.34).

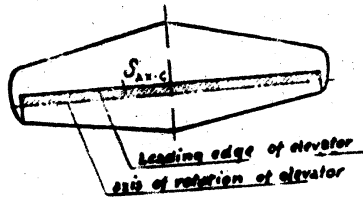


Fig.3.34 - For Determining the
Coefficient of Elevator
Efficiency

For example, if the elevator area amounts to 40% of the area of the horizontal tail surfaces, and the area of compensation equals 20% of the elevator area, eq.(3.24) we will yield a coefficient of elevator efficiency equal to:

$$n = \sqrt{0,4 \cdot 0,8} \approx 0,57;$$

$$n \approx 0,9 \sqrt{0,4} \approx 0,57.$$

In this way, a 1° deflection of the elevator is equal to a change of 0.57°

in the angle of attack of the entire tail.

In the region of $C_{L \max}$ of the horizontal tail surfaces, the linear dependence of $C_{Lh.t.}$ on δ is impaired, and eq.(3.23) is no longer correct. Owing to the downwash, however, the horizontal tail surfaces do not operate at large angles of attack in the principal states of flight, and in practice eq.(3.23) may be used in all cases for the calculation of $C_{Lh.t.}$ *

Influence of the Compressibility of Air on the Elevator Efficiency

The above expression for the coefficient of elevator efficiency, eq.(3.24), is accurate for subcritical Mach numbers. With the appearance of a shock wave on the

* For more details on the compensation, cf. infra, Chapter V.

wing, the lift coefficient, at constant angle of attack, begins to decline as a result of the nonuniform development of the shock on the upper and lower surfaces. On transition to supersonic flying speeds ($M > 1$), the lift coefficient again increases. With further increase of M , however, it once more decreases, following the law expressed by eq.(2.37) of Chapter II.

After a zone of supersonic velocities has formed on the tail, the deflection of the elevator is no longer able to vary the pressure distribution over the entire tail, since the disturbances in the flow caused by the deflected elevator are unable

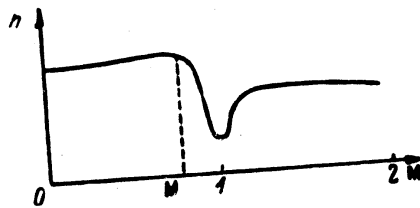


Fig.3.35 - Relation of the Coefficient of Elevator Efficiency to the Mach Number M

to penetrate through the front of sonic velocities. When the elevator is deflected in the region of transcritical Mach numbers, the pressure distribution varies only on the downstream part of the tail profile. The distribution of the pressures along the upstream part of the profile, however, remains unchanged. A local sonic velocity is reached first at about the point of the profile contour at which the rarefaction was greatest at small Mach num-

bers. When the Mach numbers of the inflowing stream increase above M_{crit} , a region of supersonic velocities on the profile contour is propagated toward the trailing edge of the profile. Accordingly, the pressure distribution on deflection of the elevator varies over an ever smaller portion of the tail profile. In other words, the elevator efficiency begins to drop when the Mach number of the tail exceeds the critical value. Experiment shows that, at an unfavorable tail profile and at small angles of elevator deflection, the tail moment may decrease to zero or even change its sign, beyond the critical Mach numbers. Under such conditions, the elevator

must be deflected through a larger angle in order to create a moment of the necessary value at subcritical Mach numbers.

At $M > 1$, the elevator efficiency is less than at subcritical Mach numbers. If we neglect the influence of the viscosity of air, then theoretically, at $M > 1$, we have the following expression for the coefficient n :

$$n \approx \frac{S_B}{S_{h.t.}}$$

However, at subcritical Mach numbers, the coefficient M was approximately proportional to the square root of this ratio.

The relationship between the coefficient of elevator efficiency and the Mach number is shown schematically in Fig. 3.35. As will be seen, one and the same elevator is only about half as efficient at supersonic Mach numbers as at subcritical ones. This fact, in conjunction with the already mentioned shift in position of the aerodynamic center at supersonic Mach numbers from about 25 to 50% of the chord require the adoption of special measures to ensure good controllability of the aircraft at both small and large Mach numbers.

General Expression for the Moment of the Horizontal Tail Surfaces

If L denotes the distance from the center of gravity of the aircraft to the center of pressure of the tail, we have the following expression for the moment of the horizontal tail surfaces relative to the axis or passing through the center of gravity of the aircraft:

$$M_{z \text{ h.t.}} = Y_{h.t.} L \quad (3.25)$$

According to the rule of signs adopted, this moment, for an aircraft of conventional design, must be taken with a minus sign, while for an aircraft of the duck type, it is taken with a plus sign.

In the general case, when the elevator is deflected, the tail profile can be considered concave since the center of pressure of the horizontal tail surfaces is

shifted along its chord on variation in the C_L of the tail. For this reason, speaking generally, the arm L is a variable quantity. However, $L = \text{const}$ may be taken without great error. Indeed, in modern aircraft, the tail area amounts to 20-25% of the wing area, while the distance from the center of gravity of the aircraft to the axis of the elevator hinges $L_{h.t.}$ is about 2.5 to 3 times as great as the mean wing chord. If we assume that the displacement of the center of pressure of the horizontal tail surfaces relative to the line of elevator hinges, within the limits of the flight angles of attack, amounts to 20% of its chord, then the value of L will vary approximately within the limits $(2.75 \pm 0.1)b_A$. For this reason, with an accuracy sufficient for practical purposes, we may take

$$L \approx L_{h.t.} = \text{const}$$

The lift of the horizontal tail surfaces may be represented in the form

$$Y_{ht} = c_{i,ht} S_{ht} \frac{\rho V_{ht}^2}{2} \quad (3.26)$$

where $V_{h.t.}$ is the velocity of the relative airflow at the tail. This velocity is connected with the speed of flight, in the general case when the tail is washed by the slipstream, by the relation

$$V_{h.t.} = V \sqrt{k_1} \quad (3.27)$$

On passing from the moment to the moment coefficient of the aileron, eq.(3.25) will yield, taking eqs.(3.26) and (2.27) into consideration,

$$M_{zh.t.} = - \frac{S_{h.t.} L_{h.t.}}{Sb_A} k_1 c_{i,ht} \quad (3.28)$$

The factor $\frac{S_{h.t.} L_{h.t.}}{Sb_A}$, representing the static moment of the aileron area related to the wing area and the mean aerodynamic chord, is denoted by A .

Since the true angles of attack of the tail are less than the angles of attack



of the wing, there is a linear dependence between $C_{Lh.t.}$ and $\alpha_{h.t.}$, within the limits of the flying range of angles of attack, so that we may put

$$C_{Lh.t.} = a_{h.t.} (\alpha_{h.t.} = n\delta)$$

Thus, the expression for the moment coefficient of the aileron, for the most general case, takes the following form:

$$m_{z \text{ h.t.}} = -k_e A a_{h.t.} (\alpha = \varphi - \epsilon + n\delta) \quad (3.29)$$

The derivative $a_{h.t.}$ of the curve $C_{Lh.t.} = f(\alpha_{h.t.})$ depends on the elongation of the horizontal tail surfaces. This relation is shown in Fig.3.36.

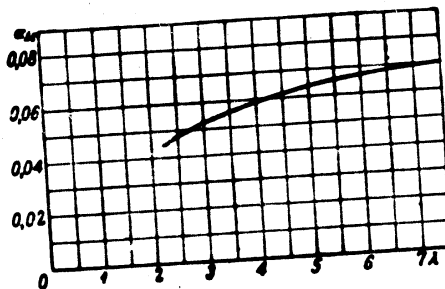


Fig.3.36 - Relation of $a_{h.t.}$ to $\lambda_{h.t. \text{ eff}}$

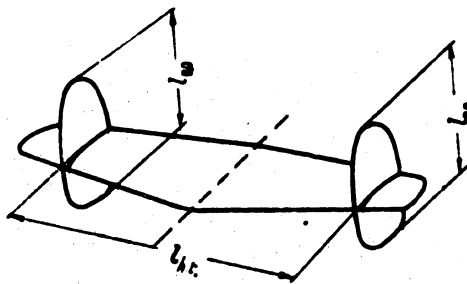


Fig.3.37 - For Determining $\lambda_{h.t. \text{ eff}}$ for a Two-Fin Tail



In some airplane designs, the vertical tail surfaces are designed in the form of two plates (Fig.3.37) located at the ends of the horizontal tail surface. This position of the vertical tail surface improves the efficiency of the horizontal tail surface. The elongation of the horizontal empennage for this case must be determined by the empirical formula

$$m_{z.h.t.} = -kA_{h.t.} (\alpha + \varphi - \epsilon_{kp} - \epsilon_f + n\delta)$$

where $\lambda_{h.t.}$ is the geometric elongation of the horizontal tail surface;

$l_{v.t.}$ is the height of the vertical tail surface (disks);

$l_{h.t.}$ is the distance between the fins (cf. Fig.3.37).

When a propeller aircraft is gliding, or when an airplane with a jet engine is in flight, the tail is not washed by the slipstream and there is no downwash from the propeller. For these cases, $m_{zh.t.}$ is expressed by the formula

$$m_{zh.t.} = kA_{h.t.} (\alpha + \varphi - \epsilon_{kp} - \epsilon_f + n\delta)$$

On substituting here the expression for ϵ_{kp} by eq.(3.18'), we have

$$m_{z.t.} = -kA_{h.t.} (\alpha + \varphi - Dc_p - \epsilon_f + n\delta). \quad (3.30)$$

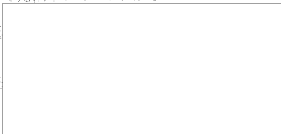
where, for shortness, we use the notation

$$D = \frac{46.3}{\lambda} \lambda_1 \lambda_2 \lambda_3. \quad (3.31)$$

Confining ourselves to the region of linear variation of the curve $C_L = f(\alpha)$ and noting that ϵ_f is a constant quantity, we are able to conclude that, in first approximation, $m_{zh.t.}$ is a linear function of the C_L of the aircraft or of α^0 . For calculating aircraft of the duck type it may be considered, with an accuracy sufficient for practical purposes, that the angle of downwash at the ailerons is equal to zero and that there is no deceleration of velocity. For such an aircraft, $m_{zh.t.}$

can be determined by the formula

$$m_{e.a.t.} = A_{e.a.t.}(s + \varphi + ns). \quad (3.32)$$



CHAPTER IV

TOTAL MOMENT OF AIRCRAFT IN STEADY
RECTILINEAR FLIGHTMoment Coefficient Acting on the Aircraft

The total moment coefficient acting on an aircraft in steady rectilinear flight is the algebraic sum of the moment coefficient of an aircraft without horizontal tail surface and the moment coefficient of the horizontal tail surface:

$$m_z = m_{z\text{bh.t.}} + m_{z\text{h.t.}}$$

In the simplest case, when $\bar{y}_T = 0$, $\bar{y} = 0$, and the effect of the slipstream on the tail is absent (for example, in an aircraft with jet engines or in an airplane flying with windmilling propellers), eqs.(2.59) and (3.30), for an aircraft of conventional design, will give

$$m_z = m_{z\text{bh.t.}} - (x_{\text{Pbh.t.}} - x_T)C_L - kA_{\text{h.t.}}(\alpha + \varphi + \varepsilon + n\delta) \quad (4.1)$$

It has been shown above, in Chapter III, that the angle of downwash ε may be considered a linear function of the coefficient C_L . Within the limits of the flight angles of attack, C_L is a linear function of the angle of attack α , and therefore the moment coefficient m is a linear function of m_z or C_L . The relation between m_z and C_L is plotted on the diagram in the form of a family of parallel lines. The value of the dihedral of the tail φ or the value of the angle of deflection of the rudder δ or, finally, the sum $\varphi + n\delta$, as may be seen from eq.(4.1), may serve as a parameter of the family of such straight lines for a given aircraft. Figure 4.1 shows roughly the form of the relation $m_z = f(\alpha)$.

With increasing values of C_L and its approach to $C_{L\text{max}}$, as indicated in Fig.4.1, the linearity of $m_z = f(\alpha)$ is impaired, and on the curve a "spoon", may sometimes appear, which has already been mentioned in Chapter II. It must be borne

in mind that, in this case, the "spoon" is not formed for the reasons indicated in Chapter II, since here $\bar{y}_T = 0$. The impairment of linearity in the case of a low plane is explained by the fact that, at sufficiently high angles of attack, the

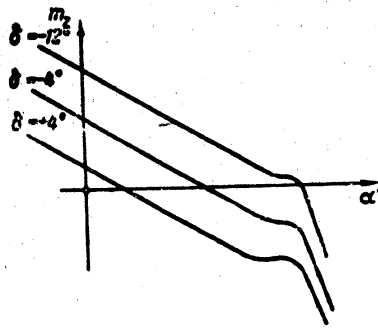


Fig.4.1 - Approximate Relation $m_z = f(\alpha)$

horizontal tail surface enters the zone of the most intense velocity deceleration (Fig.4.2), causing the deceleration coefficient to drop sharply and the absolute value of the coefficient m_z to decrease correspondingly.

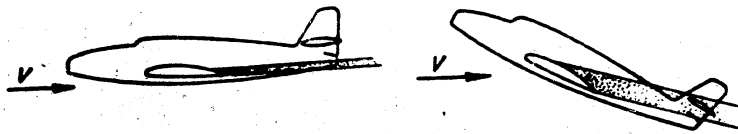
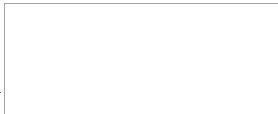


Fig.4.2 - Zone of Deceleration at Small and Large Values of α

Equivalents of Elevator Deflection and Variation
in Tail Dihedral

It has been shown above that the displacement of the curves $m_z = f(C_L)$ or



$m_a = f(\alpha)$ is affected by the magnitude of the algebraic sum $\varphi + n\delta$, which may be denoted by

$$\varphi_e = \varphi + n\delta.$$

With respect to the slope of the curves m_a , it makes no difference whether φ_e is varied by varying φ or by varying δ . But for a variation of φ_e by one and the same value, different variations of the values of φ and δ are required. For example, if the coefficient of the elevator efficiency is $n = 0.6$, then in order to create $\varphi_e = 3^\circ$ it is necessary either to vary the dihedral of the entire tail assembly by $\varphi = 3^\circ$, or to deflect the elevator through the angle $\delta = \frac{3}{0.6} = 5^\circ$.

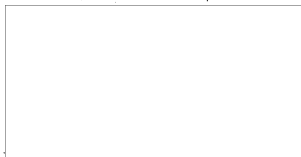
It follows from this that the longitudinal motion of the aircraft may be controlled either by deflecting the elevator or by resetting the stabilizer.

A stabilizer that can be moved during flight is, generally speaking, undesirable because of design difficulties and because of aerodynamic complications in the controllability and stability, produced by any deflection of large surfaces. In some cases, however, the use of a fully deflectable tail assembly is expedient. Thus, if an unskillful selection of the tail profile causes a drop in the efficiency of the elevator at high Mach numbers, it may be more advantageous to vary the angle of setting of the entire tail instead of deflecting the elevator.

Aerodynamic Center of Aircraft, Neutral Centering

The aerodynamic center of the aircraft, by analogy with the a.c. of the wing, is a term we will use for designating that point on the wing chord with respect to which the moment coefficient of the entire aircraft does not depend on the coefficient C_L .

To determine the position of the aircraft a.c., we will take the derivative of eq.(4.1) with respect to C_L , setting $k = \text{const.}$



$$m_i' = \frac{dm_i}{d\alpha_i} = -(\bar{x}_{P.A.C.} - \bar{x}_c) - A a_{h.t.} \left(\frac{1}{a} - D \right). \quad (4.2)$$

where, for brevity, the following notation is used:

$$a = \frac{dx_c}{d\alpha_i}$$

$$D = \frac{a}{a_{h.t.}}$$

When the center of gravity coincides with the aerodynamic center of the aircraft, the derivative $\frac{dm_i}{d\alpha_i}$ must vanish. From this condition we obtain, setting $\bar{x}_T = \bar{x}_{Pc}$,

$$\bar{x}_{Pc} = \bar{x}_{P.A.C.} + A a_{h.t.} \left(\frac{1}{a} - D \right). \quad (4.3)$$

In view of the fact that $\frac{1}{a}$ is always greater than D , the a.c. of an aircraft of conventional design is always located behind the a.c. of an aircraft without horizontal tail surface. On the other hand, in a duck type aircraft, for which the moment coefficient of the horizontal tail surface must be taken with the plus sign, the a.c. of the entire aircraft is located in front of the a.c. of an aircraft without horizontal tail surface. The displacement of the a.c. of the entire aircraft, relative to the a.c. of an aircraft without tail, reaches a very appreciable value. For example, if $\bar{x}_{P.h.t.} = 0.18$, then, at $k = 0.9$, $A = 0.5$, $a_{h.t.} = 0.06$, $a = 0.07$, and $D = 8$, we will have

$$\bar{x}_{Pc} = 0.18 + 0.9 \cdot 0.5 \cdot 0.06 \frac{1}{0.07} = 0.35.$$

On the basis of eqs.(4.1) and (4.2), the moment coefficient of the aircraft may be represented in the following form

$$m_i = m_{i,0} + \left(\frac{dm_i}{d\alpha_i} \right) \epsilon_{\alpha_i} \quad (4.4)$$

where

$$m_{z0c} = m_{z0a.c.} - kAa_{Ac}(\alpha_0 + \varphi - \epsilon_f + \pi^2) \quad (4.5)$$

and corresponds to $C_L = 0$.

It will be seen from eq.(4.2) that the angle of tail setting and the angle of elevator deflection δ do not affect the degree of longitudinal static stability of the aircraft; they affect only the value m_{z0c} , as follows from eq.(4.5).

If the center of gravity of the aircraft coincides with the a.c. of the aircraft, then, in accordance with the definition of the concept of the aerodynamic center, the moment coefficient of the aircraft will not depend on C_L . In other words, in this case, the aircraft will be statically neutral.

Now let

$$\bar{x}_c = x_{FAAc} = x_{FAAc} + kAa_{Ac}\left(\frac{1}{\sigma} - D\right) \quad (4.3')$$

If we introduce this expression in eq.(4.2), we will see that

$$m_{z'c} = \frac{\partial m}{\partial x_c} = 0.$$

The centering of an aircraft which satisfies the condition (4.3') is called neutral centering.

A somewhat different expression may be obtained for defining neutral centering.

With this in mind, let us write eq.(4.2), once for actual centering and once for neutral centering

$$m_{z'c} = -(x_{FAAc} - x_c) - kAa_{Ac}\left(\frac{1}{\sigma} - D\right);$$

$$0 = -(x_{FAAc} - x_{c0}) - kAa_{Ac}\left(\frac{1}{\sigma} - D\right).$$

By subtracting the first expression from the second, we get

STAT

$$x_{T,n} = x_T - m_z^c \quad (4.3^{**})$$

Knowing the degree of longitudinal static stability of an aircraft at a given centering, it is easy to determine the neutral centering from eq.(4.3**). Let, for example, at $x_T = 0.25$, $m_z^c = -0.10$. Then,

$$x_{T,n} = 0.25 + 0.10 = 0.35.$$

It is obvious that, to secure longitudinal static stability, the center of gravity of the aircraft must be moved forward with respect to its position at neutral centering.

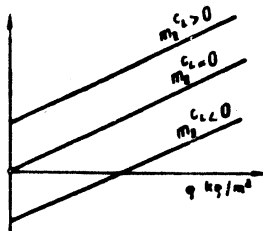


Fig.4.3 - Approximate Relations $M_z = f(q)$

Let us now determine the relationship between the total longitudinal moment acting on the aircraft and the velocity head. Obviously,

$$M_z = m_z S b_A q = m_{z0} S b_A q + \left(\frac{\partial m_z}{\partial c_z} \right) c_z S b_A q.$$

But in horizontal flight or in flight at low angles θ of inclination of the flight path, as is well known,

$$C_L S q = G$$

so that

$$M_z = m_{z0} c S b_A q + \left(\frac{\partial m_z}{\partial c_z} \right) G b_A. \quad (4.6)$$

The linear relation of M_z and q has been obtained (Fig.4.3). A variation in the degree of longitudinal static stability of an aircraft does not affect the angular

STAT

coefficient of the straight line $M_x = f(q)$, and changes only the segment cut off by the straight line on the ordinate.

Balancing of Aircraft with Respect to Moment

In Chapter I we already used the concept of aircraft balancing. Let us now find the analytical expression for the balancing angle of deflection of the elevator δ . From eq.(4.1) we find* that the points of equilibrium of the aircraft, at which $m_x = 0$,

$$\delta = \frac{1}{n} \left[\frac{m_{\delta} \Delta A_L}{k A a_{\delta L}} - \alpha_0 + \varepsilon_f - \varphi - \left(\frac{x_F b_{\delta L} - x_i}{k A a_{\delta L}} + \frac{1}{a} - D \right) c_L \right] \quad (4.7)$$

Equation (4.7) shows that the balancing angle of deflection δ of the elevator is a linear function of C_L . Now, bearing in mind that

$$\varepsilon = \varepsilon_f + \varepsilon_{sp} = \varepsilon_f + D c_L$$

and

$$\alpha = \alpha_0 + \frac{c_L}{a},$$

eq.(4.7) may be rewritten in the form

$$\delta = \frac{1}{n} \left[\frac{m_{\delta} \Delta A_L}{k A a_{\delta L}} - \alpha_0 + \varepsilon_f - \varphi - \left(\frac{x_F b_{\delta L} - x_i}{k A a_{\delta L}} + \frac{1}{a} - D \right) c_L \right] \quad (4.8)$$

or in the form

$$\delta = \frac{1}{n} \left[\frac{m_{\delta} \Delta A_L}{k A a_{\delta L}} - \alpha_0 + \varepsilon_f - \varphi + \frac{1}{k A a_{\delta L}} \left(\frac{\partial m_x}{\partial c_L} \right) c_L \right] \quad (4.8^*)$$

*Hereafter, unless otherwise specified, all our reasoning will relate to an aircraft of conventional design, i.e., to an aircraft with the horizontal tail surface located behind the wing.

Figure 4.4 schematically shows the relation of δ to C_L . For a stable aircraft, δ decreases as C_L increases. On the other hand, for an unstable aircraft, δ increases with increasing C_L . We now present still another expression for the moment coefficient of an aircraft m_z , which may be easily obtained from eq.(4.1). On taking the partial derivatives of this expression with respect to C_L and to δ , we may write

$$m_z = m_{z0} + k A a_{\delta} \delta + k A a_{C_L} C_L + m_z^{\delta} \delta + m_z^{C_L} C_L \quad (4.9)$$

where

$$m_z^{\delta} = -k A a_{\delta} n \quad (4.10)$$

On the basis of eq.(4.1) we may write that still another expression for δ :

$$\delta = -\frac{m_{z0} + k A a_{C_L} C_L}{m_z^{\delta}} - \frac{1}{n} (\alpha - \epsilon_{sp} - \epsilon_f + \varphi)$$

The Balancing Curve

As already mentioned, the term balancing curve is used for a curve showing the dependence of a balancing angle of elevator deflection on a parameter characterizing the state of flight. The flying speed V or the velocity head q may be taken as

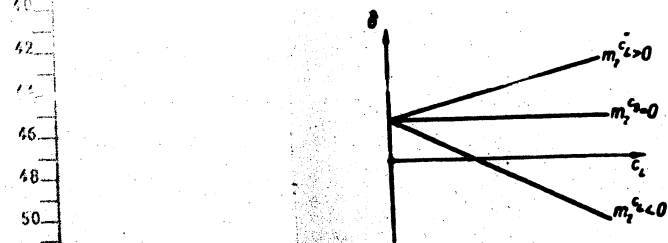


Fig.4.4 - Approximate Relation $\delta = f(C_L)$

such parameter. If the deflection of the elevator follows the law of the balancing curve, then the aircraft will be in equilibrium at all flying speeds. In view of the fact that, in steady rectilinear flight differing only slightly from horizontal flight, the equation

$$C_L = \frac{G}{Sq}$$

is valid, let us rewrite eq.(4.8') in the following form

$$\delta = \frac{1}{n} \left[\frac{m_{\delta} \Delta a_{\delta}}{k A a_{\delta t}} - \alpha_0 + \epsilon_f - \varphi + \frac{G}{S} \frac{1}{k A a_{\delta t}} m_z^{c_L} \frac{1}{q} \right], \quad (4.11)$$

where

$$m_z^{c_L} = \frac{\partial m_z}{\partial c_L}$$

This expression shows that, for an aircraft with longitudinal static stability, for which $m_z^{c_L} > 0$, the angle of deflection of the elevator required for balancing, increases with the velocity head q , since the last summand within the brackets of eq.(4.11) is negative in sign but decreases in absolute value with increasing q .

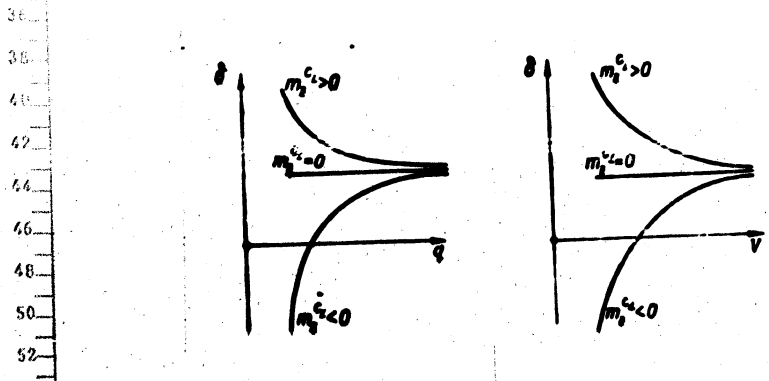


Fig.4.5 - Approximate Form of the Relation $\delta = f(q)$ and $\delta = f(V)$

0 For a statically unstable aircraft, $m_z^c > 0$, while δ decreases with increas-
 2 ing q . For a neutral aircraft, δ does not depend on the velocity head. Figure 4.5
 4 shows the approximate form of the balancing curves. As demonstrated below, the
 6 force applied by the pilot to the control stick determines, to a considerable
 8 extent, the value of the angle of deflection δ of the elevator. To reduce the mag-
 10 nitude of the elevator deflection δ , the angle of setting of the tail unit φ can be
 12 correspondingly increased. If, at any state of horizontal steady flight it is
 14 necessary to have $\delta = 0$, then the corresponding value of φ can be obtained from
 16 eq.(4.11) or eq.(4.8). From these equations we find, by equating their right-hand
 18 sides to zero,
 20

$$22 \quad \varphi = \frac{m_{\delta} \Delta A_L}{b A_{\delta} A_L} - \alpha_0 + \epsilon_f + \frac{G}{S} \frac{m_z^c}{b A_{\delta} A_L} \frac{1}{q_0} \quad (4.12)$$

24
 26
 28 or

$$30 \quad \varphi = \frac{m_{\delta} \Delta A_L}{b A_{\delta} A_L} - \alpha_0 + \epsilon_f + \frac{1}{b A_{\delta} A_L} m_z^c c_L \epsilon \quad (4.12')$$

32
 34 where C_L and q_0 correspond to the balanced state of flight at which $\delta = 0$. From
 36 eq.(4.2) it follows that, for a statically stable aircraft in which $m_z^c < 0$, the
 38 higher the velocity head q_0 the higher will be the angle of tail setting φ . For a
 40 statically unstable aircraft, we obtain the opposite relation: the higher q_0 , the
 42 smaller must be the required angle φ . Indeed, in stable aircraft, the last term of
 44 eq.(4.12) is negative and decreases in absolute value with increasing q_0 . This
 46 leads to an increase in the angle of tail setting φ . In unstable aircraft, the
 48 picture is reversed.
 50

52 Maximum Permissible Forward Centering

54 As shown in Fig.4.4, negative elevator deflection angles are necessary for
 56

ensuring the equilibrium of a stable aircraft at high values of C_L .

It follows from eq.(4.8) that the negative angle of deflection of the elevator required for balancing at high C_L close to $C_{L \max}$, increase in absolute value when the center of gravity of the aircraft is shifted forward. On determining the value of \bar{x}_T from eq.(4.7), we will have

$$\bar{x}_T = \bar{x}_{P \Delta A \Delta} + \left\{ k A a \bar{n} + k A a_{\Delta} [\alpha - \epsilon + \varphi] - m_{\Delta} \Delta A \Delta \right\} \frac{1}{c_z} \quad (4.13)$$

If the maximum negative angle of elevator deflection is limited, a certain maximum permissible centering of the aircraft, $\bar{x}_{T \text{ form.}}$ at which it is still possible to balance the aircraft at the assigned angle δ . For any position of the center of gravity forward of $\bar{x}_{T \text{ form.}}$, balancing is no longer possible.

A study of eq.(4.13) leads to the conclusion that the value of $\bar{x}_{T \text{ form.}}$ will be the greater, the smaller C_L , the larger in absolute value the negative quantity $m_{\Delta} b \text{ h.t.}$, and the smaller the downwash ϵ . We know from Chapter II that the maximum value of $m_{\Delta} b \text{ h.t.}$ is obtained when the flaps are deflected at landing. In this case the smallest angle of downwash ϵ is also obtained. Thus the case of calculating the maximum permissible forward centering will be the case of landing with deflected flaps. The value of $\bar{x}_{T \text{ form.}}$ determined from this condition will be more than sufficient to ensure all remaining attitudes.

As an example, let us determine the maximum permissible forward centering for the following conditions:

- Coordinate of a.c. of aircraft without horizontal tail surface, with deflected flaps: $\bar{x}_{P \text{ h.t.}} = 0.16$;
- Coefficient of velocity deceleration on landing $k = 0.9$;
- Coefficient of static tail moment $\lambda = 0.5$;
- Derivative curve of coefficient of tail lift $a_{\Delta} \text{ h.t.} = 0.06$;
- Moment coefficient without horizontal tail surface, with extended flaps $m_{\Delta} b \text{ h.t.} = 0.1$;

Landing angle of attack $\alpha_{\text{land.}} = 14^\circ$;

Landing value of $C_L = 1.4$;

Angle of downwash on landing, allowing for influence of ground, $\epsilon_{\text{land.}} = 6^\circ$;

Angle of dihedral of tail $\varphi = -1^\circ$;

Maximum permissible angle of elevator deflection on landing $\delta_{\text{max}} = -15^\circ$;

Coefficient of elevator efficiency $n = 0.58$.

From eq.(4.13) we obtain

$$x_{T \text{ form.}} = 0.16 - \left\{ 0.9 \cdot 0.5 \cdot 0.06 \cdot 0.58 \cdot 15 - 0.9 \cdot 0.5 \cdot 0.06 (14 - 6 - 1) - 0.1 \right\} \frac{1}{1.4} = 0.20.$$

Thus, for the initial data taken as an example, the maximum permissible forward centering is 20% of the MAC. At the same initial data, but in flight at minimum speed with undeflected flaps, we would have, at $m_{z \text{ @ h.t.}} = -0.02$, $\epsilon = 9^\circ$, $C_L = 1.0$

$$x_{T \text{ form.}} = -0.05$$

i.e., the permissible centering would be far more forward.

A stabilizer, movable during flight, is a powerful means for extending the permissible forward centering. In the preceding example, if the pilot had been able to vary the angle of stabilizer setting on landing, by bringing it down to -5° , then the permissible forward centering would have been shifted from $\bar{x}_{T \text{ form.}} = 0.20$ to $\bar{x}_{T \text{ form.}} = 0.12$.

Later, in Chapter X, we will return to the case of landing with deflected flaps, in connection with the selection of the degree of stability of the aircraft; for the present, let us turn to the influence of the compressibility of the air on the moment of the aircraft.

Aircraft Moment at High Flying Speeds

In Chapters II and III, in analyzing the moment of an aircraft without a horizontal tail surface and of one with a horizontal tail surface, we considered the

influence of the compressibility of air, manifested at high flying speeds, on the moment characteristics. Let us apply the results we obtained there to analyzing the question of the influence of the compressibility of air on the moment coefficient of the entire aircraft.

As we have seen, at $M < M_p$, the influence of compressibility is negligible and mainly causes an increase of the coefficients a and $a_{h.t.}$ at approximately the same ratio $1 : 1 - M^2$. Thus, in this region of Mach numbers, a certain small reduction in static stability occurs, which is caused by the increase of the term $kAa_{h.t.}$ in eq.(4.2).

At $M < M_{kp}$, the wing aerodynamic center is shifted rearward in most cases, the coefficient m_x^0 increases in absolute value, and the derivative a of the curve $C_L = f(a)$ of the wing and the coefficient D in the expression for the downwash, decrease. As a net result, the derivative m_x^L increases in absolute value, and the longitudinal static stability of the aircraft also increases, as shown in eq.(4.2). Accordingly, the value of the balancing angle of elevator deflection δ required for equilibrium at a certain value of C_L also decreases. This decrease in δ , at an unfavorable combination of the design aerodynamic parameters in aircraft, may prove to be so considerable that instead of the increase of δ with increasing flying speed, as follows from eq.(4.11), we may obtain a drop in δ , and at high flying speeds we might even require negative angles of δ . In this case, the pilot would sense a tendency of the aircraft to spontaneously increase its speed; at this instant, the so-called "pulling into a dive" on which we shall dwell in more detail below, in Chapter II, appears. Figure 4.6 gives the approximate character of the variation of δ as a function of flying speed for this case.

At supersonic flying speeds, the wing a.c. is shifted to about 50% of the mean aerodynamic chord, the downwash at the tail vanishes, the coefficient of elevator

* If we neglect the deceleration of the velocity at the tail.

efficiency decreases and, as the M numbers increase, the coefficients a and $a_{h.t.}$ decline. As a result there is a distinct change in the level of longitudinal static stability of the aircraft and of the balancing curve.

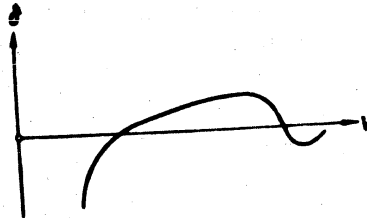


Fig.4.6 - Form of the Balancing Curve on Going into a Dive

In the special case when the aircraft wing is composed of symmetric profiles and the fuselage is a body of revolution, whose aerodynamic center coincides with that of the wing, we have

$$a_0 = 0, \quad m_{s.o.b.h.t.} = 0$$

so that eq.(4.8) takes the following form

$$\delta = \frac{1}{M} \epsilon \varphi - \varphi - \left(\frac{\bar{x}_{f.b.h.t.} - \bar{x}_T}{K a_{h.t.}} + \frac{1}{M} - D \right) C_L \quad (4.14)$$

For subcritical Mach numbers let us take, for a certain medium aircraft,

$$\pi \approx 0,9 \sqrt{\frac{s_0}{s_{h.t.}}} = 0,6; \quad k = 0,9; \quad a = \frac{0,07}{\sqrt{1-M^2}};$$

$$\epsilon_f \approx 1,0^\circ; \quad A = 0,5; \quad D = 8;$$

$$\bar{x}_T \approx 0,24; \quad a_{h.t.} \approx \frac{0,06}{\sqrt{1-M^2}}; \quad \varphi = 0; \quad \bar{x}_c \approx 0,22.$$

At $M = 0.6$ and $C_L = 0.2$, we have

$$a = 0.0875; \quad a_{ht} = 0.073;$$

$$\delta = \frac{1}{0.6} \left[1.0 - \left(\frac{0.24 - 0.22}{0.9 \cdot 0.5 \cdot 0.073} + \frac{1}{0.0875} - 8 \right) 0.2 \right] \approx +0.33^\circ.$$

For supersonic Mach numbers, for example, for $M = 1.6$, we have, for the same aircraft,

$$n \approx 0.36; \quad k \approx 1.0; \quad a \approx \frac{4}{57.3 \sqrt{M^2 - 1}} = 0.056$$

$$x_F = 1.0; \quad x_F \approx 0.5; \quad a_{ht} \approx 0.056 \text{ and } D = 0;$$

At the same flying height, C_L varies in the ratio

$$\frac{a_1^2}{a_2^2} = \left(\frac{0.6}{1.0} \right)^2 = 0.14.$$

Consequently, for

$$M = 1.6$$

$$\delta = \frac{1}{0.36} \left[1.0 - \left(\frac{0.36 - 0.22}{0.5 \cdot 0.056} + \frac{1}{0.056} \right) 0.028 \right] \approx -0.61^\circ.$$

This example gives an idea of the change in the balancing curve on transition from subcritical Mach numbers to supersonic Mach numbers. Obviously, the balancing angle of elevator deflection may even change its sign. Physically, this is explained as follows:

As a result of the rearward shift of the aerodynamic center of the wing, a moment arises tending to diminish the angle of attack. To balance this moment, the tail must be given a moment tending to increase the angle of attack, i.e., the downward elevator deflection must be reduced. Because of the decrease or even complete disappearance of the downwash at $M > 1$, the angle of attack of the tail in-

increases and, at constant, elevator deflection, a moment tending to decrease the angle of attack during a dive appears on the tail. All this taken together, leads to a substantial change in the balancing angle of elevator deflection.

Influence of Horizontal Tail Surface on the Aircraft Lift

Determination of polar curves in flight tests of an aircraft gives gives operating polars that differ more or less sharply from the polar obtained in tests of geometrically similar model of the same aircraft in the wind tunnel at the same Reynolds and Mach numbers.

This is explained by the fact that, in model wind-tunnel tests, the elevators occupy one and the same position at all values of C_L ; usually the polar are determined at $\delta = C$. In this case, equilibrium of moments is not obtained at all values of C_L , since each position of the elevator corresponds to a unique balancing value of C_L . In determining the polar of aircraft in flight from a series of steady states at various speeds, i.e., at various values of C_L , each point of the polar corresponds to its own angle of elevator deflection δ , which may be determined from the balancing curve. The deflection of the elevator introduces certain changes in the lift and drag of the aircraft, a fact that explains the difference in the polars.

Let us determine the magnitude of the change in lift of the whole aircraft in flight at a displacement by the balancing curve compared to a lift of the aircraft without horizontal tail surface.

As shown above, a prerequisite for displacement by the balancing curve is equilibrium of the moments acting on the aircraft. Consequently, at any value of C_L , the condition

$$M_z = M_{zh.t.} + M_{zh.t.} = 0$$

must be met, whence

$$M_{zh.t.} = -M_{zh.t.}$$

The moment coefficient of the horizontal tail surface may be represented in the form

$$m_{z,At} = \pm \frac{V_{At} L_{At}}{S_{\Delta} q} \quad (4.15)$$

while, for an aircraft with horizontal tail surface located behind the wing, this expression must be taken with a minus sign, and for an aircraft of the duck type, with a plus sign. The ratio $\frac{Y_{h.t.}}{S_q}$ entering into eq.(4.15) is nothing other than the additional coefficient of lift, supplementing the lift coefficient of the aircraft without tail; this additional coefficient, ΔC_L is produced by the horizontal tail surface, relative to the wing area and to the velocity head determined from the flying speed.

For this reason we can replace eq.(4.15), by

$$m_{z,At} = \pm \Delta C_L \frac{L_{At}}{b_s}$$

whence

$$\Delta C_L = \pm \frac{b_s}{L_{At}} m_{z,At} \quad (4.16)$$

where the plus sign refers to an aircraft of the usual design and the minus sign to a duck type craft.

According to eq.(2.59) in Chapter II,

$$m_{z,bh.t.} = m_{zobh.t.} - (\bar{x}_{Fbh.t.} - \bar{x}_T) C_L$$

On introducing this expression in eq.(4.16), we obtain

$$\Delta C_L = \pm \frac{b_s}{L_{At}} (m_{zobh.t.} - (\bar{x}_{Fbh.t.} - \bar{x}_T) C_L) \quad (4.17)$$

Equation (4.17) contains neither the area of the horizontal tail surface $S_{h.t.}$ for the angle of tail setting ϵ , nor the angle of elevator deflection δ . This is understandable enough since, under the condition of equilibrium, the tail lift

necessary for equilibrium is entirely determined by the moment of the aircraft without tail.

Let us evaluate the additional lift produced by the horizontal tail surface. With this in mind, let us put

$$\frac{b_A}{L_{ht}} \approx 0.4; m_{\Delta h.t.} \approx -0.02; \bar{x}_{r.b.h.t.} \approx 0.18$$

For an aircraft of conventional design, on the average, we may take $\bar{x}_T \approx 0.22$. In this case,

$$\Delta c_L = 0.4[-0.02 + 0.04c_L] = -0.008 + 0.016c_L$$

For an aircraft of the duck type, $\bar{x}_T \approx -0.05$ and

$$\Delta c_L = -0.4[-0.02 - 0.23c_L] = 0.008 + 0.112c_L$$

For various values of C_L we obtain the following values of ΔC_L

	C_L	0.1	0.3	0.6	0.9	1.2
ΔC_L	Standard design	-0.008	-0.008	+0.002	+0.006	-0.011
	Duck design	+0.019	+0.042	+0.075	+0.109	+0.142

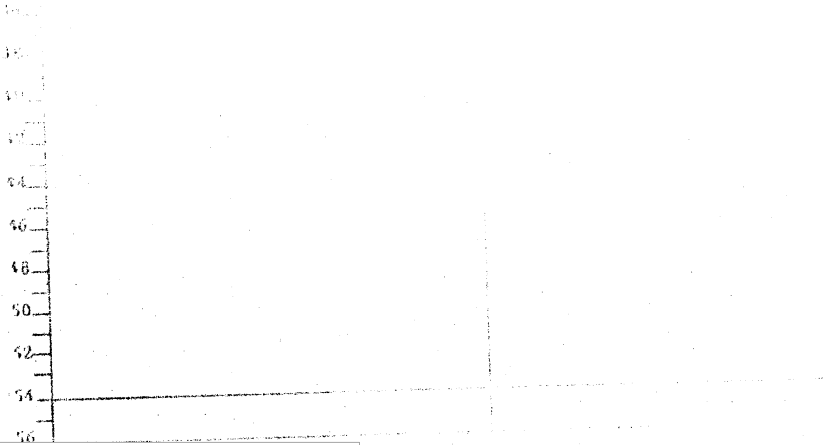
This Table shows that the influence of the horizontal tail surface on the lift is small for an airplane of standard design. For this reason, the influence of C_L of the horizontal tail surface on the ΔC_L of the whole aircraft is neglected in aerodynamic calculations of such aircraft.

The Table also shows that, in the case of a duck type aircraft, the role of the lift produced by the horizontal tail surface markedly increases, so that it can no longer be neglected in the aerodynamic calculation of the aircraft. In principle, the duck design is more advantageous than the conventional design, since the

tail of a duck-type aircraft not only ensures stability and controllability of the aircraft but also produce a lift useful for the aircraft.

At supersonic flying speeds ($M > 1$), as indicated in eq.(4.17), the horizontal tail surface will yield a negative lift at all values of C_L for an aircraft of conventional design since \bar{x}_p b h.t. increases. In a duck-type aircraft, on the contrary, at $M > 1$, the positive lift created by the horizontal tail surface increases still more.

It must be remarked, however, that in duck type aircraft it is hard to obtain a proper landing mechanization of the wing. In an ordinary type aircraft the deflection of the flaps, yielding an additional moment acting on the aircraft without tail, is compensated by the additional moment of the horizontal tail surface, produced by the increase in downwash angle. In an aircraft of the duck type, this compensating moment of the tail, for all practical purposes, is absent since the downwash in this case is negligibly small. For this reason, on deflection of the flaps in a duck-type aircraft the horizontal tail surface cannot compensate the moment created by the wing, unless a special mechanization of the tail is provided, which is very difficult to design.



CHAPTER V

THE ELEVATOR HINGE MOMENT AND THE STICK FORCE

The Elevator Hinge Moment

Up to now we have considered the moments of the aerodynamic forces acting on the aircraft with respect to an axis passing through the center of gravity of the aircraft. Besides these moments, the calculation of the stability and controllability of an aircraft is greatly influenced by the moments of the aerodynamic forces acting on the control surfaces with respect to their axis of rotation. Such moments comprise the hinge moments, i.e., the moments with respect to the axes of the hinges about which the control surfaces rotate.

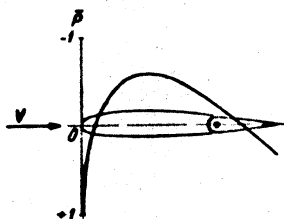
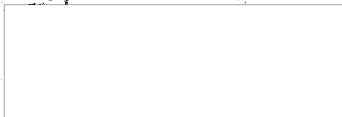


Fig.5.1 - Distribution of Pressure along the Tail Profile at $\delta = \alpha_{h.t.} = 0$.

The value of the hinge moment determines the value of the force that the pilot must apply to control the aircraft. The greater the hinge moment the greater that force.

Let us imagine that a horizontal tail surface with a symmetrical profile is set at a zero angle of attack to the relative air flow ($\alpha_{h.t.} = 0$) and that the elevator is not deflected ($\delta = 0$), as shown in Fig.5.1. Since the tail profile has a certain thickness, the pressures acting on this tail will differ from atmospheric pressure and will vary along the tail chord and, in particular, along the elevator chord. However, because of the symmetry of flow, the aerodynamic forces acting on the elevator will yield no moments with respect to its axis of rotation. The resultant of these forces, perpendicular to the elevator chord, will be equal to zero.



If the pilot, wishing to produce a certain aerodynamic force on the tail, deflects the elevator (Fig.5.2), the symmetry of flow about the body is impaired, and

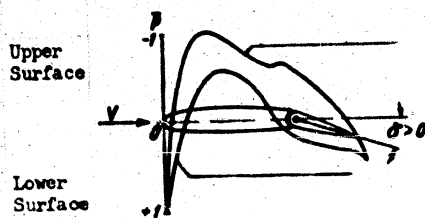


Fig.5.2 - Pressure Distribution along the Tail Profile on Deflection of the Control Surface

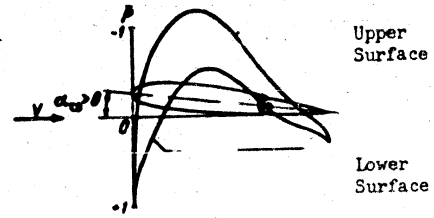


Fig.5.3 - Pressure Distribution along the Tail Profile with Varying Angles of Attack

the aerodynamic force appearing on the elevator will not, generally speaking, pass through the axis of rotation of the control surface. The same takes place if, at

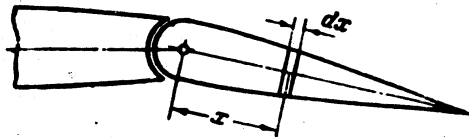


Fig.5.4 - For Determining the Hinge Moments of the Elevator

unchanged position of the elevator ($\delta = 0$), the angle of attack of the horizontal tail surface is changed (Fig.5.3). In these, a hinge moment arises, but its value will be different in the two cases.

Since, at small Mach numbers, the curve of the pressures acting on the tail remains practically unchanged when the velocity of the flow varies, the value of the hinge moment can be obtained from the formula

$$M_h = - \int_{S_h} \Delta \bar{p} q_{h.t.} x dS, \quad (5.1)$$

where $\Delta \bar{p}$ is the pressure difference acting on an element of elevator surface;

$q_{h.t.}$ is the velocity head of the relative air flow on the tail;

x is the arm of an element of the control-surface area, with respect to its axis of rotation (Fig.5.4);

$dS = b dx$ is an element of the elevator area;

and the integration is extended over the entire area of the elevator. Since $q_{h.t.}$ can be considered constant at all points of the tail, eq.(5.1) can be presented in the form

$$M_h = - q_{h.t.} \int \Delta \bar{p} x dS = - q_{h.t.} b_0 S_0 \int \Delta \bar{p} x dS, \quad (5.2)$$

where

$$\bar{x} = \frac{x}{b_0}, \quad dS = \frac{dS}{S_0}$$

and

b_B is the mean elevator chord.

The integral entering into eq.(5.2), as obvious from the above statements, is a dimensionless quantity which, at small Mach numbers, is a function only of the angle of attack of the horizontal tail surface $\alpha_{h.t.}$, of the angle of deflection of the elevator δ , and in addition also depends on the geometric relations between elevator and entire horizontal tail surface. This dimensionless coefficient is called the coefficient of hinge moment of the elevator and is denoted by m_h .

Thus,

$$M_h = m_h S_B b_B q_{h.t.} \quad (5.3)$$

Equation (5.3) shows that the condition of geometric and aerodynamic similitude

is satisfied (i.e., if the angles of attack of the horizontal tail surface and the deflections of the elevator are kept constant); however, at increasing dimensions of the tail and increasing velocity head the hinge moment increases in absolute value. For example, if the elevator in one case has the area $S = 0.5 \text{ m}^2$, the chord $b_B = 0.2 \text{ m}$, and the indicator speed is $V_i = 50 \text{ m/sec}$, $\rho = \frac{1 \text{ kg-sec}^2}{\text{m}^4}$, then

$$M_{h1} = m_h \cdot 0.5 \times 0.2 \frac{50^2}{16} \approx 15.6 m_h \quad (\text{kg-m})$$

If, while preserving geometric similarity of the tail, the elevator area is increased to $S_B = 3 \text{ m}^2$, the elevator chord to $b_B = 0.49 \text{ m}$, and the indicator speed to $V_i = 200 \text{ m/sec}$, then the hinge moment will become equal to

$$M_{h2} = m_h \cdot 3 \times 0.49 \frac{200^2}{16} \approx 3675 m_h$$

This shows that, at unchanged m_h , the hinge moment has increased over 200 times.

Aerodynamic Balance of the Elevator

The example just presented shows that, if no special measures are taken to reduce the coefficient m_h , then any increase in flying speed and aircraft size will cause the hinge moment of the elevator, and with it the stick force, to increase sharply.

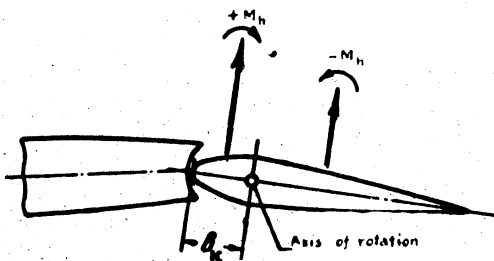
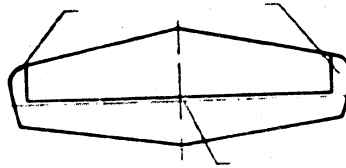


Fig. 5.5 - Diagram of Axial Aerodynamic Balance

Equation (5.2) shows that placing the axis of rotation of the control surface at a certain distance b_k to the rear of its leading edge will cause the various parts of the control-surface area to yield moments of the same sign about the axis of rotation (Fig.5.5), so that the total moment may be considerably reduced in magnitude. This is the idea of an aerodynamic control-surface balance, i.e., an arrangement of the control surfaces such that the aerodynamic forces acting on them will yield, with respect to the axis of rotation, a total moment of the desired small value. Such a type of aerodynamic balance, when the axis of rotation of the control surface is shifted rearward with respect to the leading edge, is known as axial compensation.

Horn
compensation



Axis of rotation

Fig.5.6 - Diagram of Horn Compensation

It is also possible to obtain aerodynamic balance in other ways. There exists the horn balance (Fig.5.6) in the case of elevators with flanges projecting in front of the axis of rotation and yielding a moment with a sign opposite to that of the moment produced by the main part of the elevator. There is also a servo-balance (which may be produced in two variants (Fig.5.7)). An additional deflecting surface, like a small rudder, kinematically connected with the stabilizer in such a way that on deflection of the main rudder by a positive angle, the servo tab is deflected by a negative angle, and vice versa, may also be installed in the rear part of the elevator. In this case, the pressures acting on the elevator are redistributed in such a way that the center of pressure approaches the axis of rotation of the

elevator, and, consequently, the hinge moment decreases. In the other variant, the servo tab is in the form of an individual auxiliary control surface, installed in the rear (Fig.5.7,2); the mechanism of action of the servo tab in this model remains the same as in the preceding one.

The servo tab took its name from the servo rudder (auxiliary rudder) which was proposed about 20 years ago. In such an auxiliary control surface the control stick is not connected with a main control surface free to rotate about its axis, but with a servo rudder, so that the pilot controls the servo rudder which, in turn, deflects the main control surface.

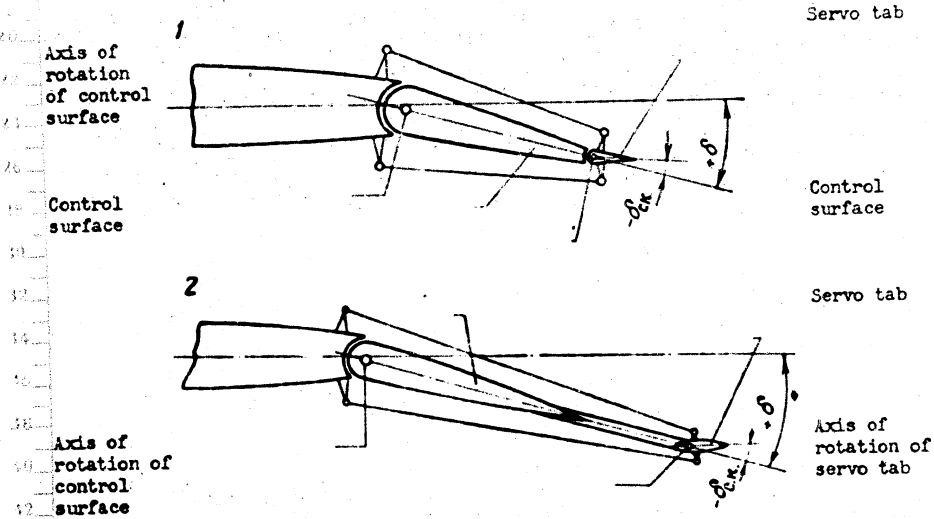


Fig.5.7 - Diagram of Servo Balance

Of all the above forms of aerodynamic balance, the most widespread is the axial type, in view of its structural simplicity and aerodynamic perfection. For practical purposes, the axial compensation has no influence on efficiency of the rudder and thus does not increase the drag of the tail, while a deflection of the servo tab creates aerodynamic forces which are directed toward the side of the

forces on the control surface, thus lowering the efficiency of this surface. The servo tab so introduced increases the tail drag. The horn tab, at high angles of rudder deflection, leads to a poor flow around the tail, with separation of the flow, and may produce a shock in the horizontal tail surface. Owing to the small structural heights it is difficult to ensure a sufficiently rigid construction of the servo tab and its control, which under certain conditions may lead to vibrations of the tail and to flutter of the whole aircraft.

On the basis of all these considerations, axial compensation is most often used at present while the servo tab is less popular.

It is also possible to reduce the hinge moment of the elevator by installing a stabilizer that is movable during flight. With such a stabilizer the pilot, at

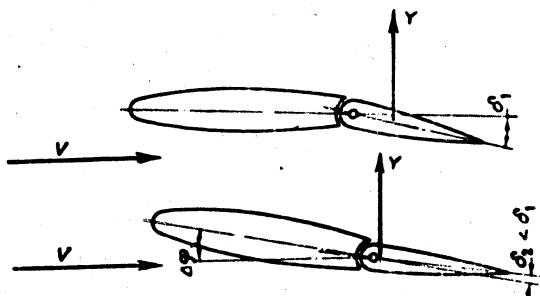


Fig.5.8 - Effect of Movable Stabilizer

attitudes where a considerable deflection of the elevator is necessary for a prolonged period of time, is able, by the aid of a special device, to vary the angle of the stabilizer installation and thereby to put more load on the stabilizer and less on the elevator (Fig.5.8). Since it makes no difference in obtaining the necessary moment of the tail with respect to the center of gravity of the aircraft, whether the pilot deflects the elevator or changes the angle of attack of the entire tail, it is possible to select the combination of δ and φ at which the hinge moment of the

rudder remains within allowable limits, by controlling the stabilizer.

The realization of a stabilizer movable during flight involves a certain complication of design, and, as shown later, results in certain difficulties at large Mach numbers. For this reason, in most cases of a movable stabilizer, a trim tab is used to reduce the stick force for sustained attitudes.

The trim tab is an auxiliary control surface installed in the rear part of the rudder in the same way as the servo tab, except that it is not kinematically connected with the stabilizer, being controlled instead by the pilot by means of a separate handwheel (Fig.5.9). When prolonged flight is necessary in some cases in

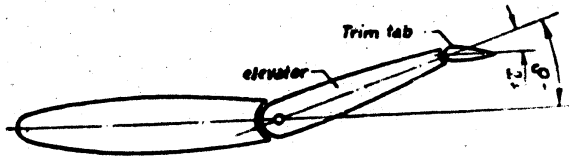


Fig.5.9 - Effect of Trim Tab Deflection

which a negative elevator deflection may be required, the pilot, by means of the handwheel, deflects the trim tab in the opposite direction (downward in Fig.5.9) by an angle such that the hinge moment vanishes or is sufficiently small.

If, at a certain elevator deflection the pilot, after setting the trim tab in some definite position does not again touch the trim-tab control wheel, then, the trim tab will remain in the same position with respect to the elevator, at all other deflections of the elevator, and a force other than zero will appear at the control stick.

The Coefficient of Elevator Hinge Moment

Within the range of the angles of attack of the horizontal tail surface and of the angles of elevator deflection used in practice, the coefficient of hinge moment of the elevator without the trim tab is a linear function of these two angles.

On introducing the generally adopted notation

$$\frac{\partial m_h}{\partial a} = m_h^a; \quad \frac{\partial m_h}{\partial b} = m_h^b,$$

we obtain the following expression for the coefficient of hinge moment

$$m_h = m_h^a a_{h.t.} + m_h^b \delta. \quad (5.4)$$

The work-up of experimental data leads to the following approximate expression for the coefficients m_h^a and m_h^b for elevators with axial compensation ($M \Delta M_{kp} \delta$):

$$m_h^a \approx -0.12 \frac{S_u}{S_{h.c.}} \left(1 - 3.6 \frac{S_{ax.c.}}{S_b} \right) a_{h.t.}; \quad (5.5)$$

$$m_h^b \approx -0.14 \left[1 - 6.5 \left(\frac{S_{ax.c.}}{S_b} \right)^{\frac{2}{3}} \right] a_{h.t.} \quad (5.6)$$

Here $S_{ax.c.}$ denotes the area of axial compensation.

Equations (5.5) and (5.6) show that, with increasing degree of axial compensation, the coefficients m_h^a and m_h^b decline (Fig. 5.10). At $\frac{S_{ax.c.}}{S_b} = 0.28$ both coefficients vanish, and with further increase of the compensation they change their sign, initiating an overcompensation of the elevator.

If, in designing the elevator, a 25% compensation is selected, then, at small industrial deviations during the construction of the aircraft, overcompensation may occur. For this reason, an axial compensation over 25-27% is rarely used in practice. The order of magnitude of the coefficients m_h^a and m_h^b for the mean ratios used in practice: $\frac{S_o}{S_{h.t.}} = 0.4$; $\frac{S_{ax.c.}}{S_b} = 0.24$ and $a_{h.t.} = 0.06$ is found to be as follows:

$$m_h^a \approx -0.0004; \quad m_h^b \approx -0.0020$$

It will be seen that the coefficient m_h^δ is a few times the value of m_h^α . In the flying range, the angle of attack of the horizontal tail varies within far narrower

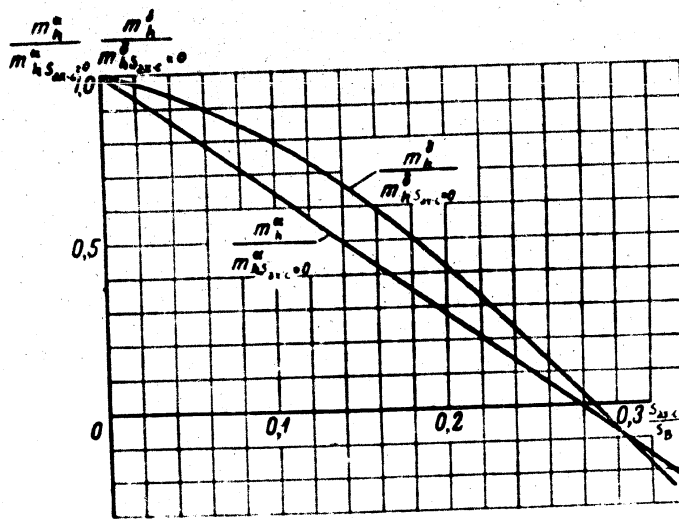


Fig. 5.10 - m_h^α and m_h^δ Plotted Against Degree of Axial Compensation

limits than the angle of elevator deflection; for this reason the hinge moment is determined primarily by the angle δ of elevator deflection. Due to this fact, the summand $m_h^\alpha \alpha_{h.t.}$ in the expression for m_h is sometimes neglected in practice and replaced by the following:

$$m_h \approx m_h^\delta \delta \quad (5.4')$$

As already indicated, deflection of the trim tab is generally used for reducing the hinge moment. The variation in the hinge moment, produced by a deflection of the trim tab can be determined from the formula

$$\Delta m_{h,\tau} \approx -0,017 \frac{S_\tau b_{st}}{S_b b_s} \sqrt{\frac{b_{st}}{b_\tau} \tau^\circ} = m_h^\tau \tau^\circ, \quad (5.7)$$



where S_T is the area of the trimmer;

b_{Bl} is the mean chord of that part of the elevator on which the trim tab is located (Fig.5.11);

b_B is the mean chord of the entire elevator;

b_T is the trim-tab chord;

τ^0 is the angle of deflection of the trim tab.

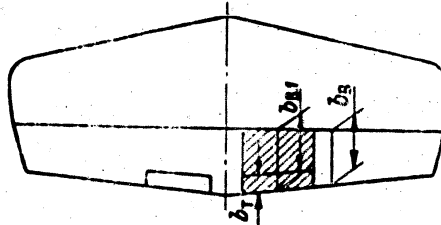


Fig.5.11 - For Determining the Hinge Moment Due to Trim Tab Deflection

Influence of the Compressibility of Air on the Hinge Moment

We mentioned in Chapter II, that, as shown by S.A.Khrstianovich, in the sub-critical region of Mach numbers the pressure curve varies with increasing Mach number in such a way that the greater the initial ordinate of the curve at $M = 0$, the greater will be the relative variation of this ordinate.

The pressure distribution along the profile of the horizontal tail surface at small Mach numbers has the form schematically shown in Fig.(5.12). It may be concluded that, as the Mach number increases, the pressures acting on the forward part of the elevator increase in a greater ratio than the pressures on the rear part of the elevator (cf. Fig.5.12). It follows from eq.(5.2) that the coefficient of the elevator hinge moment also varies in this case. If the elevator has axial compensation, then the relative role of the compensation in the general balance of moments increases. At first, the total hinge moment varies only slightly at relatively

increases. At first, the total hinge moment varies only slightly at relatively small Mach numbers (lower than M_{kp}) despite the more rapid rate of increase of the

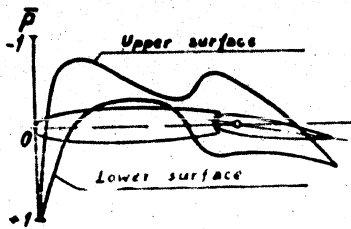


Fig. 5.12 - Pressure Distribution Along the Tail Profile at Low Mach Numbers

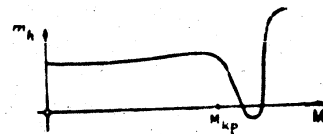


Fig. 5.13 - Slope of the Curve $m_h = f(M)$ at Mach Numbers Near the Critical Values

relative contribution of the trim tab to that moment (Fig. 5.13). Then, above a certain Mach number, the aerodynamic moment acting on the trim tab approaches the value of the aerodynamic moment acting on the rest of the elevator, the coefficient of hinge moment begins to decline, and with further increase of M , it may even change its sign.

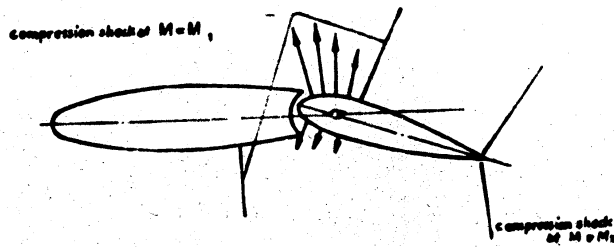


Fig. 5.14 - Influence of Compression Shocks on the Coefficient m_h

Thus, on the basis of theoretical considerations, we must expect that, when the Mach number of the relative flow at the tail increases beyond the critical Mach

number of the tail, the coefficient m_{η} of the elevator with axial compensation will decrease and that overcompensation may set in. In this case, the force on the control stick may change its sign and the control of the aircraft will be made more

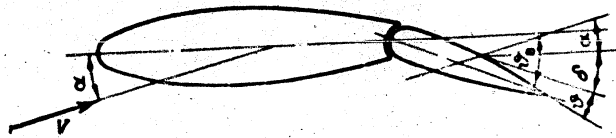


Fig.5.15 - For Determining the Angles θ in Supersonic Flow

difficult. After exceeding the critical Mach number on the tail, the phenomenon becomes still more complex. Compression shocks appear which, at increasing Mach number, shift toward the trailing edge of the tail and at a certain critical Mach number will impinge on the elevator. This shift will not be the same for the upper and lower tail surfaces, so that the picture of flow around the elevator is substantially changed. For example, let a compression shock appear on the upper surface of the wing at a positive angle of elevator deflection (Fig.5.14). In this case, high rarefactions will act on the trailing part of the elevator (on the tab). Owing to the confluent flow created by the depression of the elevator, at this moment, on the lower surface, the compression shock will still be located on the stabilizer, and on the compensator small rarefactions will act. As a result, overcompensation will take place. At somewhat higher values of $M = M_2$, the compression shocks on both upper and lower elevator surfaces may prove to be located close to the trailing edge of the elevator. In this case the coefficient of hinge moment increases sharply, since the tail will now be entirely in a supersonic flow.

As we already know (cf. Chapter II), the additional pressure at a certain point of the profile contour in a supersonic flow is proportional to the angle between the tangent to the profile contour at that point and the direction of the

0 undisturbed flow:

$$p = \frac{2}{\sqrt{M^2 - 1}} \theta.$$

Let us imagine a horizontal tail surface with an elevator deflected by a certain angle δ , the elevator having a constant chord and being set at a certain angle of attack (Fig. 5.15). The angle of an element of the upper elevator surface with the direction of the undisturbed flow is equal to

$$\theta_u = \theta + \delta + \alpha.$$

Correspondingly, for an element of the lower elevator surface,

$$\theta_n = \theta - \delta - \alpha.$$

where θ denotes the angle between the elevator contour profile at any point, and its chord.

The excess pressure on an element of the upper surface of an elevator will be

$$p_u = \frac{2}{\sqrt{M^2 - 1}} \theta_u = \frac{2}{\sqrt{M^2 - 1}} (\theta + \delta + \alpha). \quad (5.8)$$

For the corresponding elements of the lower elevator surface, the pressure is equal to

$$p_n = \frac{2}{\sqrt{M^2 - 1}} \theta_n = \frac{2}{\sqrt{M^2 - 1}} (\theta - \delta - \alpha). \quad (5.9)$$

The resultant of the aerodynamic force acting on the element of elevator surface $dS = l dx$, where l is the elevator span, is obtained by subtracting eq. (5.8) from eq. (5.9) and multiplying the difference by the velocity head and by the surface element

$$dY = (P_n - P_0) q dx = \frac{4}{\sqrt{M^2 - 1}} (\delta + \alpha) q dx. \quad (5.10)$$

The moment of this force with respect to the axis of rotation of the elevator is equal to (Fig. 5.16)

$$dM_h = \frac{4}{\sqrt{M^2 - 1}} (\delta + \alpha) q l dx. \quad (5.11)$$

On integrating eq.(5.11) from $x = -b$ to $x = b - b$, where b is the chord of the axial compensator, we find the hinge moment acting on the whole elevator

$$M_h = -\frac{4}{\sqrt{M^2 - 1}} (\delta + \alpha) q l \frac{(b_n - b_n)^2 b_n^2}{2} = \frac{2}{\sqrt{M^2 - 1}} (\delta + \alpha) q l b_n (b_n - 2b_n) = \frac{2}{\sqrt{M^2 - 1}} (\delta + \alpha) q S_n b_n \left(1 - 2 \frac{S_{ax.c}}{S_n}\right). \quad (5.12)$$

On dividing eq.(5.12) by $S_n b_n q$ and then taking the partial derivatives obtained, with respect to α and δ , we find

$$m_h^\alpha = m_h^\delta = \frac{2}{57.3 \sqrt{M^2 - 1}} \left(1 - 2 \frac{S_{ax.c}}{S_n}\right). \quad (5.13)$$

where, for calculating m_h^α , the angles α and δ must be taken in degrees.

The expression (5.13) shows that, in a supersonic flow, the coefficients m_h^α

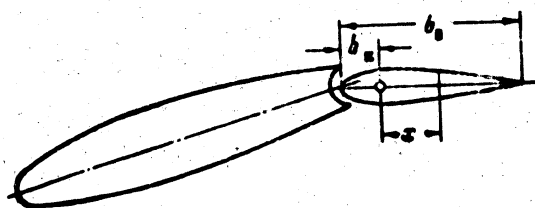


Fig. 5.16 - For Determining the Coefficient m_h in a Supersonic Flow

and m_h^δ are equal and that overcompensation sets in at $\frac{S_{ax.c}}{S_B} > 0.5$. We recall that, in a subsonic flow, m_h^α was considerably smaller than m_h^δ , and that overcompensation in that case began at $\frac{S_{ax.c}}{S_B} > 0.28$.

In deriving eq.(5.13) we did not allow for the influence of the viscosity of the air, which, particularly for the trailing part of the rudder, may introduce considerable corrections in the result obtained (cf. Chapter II). However, the expression so obtained does give an idea of the order of magnitude of the coefficients m and m_h^δ in a supersonic flow.

For example, for a tail having the dimension of the previous example, let $M = 1.5$. Let us calculate the coefficients m_h^α and m_h^δ . From eq.(5.13) we have

$$m_h^\alpha = m_h^\delta = -\frac{2}{57.3 \sqrt{2.25-1}} (1-2 \cdot 0.24) = -0.0162.$$

For subsonic velocities, with this example, we had

$$m_h^\alpha = -0.0004; \quad m_h^\delta = -0.0020.$$

Thus, the hinge moments obtained in the supersonic flow are actually considerably greater than in a subsonic flow. In addition, in a supersonic flow it is absolutely impossible to disregard the dependence of m_h on the angle of attack of the horizontal tail surface, which is sometimes done in analyzing a subsonic flow, the more so since, as we know from Chapter III, in a supersonic flow there is no downwash at the tail and the angles

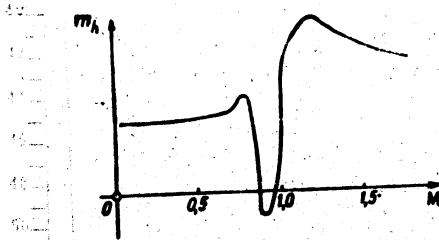


Fig.5.17 - Approximate Course of

$$m_h = f(M)$$



of attack of the tail differ from the angles of attack of the wing only by the quantity φ , which is the dihedral of the tail.

Figure 5.17 schematically shows the slope of the curve $m_h = f(M)$ for an elevator.

By giving sweepback to the entire horizontal tail surface and thus also to the elevator, the shock wave can be shifted toward considerably higher Mach numbers, in this way obtaining a satisfactory slope of the curve $m_h = f(M)$ over a wide range of Mach numbers.

Forces at the Elevator Control Stick

The stick or control wheel for the elevator is kinematically connected as shown in Fig. 5.18. In the general case, the kinematic chain may be established in

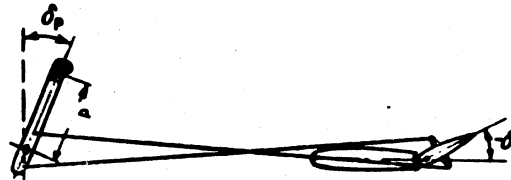


Fig. 5.18 - Kinematic Diagram of the Elevator Control

such a way that the angle of deflection of the stick δ_p is not equal to the angle of deflection of the elevator δ . It is obvious that, for an assigned hinge moment, the force at the stick is equal to

$$P = -\frac{M_h}{b_p} \frac{d\delta}{d\delta_p} = -\frac{1}{57.3} \frac{d\delta}{dx} M_h = -k_h M_h, \quad (5.14)$$

where b_p is the distance from the axis of rotation of the stick to the point of application of the force by the pilot.

The coefficient

$$k_h = \frac{1}{b_p} \frac{d\delta}{dx_p} = \frac{1}{57.3} \frac{d\delta^\circ}{dx_p} \quad (5.15)$$

is usually called the coefficient of elevator transmission (although this term is incorrect).

In eqs.(5.14) and (5.15), b_p is the working height of the stick (from its axis of rotation to the point of application of force by the pilot) and x_p is the linear displacement of the stick. The rule of signs for forces on the stick is such that when the pilot must push the stick away from him the force is positive, and when he pulls it toward him, it is negative.

Bearing in mind eqs.(5.4) and (5.7), eq. 5.14 may now be rewritten in the following form

$$P = -k_h (m_h^a x_{h,t} + m_h^b \delta + m_h^c \epsilon) S_h b_p k^2 \frac{V^2}{2} \quad (5.16)$$

By means of eqs.(5.14) and (5.16), if we know the coefficients m_h^a , m_h^b , and m_h^c from experiment or calculation, the force on the stick may be calculated for all states of flight.

For example, given the following data for an aircraft:

Wing loading

$$\frac{G}{S} = 200 \text{ kg/m}^2$$

Elevator area

$$S_B = 2.0 \text{ m}^2$$

Mean elevator chord

$$b_B = 0.6 \text{ m}$$

Axial compensation

$$\frac{S_{ax,c}}{S_B} = 0.2$$

Horizontal tail area

$$S_{h,t} = 5.0 \text{ m}^2$$

Angle of tail setting

$$\varphi = 0$$

Coefficient of deceleration

$$k = 0.9$$

Downwash at tail given by the expression

$$C^o = 0.5 + C_L$$

Derivative of the curve $C_{Lh.t.} = f(\alpha_{h.t.})$ of tail	$a_{h.t.} = 0.06$
Derivative of the curve $C_L = f(\alpha)$ of wing	$a = 0.075$
Angle of zero wing lift	$\alpha_0 = -1^\circ$
Coefficient of transfer from elevator to stick	$k_m = 1.6$

Let the flier, by means of the trim tab, ensure zero stick force at the indicated flying speed $V_{ib} = 150$ m/sec and at a rudder deflection angle of $\delta_b = -1^\circ$ (state of balancing by force). Let us determine the value of the stick force at the indicated speed $V_i = 200$ m/sec and at a rudder deflection angle $\delta = +1^\circ$.

The lift coefficient in the state of balancing by force is determined by the formula

$$c_{Lb} = \frac{160}{5V_{ib}^2} = \frac{16 \cdot 210}{150^2} = 0.142.$$

In the new state, $V_i = 200$ m/sec and

$$c_L = \frac{16 \cdot 200}{200^2} = 0.080.$$

The angle of attack of the wing in the initial state is

$$\alpha_0 = \frac{0.142}{0.075} - 1 = 0.9^\circ.$$

In the new state of flight, it is

$$\alpha = \frac{0.080}{0.075} - 1 = 0.07^\circ.$$

The true angle of attack of the tail at these states of flight is

$$\alpha_{h.t.} = \alpha_0 + \varphi - \alpha_0 = 0.9 - 0.5 - 5 \cdot 0.142 = -0.31^\circ.$$

$$\alpha_{h.t.} = \alpha + \varphi - \alpha = 0.07 - 0.5 - 5 \cdot 0.080 = -0.83^\circ.$$

Since the force during the initial state of flight was zero, the coefficient m_h in this case is also zero:

$$m_h = m_h^* s_{h,t} + m_h^* i_0 + m_h^* \tau = 0.$$

In the new state, the coefficient of hinge moment is equal to

$$m_h = m_h^* s_{h,t} + m_h^* i_0 + m_h^* \tau = m_h^* (s_{h,t} - s_{h,t}^0) + m_h^* (i_0 - i_0^0) \quad (5.17)$$

From eqs.(5.5) and (5.6), we have

$$m_h^* = -0.12 \frac{2}{3} (1 - 3.6 \cdot 0.2) 0.06 = -0.00081$$

$$m_h^* = -0.14 (1 - 6.5 \cdot 0.2^{0.75}) 0.06 = -0.00351$$

On introducing these numerical values in eq.(5.17), we get

$$\begin{aligned} m_h &= -0.00081 (-0.83 + 0.31) - 0.00351 (1 + 1) = \\ &= -0.00142 - 0.00706 = -0.0075 \end{aligned}$$

Equation (5.16) yields

$$P = -1.6 (-0.0075) 2.0 \times 0.6 \times 0.9 \frac{200}{16} = +3.2 \text{ kg}$$

If we neglected the summand $m_h^* \alpha_{h,t}$ and made our calculations from eq.(5.4'), we would get

$$P = +3.0 \text{ kg}$$

In calculating P we did not need to determine the angle of deflection of the trim tab τ .

Relation of the Stick Force and the Velocity of Horizontal Flight

In order to establish the relation between stick force and speed, in the special case of horizontal steady flight, the functional relationships of $\alpha_{h,t}$.

and δ of the flying speed must be substituted in eq.(5.16). For the time being, we consider that the compressibility of the air has no influence on the aerodynamic coefficients. In the state of balancing, the equation $m = 0$ is obviously valid. From eqs.(4.8') and (4.10) of Chapter IV, at balancing states, we have

$$\alpha_{h.t.} = \frac{m \Delta \alpha \epsilon}{m_0} = \frac{m_0^2}{m_0^2} \epsilon_i$$

The angle of attack of the horizontal wing is equal, on the basis of eq.(3.19) of Chapter III, to

$$\alpha_{h.t.} = \left(\frac{1}{\sigma} - D \right) \epsilon_i + \varphi + \alpha_0 - \epsilon_f$$

Thus the coefficients of hinge moment in states of balancing in horizontal flight are equal to

$$\begin{aligned} m_h &= m_0^2 \alpha_{h.t.} + m_h^2 \delta + m_h^2 \tau = m_0^2 \left[\left(\frac{1}{\sigma} - D \right) \epsilon_i + \varphi + \alpha_0 - \epsilon_f \right] + \\ &+ m_h^2 \left[- \frac{m_0 \Delta \alpha \epsilon}{m_0^2} - \frac{\alpha_0 + \varphi - \epsilon_f}{\sigma} - \frac{m_0^2 \epsilon_i}{m_0^2} \right] + m_h^2 \tau = \\ &= - m_h^2 \frac{m_0 \Delta \alpha \epsilon}{m_0^2} + \left(m_h^2 - \frac{m_0^2}{\sigma} \right) (\alpha_0 + \varphi - \epsilon_f) + \\ &+ \left[m_h^2 \left(\frac{1}{\sigma} - D \right) - m_h^2 \frac{m_0^2 \epsilon_i}{m_0^2} \right] \epsilon_i + m_h^2 \tau \end{aligned}$$

The stick force for these states of flight is found from eq.(5.16):

$$\begin{aligned} P &= -k_h S_0 b_0 b q \left\{ - m_h^2 \frac{m_0 \Delta \alpha \epsilon}{m_0^2} + \left(m_h^2 - \frac{m_0^2}{\sigma} \right) (\alpha_0 + \varphi - \epsilon_f) + m_h^2 \tau \right\} + \\ &+ \left[m_h^2 \left(\frac{1}{\sigma} - D \right) - m_h^2 \frac{m_0^2 \epsilon_i}{m_0^2} \right] \epsilon_i \end{aligned}$$

Since, during horizontal steady flight, the equation



$$G = C_L S q$$

is valid, the preceding equation may, after certain simplifications, be rewritten in the form

$$P = - \frac{m_h^i \Delta S_{\text{eff}} \Delta h}{m_i^i} \frac{G}{S} \left[-m_{\text{rot}} b h t + m_i^i \left(\frac{m_h^i}{m_i^i} - \frac{1}{a} \right) (a_0 + \tau - e_f) + m_i^i \frac{m_h^i}{m_i^i} \right] \frac{q}{S} + \left[m_i^i \frac{m_h^i}{m_i^i} \left(\frac{1}{a} - D \right) - m_i^i f \right] \quad (5.18)$$

The factor $\frac{m_h^i \Delta S_{\text{eff}} \Delta h}{m_i^i} \frac{G}{S}$ entering into this expression may be termed the coefficient of stick force. This factor characterizes the magnitude of the force which must be applied by the pilot when displacing the balance of the aircraft to maintain the

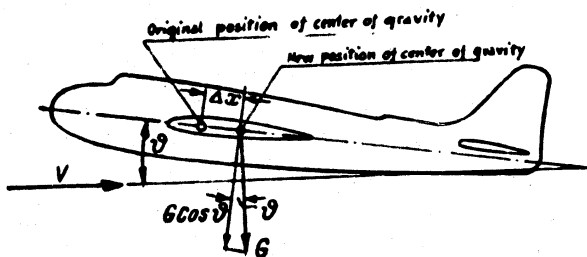


Fig.5.19 - Additional Moment on Changing the Balance of the Aircraft

preceding state of flight, i.e., when shifting the center of gravity of the aircraft by a quantity equal to the length of the mean aerodynamic chord.

Now let us assume that in flight, due to any cause, the center of gravity of the aircraft is displaced by the quantity Δx (Fig.5.19). Then a moment equal



to $G \cdot \Delta x \cdot \cos \theta$ will be produced with respect to the original position of the center of gravity of the aircraft.

In order to keep the balancing of the aircraft from changing, it is necessary to create an equal moment of weight and a moment of opposite sign on the tail, i.e., to deflect the elevator through an angle $\Delta \delta$.

The required elevator deflection is found from the condition:

$$G \cos \theta \Delta x = -m_1^1 q S b_1 \Delta \delta.$$

However, with sufficient approximation, at small angles θ :

$$G \cos \theta \approx G \approx c_L S q,$$

so that

$$c_L \Delta x = -m_1^1 b_1 \Delta \delta.$$

Hence,

$$\Delta \delta = -\frac{c_L}{m_1^1} \frac{\Delta x}{b_1} = -\frac{c_L}{m_1^1} \Delta x. \quad (5.19)$$

The additional force on the stick due to the elevator deflection is then equal

to

$$\begin{aligned} \Delta P &= -k_h m_h^1 \Delta^2 S_0 b_0 k q = k_h m_h^1 \frac{c_L}{m_1^1} S_0 b_0 k \frac{q}{c_L} \Delta x = \\ &= -k_h \frac{m_h^1}{m_1^1} S_0 b_0 k \frac{q}{S} \Delta x. \end{aligned}$$

whence

$$\frac{\partial_h m_h^1 S_0 b_0 k}{m_1^1} \frac{q}{S} = \frac{\Delta P}{\Delta x}. \quad (5.20)$$

STAT

as can be demonstrated.

If we use $\frac{\Delta P}{\Delta x} = P^x$, we have

$$P = -P^x \left[-m_{\delta} b h t + m_z^x \left(\frac{m_h^x}{m_h^x} - \frac{1}{a} \right) (a_0 + \varphi - e) + m_z^x \frac{m_h^x}{m_h^x} \tau \right] \frac{q}{S} + \left[m_z^x \frac{m_h^x}{m_h^x} \left(\frac{1}{a} - D \right) - m_z^x \right] \frac{1}{q_0} \quad (5.21)$$

At a certain value of the velocity head $q = q_0$, in the state of balancing by force, the force on the stick is zero; therefore,

$$\left[-m_{\delta} b h t + m_z^x \left(\frac{m_h^x}{m_h^x} - \frac{1}{a} \right) (a_0 + \varphi - e) + m_z^x \frac{m_h^x}{m_h^x} \tau \right] \frac{1}{S} = - \left[m_z^x \frac{m_h^x}{m_h^x} \left(\frac{1}{a} - D \right) - m_z^x \right] \frac{1}{q_0}$$

On substituting this expression in the general formula (5.21), we get

$$P = -P^x \left[m_z^x \frac{m_h^x}{m_h^x} \left(\frac{1}{a} - D \right) - m_z^x \right] \left(1 - \frac{q}{q_0} \right) \quad (5.22)$$

In the absence of elevator overcompensation, as we already know, $m_h^x < 0$, $m_h^{\delta} < 0$ and the coefficient m_h^x is substantially less than m_h , while the coefficient $m_z^{\delta} = -k A a_{h.t.}$ is always less than zero.

Thus, in an aircraft without longitudinal static stability ($m_z^{C_L} > 0$) and with overcompensated control surfaces, the force on the stick declines with increasing velocity head (Fig. 5.20). For a statically stable aircraft, if the condition

$$|m_z^x| > \left| m_z^x \frac{m_h^x}{m_h^x} \left(\frac{1}{a} - D \right) \right|,$$

is satisfied, the force on the stick also increases with the velocity head. If, however, this condition is not satisfied, then even for a statically stable air-

craft, the force on the stick decreases with increasing velocity head.

The increase of the stick force with increasing velocity head ($\frac{dP}{dq} > 0$) is necessary for normal control of the aircraft. In this case, the pilot must apply additional force to increase the flying speed; the general impression is that of resistance of the aircraft to the effort of the pilot to increase the flying speed. In the case of a negative derivative of the curve of stick force versus velocity head ($\frac{dP}{dq} < 0$), the pilot must counteract the tendency of the aircraft to increase its speed. It is evident that, in the former case, the aircraft is far more easily controlled than in the latter.

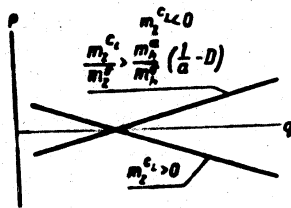


Fig. 5.20 - Stick Force Versus Velocity Head

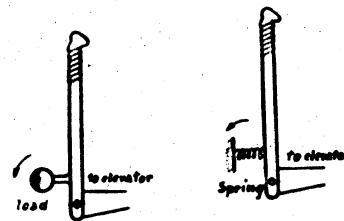


Fig. 5.21 - Loads and Springs in the System of Elevator Control

As we will see later, the slope of the curves $P = f(q)$ or $P = f(V)$ is closely related to the degree of longitudinal static stability of the stick-free aircraft.

Influence of Balancers and Springs on Force on Stick

Sometimes, to improve the stability of the stick-free aircraft, special weights (balancers) or springs are introduced into the control system. Figure 5.21 shows the devices placed on the control stick itself, although in reality they may be located on other parts of the elevator control system.

Obviously, this hinge moment, produced by these devices, in contrast to the

aerodynamic hinge moment, which is proportional to the velocity head, does not depend on the velocity head at all and is determined by the mass of the weight and its location, or by the tensile force of the spring. However, the coefficient of the hinge moment due to a balancer or a spring, does strongly depend on the velocity head and is inversely proportional to it.

It must be borne in mind that in flight at constant load factor, both these devices, the balancer and the spring, act in entirely the same way when the state of flight changes: the hinge moment due to either device does not change. On the other hand, in flight with a varying load factor, the action of the spring and that of the balancer differ substantially. When the load factor varies, the hinge moment produced by the balancer varies proportionally to the load factor while the hinge moment produced by the constant tension of a spring, remains constant.

If the pilot releases the control stick whose system includes balancers or springs, then, in addition to the force due to the aerodynamic hinge moment, a fixed force will act on the stick and will be determined by the mass of the load, multiplied by the load factor, or by the tensile force of the spring. Under the influence of this force, the elevator will be deflected in the same way and will produce a moment with respect to the center of gravity of the aircraft.

Let us determine the degree of longitudinal static stability for this case.

When the state of flight varies, the rotation of the elevator takes place relatively slowly; for this reason, the influence of the angular velocity of elevator rotation on its hinge moment will be neglected. In this case, two forces act on the control stick: the force $P_{b\ sp}$ produced by the weights and springs in the control system and the force P_a created by the aerodynamic hinge moment of the elevator. At each instant of time, with a free stick, these forces will be in equilibrium, so that the equality

$$P_{b\ sp} + P_a = 0$$

is valid. In the general case, when the flight takes place at a load factor $n \neq 1$,

STAT

the load on the stick due to the balancer and springs is equal to

$$P_{b\ sp} = -nP_b - P_{sp}$$

The force on the stick due to the aerodynamic hinge moment will be:

$$P_a = -k_h m_h S_B b k_q = -k_h S_B b k_q (m_h^{\alpha^{\circ}} h.t. + m_h^{\delta^{\circ}} + m_h^{\tau^{\circ}})$$

Thus,

$$nP_b + P_{sp} = -k_h S_B b k_q (m_h^{\alpha^{\circ}} + m_h^{\delta^{\circ}} + m_h^{\tau^{\circ}})$$

From this we find the angle of elevator deflection with the stick free:

$$\delta^{\circ} = \frac{nP_b + P_{sp}}{k_h S_B b k_q} = \frac{m_h^{\alpha^{\circ}} + m_h^{\delta^{\circ}} + m_h^{\tau^{\circ}}}{m_h^{\delta^{\circ}}} \quad (5.23)$$

Because of the deflection of the elevator, the moment coefficient acting on the aircraft varies by the quantity $\Delta m_2 = m_2^{\delta^{\circ}}$ and the total coefficients of moment of an aircraft, with the stick free, will be equal to

$$m_{2,cf} = m_{2,0} + m_2^{\delta^{\circ}} = m_{2,0} + \frac{m_h^{\delta^{\circ}}}{m_h^{\delta^{\circ}}} (nP_b + P_{sp}) = m_{2,0} + \frac{m_h^{\delta^{\circ}}}{m_h^{\delta^{\circ}}} (nP_b + P_{sp}) \quad (5.24)$$

In accordance with the definition of the concept of overload:

$$nG = C_L S_q$$

we have

$$\frac{1}{\sigma} = \frac{C_L}{\sigma} \frac{1}{S} \quad (5.25)$$

Noting that the angle of attack of the horizontal tail surface according to eq.(3.19) of Chapter III, is equal to



$$a_{hc} = \left(\frac{1}{s} - D \right) c_L + \dot{\psi} + a_0 - i_0$$

and making use of eq.(5.20), we may, after certain transformations, write eq.(5.24) for the coefficient of stick-free moment, in the form

$$m_{1,0} = m_{1,0} - \frac{1}{\rho} \left(c_L P_0 + \frac{s}{\rho} \nu_{\infty} \right) - m_{1,0} \left[\left(\frac{1}{s} - D \right) c_L + \dot{\psi} + a_0 - i_0 \right] - m_{1,0} \frac{\dot{\psi}}{h} \quad (5.26)$$

Let us now consider two special cases of flight. In the first case, let the flying speed remain constant during a variation in the angle of attack α or of the lift coefficient C_L ; consequently, let a certain load factor $n \neq 1$ appear, since the lift is no longer equal to the weight of the aircraft. In the second case, let the flying speed vary in such a way with varying α or C_L , that the equality* $Y = G$ is satisfied, and, consequently, the load factor remains, as before, $n = 1$.

The former corresponds, for example, to a sharp maneuver of the aircraft, when the speed is unable to vary, or to a flight in a disturbed atmosphere ("bump"), when, due to vertical wind gusts, the angles of attack vary, while the flying speed remains practically the same. An example of the latter case of flight is the take-off run or the deceleration of the aircraft in horizontal flight, when the pilot simultaneously moves the elevator and the throttle of the engine.

The degree of longitudinal static stability in the former case, as we already know (cf. Chapter I or Chapter IV), is evaluated by the partial derivative

* It would be more accurate in these arguments, to take the total aerodynamic force R instead of the lift Y ; but in practice, at the flight angles of attack, R differs little from Y .

STAT

$\frac{\partial m_z}{\partial C_L} = m_z \frac{C_L}{m_z}$. This derivative is called a measure of the static stability with respect to overload, emphasizing by this term that we are dealing with a flight at varying load factor and constant speed.

In order to evaluate the degree of longitudinal static stability in the latter case*, it is necessary to bear in mind that, on any variation in C_L , the coefficient m_z likewise varies, owing to the variation of the flying speed V or the velocity head q . In this case the degree of longitudinal static stability is evaluated by the value of the total derivative $\frac{dm_z}{dC_L}$ which may be represented in the form

$$\frac{dm_z}{dC_L} = \frac{\partial m_z}{\partial C_L} + \frac{\partial m_z}{\partial q} \frac{dq}{dC_L} = m_z' + m_z'' \frac{dq}{dC_L}$$

In the special case of horizontal flight the derivative $\frac{dq}{dC_L}$ may be found from the general equation

$$0 = c_l S q$$

By differentiating this equation, we get

$$0 = q dc_l + c_l dq$$

whence

$$\frac{dq}{dC_L} = - \frac{c_l}{c_l'}$$

The derivative $\frac{dm_z}{dC_L}$ is called the measure of static stability with respect to velocity. This term emphasizes the fact that we are dealing with flight at varying speed and constant overload.

*Stability with respect to load factor and stability with respect to flying speed will be considered in detail below, in Chapter VIII.

Taking the partial and total derivative of eq.(5.26) with respect to C_L , we obtain the degree of stability with respect to the overload (at $q = \text{const}$) and with respect to speed (at $n = \text{const} = 1$) in stick-free flight, bearing in mind that in the absence of the influence of compressibility, $\frac{dm_z}{dC_L} = m \frac{C_L}{z}$

$$m_{z00}^{c_L} = m_{z0}^{c_L} \frac{P_0}{P} = m \frac{m_z'}{m_z} \left(\frac{1}{z} - D \right). \quad (5.27)$$

$$\left(\frac{dm_z}{dC_L} \right)_{z=0} = m_{z0}^{c_L} - m_{z0} \frac{m_z'}{m_z} \left(\frac{1}{z} - D \right) \frac{P_0 - P_{sp}}{P}. \quad (5.28)$$

As mentioned above, and as will be clear from the expressions obtained, the stability with respect to overload is effected only by the balancers, while the stability with respect to speed is effected by both balancers and springs. The stability with respect to load factor increases with the force due to balancers; the stability with respect to speed increases with the force from the balancers and from the springs.

It is obvious that, in the general case, when the control system includes both springs and balancers, the force on the stick will be obtained, in horizontal steady flight, by adding the forces due to the spring and balancers to the force defined by eq.(5.21). On performing this operation, we have

$$P_{sp} = -P_0 \left\{ -m_{sp} \frac{m_z'}{m_z} + m_{z0} \left(\frac{m_z'}{m_z} - \frac{1}{z} \right) (v_0 + v - v_0) + \right. \\ \left. m_{z0} \frac{m_z'}{m_z} \right\} \frac{v}{s} + \left[m_{z0} \frac{m_z'}{m_z} \left(\frac{1}{z} - D \right) - m_{z0}' \right] \frac{v}{s} - P_0 - P_{sp} \quad (5.21')$$

In the state of balancing by force, at $q = q_0$, the force on the stick is equal to zero. From this, by analogy to the preceding equation, we obtain



$$\left[-m_{\delta} \delta h \dot{c} + m_{\delta}^{\prime} \left(\frac{m_{\delta}^{\prime}}{m_{\delta}} - \frac{1}{\sigma} \right) (z_0 + \psi - \psi_f) + m_{\delta}^{\prime} \frac{m_{\delta}^{\prime}}{m_{\delta}} \psi \right] \frac{1}{\sigma} -$$

$$= \frac{1}{q_0} \left[m_{\delta}^{\prime} \frac{m_{\delta}^{\prime}}{m_{\delta}} \left(\frac{1}{\sigma} - D \right) - m_{\delta}^{\prime} c + \frac{P_0 + P_{\delta}}{P^*} \right]$$

By substituting this equation in eq.(5.21'), we obtain

$$P = -P^* \left[m_{\delta}^{\prime} \frac{m_{\delta}^{\prime}}{m_{\delta}} \left(\frac{1}{\sigma} - D \right) - m_{\delta}^{\prime} c + \frac{P_0 + P_{\delta}}{P^*} \right] \left(1 - \frac{q}{q_0} \right). \quad (5.22')$$

On comparing eq.(5.22') and eq.(5.28), we come to the conclusion that

$$P = P^* \left(\frac{dm_{\delta}^{\prime}}{dq} \right)_{q_0} \left(1 - \frac{q}{q_0} \right). \quad (5.29)$$

may be written instead of eq.(5.22').

We remind the reader again that eq.(5.29) was derived under the assumption of horizontal flight and the absence of any influence of the compressibility of air. A more general case, allowing for the influence of compressibility, as well as for a load factor $n \neq 1$, will be discussed in Chapter IX.

From eq.(5.29), we can draw the following conclusions:

1. The character of the slope of the curve $P = f(q)$ is completely determined by the degree of stick-free longitudinal static stability of the aircraft.
2. For an aircraft that is neutral with the stick free, the force on the stick for all flying speeds is equal to zero.
3. For an aircraft that is unstable with stick free, the stick force declines with increasing velocity head.

If the relation between stick force and flying speed is known from flight tests of an aircraft and the coefficient P^* is determined by some method (by

wind-tunnel model tests or from flight tests) the degree of stick-free stability of an aircraft may be determined from eq.(5.29).

From eq.(5.29), we get

$$\left(\frac{dm_s}{dq}\right)_{cs} = \frac{P}{P^*} \frac{1}{1 - \frac{q}{q_0}} = \text{const} \frac{P}{1 - \frac{q}{q_0}} \quad (5.30)$$

By using springs or balancers, the characteristic $\frac{dP}{dq}$, which plays a substantial role in evaluating the controllability of an aircraft, can be varied to a considerable extent.

If the value of the force on the stick due to aerodynamic forces, as determined by eq.(5.22), is added to the force on the stick due to the balancers and springs, then the total stick force in horizontal flight will obviously be equal to *

$$P = P^* \left[m \frac{m_A}{m_h} \left(\frac{1}{s} - D \right) - m_s^* \left(1 - \frac{q}{q_0} \right) - P_b - P_{sp} - c \left(1 - \frac{q}{q_0} \right) - P_v - P_{sv} \right] \quad (5.31)$$

This expression shows that the value of the velocity head $q = q_0$, at which the stick force will vanish in the absence of springs and weights will no longer yield a zero stick force when springs and weights are present, since this velocity head only causes the force due to the aerodynamic hinge moment to vanish.

*In eq.(5.22'), giving the value of the force applied by the pilot to the stick, the quantity P_b and P_{kp} must be taken with opposite signs, as we have done, since the force applied by the pilot is opposite in sign and equal in magnitude to the force due to the loads or springs; if the spring tends to deflect the stick "away from the pilot", then the pilot must apply force in the direction "toward him", and vice versa.

The vanishing of the stick force will take place at another velocity head $q = q_b'$ which is determined from the condition

$$-c \left(1 - \frac{q_a}{q_b} \right) - P_s - P_{sp} = 0,$$

whence

$$q_b' = q_a \left(1 + \frac{P_s + P_{sp}}{c} \right).$$

In order to obtain a balancing by force in this state of flight, the pilot must make use of the trim tab or must vary the angle of stabilizer setting, if the aircraft has an adjustable stabilizer (in such a way that the resultant additional stick force is equal to $(P_b + P_{sp})$). The hinge moment obtained as a result of the deflection of the trim tab $\Delta M_{ht} = m_h^a S_B b k q$ or of the variation in the angle of stabilizer setting $\Delta M_{hp} = m_h^a S_B b k q$ and the corresponding stick force, are proportional to the velocity head q . For this reason, at a velocity head different from q_b , the additional force on the stick will be equal to

$$\Delta P = (P_b + P_{sp}) \frac{q}{q_b}$$

Thus the derivative of P with respect to q , in the presence of springs and weights, will be equal to

$$\frac{dP}{dq} = \frac{dP}{dq} + \frac{dP}{dq} = \frac{P_s + P_{sp}}{q_b} \quad (5.32)$$

If for any cause, a negative derivative $\frac{dP}{dq}$ is obtained in flight tests, thus interfering with the normal control of the aircraft, the position may be corrected by introducing springs or weights, of a definite tensile force or mass, as the case may be, in the control system. This is illustrated in Fig. 5.22.

For example, let the derivative of the force with respect to velocity head in the flight tests of an aircraft be $\frac{dP}{dq} = -0.0025$ with a velocity head in the state

of balancing by force, of $q_p = 1000 \text{ kg/m}^2$.

To obtain on this aircraft a derivative of stick force $\frac{dP}{dq} = + 0.0025$, it would be required to introduce a spring or weight in the control system of such

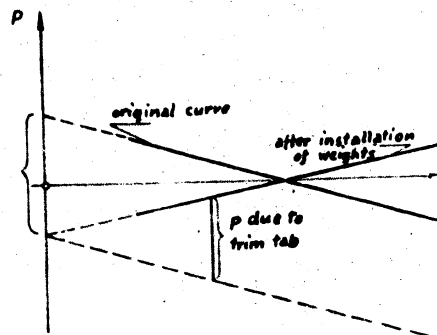


Fig.5.22 - Change in the Gradient $\frac{dP}{dq}$ by Means of Weights

and Springs

dimensions that the resultant force on the stick would be

$$P_b + P_{tr} = q_b \left(\frac{dP}{dq} - \frac{dP}{dq} \right) = 1000 (0,0025 + 0,0025) = 5 \text{ kg.}$$

If, for example, the arm of the load with respect to the axis of location of the stick were equal to 0.25, while the operating height of the stick $b_p = 0.5 \text{ m}$, then the load required would be

$$G_b = 5 \frac{0,5}{0,25} = 10 \text{ kg.}$$

Together with the weight, a spring with a corresponding tensile force might also be used.



Hydraulic Boosters and Automatic Rudder Control

As we have seen, at high flying speeds, when the influence of the compressibility of the air is pronounced, the stick forces undergo considerable variations and may reach high levels, thus making control difficult. These difficulties can be overcome by using a so-called "nonlinear" transmission from the rudder to the stick or by introducing hydraulic boosters into the control system. As we know, the stick force is equal to

$$P = k_h M_h^2$$

while the hinge moment, other conditions being equal, is proportional to the square of the flying speed.

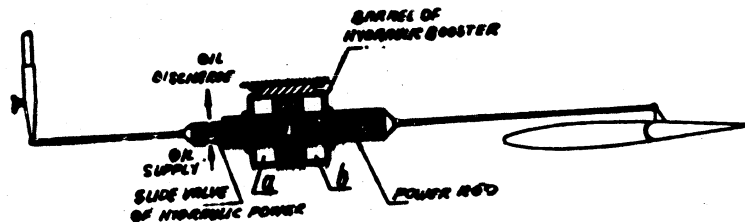


Fig.5.23 - System of Irreversible Hydraulic Booster

For this reason, to avoid too high a force on the stick at high flying speeds, it is desirable to have a k_h , variable during flight, which decreases at high flying speeds. Such a nonlinear transmission can be obtained by selecting the proper kinematics of rudder control. Since high flying speeds correspond to small angles of rudder deflection, the kinematics might be so selected that the derivatives $\frac{d\delta}{d\delta_p}$ decrease at small negative or positive angles of rudder deflection. In this case, however, one and the same elevator deflection, at high speeds, would correspond to greater stick deflections than at low speeds.

This method of reducing the stick force does not eliminate all the drawbacks

and is difficult for the designer to solve. For example, at $M > M_{kp}$, as already mentioned, the generation of a force of opposite sign is possible. A nonlinear transmission cannot correct such a situation.

A far more effective means of normalizing the efforts is to introduce hydraulic boosters, reversible or irreversible, in the control system. The mechanism of action of the irreversible hydraulic booster is shown in Fig.5.23.

On pushing the control stick forward, which is not directly connected with the rudder, the pilot displaces the valve slide of the hydraulic booster in such a way

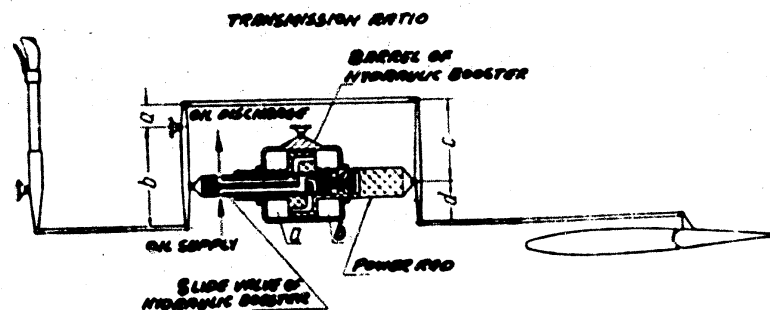


Fig.5.24 - Diagram of Reversible Hydraulic Booster

that oil under a definite pressure, produced by a pump, begins to enter the cavity (a) of the cylinder. Under the pressure of the oil, the piston is displaced, and thus deflects the control surface. On deflecting the stick in the opposite direction, the oil enters the cavity (b) of the cylinder, instead, and the rudder is deflected toward the other side. In this way, the total hinge moment of the rudder is taken up by the piston of the hydraulic booster, and the pilot needs only a minor effort to displace the valve. Since these negligible forces will not give the pilot "the feeling of control", the desired feeling of effort is ordinarily created by including special springs or weights in the control system, whose forces do not depend on the velocity head nor the Mach number of flight. In this case, the pilot is not at all confronted with variations in the rudder hinge moment due

to the influence of the compressibility of the air. Such a booster is therefore "irreversible".

The reversible hydraulic booster in Fig. 5.24, differs from the irreversible in that it absorbs only a portion instead of the entire elevator hinge moment. In this case, the force of the spring or weights still acts on the stick in addition to a partial force due to the aerodynamic hinge moment of the rudder. Thus, if the aerodynamic hinge moment undergoes sharp variations, the pilot feels these variations on

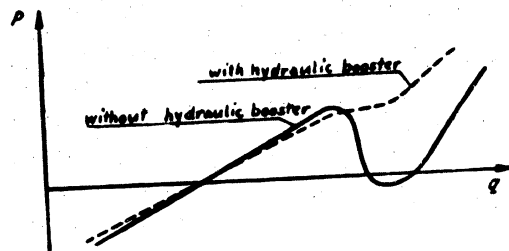


Fig. 5.25 - Curves of Stick Force with and without Reversible Hydraulic Booster

a reduced scale. Depending on the selected parameters for the reversible hydraulic booster, stick forces may be obtained with a sign required for the normal control of the aircraft, although the aerodynamic hinge moment of the rudder may change its sign (Fig. 5.25).

It should be pointed out that hydraulic boosters may be used not only on high-speed aircraft but also on heavy aircraft where extensive rudder balance is required, which is hard to produce accurately in industrial manufacture.

Influence of Friction in the Control Transmission on the Stick Force

Friction in the elevator control system leads to additional forces on the control stick and impairs the accuracy of elevator motion. At high friction forces, there may be serious difficulty in controlling an aircraft.

The force that the pilot must apply to overcome the friction forces is always

opposite in direction to the motion of the stick.

On the diagram, the relation of the stick force to the velocity head is shown in the form of a certain strip (Fig.5.26), the so-called friction path, instead of

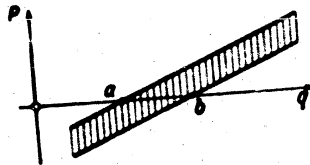


Fig.5.26 - Relation $P = f(q)$ in the Presence of Friction in the Control System

in the form of a straight line, as it would be if friction were absent. On releasing the stick in the presence of friction, the aircraft may be balanced with respect to force within a certain interval ab instead of at a single value of the velocity head, as was the case earlier (cf. Fig.5.26). In the presence of high friction, the pilot cannot push the stick smoothly forward and has to move it with more or less sharp jerks, which, of course, adversely affects the aircraft behavior in the air. The influence of friction is particularly unpleasant at high flying speeds, when the pilot must make the elevator execute accurate and very small motions. The pilot finds himself unable to effect these motions in the presence of friction. For this reason, in designing and constructing an aircraft, all possible measures must be taken to reduce friction in the rudder control transmission.

CHAPTER VI

ADDITIONAL MOMENTS ACTING ON THE AIRCRAFT IN UNSTEADY MOTION

Influence of the Unsteady Character of Motion on the Longitudinal Moment

In the preceding Chapters we considered the moments of the aerodynamic forces acting on an aircraft in steady motion, when all parameters of motion (for example, angle of attack, angle of inclination of flight path to horizon, flying speed, etc.) are independent of time. It was established that these moments, at a given Mach number and for a given aircraft, at constant engine operation, are completely determined by the angle of attack and the velocity head of flight*.

In the case of unsteady motion, the parameters of motion are a function of time, so that, in the general case, the aerodynamic forces and their moments will depend not only on the kinematic parameters of motion at the given instants of time, but also on the entire history of the motion in the preceding instants of time: on the angular velocity of rotation of the aircraft and its derivatives with respect to time, on the derivatives $\frac{dV}{dt}$, $\frac{d^2V}{dt^2}$, etc. This is explained by the fact that the conditions of unsteady flow around parts of the aircraft (for example, the wing, the tail, etc.) may markedly differ from the conditions of flow around the same parts by a stationary, steady stream. This difference in the conditions of flow around these parts results in a difference in the aerodynamic forces and their moments.

In certain cases (usually in rapidly changing processes) the variations in aerodynamic forces may be considerable, by comparison with a stationary flow. It

*For the horizontal tail surface, the invariance of the elevator deflection angle must be added to these, and for the wing, the invariance of the angle of flap deflection.

is well known that a wing, rapidly vibrating in a vertical plane, may produce traction, although under stationary conditions the very same wing (as we know) produces drag.

In the general case, for all aerodynamic forces and moments at unsteady motions of the aircraft, a relation of the following type would have to be adopted:

$$m_x = f\left(\alpha, \frac{d\alpha}{dt}, \frac{d^2\alpha}{dt^2}, \dots, \frac{dV}{dt}, \frac{d^2V}{dt^2}, \dots \text{ etc.} \right)$$

and we would have to consider that m_x depends on the entire preceding history of the motion.

Hypothesis of the Stationary State

In most problems connected with an analysis of aircraft stability, the kinematic parameters of motion vary relatively slowly. For this reason, it may be considered, in first approximation, that the primary influence on the structure of the flow at each given instant of time is exerted by the kinematic parameters of motion of precisely that instant of time. The hypothesis of stationary condition is thus used in the analysis of aircraft stability. According to this proposition, the magnitude of the forces acting on an aircraft in unsteady motion is completely determined by the kinematic parameters of motion at the given instant of time. With respect to the longitudinal motion of the aircraft, these kinematic parameters are, at an assigned altitude: flying speed V , angle of attack α , and angular velocity of rotation of the aircraft ω_z . The use of such a hypothesis, of course, is an extraordinary simplification of the analysis. It must be remembered that the hypothesis of the stationary state is merely one of first approximation, a rough model of the actual phenomenon. As an example of the obvious inapplicability of the hypothesis of the stationary condition, we may mention the case of flow around a wing set at a high angle of attack. The slope of the curve $C_L = f(\alpha)$ at certain profiles near an angle of attack corresponding to $C_{L \max}$, even at a very smooth

variation in the angle of attack, depends on the direction in which the angle of attack varies (Fig.6.1). At a continuous increase in angle of attack, curve (1) may be obtained for such profiles, while at a continuous decrease in angle of attack from values exceeding the angle corresponding to $C_{L \max}$, curve (2) is obtained. Here aerodynamic hysteresis takes place.

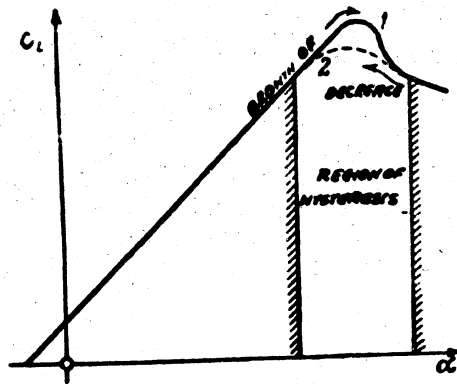


Fig.6.1 - Approximate Character of the Curve $c_v = f(\alpha)$ for Several Profiles

It is obvious that, in the region delineated in Fig.6.1, without knowing the character of the wing motion in the preceding instant of time, we are unable to say what value of C_L will correspond to some definite angle of attack of the wing at the given instant of time.

At a higher angular velocity, the phenomenon of hysteresis at high angles of attack will evidently be reflected more or less for all wing profiles. On the linear segments of the curve $C_L = f(\alpha)$, to which we will confine our investigation, there will be practically no hysteresis, so that the example presented can be considered merely as an illustration of the arbitrary nature of the hypothesis of stationary conditions in general. However, we will show later that, even within the limits of the linear relation $C_L = f(\alpha)$, the hypothesis of stationary condition

can not be used in all cases.

Influence of Angular Velocity on the Moment of the Wing, Fuselage, and Tail

Let an aircraft, flying at a speed V , rotate at the same time about the axis oz at an angular velocity ω (Fig.6.2).

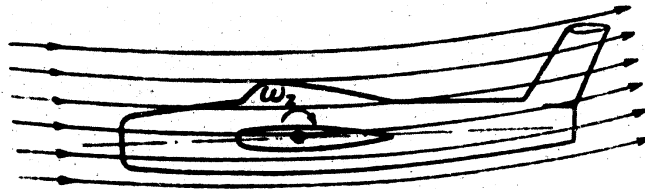


Fig.6.2 - Flow Around an Aircraft in Curvilinear Flight

As a result of the composition of the translational and rotational motions, the streamlines of the air meeting the aircraft will be curved, as shown in Fig.6.2. The angles of impact of the resultant curved stream on the elements of the aircraft at various points of these elements will differ; both the values of the aerodynamic

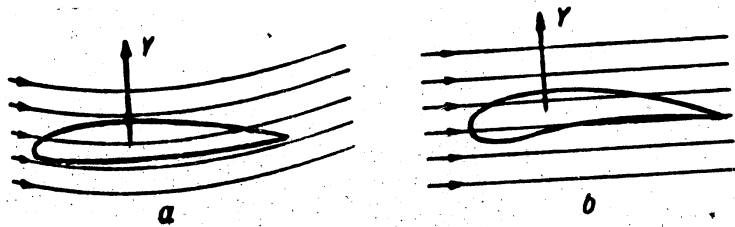


Fig.6.3 - The Hypothesis of Curvature

forces acting on the elements of the aircraft and the moments of these forces, will differ from their values during a purely translational motion of the aircraft.

Instead of using the conditions of motion of the aircraft in a curved flow (Fig.6.3,a), it is possible to use the conditions of flow around elements of a



correspondingly curved aircraft in a rectilinear flow (Fig.6.3,b). The results obtained on the basis of this "hypothesis of curvature" for the aircraft wing, are in rather good agreement with experimental data. To determine the moments of a horizontal tail surface, as demonstrated below, there is no need to resort to the hypothesis of the curvature, since in this case the results may be obtained by an elementary method. We will start with a discussion of this simplest case.

The Damping Moment of the Horizontal Tail Surface

When an aircraft rotates with respect to the axis oz at an angular velocity ω_z , there appear at all points of the aircraft additional components of linear velocity of the relative flow $\Delta V = \omega_z r$ (Fig.6.4) directed along the perpendicular to the

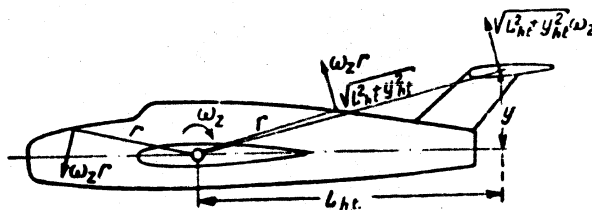
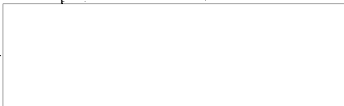


Fig.6.4 - Additional Velocities of the Relative Flow Produced by the Rotation of the Aircraft at an Angular Velocity ω_z

radius-vector r in a direction opposite to that of the circular velocity $\omega_z r$. In particular, at the location of the elevator hinges at the horizontal tail surface, the additional component of velocity will be equal to

$$\Delta V_{h.t.} = \sqrt{L_{h.t.}^2 + y_{h.t.}^2} \omega_z.$$

Since the value of $y_{h.t.}$ in ordinary cases is considerably less than the value of $L_{h.t.}$ we can assume within a certain error, that



$$\Delta V_{ht} \approx L_{ht} \omega_z \quad (6.1)$$

and consider that ΔV_{ht} is directed perpendicularly to the velocity of flight V .

At other points of the horizontal tail profile, the additional component of velocity, strictly speaking, will differ from that given by eq.(6.1), since the distance of these points from the center of gravity of the aircraft will not be equal to L_{ht} .

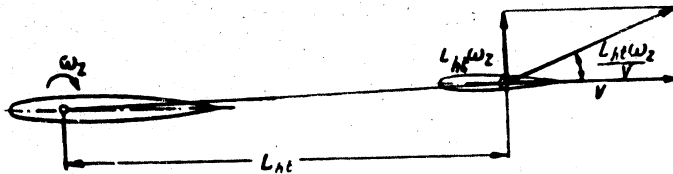


Fig.6.5 - Variation in Angle of Attack of the Horizontal Tail Surface during Rotation of the Aircraft

The value of the horizontal tail chord, however, is considerably less than the arm of the horizontal tail surface L_{ht} , and it may be assumed without great error that, over the entire tail chord, the velocity ΔV_{ht} is constant in magnitude and in direction and is equal to $L_{ht}\omega_z$.

The additional component ΔV_{ht} changes not only the value of the velocity of the relative flow at the tail, but (Fig.6.5) also the angle of attack of the horizontal tail surface by the quantity

$$\Delta \alpha_{ht} = \arctg \frac{\omega_z L_{ht}}{V} \approx \frac{\omega_z L_{ht}}{V} \quad (6.2)$$

A consequence of the variation in angle of attack of the horizontal tail surface is the change in the lift of the tail by the quantity



STAT

$$\Delta Y_{ht} = \Delta c_{Lht} S_{ht} q k, \quad (6.3)$$

where k is the coefficient of deceleration of velocity in the tail region.

At the positive angular velocity ω_z , the additional lift of the horizontal tail surface will be directed upward. By multiplying the value of the additional lift of the tail according to eq.(6.3) by the arm of the horizontal tail surface relative to the center of gravity of the aircraft, L_{ht} , we obtain the additional moment produced by the horizontal tail surface on rotation of the aircraft

$$M_{zht-\omega_z} = -\Delta c_{Lht} S_{ht} q k L_{ht} \quad (6.4)$$

According to eq.(6.2), the additional coefficient of lift of the horizontal tail surface is equal to

$$\Delta c_{Lht} = a_{ht} \Delta a_{ht} = a_{ht} \frac{\omega_z L_{ht}}{V \sqrt{k}}. \quad (6.5)$$

On substituting the value of Δc_{Lht} from eq.(6.5) in eq.(6.4), we get

$$M_{zht-\omega_z} = -a_{ht} S_{ht} L_{ht} q V \sqrt{k} \frac{\omega_z L_{ht}}{V}. \quad (6.6)$$

Equation (6.6) shows that the moment of the horizontal tail surface caused by the rotation of the aircraft about the axis oz is directly proportional to the angular velocity of rotation ω_z and has a direction opposite to that of the rotation. This moment, which always counteracts the rotation of the aircraft, is known as the damping moment of the horizontal tail surface.

It is easy to prove that, at a negative angular velocity of rotation $\omega_z < 0$, the damping moment is positive, i.e., opposes the rotation of the aircraft. In a duck-type aircraft, in which the horizontal tail surface is located in front of the center of gravity of the aircraft, the damping moment is negative at positive ω_z .

(Fig.6.6), and positive at negative ω_z .

The damping moment actually counteracts the rotation of the aircraft, but at the beginning of a rotation it is unable to restore the aircraft to its original

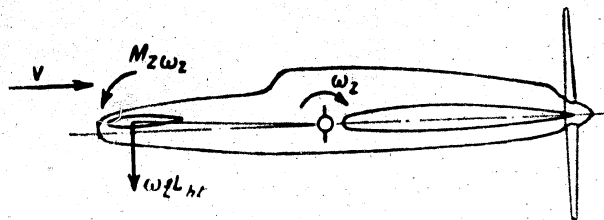


Fig.6.6 - Damping Moment of Tail in Duck-Type Aircraft

position. As shown by eq.(6.6), the damping moment changes its sign with any change in the sign of the angular velocity ω_z . Thus, if for any reason, whatever, an incipient rotation from the position of equilibrium is interrupted, and is replaced by a rotation toward the original position of equilibrium, then the damping moment will counteract this rotation just as it counteracted the initial rotation from the equilibrium position.

In the analysis of stability problems, the actual angular velocity ω_z can be conveniently replaced by the dimensionless angular velocity

$$\omega_z = \frac{v \omega_z}{v} \quad (6.7)$$

On substituting the dimensionless angular velocity ω_z , according to eq.(6.7), in the expression for the damping moment, eq.(6.6), we get

$$M_{z \omega_z} = -a_z S_{ref} l_{HT} \omega_z$$

or, passing to the moment coefficient,



$$m_{z, \dot{\omega}_z} = \frac{M_{z, \dot{\omega}_z}}{S_{h.t.}} = -a \cdot \frac{S_{h.t.} L_{h.t.}}{S_{b_A}^2} \dot{\omega}_z \quad (6.8)$$

In our subsequent analysis, we will frequently use the derivative of $M_{z, \dot{\omega}_z}$ with respect to the dimensionless angular velocity ω_z . If we denote this derivative by $m_{z, \dot{\omega}_z}^{\dot{\omega}_z}$, eq. (6.8) will yield

$$m_{z, \dot{\omega}_z}^{\dot{\omega}_z} = -a \dot{\omega}_z \frac{S_{h.t.} L_{h.t.}}{S_{b_A}^2} \quad (6.9)$$

On comparing eq. (6.8) with eq. (3.30) in Chapter III, for the moment coefficient of the horizontal tail surface, we note that if the moment coefficient of the horizontal tail $m_{z, \dot{\omega}_z}$ is proportional to the coefficient $A = \frac{S_{h.t.} L_{h.t.}}{S_{b_A}}$, representing the dimensionless static moment of the horizontal tail area, relative to the center of gravity of the aircraft, then the coefficient of damping of the moment will be proportional to the ratio $\frac{S_{h.t.} L_{h.t.}}{S_{b_A}^2}$, representing the dimensionless moment of inertia of the horizontal tail area relative to the center of gravity of the aircraft.

At a given value of A , it makes no difference in obtaining a definite value of the coefficient moment of the horizontal tail surface whether we vary the ratio $\frac{S_{h.t.}}{S}$ or $\frac{L_{h.t.}}{b_A}$. To obtain a definite coefficient of damping moment, however, this does make a difference; the aircraft in which the dimensionless arm of the horizontal tail surface $\frac{L_{h.t.}}{b_A}$ is greater will have a higher coefficient of damping moment at various values of A .

It must be borne in mind that the damping properties of the horizontal tail surface at high angles of attack may decrease or even vanish entirely. At an angle

of attack of the wing so high that the true angle of attack of the tail exceeds the angle of attack at which the C_L of the tail becomes equal to $C_{L \max}$, an increase in angle of attack of the horizontal tail surface obtained on rotation will not lead to an increase of the C_L of the tail, as was obtained on the linear segment of the curve $C_{L_{h.t.}} = f(\alpha_{h.t.})$. On the other hand, the increment in angle of attack of the tail leads to a decrease in $C_{L_{h.t.}}$ (in this case $\Delta C_{L_{h.t.}}$ will be negative), and the horizontal tail will not damp the rotation but will tend to intensify it. However, at large angles of attack, as may occur in a tail spin, the whole theory of stability becomes inapplicable. In the present discussion, we confine ourselves to the consideration of small angles of attack, when the relation $C_L = f(\alpha)$ may be considered linear.

Damping Moment of the Wings

Within the limits of the wing chord located near the center of gravity of the aircraft, the change in angle of attack produced by the rotation of the aircraft can no longer be considered constant, as was the case in the analysis of the damping by the horizontal tail surface. In this case (Fig.6.7) the signs of the additional angle of attack come out different in the leading and trailing parts of the wing.

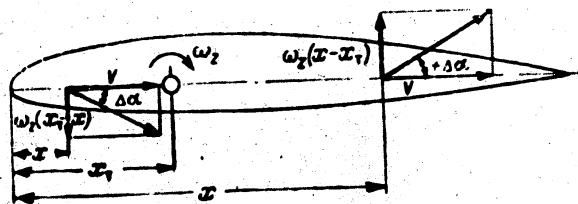


Fig.6.7 - Variation of the Flow around the Wing on Rotation of the Aircraft

The additional angle of attack at any point of the wing chord, due to the



STAT

rotation of the aircraft, is equal to

$$\Delta \alpha = \frac{c_{x_T}(\alpha, -\alpha)}{V} \quad (6.10)$$

where x_T is the coordinate of the center of gravity of the aircraft relative to the leading edge of the wings.

The occurrence of these additional angles of attacks, according to the curvature hypothesis, is equivalent to the corresponding camber of the profile; the aerodynamic characteristics of the fictive profile of such camber will not coincide with the aerodynamic characteristics of the actual profile. As a result of this, an additional moment, damping the rotation, will act on the profile.

Without going into detail, we will present only the final result obtained for a wing of finite span and rectangular planform (Bibl.8)

$$m_{\dot{\alpha}}^* = -\frac{a}{4} (1 - 2x_T^2 - \frac{2a}{16} \dots) \quad (6.11)$$

Equation (6.11) may be also used in first approximation for calculating trapezoidal wings with a slight sweepback*.

Figure 6.8 shows the calculation results when using eq.(6.11) for various centerings of the aircraft \bar{x}_T and for various aspect ratios of the wings (since

$a = \frac{\partial C_L}{\partial \alpha}$ is a function of the aspect ratio).

The damping produced by wings without sweepback is considerably less than the damping by the horizontal tail surface. Let us take the following starting data as

* It must be borne in mind that eqs.(6.9) and (6.11), in calculating the derivatives of a_{ht} and a , the angle of attack must be taken in radians, instead of in degrees, as was done earlier.

example

$$A = 0.5; \quad L_1 = 2.5; \quad h = 0.9; \quad a_1 = 4; \\ b_A = 5; \quad x_1 = 0.25.$$

From eq.(6.9) we have

$$m_{i,1}^* = -4 \cdot 0.5 \cdot 2.5 \cdot 0.9 = -4.75.$$

Equation (6.11) yields

$$m_{i,2}^* = \frac{5}{4} (1 - 2 \cdot 0.25)^2 - \frac{2^2 - 5}{10} = 0.99.$$

Obviously, the coefficient of damping moment of the wing was only about a twelfth the coefficient of damping moment of the tail.

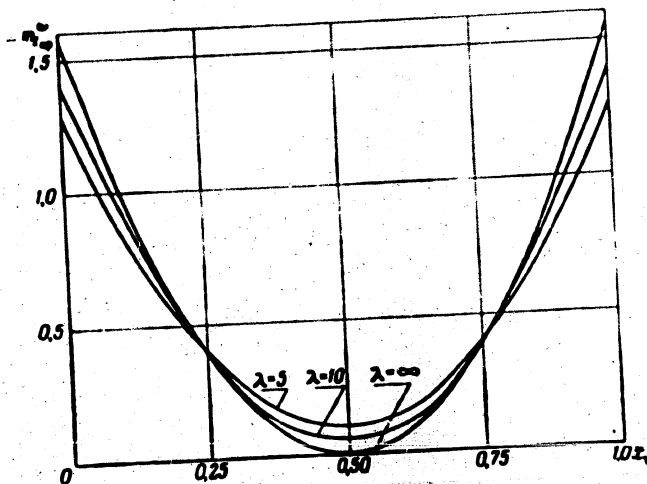


Fig.6.8 - Influence of Centering of Aircraft and Aspect Ratio of the Wing on the Damping Moment

Influence of Sweepback on Damping Moment of Wings

The distance from the axis oz passing through the center of gravity of the aircraft to the segment of elements of a sweptback wing (Fig.6.9) are greater than the

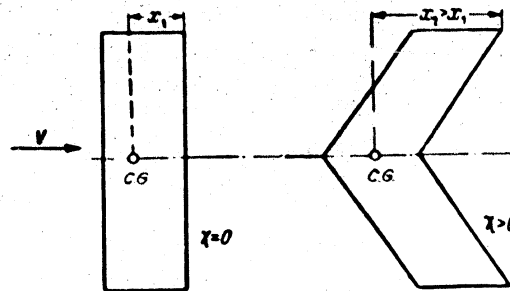


Fig.6.9 - Damping of Sweptback and Non-Sweptback Wings

same distances on a wing of the same planform but without sweepback. For this reason, the damping properties of the wing increase with increasing sweepback.

The approximate value of the moment coefficient of damping of a wing of constant chord with sweepangle may be determined on the basis of the following considerations.

The elementary moment due to rotation about the center of gravity of the aircraft in any wing section, at the distance x (Fig.6.10) of the plane of symmetry of the aircraft, will be equal to

$$dM_z = bdzq [\Delta c_m b + \Delta c_l x], \quad (6.12)$$

where x is the distance from the leading edge of the section taken as the axis of rotation; Δc_m , Δc_l are the increments of c_m and c_l due to the rotation of the aircraft.

The total moment acting on the whole wing is obtained by integrating eq.(6.12) along the wing span:



$$M_z = bq \left\{ b \int_{-\frac{l}{2}}^{+\frac{l}{2}} \Delta c_m dz + \int_{-\frac{l}{2}}^{+\frac{l}{2}} \Delta c_l x dz \right\}.$$

Introducing the dimensionless coordinate $\bar{z} = \frac{z}{l}$ and taking $\bar{x} = \frac{x}{b}$, we may rewrite this expression in the form

$$M_z = b^2 l q \left\{ \int_0^1 \Delta c_m d\bar{z} + \int_0^1 \Delta c_l \bar{x} d\bar{z} \right\}.$$

so that the moment coefficient becomes

$$m_z = \int_0^1 \Delta c_m d\bar{z} + \int_0^1 \Delta c_l \bar{x} d\bar{z}. \quad (6.13)$$

On the basis of the above-mentioned curvature hypothesis, the following approximate expressions can be obtained for Δc_m and Δc_l :

$$\left. \begin{aligned} \Delta c_m &= - \left[0.25a(0.75 - \bar{x}_c) + \frac{\pi}{8} \right] \alpha_c \\ \Delta c_l &= a(0.75 - \bar{x}_c) \alpha_c \end{aligned} \right\} \quad (6.14)$$

where, in determining $a = \frac{\partial C_L}{\partial \alpha}$, the angle of attack α must be taken in radians.

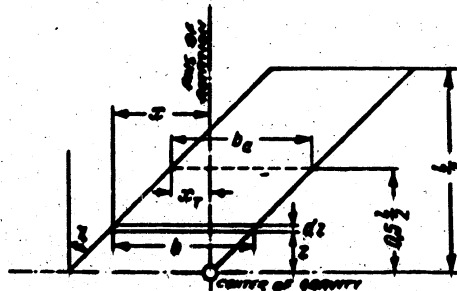


Fig.6.10 - For Determining the Damping Moment of a Sweptback Wing

STAT

It is clear from Fig. 6.10 that

$$\bar{x} = \bar{x}_T - \frac{l}{2b} (z - 0.5) \lg \chi = x_T - \frac{l}{2} (z - 0.5) \lg \chi. \quad (6.15)$$

On substituting eqs. (6.14) and (6.15) in (6.13), after integration and simplifications, we obtain the following expression for m_z^w of a sweptback wing with constant chord:

$$m_{T,sp}^w = - \left\{ \frac{a}{4} (1 - 2\bar{x}_T)^2 + \frac{2a - a}{16} \right\} + \frac{a^2 \lg^2 \chi}{48}. \quad (6.16)$$

Bearing in mind that the taper of sweptback wings, generally speaking, differs from $\eta = 1$, while in the theory we are considering a wing of constant chord ($\eta = 1$), and applying a correction to the general approximation of the arguments, we obtain the following final expression for the m_z^w of a sweptback wing

$$m_{T,sp}^w = - \left\{ \frac{a}{4} (1 - 2\bar{x}_T)^2 + \frac{6 - a}{16} \right\} + 0.019a^2 \lg^2 \chi. \quad (6.17)$$

As an example, let us use eq. (6.17) for calculating the value of m_z^w for $a = 4$; $\lambda = 5$; $\bar{x}_T = 0.25$, assuming that in one case $\chi = 0$, and in the other case $\chi = 45^\circ$.

We then have, for wings without sweepback ($\chi = 0$)

$$m_{T,sp}^w = - \left[\frac{4}{4} (1 - 2 \cdot 0.25)^2 + \frac{6 - 4}{16} \right] = -0.375$$

For a wing with sweepback $\chi = 45^\circ$:

$$m_{T,sp}^w = - [0.375 + 0.019 \cdot 4 \cdot 25] \cdot 0.707 = -1.61$$

* It must be borne in mind that the gradient of the lift a of a sideslipping wing is smaller by a factor of $\cos \chi$ than for a rectangular wing of the same aspect ratio: $a_\chi = a \cos \chi$

As seen from this example, sweepback considerably increases the damping property of a wing.

Damping of Fuselage. Resultant Damping Moment

With respect to the fuselage, the same reasoning is applicable as to the wing. For this reason, on the basis of the curvature hypothesis, an expression for the moment coefficient of damping of the fuselage may be obtained. Calculations show that the quantity m_2^w of the fuselage is small; for practical purposes, this coefficient may just as well not be separately calculated, if, instead, we take the damping properties of the fuselage into account by applying some correction factor to eq.(6.9), which value must be taken from statistical data.

In this way, the resultant moment coefficient of damping of an aircraft may be determined by the formula

$$m_2^w \approx -1.20 \frac{S_{HL} L_{HL}^2}{S_A^2} V^2 \left[\frac{1}{4} (1 - 2\tau)^2 + \frac{6}{15} \tau + 0.019 \alpha^2 (1.5)^2 \right] \quad (6.18)$$

where the damping of the fuselage is taken into account by the factor 1.2 in the first summand.

For modern aircraft with sweptback wings, the value of m_2^w usually ranges from -5.5 to -7. In view of the fact that a number of assumptions were made in deriving eq.(6.18), it is recommended that experimental data, obtained in special installations in wind tunnels, be used in calculating m_2^w .

Lag of the Downwash at the Tail

In comparing the results of calculation by the above methods with empirical data, a marked discrepancy between theory and experiment was found. The experimental data were considerably larger (about 1.5 times) than the results obtained by calculation. The primary reason for this discrepancy between theory and experiment

STAT

is the inapplicability of the stationary state hypothesis to an evaluation of the damping of the horizontal tail surface.

It is found that in unsteady motion of an aircraft the conditions of flow around the horizontal tail surface cannot be evaluated by means of the kinematic parameters of motion at the given instant of time alone. It is also necessary to allow for the character of motion of the aircraft in the preceding instants of time. To prove this, let us turn to a more detailed consideration of the conditions of flow about horizontal tail surfaces during unsteady motion of an aircraft.

Let the aircraft have a translational velocity and at the same time rotate about the axis oz . Here, to each instant of time t corresponds a definite angle of attack of the wings α and, consequently, a definite value of the lift coefficient C_L .

The downwash at the wing is created by the circulation of the velocity corresponding to the time t . However, in view of the fact that the tail is located at a certain distance downstream of the wing, a certain time is required for the velocity induced by the wing to reach the horizontal tail surface. At a flying speed V of the aircraft and a distance $l_{h.t.}$ between the wing and the horizontal tail surface, the velocity induced by the wing will reach the tail after the time interval:

$$\tau = \frac{l_{h.t.}}{V}$$

For this reason, at the time t , the downwash in the region of the horizontal tail surface will correspond to the angle of attack of the wing which existed at the time

$$t_1 = t - \tau$$

This angle of attack will differ from the angle of attack at the time t by the quantity

$$\Delta\alpha = -\frac{d\alpha}{dt} \tau = -\alpha \frac{l_{h.t.}}{V} \quad (6.19)$$

STAT

The downwash at the tail due to the wing may be represented in the form

$$w = D\alpha, \quad (6.20)$$

where D is the coefficient depending on the law of spanwise distribution of circulation and on the mutual position of tail and wings.

Taking the derivative of eq.(6.20) with respect to α , we may determine the amount by which the downwash at the tail will differ from the quantity which, by the stationary state hypothesis, corresponds to the time t

$$\Delta w = D \frac{d\alpha}{dt} \Delta t = D \alpha \frac{L_{ht}}{V V_0} \quad (6.21)$$

The result of this lag of the downwash will be an additional lift of the horizontal tail directed upward (at positive α_2)

$$\Delta Y_{ht} = -\alpha_{ht} \Delta w S_{ht} q_0 = -\alpha_{ht} D \alpha \frac{L_{ht}}{V} S_{ht} q_0 \quad (6.22)$$

and additional moment of the horizontal tail surface

$$\Delta M_{ht} = -\alpha_{ht} D \alpha \frac{L_{ht}}{V} S_{ht} q_0 l_{ht} \quad (6.23)$$

tending to diminish the angle of attack.

Let us introduce the dimensionless derivative of the angle of attack with respect to time

$$\alpha' = \frac{d\alpha}{dt}$$

and let us determine, by eq.(6.23), the coefficient of additional moment

$$m_{\alpha' ht} = -\alpha_{ht} D \alpha \frac{L_{ht}^2}{V} S_{ht} q_0$$

Taking the derivative of the expression obtained for $m_{\alpha' ht}$ with respect to α ,

we obtain the derivative of the coefficient of moment due to the lag of the downwash:

$$m_i' = -a_{ht} D a \frac{\partial a_{ht}}{\partial \alpha_{ht}} \quad (6.24)$$

On comparing eqs. (6.24) and (6.9), we note that the coefficients m_z and $m_{zh.t.}^{\omega}$ are connected with each other by the relation:

$$m_i' = -m_{ht}^{\omega} D a$$

On the average, for aircraft flying at subsonic speeds, $D \approx 6 - 8$; $a = 0.07 - 0.08$, so that

$$m_i' \approx 0.4 m_{ht}^{\omega} \quad 0.6 m_{ht}^{\omega}$$

As will be seen, the error due to neglecting the lag of the downwash in calculating the moment of the horizontal tail surface in unsteady motion would be an appreciable quantity.

Influence of the Compressibility of Air on the Moment of Damping

With the variation of the Mach number, all the basic aerodynamic characteristics of the aircraft also vary, while these variations become particularly great at $M > M_{tor}$. It is only natural that, at any variation in M , the coefficients m_z^{ω} and m_z^{α} will also vary.

At the present time we have no experimental data on values of these coefficients at high Mach numbers. For this reason, in the analysis of the influence of the Mach numbers on these coefficients, we must confine the study to merely qualitative considerations.

As M increases in the region $M < M_h$, the derivatives $a = \frac{\partial C_L}{\partial \alpha}$ and $a = \frac{\partial C_{Lh.t.}}{\partial \alpha_{h.t.}}$ increase, the coefficient $D = \frac{\partial g}{\partial C_L}$ varies only slightly. On turning to eqs. (6.9) and (6.24), we see that, in this case, the coefficients $m_{zh.t.}^{\omega}$ and m_z^{α} likewise

0
2
4
6
8
10
12
14
16
18
20
22
24
26
28
30
32
34
36
38
40
42
44
46
48
50
52
54
56

increase, at greater increases in m^a . Equation (6.17) shows that m_z^{ω} likewise increases. Thus, in this region of high Mach numbers, the damping properties of an aircraft increase with increasing M .

At $M < M_{tor}$, the coefficient a begins to decrease, the coefficient $a_{h.t.}$ slows its rate of growth and decreases on further increase of M , while the coefficient D declines. As a result, the coefficients m_z^{ω} and m_z^a decrease.

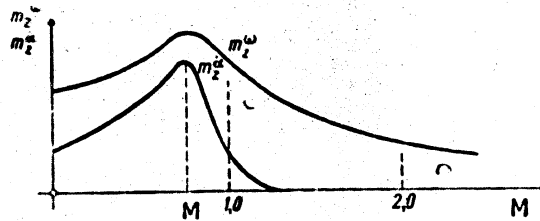


Fig.6.11 - Approximate Character of the Variation of m_z^{ω} and m_z^a with M

38
40
42
44
46
48
50
52
54
56

In the region of supersonic speeds at $M > 1$, the values a and $a_{h.t.}$ continue to decline with increasing M , and the downwash at the tail vanishes ($D = 0$). Thus, in this region of Mach numbers, the coefficient m_z^{ω} continues to decrease monotonously, while the coefficient m_z^a vanishes. Figure 6.11 shows the approximate character of the slopes of the coefficient m_z^{ω} and m_z^a .



CHAPTER VII

LONGITUDINAL MOTION OF THE AIRCRAFT AND ITS STABILITY

Resolution of the Aircraft Motion into Longitudinal and Lateral Components

In the most general case, the motion of an aircraft must be considered as a motion in space by a body having six degrees of freedom, i.e., as the sum of three translational motions with respect to three axes of coordinates and three rotary motions about these axes. Such motion is described by six equations, whose solution in the general case is highly complex. In studying the controllability and stability of the aircraft, the motion of the aircraft in space is customarily resolved into longitudinal and lateral components, these two motions being usually taken as independent of each other.

Longitudinal motion is the term applied to the motion of an aircraft taking place in a plane coinciding with the plane of symmetry of the aircraft, that is in the plane passing through the longitudinal axis of the aircraft and perpendicular to the transverse axis of the aircraft oz directed along the wing span (Fig.7.1).

The basis for the resolution of the aircraft motion into longitudinal and lateral is the fact that, at small deviations of the aircraft motion from symmetrical motion (and it is such deviations that are in fact considered by the theory in most cases), it may be considered that the forces and moment acting in the longitudinal plane do not vary. In exactly the same way the forces and moments acting in the two other coordinate planes do not vary at small deviations of the aircraft

motion in its plane of symmetry.

In the longitudinal motion of an aircraft, there is variation of only three of

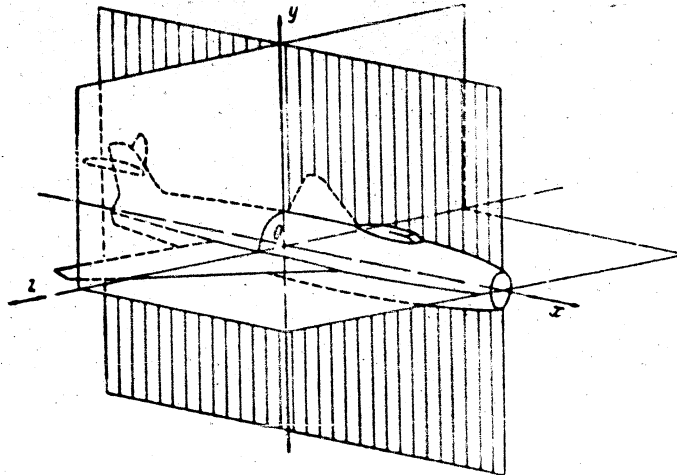


Fig.7.1 - Plane of Symmetry of the Aircraft, xy

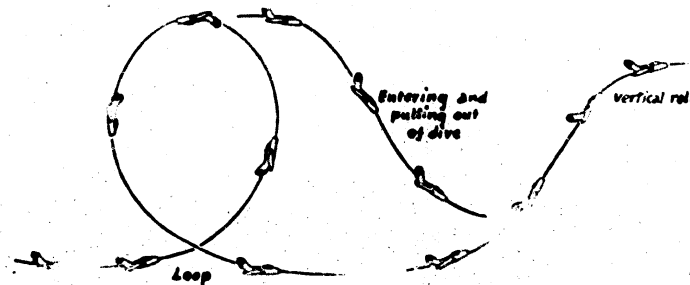


Fig.7.2 - Flight Path of the Aircraft and Position of the Aircraft in Executing Loop, Climb, and Dive

the six independent parameters which in the general case determine its position and motion in space as a solid body; for example, the speed of flight, the angle of

attack and the angle of inclination of the flight path, or the components of velocity with respect to the axes of coordinates fixed with respect to the aircraft and the angle of pitching, etc. Some examples of longitudinal motion of an aircraft are the loop, the climb, and the dive (Fig.7.2). The longitudinal motion of an aircraft is described by three equations, which simplify the solution of the problem by comparison with the most general case.

Lateral motion is the term applied to the motion of the aircraft in the xz and yz planes, when the center of gravity of the aircraft remains in the horizontal plane. In lateral motion, of the six independent parameters likewise only three vary; as such three independent parameters, we may take for example, the angle of sideslip, the angle of bank, and the angular velocity with respect to the normal axis of the aircraft; or the components of the angular velocity with respect to the ox and oy axes connected with the aircraft and the angle of yaw, etc*.

Examples of lateral motion of an aircraft are the turn of an aircraft in a horizontal plane, sideslip, and free lateral oscillations.

Strictly speaking, only gliders or multi-engine aircraft with an even number of engines in which the engines are symmetrically located and the propellers are of the counterrotating type can be considered fixed with respect to the xy plane. Usually, however, an aircraft is also asymmetric due to rotation of the engine and propeller parts in a single direction, asymmetric setting of the vertical tail surfaces, etc.

In a strictly symmetrical glider or aircraft, all types of longitudinal motions or maneuvers may be effected by deflecting only the elevator, with the ailerons and

* The angle of sideslip is the term applied to the angle between the projection of the vector of velocity on the xz plane and the x axis; the angle of bank is used for the angle between the z axis and the horizontal plane. The angle of yaw is used for the angle of rotation of the aircraft in the horizontal plane.

rudder held motionless. If, in a strictly symmetrical aircraft or glider, a gust exerts a symmetrical action, then the following disturbed motion of the aircraft (if the pilot does not intervene in the control) will also be symmetric, i.e., it will take place in the same vertical plane as before the start of the disturbance.

Since the aircraft is usually not strictly symmetric, it follows that in performing maneuvers in a vertical plane, moments and forces that tend to bring the flight path out of the vertical plane appear together with the longitudinal moments and forces acting on the aircraft. Of these asymmetric moments and forces, the most substantial in magnitude are the forces connected with the gyroscopic effect of the propellers and the rotating part of the engines, and with the twist imparted to the air flow by the propellers. To enable the pilot to perform any maneuver, for example a loop in a vertical plane, he is compelled, while deflecting the elevator, to produce longitudinal moments by deflecting in a definite manner the ailerons and rudder, in order to counteract the lateral moments that are produced on the execution of the maneuver. In propeller aircraft, these asymmetric moments are rather considerable and noticeable to the pilot; from flying practice, the difference is well known in piloting technique when executing so-called left and right figures, for example, a left and right turn.

In aircraft with jet engines, the engine parts rotate on relatively short radii, but the effect of twist of the air flow passing through the engine is small or even entirely absent. For this reason, the asymmetric moments are considerably smaller in jet aircraft than in propeller aircraft.

As stated above, in studying the behavior of an aircraft in the air with the object of obtaining more easily visualized results, it is expedient to consider the longitudinal motion of the aircraft in the plane of symmetry independently of its asymmetric lateral motion. Such a separate study of the longitudinal motion presupposes that the pilot, if necessary, will be able to actuate the ailerons and rudder in an ideal manner, and will always be able to maintain the flight path in

the vertical plane coinciding with the plane of symmetry of the aircraft, and that the longitudinal forces and moments in this case will not depend on the action of the ailerons and rudder. Of course, a number of maneuvers such as a turn, a complete combat rotation of the tail wing, etc., require the simultaneous consideration of longitudinal and lateral motion, i.e., the consideration of the general case of the motion of the body with six degrees of freedom. In this book, however, we will not take up this problem.

Forces and Moments Acting on the Aircraft

The motion of an aircraft in the vertical plane will be characterized by three independent equations: two equations connected with the projection of forces and one equation connecting the moments acting on the aircraft.

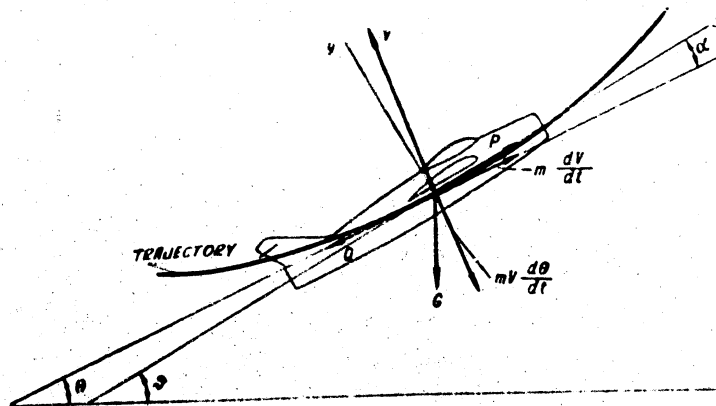


Fig.7.3 - Trajectory of Motion and Diagram of Forces Applied to Center of Gravity of Aircraft

The forces applied in flight to the individual parts of the aircraft, in setting up the equations of motion, may be reduced to systems of forces applied to the

center of gravity of the aircraft (Fig.7.3), and to moments with respect to the transverse axis of the aircraft passing through its center of gravity.

The external forces applied to the aircraft will be as follows: the engine thrust P , the lift Y , the drag Q , and the force of gravity G .

In theoretical studies and calculations of the stability and controllability of aircraft, with the exception of aircraft equipped with liquid-jet engines, the weight and mass of the aircraft are usually considered to be constant.

In working up the results of flight measurements, and in particular for determining the characteristics of longitudinal stability and controllability of an aircraft from flight tests, it is necessary in some cases to allow for the variation of the weight and mass of the aircraft with time, that is, it is necessary to allow for the relation

$$G = f(t); \quad (7.1)$$

In the present course, however, we will consider the weight and mass of the aircraft to be independent of time.

For the general case of unsteady controlled motion of an aircraft in air, the longitudinal aerodynamic moment may be expressed by the function

$$M_x = F(\alpha, \dot{\alpha}, \omega, \dot{\omega}, V, H, t) \quad (7.2)$$

In allowing for the influence of the compressibility of air on the longitudinal aerodynamic moment in the functional relation given by eq.(7.2), it is in practice more convenient to express the parameter V in terms of the Mach number.

General Equation of the Longitudinal Motion of an Aircraft

In the general case of unsteady motion, the forces and moments applied to the aircraft are unbalanced. As a result of the fact that the forces are unbalanced, i.e., owing to the fact that the resultant of all external forces applied to the aircraft is not equal to zero, it will move with a linear acceleration or decelera-

tion. In consequence of the fact that the resultant moment of the external forces will not be equal to zero, the aircraft will also have an angular acceleration or deceleration. This will be reflected by the equations of unsteady motion of the aircraft in their analytical form.

A convenient form of the general equations of longitudinal motion is obtained by finding equations for the magnitude of the linear accelerations along the tangent and along the normal to the flight path, and also for the value of the angular acceleration of rotation of the aircraft with respect to its transverse axis passing through the center of gravity of the aircraft.

The acceleration of motion in the direction of the tangent to the path of the center of gravity of the aircraft, i.e., in the direction of the speed of flight, is called the tangential acceleration and is equal to the derivative dV/dt .

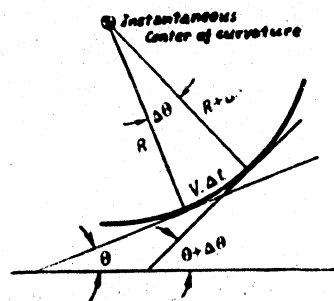


Fig.7.4 - Relation between the Variation in the Angle of Inclination of the Flight Path, the Radius of Curvature and the Flying Speed

The value of dV/dt may be found by applying the well-known law of mechanics: the product of the mass of a body by its acceleration is equal to the acting force. The force acting in the direction of the velocity of flight will represent the resultant projection of all forces applied to the flight path.

Proceeding in this way, we obtain the

first equation:

$$\frac{dV}{dt} = P \cos \alpha - Q - G \sin \theta. \quad (A)$$

If the right side of eq.(A) is positive in sign, then the speed of the aircraft will be increasing at the moment of time under consideration. With the right side

of eq.(A) negative in sign, the speed of the aircraft will decrease.

The acceleration of motion, along the normal to the flight path, of the center of gravity of the aircraft is called centripetal; as we know from the course on mechanics, its absolute value is determined by the expression $\frac{V^2}{R}$, where V is the velocity of flight and R the instantaneous radius of curvature of the flight path. In analyzing the motion of an aircraft, it is more convenient to use the expression for the centripetal acceleration related to the velocity of flight and the angular velocity of rotation of the flight path, equal to $d\theta/dt$. It is relatively easy to prove (Fig.7.4) that, at any instant of motion,

$$V = R \frac{d\theta}{dt} \quad (7.3)$$

so that the centripetal acceleration may be represented in the form

$$V \frac{d\theta}{dt}$$

The magnitude and sign of the centripetal acceleration will be determined by the magnitude and sign of the projection of the resultant of all forces, applied to the aircraft, onto the normal to the flight path. The projection of the resultant force is equal to the sum of the projections of the forces of its components. For this reason, the second of the general equations of motion of the aircraft will be represented in the form

$$m \frac{d^2 s}{dt^2} = P \sin \alpha + Y - G \cos \theta \quad (B)$$

According to this equation, the centripetal acceleration at angular velocity of rotation of the flight path $d\theta/dt$ is the sum of the lift Y of the aircraft, and the projection of the engine thrust onto the normal to the flight path will be greater than the projection of the weight onto the normal to the flight path, i.e., in the case when

$$(Y + P \sin \alpha) > G \cos \theta$$



Finally, the angular acceleration rotation of the aircraft about its transverse axis $d\theta/dt$ will be connected with the moments of the forces with respect to the same axis by the equation

$$I_y \frac{d^2\theta}{dt^2} = M_x - M_y \quad (C)$$

If the angular velocity of rotation of the aircraft with respect to its transverse axis (the angular velocity of pitching) is denoted by ω_z , then we may write

$$\frac{d\theta}{dt} = \omega_z$$

In this way we obtain a system of three differential equations

$$\begin{cases} m \frac{d^2x}{dt^2} = \cos \alpha \cdot Q - Q \sin \alpha \\ m \frac{d^2y}{dt^2} = \sin \alpha \cdot Y - Q \cos \alpha \\ I_y \frac{d^2\theta}{dt^2} = M_x - M_y \end{cases} \quad (7.4)$$

determining the motion of the aircraft in the vertical plane (plane of symmetry).

As the independent variables in these three equations we may select any three parameters out of all the parameters on which the forces and moments entering into these equations depend. In the general case, the forces and moments depend on the parameters

$$V, \alpha, \theta, H, t,$$

on their derivatives with respect to time, and on t .

It is here assumed that the position of the engine control stick (throttle control) does not change during the motion of the aircraft under consideration. As we see, the total number of variables exceeds the number of equations of the system (7.4). For this reason the system of equations (7.4) must be supplemented by an additional relation or connection between the variables to make the problem of finding a solution of this system mathematically realizable, at least in principle.



If we consider the disturbed motion of the aircraft, without intervention by the pilot, then the position of the elevator will be either constant ($\delta = \text{const}$), or will be determined by the variation in the remaining parameters of motion [$\delta = f(\alpha, V, \theta, H, \text{ and } t)$]. In both these cases the two "superfluous" variables may be eliminated from the system of equations (7.4) by means of two auxiliary equations:

$$\left. \begin{aligned} \frac{dH}{dt} &= V \sin \theta, \\ \alpha &= \theta - \theta_0. \end{aligned} \right\} \quad (7.5)$$

On considering the controlled motion, eq.(7.4) and eq.(7.5) must be supplemented by defining either the variation of the elevator position with time $\delta = f(t)$, or the variation, as a function of time, of any other of the parameters of motion of the aircraft, for example, the angle of attack.

The first of the equations (7.5) is easy to obtain if the velocity of the center of gravity of the aircraft along the vertical is represented, on the one hand, in the form of the derivative dH/dt , and on the other hand, as the projection of the velocity along the flight path onto the vertical. The second equation results from the geometric relations which are indicated in Fig.7.3.

Integration of the Equations of Motions

The system of differential equations of motion of the aircraft (7.4) cannot be solved analytically in its general form, since their right-hand sides are complex functions of the parameters of aircraft motion and of the aircraft position in space. The forces and moments entering onto the right-hand sides cannot, in the general case, be represented by sufficiently simple analytical expressions. The dependence of the forces and moments on the parameters of motion of the aircraft in many cases is determined by means of experimental plots, for example plots of the coefficients C_D and C_L as functions of the angle of attack and the Mach number, curves of the coefficient of longitudinal moment m_x as a function of the coefficient C_L , the Mach number, etc. As a result of this, the initial equations of motion of

the aircraft in the general form consist of a complex system of nonlinear differential equations.

To determine the motion of the aircraft itself from its equations, we must either make simplifying assumptions, under which it becomes possible to integrate the equations in the general analytical form, or we must use approximate methods of integrating these differential equations.

Simplifying assumptions may be made to obtain analytical solutions of these equations of motion only in the investigation of special problems of the dynamics, stability and controllability of aircraft. As an example of such a simplification we might mention the assumption that the flying speed or the angle of attack remain unchanged during unsteady motion. The most widely used and highly useful assumption is that the unsteady disturbed motion of an aircraft differs from the initial steady state of flight only by minor deviations of the parameters of motion from their values, corresponding to the initial state of flight. This assumption forms the basis for the method of small disturbances, which will be discussed in greater detail below and which is widely used in the various fields of technology.

Numerical Integration of the Equation of Motion

In cases where the above assumptions are inapplicable, the motion of an aircraft, for example, in studying the dive and other maneuvers must be determined by approximate methods of integration of the total differential equations of motion.

The use of these methods gives a picture of the motion of the aircraft in space under any forms of the relation of the forces and moments to the parameters of motion and time, for any maneuvers of the aircraft, and with any initial deviations of the aircraft from the original state of flight.

There are many methods of approximate integration of differential equations: numerical, graphical, and mixed; all of these methods are very time-consuming in performing the calculations.

The one with the simplest idea is the method of numerical integration, which is

widely used in technology and will be briefly described below.

Starting from the differential equations (7.4) and the auxiliary equations, we can write the approximate equations in which the infinitesimal increments of the variables are replaced by small but finite increments ΔV , $\Delta \theta$, etc.

In each specific case of aircraft motion investigated, relations, assigned by some method or other, must exist between the forces and their moments and the parameters of motion of the aircraft, or the angle of elevator deflection δ , as well as with the atmospheric conditions, which are defined on the one hand by the values of the density ρ and the atmospheric pressure p , and on the other hand by the parameters of the motion of the air itself.

$$\begin{aligned} \Delta V &= \frac{\Delta t}{m} (P \cos \alpha - Q - G \sin \theta) \\ \Delta \theta &= \frac{\Delta t}{mV} (P \sin \alpha + Y - Q \cos \theta) \\ \Delta \omega_x &= \Delta t \frac{M_x - PY_z}{I_x}; \\ \Delta \omega_y &= \Delta t \frac{M_y - PZ_x}{I_y}; \\ \Delta H &= \Delta V \sin \theta; \\ \Delta \alpha &= \Delta \theta - \Delta \omega_x. \end{aligned} \quad (7.6)$$

If necessary, the laws of the variation of the aircraft weight with time and with the parameters of motion of the aircraft must also be assigned.

The solution of the equations of motions by this method of integration reduces to the following operations: Knowing the parameters of motion of the aircraft and the forces and moments entering the right-hand sides of the eq.(7.6), for the initial instant of time $t_0 = 0$, and having assigned, in accordance with the required accuracy of calculation, a definite time interval Δt , we find the increments of the parameters in the left-hand sides of eq.(7.6). On summing them from the initial values of the parameters, we determine the velocity, height, angular attack, etc., corresponding to the new instant of time $t_1 = t_0 + \Delta t$. From the resultant parameters of motion

and time t_1 we determine the new values of the forces and moments, allowing for the changes in density and pressure of the air, and also the new value of the aircraft mass (if it is necessary to allow for the variation of mass with time). We then find the new increments $\Delta V_1, \Delta \theta_1$, etc. This process of calculations is repeated, step by step, until the final result is obtained.

In practice, within the limits of the required accuracy of calculation, it is often more expedient to assign not a definite time interval, but a definite increment of one of the parameters of motion, for instance, ΔV . Then, at each stage of the computations, we determine the corresponding increment Δt by the formula

$$\Delta t = \frac{\Delta V}{P \cos \alpha - Q - G \sin \theta} \quad (7.7)$$

and for the calculation of the increments of the other parameters this value of Δt , new each time, is used.

The accuracy of the methods of numerical integration will be greater the shorter the time interval Δt is taken or the smaller the increment of a given parameter of motion.

In many cases, a considerable simplification of the calculations is possible because of the smaller number of general equations used in this case and because of the reduction in the number of variables entering the equation. In the analysis of longitudinal motion of an aircraft, such cases might include calculations of the take-off run or deceleration of the aircraft along a horizontal straight line, dive of the aircraft at a constant angle of inclination of the flight path, or a dive at constant angle of pitch. In such cases, the method of numerical integration may give an answer to the questions under consideration with a considerably smaller expenditure of time.

The Method of Small Disturbances

The above method of numerical integration of the equations of motion of an aircraft allow the character of the motion to be determined under the given concrete

conditions. This is very laborious and gives no indications of the general relations and laws of motion. For example, in order to prove by this method that an aircraft is stable in flight under the effect of various external influences, it would be necessary to perform laborious calculations for each of these disturbances.

The method of small disturbances is free from the shortcomings inherent to the method of numerical integration. As already stated, the use of the method of small disturbances assumes that, during the disturbed motion or controlled maneuver under consideration, there arise only small deviations of the parameters, characterized in the motion of the aircraft from their values corresponding to the initial steady state of flight. Under this assumption, the system (7.4) may be reduced to a system of linear differential equations which may be integrated. The widely disseminated classical theory of the dynamic stability of aircraft is founded on this method.

Let us apply the method of small disturbances to the study of stability of the longitudinal motion of an aircraft. Let us write the general equations of motions, instead of the system (7.4), in the following form:

$$\left. \begin{aligned} m \frac{dv}{dt} - X_c \cdot \sin \theta &= 0 \\ m v \frac{d\theta}{dt} - Y_c \cdot G \cos \theta &= 0 \\ I_{yy} \frac{d\omega}{dt} - M_x &= 0 \end{aligned} \right\} \quad (7.8)$$

Here X_c denotes the algebraic sum of the projections of the forces of the engine thrust onto the tangent to the flight path, and the drag of the aircraft; and Y_c the algebraic sum of the projection of the force of engine thrust onto the normal, the flight path, and the lift*

* The form of the equations of aircraft motion in (7.8) have the advantage over the form of eq.(7.4), that eq.(7.8) has one and the same form for (cont'd. next page)

$$\left. \begin{aligned} X_c &= Q - P \cos \alpha \\ Y_c &= Y + P \sin \alpha \end{aligned} \right\} \quad (7.9)$$

Analogously, M_{zc} denotes the algebraic sum of the aerodynamic moment and the moment due to the direct engine thrust

$$M_{zc} = M_z - P y_f \quad (7.10)$$

In all subsequent discussions we will assume that the initial state of steady rectilinear flight corresponds to constant values of the parameters of motion

$$V, \alpha, \theta, \dot{\theta} = 0$$

Then, from eq.(7.8), since for steady motion

$$\frac{d}{dt} - \frac{d}{dt} = \frac{d}{dt} - \frac{d}{dt} = 0$$

we obtain the following equations of the initial steady state of flight:

$$\left. \begin{aligned} X_{c0} + Q \sin \theta_0 &= 0 \\ -Y_{c0} + Q \cos \theta_0 &= 0 \\ M_{zc0} &= 0 \end{aligned} \right\} \quad (7.11)$$

Where the subscript "0" denotes the initial values of the forces and parameters of motion.

Disturbed motion will be characterized by a small variation in time of the variables V , α , θ and $\dot{\theta}$ (variations) which may be represented in the form:

(contin) both aircraft and glider, and for engine and engineless flight. In analyzing the results of flight tests it is practically impossible to determine the drag or lift and the corresponding summand of engine thrust separately.

$$\left. \begin{aligned} V &= V_0 + \Delta V \\ \alpha &= \alpha_0 + \Delta \alpha \\ \theta &= \theta_0 + \Delta \theta \\ \dot{\theta} &= \dot{\theta}_0 + \Delta \dot{\theta} \end{aligned} \right\} \quad (7.12)$$

If, after a certain time has elapsed, the quantities ΔV , $\Delta \alpha$, $\Delta \theta$, $\Delta \dot{\theta}$ become smaller than certain assigned values, then, according to the definition at the beginning of this book, the airplane is stable. In the opposite case, the aircraft is unstable in the assigned initial state of flight.

Since, by definition, ΔV , $\Delta \alpha$, $\Delta \theta$ and $\Delta \dot{\theta}$ are small quantities, then each force and moment depending on the parameters of motion of the aircraft may be represented by a Taylor power series of the increments of these parameters. Owing to the smallness of the increments ΔV , $\Delta \alpha$ etc., the terms beginning with the second order of smallness and higher orders, may be neglected in each Taylor series.

Let us now set up the equations of motion, taking account of the assumptions made. The weight, mass, and moment of inertia of the aircraft will be considered constant. The density of the air, within the range of variation of flying height under consideration, will also be considered constant and equal in value to the density of air at the level of the initial steady state of motion.

On the basis of the above assumptions, at unsteady disturbed motion, the external forces and moments may be represented by the following expressions*:

* In the general case, in eq.(7.13), for X and Y we would have to add terms depending on the angular velocity of rotation as was done for M_{zC} . But in view of the lack of sufficient information on the influence of ω_z on X_C and Y_C , these terms will be neglected.

$$\begin{aligned}
 X_1 &= X_{10} + \left(\frac{\partial X_1}{\partial V}\right)_0 \Delta V + \left(\frac{\partial X_1}{\partial \alpha}\right)_0 \Delta \alpha \\
 Y_1 &= Y_{10} + \left(\frac{\partial Y_1}{\partial V}\right)_0 \Delta V + \left(\frac{\partial Y_1}{\partial \alpha}\right)_0 \Delta \alpha \\
 G \sin \theta &= G \sin \theta_0 + \left[\frac{\partial (G \sin \theta)}{\partial \theta}\right]_0 \Delta \theta \\
 G \cos \theta &= G \cos \theta_0 + \left[\frac{\partial (G \cos \theta)}{\partial \theta}\right]_0 \Delta \theta \\
 M_{1c} &= M_{1c0} + \left(\frac{\partial M_{1c}}{\partial V}\right)_0 \Delta V + \left(\frac{\partial M_{1c}}{\partial \alpha}\right)_0 \Delta \alpha + \\
 &\quad + \left(\frac{\partial M_{1c}}{\partial \omega}\right)_0 \Delta \omega + \left(\frac{\partial M_{1c}}{\partial \dot{\alpha}}\right)_0 \Delta \dot{\alpha}
 \end{aligned} \tag{7.13}$$

By hypothesis, the initial motion is steady, so that V , α , θ and $\dot{\theta}$ are constants and their derivatives with respect to time are zero.

Therefore,

$$\frac{dV}{dt} = \frac{d\Delta V}{dt}; \quad \frac{d\alpha}{dt} = \frac{d\Delta \alpha}{dt}; \quad \frac{d\theta}{dt} = \frac{d\Delta \theta}{dt}; \quad \frac{d\dot{\theta}}{dt} = \frac{d\Delta \dot{\theta}}{dt}$$

Since the weight G of the aircraft is taken as constant, we have

$$\left[\frac{\partial (G \sin \theta)}{\partial \theta}\right]_0 = G \cos \theta_0; \quad \left[\frac{\partial (G \cos \theta)}{\partial \theta}\right]_0 = -G \sin \theta_0$$

We now substitute in eq.(7.8) the forces and moments by eq.(7.13), introducing

the notation

$$\left(\frac{\partial X_1}{\partial V}\right)_0 = X_V; \quad \left(\frac{\partial X_1}{\partial \alpha}\right)_0 = X_\alpha \quad \text{etc.}$$

and obtain

$$\begin{aligned}
 m \frac{dV}{dt} + X_{10} + X_V \Delta V + X_\alpha \Delta \alpha + G \sin \theta_0 + G \cos \theta_0 \Delta \theta &= 0 \\
 m (V_0 + \Delta V) \frac{d\Delta \alpha}{dt} - Y_{10} - Y_V \Delta V - Y_\alpha \Delta \alpha +
 \end{aligned}$$

$$\begin{aligned}
 &+ Q \cos \theta_0 - Q \sin \theta_0 \Delta \theta = 0 \\
 I_x \frac{d^2 \Delta \theta}{dt^2} - M_{x, \alpha} \Delta V - M_{x, \dot{\alpha}} \dot{\Delta \alpha} - M_{x, \ddot{\alpha}} \ddot{\Delta \alpha} - \\
 &- M_{x, \dot{\theta}} \dot{\Delta \theta} - M_{x, \ddot{\theta}} \ddot{\Delta \theta} = 0.
 \end{aligned}
 \tag{7.14}$$

According to eq.(7.11), we have

$$\begin{aligned}
 X_{x, \alpha} + Q \sin \theta_0 &= 0; \\
 -Y_{x, \alpha} + Q \cos \theta_0 &= 0; \\
 M_{x, \alpha} &= 0.
 \end{aligned}$$

In the second equation of system (7.14), the term $m \Delta V \frac{d\Delta \theta}{dt}$ is of the second order of smallness and may be disregarded.

The three equations of the system (7.14) contain four variables ΔV , $\Delta \alpha$, $\Delta \theta$, and $\dot{\Delta \theta}$ and their derivatives. Let us eliminate $\Delta \theta$ and $d\Delta \theta/dt$ from these equations by making the substitutions:

$$\begin{aligned}
 \Delta \theta &= \Delta \theta - \Delta \theta; \\
 \frac{d\Delta \theta}{dt} &= \frac{d\Delta \theta}{dt} - \frac{d\Delta \theta}{dt}.
 \end{aligned}$$

After the above transformations, we obtain the equations of motion in the versions for small deviations of the aircraft from the initial state of flight:

$$\begin{aligned}
 m \frac{d^2 \Delta V}{dt^2} - X'_{y, \dot{\alpha}} \dot{\Delta \alpha} + (X'_{y, \alpha} - (Y'_{x, \alpha} - Q \sin \theta_0) \Delta \alpha + Q \cos \theta_0 \Delta \theta) &= 0; \\
 m \dot{V}'_{y, \dot{\alpha}} \frac{d\Delta \alpha}{dt} - m \dot{V}'_{y, \alpha} \dot{\Delta \alpha} - Y'_{y, \dot{\alpha}} \dot{\Delta \alpha} - \\
 - (Y'_{y, \alpha} - Q \sin \theta_0) \Delta \alpha - Q \sin \theta_0 \Delta \theta &= 0. \\
 I_x \frac{d^2 \Delta \theta}{dt^2} - M'_{x, \dot{\alpha}} \dot{\Delta \alpha} - M'_{x, \alpha} \Delta \alpha - M'_{x, \dot{\theta}} \dot{\Delta \theta} - M'_{x, \ddot{\theta}} \ddot{\Delta \theta} &= 0
 \end{aligned}
 \tag{7.15}$$

The system eq.(7.15) is a system of linear homogeneous differential equations with constant coefficients. This system is solved rather simply by the methods described in all textbooks of higher mathematics.

It must be remembered that eq.(7.15) characterizes the "free" disturbed motion of the aircraft, i.e., the unsteady motion taking place after the disturbing course has ceased to act directly on the aircraft. This may be represented physically as the motion taking place after certain entirely determinate initial deviations of the parameters of motion from their values in the initial state of flight under consideration.

If we began to consider the disturbed motion of the aircraft under the action of the disturbing causes that were invariant over the course of a certain time, or varied with time, then in the right-hand sides of eq.(7.15) the zeroes would have to be replaced by definite values or functions of time, expressing the disturbing forces or moments. The methods of solving such equations are not complicated; these will be described below, on an example of controlled longitudinal unsteady motion. For the time being, however, let us solve the system of equations (7.15) in the form in which they are shown above, i.e., a system describing the motion produced by an initial deviation of the parameters of motion from their values during the initial steady state of flight.

The Dimensionless Forms of the Equations of Motion

Solving the system of equations (7.15), will yield the expressions for the variables ΔV , $\Delta \alpha$ and $\Delta \theta$ as functions of time. These expressions contain coefficients for these variables, i.e., the quantities X_c^V , Y_c^V , X_c^a , etc. Such a form of solution is inconvenient for the analysis of the general laws and relationships defining the motion of an aircraft and its stability, since the quantities X_c^V , Y_c^V , X_c^a , etc. will vary with any variation of the initial flight condition.

A more convenient form may be obtained if the values of the aerodynamic forces

and moments are replaced by their dimensionless coefficients. Let us write the expanded expressions for X_c , Y_c and M_z

$$\left. \begin{aligned} X_c &= c_o S \frac{V^2}{2} - P \cos \alpha = c_o S \frac{V^2}{2} \\ Y_c &= c_i S \frac{V^2}{2} + P \sin \alpha = c_i S \frac{V^2}{2} \\ M_{zc} &= m_x S b_A \frac{V^2}{2} - P y_p = m_x S b_A \frac{V^2}{2} \end{aligned} \right\} \quad (7.16)$$

It will be seen from eq.(7.16) that the dimensionless coefficients C_{Dc} , C_{Lc} and m_{zc} are defined by the expressions

$$\left. \begin{aligned} c_{Dc} &= c_D - P_x \\ c_{Lc} &= c_L + P_y \\ m_{zc} &= m_x - m_{zp} \end{aligned} \right\} \quad (7.17)$$

where P_x , P_y and m_{zp} denote, respectively,

$$\left. \begin{aligned} P_x &= \frac{2P \cos \alpha}{S V^2} \\ P_y &= \frac{2P \sin \alpha}{S V^2} \\ m_{zp} &= \frac{2P y_p}{S b_A V^2} \end{aligned} \right\} \quad (7.18)$$

The expanded expressions for the derivatives X_c^V , X_c^a , Y_c^V , etc. may be written in the form

$$\left. \begin{aligned} X_c^V &= \left(\frac{\partial X_c}{\partial V} \right)_0 = c_o S \frac{1}{2} 2V_o + \frac{\partial c_o}{\partial \alpha} \frac{\partial \alpha}{\partial V} S \frac{V_o^2}{2} - \\ &= c_o S V_o + c_o^a \frac{1}{2} S \frac{V_o^2}{2} = \\ &= c_o S V_o + c_o^a S \frac{V_o^2}{2} V_o = b_1 c_o S V_o \\ X_c^a &= \left(\frac{\partial X_c}{\partial \alpha} \right)_0 = c_o S \frac{V_o^2}{2} \end{aligned} \right\} \quad (7.19)$$

STAT

$$\begin{aligned}
 Y_c^* &= \left(\frac{\partial Y_c}{\partial V_0} \right)_0 = c_{L,c} S b_1^2 + c_{L,c}^* S \frac{M_0^2}{2} b_1^2 - h_{L,c} S b_1 V_0 \\
 Y_c^* &= \left(\frac{\partial Y_c}{\partial V_0} \right)_0 = c_{L,c}^* S \frac{V_0^2}{2} \\
 M_{Y_c}^* &= \left(\frac{\partial M_{Y_c}}{\partial V_0} \right)_0 = m_{Y_c} S b_1^2 + m_{Y_c}^* S b_1 \frac{M_0^2}{2} + V_0 - \\
 &= m_{Y_c}^* S b_1 \frac{V_0^2}{2} \\
 M_{Y_c}^* &= \left(\frac{\partial M_{Y_c}}{\partial \omega_1} \right)_0 = m_{Y_c}^* S b_1 \frac{V_0^2}{2} \\
 M_{Y_c}^* &= \left(\frac{\partial M_{Y_c}}{\partial \omega_2} \right)_0 = m_{Y_c}^* S b_1 \frac{V_0^2}{2} \\
 M_{Y_c}^* &= \left(\frac{\partial M_{Y_c}}{\partial \delta_1} \right)_0 = m_{Y_c}^* S b_1 \frac{V_0^2}{2}
 \end{aligned}
 \tag{7.19}$$

The following notation has been adopted:

$$\begin{aligned}
 b_1 &= 1 + \frac{M_{Y_c}^*}{2c_{L,c}} \\
 b_2 &= 1 + \frac{M_{Y_c}^*}{2c_{L,c}^*} \\
 c_{L,c}^* &= \frac{d c_{L,c}}{d M} \cdot c_{L,c} = \frac{d c_{L,c}}{d M}
 \end{aligned}
 \tag{7.20}$$

In the initial state of flight, the aircraft is balanced with respect to moments, and, as has already been stated, the quantity $m_{zc} = 0$.

We obtain eq.(7.19) for M_{zc}^a and M_{zc}^a if we bear in mind that the dimensionless coefficient m_{zc} can be a function only of dimensionless quantities. For the dimensionless quantity of angular velocity of pitching, let us take $\omega_z = \omega_z b_A / V_0$.

(cf. Chapter VI). Then

$$\begin{aligned}
 M_{Y_c}^* &= \frac{d m_{Y_c}}{d \left(\frac{\omega_z b_A}{V_0} \right)} S b_1 \frac{V_0^2}{2} \frac{d \omega_z}{d \omega_z} = m_{Y_c}^* S b_1 \frac{V_0^2}{2} \\
 M_{Y_c}^* &= m_{Y_c}^* S b_1 \frac{V_0^2}{2}
 \end{aligned}$$

STAT

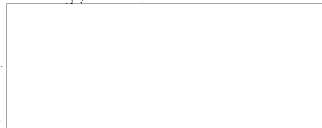
Starting out from eq. (7.17) and eq. (7.18), and bearing in mind that P is considered a function only of the single parameter V, let us find expressions for c_{xc}^M , c_{yc}^M , m_{yc}^M , etc.

$$\left. \begin{aligned} c_{xc}^M &= c_{xc}^M - \frac{2P^y \cos \alpha_0}{SM_{\phi} V_0} + \frac{4P_0 \cos \alpha_0}{SM_{\phi} V_0^2} \\ c_{yc}^M &= c_{yc}^M + \frac{2P_0 \sin \alpha_0}{S_p V_0^2} \\ c_{zc}^M &= c_{zc}^M + \frac{2P_0 \cos \alpha_0}{S_p V_0^2} \\ c_{xc}^M &= c_{xc}^M + \frac{2P^y \sin \alpha_0}{SM_{\phi} V_0} - \frac{4P_0 \sin \alpha_0}{SM_{\phi} V_0^2} \\ m_{yc}^M &= m_{yc}^M - \frac{2P^y y_p}{2b_{\phi} V_0 M_0} + \frac{4P_0 y_p}{2b_{\phi} M_0 V_0^2} \\ m_{zc}^M &= m_{zc}^M \quad m_{xc}^M = m_{xc}^M \quad m_{yc}^M = m_{yc}^M \end{aligned} \right\} (7.21)$$

Let us now return * to the system of equations (7.15). On substituting X_{co} and Y_{co} for $G \sin \theta$ and $G \cos \theta$, on the basis of the equations (7.11) of initially steady flight, we obtain

$$\left. \begin{aligned} m \frac{dV}{dt} + X'_y \Delta V + (X'_z - Y_{co}) \Delta \alpha + Y_{co} \Delta \theta &= 0; \\ mV_0 \frac{d\alpha}{dt} - mV_0 \frac{d\alpha_0}{dt} - Y'_z \Delta V - (Y'_z + X_{co}) \Delta \alpha + X_{co} \Delta \theta &= 0; \\ I_y \frac{d\alpha}{dt} - M'_{zc} \Delta V - M'_{zc} \Delta \alpha - M'_{zc} \frac{d\alpha_0}{dt} - M'_{zc} \frac{d\alpha}{dt} &= 0. \end{aligned} \right\} (7.22)$$

* We note that, physically, the derivative m_{zc}^M in the general case takes account not only of the direct influence of the compressibility of the air but also of the influence of the operating state of the engines and of the influence of structural deformations on the longitudinal moments of the aircraft. From the formal point of view, we might everywhere introduce derivatives with respect to the flying speed V instead of derivatives with respect to the Mach number.



For the further analysis, let us express the equations of motion in the so-called dimensionless form. For this purpose, the time and increments of flying speed will not be measured in dimensionless units t and ΔV but in relative or dimensionless quantities, using the following notation for the quantities:

$$\Delta V = \frac{\Delta V}{V_0}; \quad t = \frac{t}{\tau}, \quad \text{where } \tau = \frac{2m}{\rho S V_0}. \quad (7.23)$$

Here, as before, V_0 denotes the flying speed at the initial steady state of flight, m the mass of the aircraft, ρ the density of the air, S the wing area. In this way, the change in velocity ΔV will be measured in fractions of the flying speed during the initial steady state of flight, while the change in time will be measured in units (fractions) τ . As indicated by eq.(7.23), the numerical value of τ depends on the velocity and altitude of flight during the initial steady state and at the specific mass load $|m/S|$ on the aircraft wing.

The coefficient τ , having the dimension "second", may be called the time scale in converting the equations of motion into the dimensionless form.

On substituting t , ΔV , X_{co}^V , X_{co} , etc. in the system of equations (7.22) by the corresponding expressions from eqs.(7.19) and (7.23), and everywhere omitting, for the sake of simplicity, the subscript "c", we obtain:

$$m S V_0^2 \frac{d\Delta V}{dt} - b_1 c_1 S V_0^2 \Delta V + (c_2 - c_1) S V_0^2 \Delta z -$$

$$- c_2 S V_0^2 \Delta z = 0;$$

$$\frac{m S V_0^2}{2m} \frac{d\Delta z}{dt} - \frac{m S V_0^2}{m} \frac{d\Delta V}{dt} - b_2 c_1 S V_0^2 \Delta V -$$

$$- (c_1 + c_2) S V_0^2 \Delta z + c_2 S V_0^2 \Delta z = 0;$$

$$\frac{m S V_0^2}{4m} \frac{d\Delta z}{dt} - \frac{m S V_0^2}{2m} \frac{d\Delta V}{dt} - m_1 \frac{d\Delta V}{dt} -$$

$$- m_1 \frac{S V_0^2 V_0^2}{4m} \frac{d\Delta z}{dt} - m_1 \frac{S V_0^2 V_0^2}{4m} \frac{d\Delta V}{dt} = 0$$

In the last equation, the moment of inertia I_z is replaced by the expression

$$I_z = m r_z^2 - m b_A^2 r_z^2$$

where r_z is the radius of the moment of inertia with respect to the lateral axis of the aircraft, while $r_z = r_z/b_A$ is the relative value of the radius of inertia.

On dividing the first and second equations by $S_0 v^2/2$ and the third one by $\frac{r_z^2 S_0^2 v^2}{4m}$ we obtain the following:

$$\left. \begin{aligned} \frac{d\bar{V}}{dt} + 2h_1 c_{\alpha} \Delta \bar{V} + (c_{\alpha}^2 - c_{\alpha}) \Delta z + c_{\alpha} \Delta \theta &= 0; \\ \frac{d\Delta z}{dt} - \frac{d\Delta \theta}{dt} - 2h_2 c_{\alpha} \Delta \bar{V} - (c_{\alpha}^2 + c_{\alpha}) \Delta z + c_{\alpha} \Delta \theta &= 0; \\ \frac{d^2 \Delta z}{dt^2} - M \frac{r_z}{l} m_{\alpha}^2 \Delta \bar{V} - \frac{r_z}{l} m_{\alpha}^2 \Delta z - \\ - \frac{m_{\alpha}^2}{l} \frac{d\Delta z}{dt} - \frac{m_{\alpha}^2}{l} \frac{d\Delta \theta}{dt} &= 0. \end{aligned} \right\} (7.24)$$

Here the notation

$$\mu = \frac{2m}{\rho S_0 b_A}$$

has been introduced. The coefficient μ is a very important parameter in the dynamics of aircraft flight and is known as the coefficient of relative density of the aircraft. Physically, the coefficient μ may be considered as a quantity proportional to the ratio of the mass of the aircraft to the mass of air displaced by it, since the quantity $S b_A$, to a certain extent, characterizes the bulk dimensions of the aircraft.

Thus, eqs.(7.24) represent the equations of disturbed motions in variations, described in dimensionless form.

The dimensionless form of equations of motion is very convenient for an analysis of the stability and controllability of the aircraft, since this form allows

one and the same expressions and functional relations to be used for the whole range of states encountered in flight.

Solution of the Equations of Motion. Characteristic Equation

Equations (7.24), like eq.(7.15), constitute a system of homogeneous differential equations with constant coefficients. The method of finding the general solution of these equations is given in textbooks of higher mathematics and will be briefly described below.

According to the general theory of differential equations, partial solutions of such a system can be obtained by using

$$\left. \begin{aligned} \Delta V &= A e^{\lambda t} \\ \Delta z &= B e^{\lambda t} \\ \Delta \theta &= C e^{\lambda t} \end{aligned} \right\} \quad (7.25)$$

where A , B , C , and λ are constant quantities. Then,

$$\left. \begin{aligned} \frac{d\Delta V}{dt} &= A \lambda e^{\lambda t} & \frac{d\Delta z}{dt} &= B \lambda e^{\lambda t} \\ \frac{d\Delta \theta}{dt} &= C \lambda e^{\lambda t} & \frac{d\Delta \psi}{dt} &= C \lambda e^{\lambda t} \end{aligned} \right\}$$

On substituting these expressions for the variables and their derivatives in eq.(7.24), and dividing everywhere by the common multiple $e^{\lambda t}$, we obtain

$$\left. \begin{aligned} (\lambda + 2b_1 c_{11}) A + (c_{12} - c_{21}) B + c_{13} C &= 0 \\ -2b_2 c_{11} A - (\lambda + c_{22} + c_{32}) B + (\lambda + c_{33}) C &= 0 \\ -M \frac{c_{11} \lambda}{r_1^2} A - \left(\frac{c_{22} \lambda}{r_2^2} + \frac{c_{32} \lambda}{r_2^2} \right) B - \left(\lambda - \frac{c_{33} \lambda}{r_3^2} \right) C &= 0 \end{aligned} \right\} \quad (7.26)$$

Equations (7.26) constitute a system of algebraic equations with respect to the unknowns A , B , and C . As is well known from courses on higher mathematics, the quantities A , B , and C , on the basis of these equations, will be equal to the ratios

of the determinants

$$A = \frac{A_1}{\Delta}; \quad B = \frac{A_2}{\Delta}; \quad C = \frac{A_3}{\Delta}. \quad (7.27)$$

where Δ is the so-called characteristic determinant and consists of the coefficient of the unknowns on the left-hand side of eq.(7.26), namely:

$$\Delta = \begin{vmatrix} \lambda + 2k_{pp} & (c_{0p} - c_{2p}) & c_{1p} \\ -2k_{cp} & -\lambda - c_{0c} & -c_{1c} \\ -M \frac{a_1^2}{r_1^2} & -\frac{a_2^2 + a_3^2}{r_2^2} & \lambda - \frac{a_4^2}{r_2^2} \end{vmatrix} \quad (7.28)$$

The determinants Δ_1 , Δ_2 , and Δ_3 are obtained from the determinant by replacing the first, second, and third columns respectively by the coefficients on the right hand side of eq.(7.26). Since there are zeros on the right-hand side of eq.(7.26), it follows that $\Delta_1 = \Delta_2 = \Delta_3 = 0$. For the unknowns A, B, and C to have values different from zero under these conditions, it is necessary that the characteristic determinant Δ also vanishes. On developing the determinant (7.28) we obtain the characteristic equation with respect to the unknown λ . It is obvious that, by developing the determinant, we obtain terms containing λ , λ^2 , λ^3 , λ^4 and a term free from λ . Thus the characteristic equation will be an equation of the fourth degree in λ . Such an equation has, as is generally known, four roots.

On substituting in system (7.26) any root of the characteristic equation, we obtain a system of three homogeneous equations in three unknowns A, B, and C.

In view of the fact that $\Delta = 0$, these equations (7.26) are not independent of each other, and one of them is a linear combination of the other two. Consequently, by taking any two of these equations, we can determine only two of the quantities A, B, and C as a function of the third, which is for the time being, an arbitrary constant. In other words, by taking any two of the equations (7.26) we are able to determine only the ratios of two of these quantities to the third,

for example

$$\left. \begin{aligned} \frac{A}{C} &= f(\lambda) \\ \frac{B}{C} &= g(\lambda) \end{aligned} \right\} \quad (7.29)$$

These ratios will be functions of the parameter λ , the root of the characteristic equation. To each root of the characteristic equation there corresponds one particular solution of the system of differential equations (7.24) and, consequently, also one arbitrary constant. Therefore, to each root of the characteristic equation λ there corresponds its own special type of disturbed motion. The sum of all four particular solutions for each of the variables will be the general solution of the differential equations of motion. Thus, the general solution of the system of equations (7.24) will have the following form:

$$\left. \begin{aligned} \Delta V &= A_1 e^{\lambda_1 T} + A_2 e^{\lambda_2 T} + A_3 e^{\lambda_3 T} + A_4 e^{\lambda_4 T} \\ \Delta \omega &= B_1 e^{\lambda_1 T} + B_2 e^{\lambda_2 T} + B_3 e^{\lambda_3 T} + B_4 e^{\lambda_4 T} \\ \Delta \delta &= C_1 e^{\lambda_1 T} + C_2 e^{\lambda_2 T} + C_3 e^{\lambda_3 T} + C_4 e^{\lambda_4 T} \end{aligned} \right\} \quad (7.30)$$

Of the twelve coefficients A_1, A_2, \dots, C_4 , only four are arbitrary constants. If for these latter, for example, the quantities C_1, C_2, C_3 , and C_4 are taken, then the remaining eight coefficients are determined by means of the relations (7.29), namely

$$\left. \begin{aligned} A_1 &= f(\lambda_1) C_1, & A_2 &= f(\lambda_2) C_2, & A_3 &= f(\lambda_3) C_3, & A_4 &= f(\lambda_4) C_4 \\ B_1 &= g(\lambda_1) C_1, & B_2 &= g(\lambda_2) C_2, & B_3 &= g(\lambda_3) C_3, & B_4 &= g(\lambda_4) C_4 \end{aligned} \right\} \quad (7.31)$$

After substituting the expressions from eq.(7.31) for A_1, A_2 , etc. in eq.(7.30), we obtain expressions for the increments of the parameters of motion of the aircraft. These expressions contain only four constant quantities, all of them arbitrary for the time being. These arbitrary constants, for each concrete case of a disturbed motion, must be determined according to the initial conditions, i.e., ac-

ording to the values of the variables and their derivatives at the initial instants of time. If, for example, we assign, at $t = 0$, the values

$$\Delta V_0, \Delta v_0, \Delta \dot{v}_0 = \begin{pmatrix} \Delta V_0 \\ \Delta v_0 \\ \Delta \dot{v}_0 \end{pmatrix},$$

then, for determining the four constants we will have four equations

$$\left. \begin{aligned} f(0)C_1 + f(0)C_2 + f(0)C_3 + f(0)C_4 - \Delta V_0 \\ \varphi(0)C_1 + \varphi(0)C_2 + \varphi(0)C_3 + \varphi(0)C_4 - \Delta v_0 \\ C_1 + C_2 + C_3 + C_4 - \Delta \dot{v}_0 \\ \lambda_1 C_1 + \lambda_2 C_2 + \lambda_3 C_3 + \lambda_4 C_4 = \begin{pmatrix} \Delta \dot{v}_0 \\ \Delta v_0 \end{pmatrix} \end{aligned} \right\} \quad (7.32)$$

By solving the system (7.32), we obtain

$$C_1 = \frac{E_1}{E}, \quad C_2 = \frac{E_2}{E}, \quad C_3 = \frac{E_3}{E}, \quad C_4 = \frac{E_4}{E} \quad (7.33)$$

where E denotes the determinant composed of the coefficients of the variables on the left-hand sides of the system (7.32), namely

$$E = \begin{vmatrix} f(0) & f(0) & f(0) & f(0) \\ \varphi(0) & \varphi(0) & \varphi(0) & \varphi(0) \\ 1 & 1 & 1 & 1 \\ \lambda_1 & \lambda_2 & \lambda_3 & \lambda_4 \end{vmatrix} \quad (7.34)$$

$E_1, E_2, E_3,$ and E_4 denote the determinants obtained from the determinant (7.34) on replacing the first, second, etc. columns by the quantities in the right-hand sides of the system (7.32).

In this way, the solutions of the system of equations (7.24) can be found by this method, under assigned initial conditions, by using the following operations:

1. Two of the equations of the system (7.24) are arbitrarily selected. As their solutions the functions $f(\lambda)$ and $\varphi(\lambda)$ are found (cf. eq. 7.29).
2. The four roots of the characteristic equation $\Delta = 0$ are found (cf. eq. 7.28).

3. From the assigned initial conditions, by solving the system (7.32), the constants $C_1, C_2, C_3,$ and C_4 are found.
4. From eq.(7.31), the values $A, B, A',$ etc. are determined.
5. By substituting the values so obtained in eq.(7.30), the general solution for each of the variables, the parameters of motion of the aircraft, are found.

This rather laborious process of finding the solution of a system of general equations of motion of the aircraft is used infrequently. Ordinarily, in the analysis of the disturbed motion of aircraft and its stability, approximate methods are used. The evaluation of the dynamic stability of an aircraft can be obtained directly from the values of the roots of the characteristics equation. If it is only necessary to determine whether an aircraft does or does not have dynamic stability, then it is possible to start from the values of the coefficients of the characteristic equation.

Correlation of the Roots and Coefficients of the Characteristic Equation

Let us now consider the characteristic equation in more detail. If we develop, in powers of λ , the characteristic determinant of eq.(7.22) and equate it to zero, then, as mentioned before, we obtain a characteristic equation of the fourth degree in

$$F(\lambda) = \lambda^4 + a_3\lambda^3 + a_2\lambda^2 + a_1\lambda + a_0 = 0. \tag{7.35}$$

where

$$\begin{aligned} a_3 &= c_{1c}^2 - \frac{a_{1c}^2 + a_{2c}^2}{T_c^2} + (1 + 2k_1)c_{1c} \\ a_2 &= -\frac{r_{1c}^2 + c_{1c}^2 r_{2c}^2}{T_c^2} - (1 + 2k_1)c_{1c} \left(\frac{a_{1c}^2 + a_{2c}^2}{T_c^2} \right) + \\ &\quad + 2(b_{1c}^2 c_{1c} + b_{2c}^2 c_{1c} + b_{3c}^2 c_{1c} - b_{4c}^2 c_{1c}^2) \\ a_1 &= -2(b_{1c}^2 c_{1c} + b_{2c}^2 c_{1c} + b_{3c}^2 c_{1c} - b_{4c}^2 c_{1c}^2) \frac{a_{1c}^2}{T_c^2} - \end{aligned} \tag{7.36}$$



$$\begin{aligned}
 & -2(k_1 c_{11}^2 + k_2 c_{21}^2) \frac{a_1^2}{T_1^2} - (1 + 2k_1) c_{11} \frac{r_{11}^2}{T_1^2} + \\
 & \quad + M c_{11} \frac{r_{11}^2}{T_1^2}; \tag{7.36} \\
 a_4 = & -2(k_1 c_{11}^2 + k_2 c_{21}^2) \frac{r_{11}^2}{T_1^2} + (c_{11} c_{11} + c_{21} c_{21}) M \frac{r_{11}^2}{T_1^2}.
 \end{aligned}$$

All four coefficients of the characteristic equation (7.35) $a_1, a_2, a_3,$ and a_4 are real quantities. For this reason, the four roots of the characteristic equation must be either real or paired conjugate complex quantities. As is known from mathematics, an algebraic equation of the fourth degree may be represented in the form of the product

$$F(\lambda) = (\lambda - \lambda_1)(\lambda - \lambda_2)(\lambda - \lambda_3)(\lambda - \lambda_4) = 0, \tag{7.37}$$

where $\lambda_1, \lambda_2, \lambda_3,$ and λ_4 are the roots of the equation $F(\lambda) = 0$. On multiplying and equating the coefficients of the same power of λ in eq.(7.37) and eq.(7.35), we obtain

$$\begin{aligned}
 a_1 &= -(\lambda_1 + \lambda_2 + \lambda_3 + \lambda_4) \\
 a_2 &= \lambda_1 \lambda_2 + \lambda_1 \lambda_3 + \lambda_1 \lambda_4 + \lambda_2 \lambda_3 + \lambda_2 \lambda_4 + \lambda_3 \lambda_4 \\
 a_3 &= -(\lambda_1 \lambda_2 \lambda_3 + \lambda_1 \lambda_2 \lambda_4 + \lambda_1 \lambda_3 \lambda_4 + \lambda_2 \lambda_3 \lambda_4) \\
 a_4 &= \lambda_1 \lambda_2 \lambda_3 \lambda_4.
 \end{aligned} \tag{7.38}$$

It is obvious that the roots of the characteristic equation must be either real or paired conjugate complex quantities.

In our subsequent analysis of disturbed motion we will consider only the following cases:

- 1) All four roots are real numbers.
- 2) Two roots are real and two roots are mutually conjugate complex or pure imaginary numbers.



3) All four roots are complex or pure imaginary numbers, pairwise conjugate among themselves.

The Character of Disturbed Motion

Let us attempt to represent the character of the disturbed motion in each of the three combinations of roots of the characteristic equations.

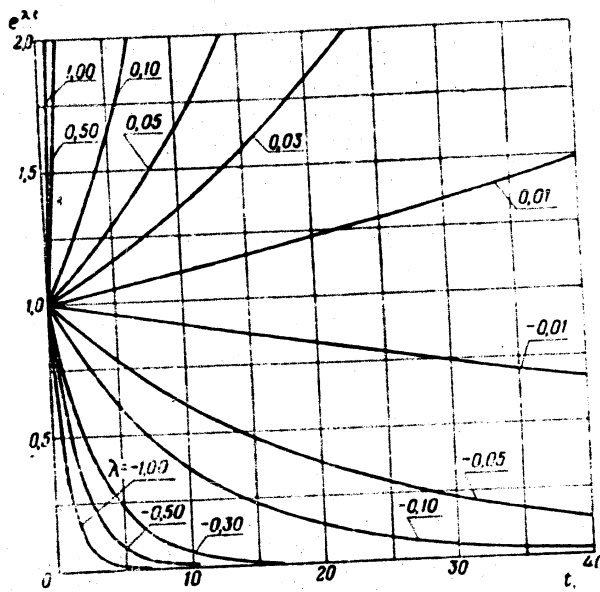


Fig.7.5 - The Function $e^{\lambda t}$ at Various Values of λ .

In the first case, where all four roots λ are real, the variation in each of the parameters of motion of the aircraft may be represented directly by eq.(7.30).

Let us take as an example Δy .

$$\Delta y = A_1 e^{\lambda_1 t} + A_2 e^{\lambda_2 t} + A_3 e^{\lambda_3 t} + A_4 e^{\lambda_4 t}$$



Each of the four summands of ΔV varies as a function of time by an aperiodic law, and will increase or decrease with time in accordance with the sign of the corresponding root λ . For a more graphic idea of the intensity of aperiodic motion, Fig. 7.5 shows the variation with time of the function $e^{\lambda t}$ for various values of λ .

The individual summands of $Ae^{\lambda t}$ for negative values of λ will decline in time, more and more (asymptotically) approaching zero. At positive values of λ , the corresponding summands of $Ae^{\lambda t}$ will increase in absolute value with time. If even one root of the characteristic equation is positive, then the values of the deviations of the parameters of motion ΔV , and $\Delta \theta$, represented by eq. (7.30), will increase in absolute value with time. The aircraft will deviate more and more from the initial state of flight. Thus the aircraft, in the initial flight condition under consideration, will be unstable.

To obtain stability of the aircraft, all roots in a characteristic equation with four real roots, must be negative.

Let us now consider the second case, when two roots of the characteristic equation are conjugate complex quantities and two roots are pure real numbers. Let us assume that the roots λ_1 and λ_2 , are conjugates, i.e., that $\lambda_1 = \lambda_2$. Let

$$\lambda_1 = a + bi.$$

Then $\lambda_2 = a - bi$, where $i = \sqrt{-1}$, and the coefficients a and b are real numbers.

Let us consider, on the example of the parameter ΔV , the partial solution of the system of equations corresponding to the pair of roots λ_1 and λ_2 :

$$\Delta V = A_1 e^{\lambda_1 t} + A_2 e^{\lambda_2 t}.$$

Since we are considering a real motion of the aircraft, all quantities entering into the final solution of the equations must be real. For this reason, in the presence of conjugate complex roots, the constant quantities corresponding to them and entering into the solutions of the equations, must likewise be mutually conjugate.

If $\lambda_1 = \lambda_2$, it is easy to demonstrate that the functions $f(\lambda_1)$ and $f(\lambda_2)$ in

eq.(7.31) will also be conjugate, i.e.,

$$A_2 = \overline{A_1}.$$

Starting from the condition of real motion, we conclude that the arbitrary constants C_1 and C_2 in eq.(7.31) in this case as well, must be taken as mutually conjugate complex quantities, i.e.,

$$C_1 = \overline{C_2}.$$

Then the constants A_1 and A_2 will likewise be mutually conjugate complex quantities and may be written in the form

$$A_1 = B - Di;$$

$$A_2 = B + Di$$

where B and D are constant real quantities.

Let us now transform the partial solution for ΔV , by writing it first in the form:

$$\begin{aligned} \Delta V &= (B - Di)e^{i\omega t} + (B + Di)e^{-i\omega t} = \\ &= (B - Di)e^{i\omega t} + (B + Di)e^{i\omega t} - 2Di e^{-i\omega t} = \\ &= 2Be^{i\omega t} - 2Di(e^{i\omega t} - e^{-i\omega t}). \end{aligned}$$

However, the Euler equations read

$$e^{i\omega t} + e^{-i\omega t} = 2 \cos \omega t;$$

$$e^{i\omega t} - e^{-i\omega t} = 2i \sin \omega t.$$

so that the expression for ΔV may be rewritten in the form

$$\Delta V = 2Be^{i\omega t} \cos \omega t + 2De^{i\omega t} \sin \omega t.$$

In order to convert the expression for ΔV into a form more convenient for practical purposes, we introduce the notation



$$A = 2\sqrt{B^2 + D^2};$$

$$\tan \phi = \frac{B}{D}.$$

Then,

$$\Delta V = A e^{-\alpha t} \sin(\bar{\omega} t + \phi).$$

For any other parameters of motion of the aircraft, solutions analogous in form and corresponding to this pair of conjugate roots of the characteristic equation may be obtained. As shown by the last formula, the motion of an aircraft corresponding to this partial solution of the equations will consist either of damped oscillations, if the quantity α is negative, or of oscillations increasing in amplitude, if the quantity α is positive. In the special case where $\alpha = 0$, these oscillations will proceed at constant amplitude, i.e., they will be harmonic *.

Analogous considerations and conclusions may be drawn also with respect to the particular solution of the equations corresponding to the other pair of complex conjugate roots of the characteristic equation. Denoting, in this case,

$$\lambda_{2,1} = \alpha \pm i\beta,$$

we obtain the corresponding partial motions of the aircraft of the type

$$\Delta V = C e^{-\alpha t} \sin(\bar{\omega} t + \gamma).$$

On the whole, as follows from the above statements, the disturbed motion of the aircraft will be characterized by one of the following four expressions, which,

* Strictly speaking, for $\alpha = 0$, as shown by A.M. Lyapunov, it is necessary in the expansion into a Taylor series to take account of the terms above the first order of smallness. But a strict consideration of this special case is not of interest for technology.

depending on their type, are applicable to any of the parameters of this motion:

$$\left. \begin{aligned} 1) \Delta \bar{V} &= A_1 e^{\lambda_1 t} + A_2 e^{\lambda_2 t} + A_3 e^{\lambda_3 t} + A_4 e^{\lambda_4 t} : \\ 2) \Delta \bar{V} &= A e^{\alpha t} \sin(\beta t + \psi) + A_2 e^{\lambda_2 t} + A_3 e^{\lambda_3 t} : \\ 3) \Delta \bar{V} &= A_1 e^{\lambda_1 t} + A_2 e^{\lambda_2 t} + C e^{\alpha t} \sin(\beta t + \gamma) : \\ 4) \Delta \bar{V} &= A e^{\alpha t} \sin(\beta t + \psi) + C e^{\alpha t} \sin(\beta t + \gamma) \end{aligned} \right\} (7.39)$$

The first type of disturbed motion of the aircraft is represented by the resultant (algebraic sum) of four partial aperiodic motions superposed on each other. The second and third type consist of the superposition of two aperiodic motions and one oscillatory motion with increasing or decreasing amplitude, depending on the signs of the quantities α and β . Although, in their form, the second and third types are entirely the same, it is preferable (because of the substantial difference in aircraft) to differentiate them with respect to the absolute value of the pair of roots λ_1 and λ_2 ; this will be substantiated below. The fourth type represents a superposition of two oscillatory motions. This type of disturbed aircraft motion is most frequently encountered.

Conditions of Stability

It follows from eqs.(7.30) and (7.39) that the deviation in time of the parameters of aircraft motion from their values in the initial state of flight will decrease without limit as to absolute value, if all the real parts of the roots of the characteristic equation are negative. It is sufficient for one of the roots to be positive or to have one positive real part for the deviation of the parameters of motion from their values in the initial state of flight, to increase without time limit. In the former case, the aircraft will be stable, in the latter, unstable.

Thus, for the stability of an aircraft it is necessary and sufficient that all roots of the characteristic equation have negative real parts.

It is well known from courses on higher algebra that for the roots of an equa-

tion of the fourth degree, of the type

$$0 = s^4 + a_3 s^3 + a_2 s^2 + a_1 s + a_0$$

to have negative real parts, it is necessary and sufficient that the conditions

$$\left. \begin{aligned} a_3 > 0; \quad a_2 > 0; \quad a_1 > 0; \quad a_0 > 0; \\ R = (a_3 a_2 - a_1 a_0) - a_1^2 > 0 \end{aligned} \right\} \quad (7.40)$$

are satisfied.

The condition (7.40), which yields a qualitative solution of the question as to whether an aircraft is stable, does not characterize the quantitative aspect of disturbed motion. Without going into a detailed analysis of the condition (7.40) (Sibl.8), we will show merely that if these conditions are violated with respect to the free term a_0 of the characteristic equation, then the roots of the characteristic equation will contain one root which will be real with a positive sign, so that the disturbed motion of the aircraft will be aperiodically unstable.

Now, eq.(7.38) shows that

$$a_0 = \lambda_1 \lambda_2 \lambda_3 \lambda_4$$

As stated above, the characteristic equation can have complex values for its roots only if they are pairwise conjugate. The products of such two conjugate roots will be positive, regardless of the sign of their real parts. For example, let the roots λ_1 and λ_2 be conjugate. Then,

$$\lambda_1 \lambda_2 = (\sigma + i\eta)(\sigma - i\eta) = (\sigma^2 + \eta^2) > 0$$

It follows from this that the condition $a_0 < 0$ can be satisfied only in the case when the roots of the characteristic equation include pure real roots. Consequently, only if the characteristic equation has one or three pure real positive roots will the free term a_0 be less than zero. To the positive real root, however, also corresponds the aperiodic motion of the aircraft. We remark in this connection that the case of three pure real positive roots does not exist for the aircraft.



Stability of Aircraft with Automatic Pilot

The purpose of the automatic pilot is to control the aircraft or other flying machines at a definite attitude, without participation of the pilot, in order to relieve him of work.

An automatic pilot consists of special devices (for example, gyroscopes) which react to any deviation of the parameters of motion (angles, angular velocities, etc.) from their assigned values, and of a servo unit which properly deflects the control surfaces of the aircraft, which in turn, correct the deviation of the parameters.

Figure 7.6 shows a schematic diagram of an automatic pilot. The parts of the automatic pilot, rigidly attached to the aircraft, are indicated by hatching. The piston of the servo unit is rigidly attached to the control surfaces of the aircraft. The slide is connected with the gyroscope and maintains a constant position in space during maneuvers of the aircraft.

The automatic pilot operates in the following way: When the aircraft deviates from its definite position in space, the air nozzle is shifted with respect to the slide by the angle φ , equal to the angle of deflection of the aircraft. Next, one of the nozzles is closed by the slide valve while the second is opened. As a result a pressure drop is produced in the air relay. This pressure drop in the relay shifts the oil valve of the servo unit to one side, away from the zero position. The shift of the valve admits oil to the servo unit whose piston then deflects the rudder in such a way that the aircraft turns, tending to return to its original position. The piston of the servo unit is connected with the nozzles by means of a follow-up system in such a way that, on motion of the piston, the nozzles tend to reduce the angle between the nozzles and the valve.

The schematic diagram in Fig.7.6 maintains proportionality between the angles

* The design of automatic pilots will not be described here; the interested reader is referred to special works on the subject (Bibl.9).

of deflection of the aircraft and those of the rudder when the deviations of the aircraft are slow. At rapid deviations of the aircraft, however, the piston of the servo unit, having only a limited rate of motion, is unable to ensure proportionality between deflections of the control surfaces and the aircraft.

Ordinary automatic pilots react both to the angle of pitch θ and to the angular velocity $\frac{d\theta}{dt}$. This reduces the lag in response of the aircraft to harmful changes in attitude.

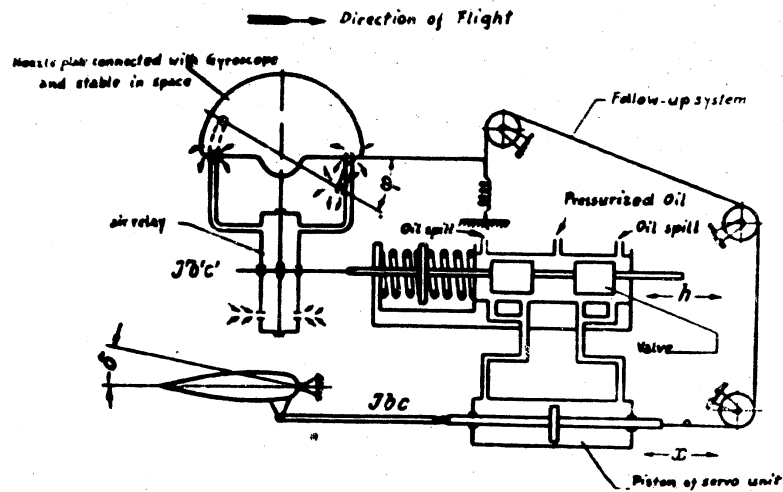


Fig.7.6 - Schematic Diagram of Automatic Pilot

Below we shall consider the stability of an aircraft with a so-called ideal automatic pilot, i.e., with an automatic device that the control surface with no lag whatever through angles that are correlated with complete accuracy and uniquely with the values of the deviations of the parameters of motion of the aircraft from their values under the initial state of flight. In reality, such automatic pilots do not exist. Each actual practical automatic pilot reacts to a deviation of the aircraft from its attitude with some lag. In any automatic pilot system friction is

STAT

0 always present, the sensitive element of the automatic pilot cannot be accurately
 1 controlled, etc. *.

The consideration of the stability of an aircraft with an ideal automatic pilot
 2 can give an idea only of the general reaction of the actual autopilot to the motion
 3 of the aircraft.

Automatic pilots of various designs are known, which react to a deviation of
 4 various parameters of aircraft motion or to a definite combination of deviations of
 5 these parameters. For example, let an autopilot react to the deviation of the para-
 6 meters of longitudinal motion above considered: ΔV , Δx , and $\Delta \theta$; and to the angular
 7 velocity of pitching $\Delta \omega_p = d\Delta \theta/dt$. Assuming the power of the servo unit of the auto-
 8 matic pilot to be sufficiently large, we may neglect the influence of the aerody-
 9 namic and inertia hinge moments of the control surfaces. Then the angle of deflec-
 0 tion of the elevator will be determined by the formula

$$\Delta \theta = v_1 \Delta V + v_2 \Delta x + v_3 \Delta \theta + v_4 \frac{d\Delta \theta}{dt}.$$

where v_1 , v_2 , v_3 , and v_4 will be considered constant quantities depending on the
 1 transmission ratios of the automatic pilot, i.e., on the ratios of the values of the
 2 deflection of the rudder to the corresponding increment of the parameter of aircraft
 3 motion causing that deviation**.

4 The deflections of the rudder caused by the automatic pilot will create an

5 * The longitudinal stability of the aircraft, allowing for the lag of an automatic
 6 pilot and limited by the rate of displacement of the rudder, has been considered
 7 by V.A.Kotel'nikov (Bibl.10).

8 ** The design of automatic pilots permits adjustment of the transmission ratios
 9 within certain limits.

additional increment of the longitudinal moment ΔM_z acting on the aircraft, equal to

$$\Delta M_z = M_z^{\delta} \Delta \delta = M_z^{\delta} \delta V + M_z^{\delta} \delta \alpha + M_z^{\delta} \delta \dot{\alpha} + M_z^{\delta} \delta \ddot{\alpha} \quad (7.41)$$

where $M_z^{\delta} = \frac{\partial M_z}{\partial \delta}$ is the partial derivative of the longitudinal moment with respect to the angle of deflection of the elevator.

In order to analyze the influence of the automatic pilot on the disturbed motion of the aircraft, this increment ΔM_z must be introduced into the equation of the moments of the system (7.14). On doing this, and grouping similar terms, we get

$$\left. \begin{aligned} I_z \frac{d^2 \Delta \theta}{dt^2} - (M_z^{\delta} + \nu_1 M_z^{\delta}) \Delta V - (M_z^{\delta} + \nu_2 M_z^{\delta}) \Delta \alpha \\ - M_z^{\delta} \frac{d \Delta \alpha}{dt} - (M_z^{\delta} + \nu_3 M_z^{\delta}) \frac{d \Delta \alpha}{dt} - \nu_4 M_z^{\delta} \Delta \alpha - Q \end{aligned} \right\} \quad (7.42)$$

On comparing eq.(7.42) with the original equation of moments (7.14), we see that the influence of the above automatic pilot was expressed, in the first place, in the variation of the value of the coefficients of the variables ΔV , $\Delta \alpha$ and $\frac{d \Delta \alpha}{dt}$, and, in the second place, in the appearance of the additional term $\nu_2 M_z^{\delta} \Delta \theta$. In this way the use of an automatic pilot is equivalent to a variation in the value of the longitudinal static stability of the aircraft M_z^{δ} and of the derivative M_z^{δ} , and to a variation in the value of the longitudinal damping moment. Consequently, in this part, the influence of the automatic pilot may be considered at the same time with the analysis of the influence of these parameters. The increase in the complexity of the equations of motion as a result of the appearance of the additional term on the left side of eq.(7.42) must be analyzed separately.

It is possible to imagine an automatic pilot which also reacts to the values $\frac{d^2 \Delta \theta}{dt^2}$ and $\frac{d \Delta \alpha}{dt}$. In this way, with respect to the dynamic stability (and with respect to the controllability if, for example, we imagine the automatic pilot to be connected with an additional rudder besides the main rudder, controlled only by the

STAT

0 pilot), in the general case, the effect of the automatic pilot is likewise equivalent to a variation in the moment of inertia and the moment due to the lag of the downwash.

The system of equations of the longitudinal aircraft motion of an aircraft with an ideal automatic pilot, reacting only to a variation in the angle of pitch, will, in the dimensionless form, be as follows

$$\begin{aligned} \frac{dV}{dt} + 2h_1 c_{D_1} V + (c_{D_1} - c_{D_2}) \beta + c_{D_2} \beta &= 0 \\ \frac{d\beta}{dt} - \frac{d\beta_0}{dt} - 2h_1 c_{D_1} V - (c_{D_1} + c_{D_2}) \beta + c_{D_2} \beta_0 &= 0 \\ \frac{d\beta_0}{dt} - M^2 \frac{m_1^2}{r_1^2} V - \frac{m_1^2}{r_1^2} \beta &= 0 \\ -\frac{m_1^2}{r_1^2} \frac{d\beta_0}{dt} - \frac{m_1^2}{r_1^2} \beta + \frac{m_1^2}{r_1^2} \frac{d\beta}{dt} &= 0 \end{aligned} \quad (7.42)$$

where $m_z^0 = \frac{\partial m_z}{\partial \beta}$ and v_3 is the transmission ratio of the automatic pilot.

On developing the characteristic determinant of this system of equations, we find that the coefficients of the characteristic equations a_1, a_2, a_3 and a_4 received the following supplements in addition to their values without the automatic pilot, $\Delta a_1, \Delta a_2, \Delta a_3$, and Δa_4 , which are equal respectively to

$$\begin{aligned} \Delta a_1 &= 0 \\ \Delta a_2 &= -\frac{m_1^2}{r_1^2} \\ \Delta a_3 &= -\frac{m_1^2}{r_1^2} \frac{(1+2h_1)c_{D_1} + c_{D_2}}{r_1^2} \\ \Delta a_4 &= -\frac{m_1^2}{r_1^2} \frac{(1-h_1)c_{D_1} + h_1 c_{D_2} - h_1 c_{D_1} c_{D_2}}{r_1^2} \end{aligned} \quad (7.44)$$

52 On regulating the transmission ratio v_3 from the automatic pilot to the rudder,
54 the automatic pilot can be used for influencing the coefficients of the character-
56



istic equation and, consequently, also the characteristics of the dynamic stability of the aircraft. More detailed information on this influence may be found, for example, in the above-mentioned books by V.S.Vedrov and V.A.Kotel'nikov (Bibl.8,10).

The Stability of a Stick-Free Aircraft

As shown by V.S.Vedrov (Bibl.8), in considering the stability of a stick-free aircraft, the influence of the inertial forces of the control system, including the rudder itself, can be neglected. In that case, the position of the rudder during disturbed motion of the stick-free aircraft will be determined by the increments of overload $\Delta n = \frac{\Delta Y}{G}$ acting on the aircraft. The first of these, at the adopted initial assumptions, will be a function of the velocity increment V , of the angle of attack $\Delta \alpha$, and of the angular velocity $\dot{\Delta \alpha}$. The increment in overload is determined by the increment in angle of attack and flying speed. Consequently, the deflection of the elevator $\Delta \delta$ under the action of the disturbances is given by

$$\Delta \delta = \varphi_1 \Delta V + \varphi_2 \Delta \alpha + \varphi_3 \frac{d\Delta \alpha}{dt} + \varphi_4 \frac{d^2 \Delta \alpha}{dt^2} \quad (7.45)$$

and the corresponding increment of moment ΔM_z , by the function

$$\Delta M_z = \varphi_1 M_z^1 \Delta V + \varphi_2 M_z^2 \Delta \alpha + \varphi_3 M_z^3 \frac{d\Delta \alpha}{dt} + \varphi_4 M_z^4 \frac{d^2 \Delta \alpha}{dt^2} \quad (7.46)$$

where $\varphi_1, \varphi_2, \varphi_3$, and φ_4 are constant quantities.

If this additional moment is introduced into the equation of moments of the system (7.24), the form of the equation will remain unchanged, while the value of the constant coefficients of the variables will change*.

In this way, in contrast to the stability with an automatic pilot, the stability of a stick-free aircraft, considered from the formal side, is completely analogous to stability with the elevator in fixed position. The characteristic equation and its coefficients will have the same form in both cases and may be distinguished only by the corresponding respective indexes of the coefficients.

* Similar expressions of these coefficients and the analysis of the influence of aerodynamic and design parameters on them are presented in Chapter IX.

CHAPTER VIII

ANALYSIS OF THE DISTURBED MOTION OF AN AIRCRAFT

Practical Method of Calculation and Analysis of DisturbedAircraft Motion

In the preceding Chapter we considered, in their general form, the equations of disturbed motions, the methods for their solution, and the condition for the stability of motion. We saw that, to determine the disturbed motion, it was necessary to solve a characteristic equation of the fourth degree, and, using the assigned initial conditions, to find the numerical values of the constant coefficients in the expressions for the parameters of aircraft motion under consideration. The expression obtained in Chapter VII for the coefficients of the characteristic equation were rather unwieldy. Calculation on the basis of these general equations and formulas requires a large expenditure of time and makes it difficult to apply the theory of dynamic stability to the solution of practical questions. The question thus, naturally enough, arises as to the formulation of approximate methods of calculation with a degree of accuracy that will satisfy the engineer.

The simplifications on which the approximate methods are founded consist mainly of the resolution of disturbed longitudinal motion into two widely differing types of motion, namely into so-called short-period and long-period motions. In order to give a clearer foundation for these engineering calculations and analyses, we will use numerical examples in the following.

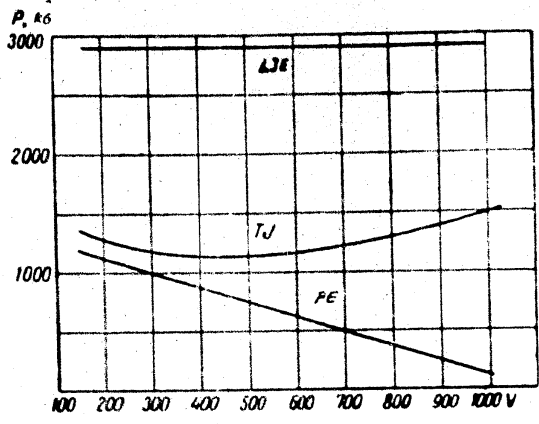


Fig.8.1 - Typical Relation between the Thrust of a Piston Engine (PE), a Turbo-jet (TJ) Engine, and a Liquid-Jet Engine (LJE) as a Function of Flying Speed

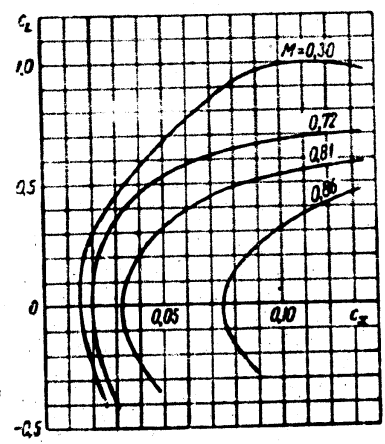


Fig.8.2 - Polars of an Aircraft, allowing for the Influence of Compressibility of Air

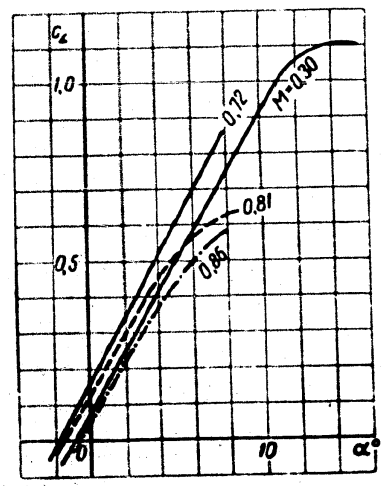


Fig.8.3 - Curves $C_L = f(\alpha)$ Allowing for the Influence of the Compressibility of Air



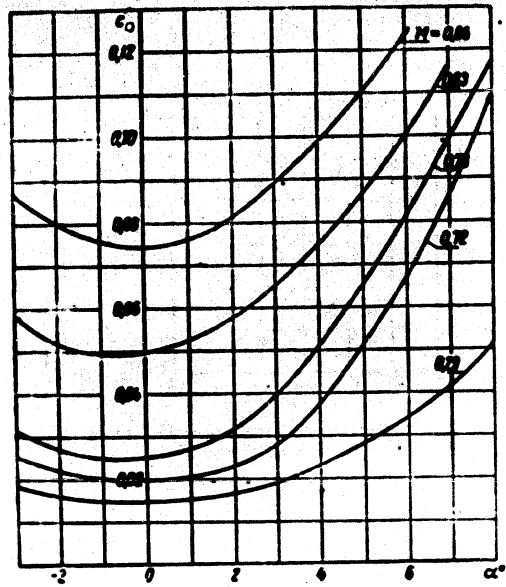


Fig.8.4 - Example of the Relation between C_D and α at Various Mach Numbers

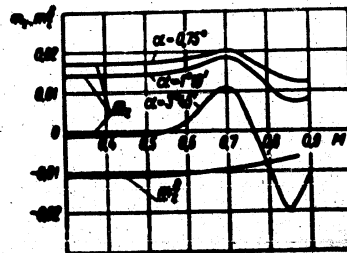


Fig.8.5 - Example of the Relation between m_2 and m_2^δ and the Mach Numbers at Various Angles of Attack



Determination of the Coefficients of the CharacteristicEquations

The calculation of the coefficient of the characteristic equation is rather laborious.

As an example we present the calculation of a turbo-jet fighter of conventional design with a rectangular wing, having the following design data:

Weight $G = 6900$ kg;

Length of aircraft $L = 10.6$ m;

Wing area $S = 21.7$ m²;

Length of mean aerodynamic chord $b_A = 1.95$ m;

Relative area of horizontal tail surface $\bar{S}_{h.t.} = \frac{S_{h.t.}}{S} = 0.175$;

Arm of horizontal tail surface with respect to center of gravity $l_{h.t.} = 6$ m

Arm of engine thrust with respect to center of gravity (engine axis passes above center of gravity) $y_p = 0.25$ m.

Let the polars of this aircraft and the curves $C_L = f(\alpha, M)$ be characterized by the curves shown in Figs. 8.2 and 8.3, and the curve of thrust of the turbo-jet engine is shown by Fig. 8.1.

The coefficients of the characteristic equation depend on the coefficients C_D , C_L , and m_z and on their derivatives relative to the angle of attack and the Mach number. For this reason, the calculations require supplementing the graphs of Fig. 8.1, 8.2 and 8.3 by graphs similar to those shown in Figs. 8.4 to 8.8. All the graphs necessary for our calculations can be constructed from the results of model tests of the given aircraft in a wind tunnel.

Let us, take for the calculation, three attitudes at full throttle at $C_L = 0.4$, 0.1 , and 0.05 and one attitude of gliding at zero thrust and $C_L = 0.4$.

The altitude of flight is taken as equal to 2000 m.

Starting from the design data given above, we obtain, on performing the corre-

STAT

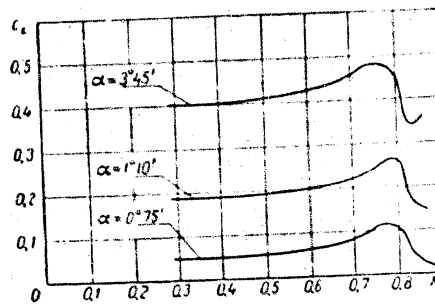


Fig.8.6 - Example of the Relation between C_L and Mach Number at Various Angles of Attack

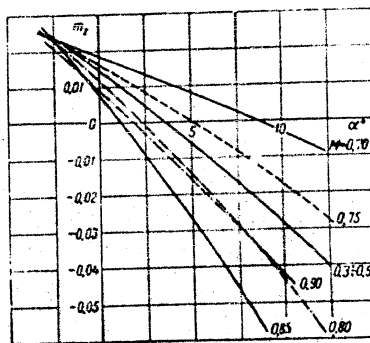
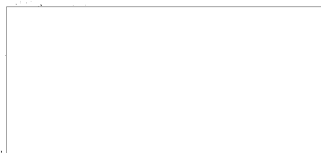


Fig.3.7 - Example of the Relation between m_z and α at Constant Elevator Position and Various Mach Numbers



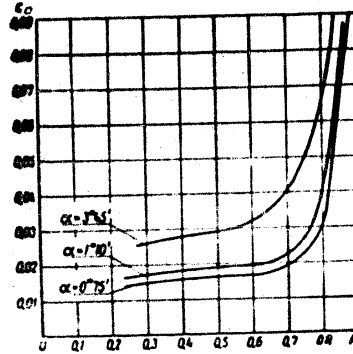


Fig.8.8 - Example of the Relation between C_D and M at Various Angles of Attack

Table 8.1

C_L	$P=0$			$P=0$
	0,4	0,1	0,05	$C_L = 0,1$
α°	3,8°	+0,75°	0°	3,8°
θ°	5,6°	0	-48,4°	-3,87°
ϕ°	9,4°	+0,75	-48,4°	-0,07°
$V, m/sec$	124	248	286	124
M	0,37	0,74	0,85	0,37
$V, km/hr$	447	893	1030	447

15°

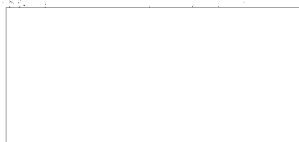


Table 8.2

Values of Initial Coefficients

2	QUANTITY c_L	P=0			P=0
		0,4	0,1	0,05	0,4
1	c_0	0,027	0,020	0,073	0,027
2	$P, \kappa z$	1140	1330	1530	0
3	$S_p V^3$	$3,43 \cdot 10^4$	$13,7 \cdot 10^4$	$18,2 \cdot 10^4$	$3,43 \cdot 10^4$
4	$c_0 c$	-0,040	0	0,056	0,027
5	$c_L c$	0,400	0,100	0,050	0,400
6	c_0^2	0,301	0,057	0,181	0,301
7	$c_0^2 c$	0,301	0,057	0,181	0,301
8	c_L^2	4,56	5,12	4,30	4,56
9	$c_L^2 c$	4,63	5,14	4,32	4,56
10	M	0,37	0,74	0,86	0,37
11	c_0^3	0,01	0,008	1	0,01
12	PV	0	1,6	2,0	0
13	$c_0^2 c$	0,37	0,145	1,04	0,01
14	c_L^3	0	0,50	-0,70	0
15	$c_L^3 c$	0,02	0,50	-0,70	0
16	A_1	0,71	$A_1 c_0 c = 0,054;$ $A_1 = \infty$	8,9	1,07
17	A_2	1,01	2,85	-4,95	1
18	m_1^M	0	-0,0615	-0,6375	0
19	$m_1^M c$	0,0460	-0,0600	0,037	0
20	m_1^c	-0,244	-0,170	-0,373	-0,244

STAT

According to the calculations, the initial values for the parameters of motion that are presented in Table 8.1.

Table 8.2 contains the results of the calculation of the coefficients C_{Dc} , C_{Lc} , C_{Dc} , etc. from eqs.(7.17), (7.18), (7.20), and (7.21).

The coefficient of damping moment of pitching m_2^d and the moment coefficient due to lag in downwash m_2^d are determined by the approximate formulas for the case of an aircraft of conventional design with a rectangular wing (Bibl.11).

$$m_2^d = 1.25 \frac{S_{ht} L_{ht}^2}{S_A} V^2$$

$$m_2^d = \frac{d}{d\alpha} m_2^d$$

Taking the aspect ratio of the horizontal tail surface $A_{h.t.} = 3$, we obtain the approximate value $a_{h.t.} \approx 3$. We will consider this constant for all four states of flight, although in reality $a_{h.t.}$, as we know from Chapter III, varies with the Mach number. This assumption is legitimate in this case, inasmuch as the calculation examples given by us are of an illustrative nature. We will consider that the $\frac{d\epsilon}{d\alpha} \approx 0.50$. Finally, the coefficient of velocity deceleration is taken as $k = 0.9$. In that case, for all four states of flight taken, we obtain

$$m_2^d = -1.25 \cdot 3 \cdot 0.175 \cdot \frac{25}{9.8} \cdot 0.25 = -3.2$$

$$m_2^d = 2.92$$

Of course, in technical, not illustrative, calculation of dynamic stability and disturbed motion of a specific aircraft, it is necessary to use for the determination of the values of $a_{h.t.} \frac{d\epsilon}{d\alpha}$ and m_2 , the more accurate methods and formulas, which, in particular, were presented in Capters III and VI of this book.

We find the square of the radius of inertia r_2^2 by the approximate formula

$$r_2^2 = 0.0312^2$$



STAT

POOR ORIGINAL

Table 8.3

Calculation of the Coefficient a_1

c_1	P=0			P=6
	0.4	0.1	0.05	0.4
$a_1 = c_1^2$	4.83	5.14	4.32	4.56
$a_1 = -\frac{m_1^2 + m_2^2}{r_1^2}$	9.65	9.85	9.65	9.65
$a_1''' = (1+2h_1) c_1$	0.0168	0.108	0.948	0.885
$a_1 = a_1' + a_1'' + a_1'''$	14.59	14.99	14.91	14.585

Table 8.4

Calculation of the Coefficient a_2

c_2	P=0			P=6
	0.4	0.1	0.05	0.4
m_2^2	-78.1	-55.1	-120.9	-78.1
$c_1^2 c_2^2$	-77.3	-38.3	-25.5	-26.9
$a_2 = -\frac{m_2^2 + c_1^2 c_2^2}{r_2^2}$	114.9	93.1	139.5	114.4
$a_2 = -(1+2h_2) c_2$	0.148	1.04	9.67	0.83
$h_2^2 c_2$	0.0014	0	0.0288	0.001
$h_2^2 c_2^2$	0.134	0.2775	1.89	0.132
$-h_2^2 c_2^3$	-0.1216	-0.0482	0.0447	-0.129
$h_2^2 c_2$	0.1613	0.0335	-0.0124	0.168
$a_2''' = 2h_2^2 c_2 + h_2^2 c_2^2 - h_2^2 c_2^3 + h_2^2 c_2$	0.24	0.269	1.914	0.348
$a_2 = a_2' + a_2'' + a_2'''$	115.5	94.72	172.5	115.58

POOR ORIGINAL

Table 8.5

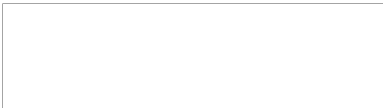
Calculation of the Coefficient a_3

c	P=0			P=0
	0.4	0.1	0.05	0.4
$a_3 = -2(h_1 c^2 + h_2 c_0 c^2 - h_3 c_1 c^2 + h_4 c^2) \frac{m^2}{r^2}$	2.18	3.73	25.30	2.23
$a_3 = -2(h_2 c^2 + h_3 c^2) \frac{m^2}{r^2}$	1.08	0.18	0.68	1.07
$a_3 = -(1+2h_1) c_0 c \frac{m^2}{r^2}$	1.43	6.400	123.90	7.23
$a_3 = -M c_0 c \frac{m^2}{r^2}$	1.81	0.907	2.08	0
$a_3 = a_3 + a_3 + a_3 + a_3$	6.46	9.438	147.1	10.53

Table 8.6

Calculation of the Coefficient a_4

c_1	P=0			P=0
	0.4	0.1	0.05	0.4
$a_4 = -2(h_2 c^2 + h_3 c^2) \frac{m^2}{r^2}$	27.33	3.02	3.77	27.1
$c_0 c^2 c$	0.012	0	0.010	-
$c_1 c^2 c$	1.853	0.514	0.716	-
$a_4 = (c_0 c^2 c + c_1 c^2 c) \frac{m^2}{r^2}$	11.07	-0.17	-2.51	0
$a_4 = a_4 + a_4$	28.40	-4.75	0.68	27.4



POOR ORIGINAL

where L is the total length of the aircraft, which in our case is 10.6 m. Then, for this aircraft, we obtained

$$c_l^* = 2.08 \text{ m}^2$$

Finally, let us calculate a very important parameter of dynamic stability and controllability of aircraft, the coefficient of relative density of the aircraft:

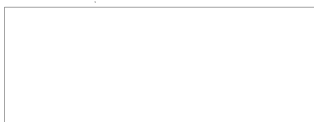
$$\rho = \frac{2m}{\rho_{0,2}} = \frac{2 \cdot 6000}{9.81 \cdot 0.1020 \cdot 21.7 \cdot 1.25} = 284$$

The calculation of each of the coefficients of the characteristic equation is presented in Tables 8.3 to 8.6. The individual summands of each coefficient are denoted by indices, for example:

$$a_1 = a_1^1 + a_1^2 + a_1^3 \dots$$

Thus, for the initial states of flight we obtained the values of the coefficient of the characteristic equations presented in Table 8.7.

λ	Flying Speed at Altitude $H=2000 \text{ m}$	Coefficient			
		a_1	a_2	a_3	a_4
1	Glide at zero engine thrust $c_L = 0.4; \theta = -3.87^\circ; V_1 = 405 \text{ km/hr}$	14.30	115.58	10.53	27.4
2	Flight at full engine thrust $c_L = 0.4; \theta = 5.6^\circ; V_1 = 405 \text{ km/hr}$	14.17	115.5	6.46	38.40
3	$c_L = 0.1; \theta = 0^\circ; V_1 = 810 \text{ km/hr}$	14.90	94.72	9.50	4.75
4	$c_L = 0.05; \theta = -48^\circ.4; V_1 = 939 \text{ km/hr}$	14.91	172.50	147.10	0.16



POOR ORIGINAL

In Table 8.7, for a fuller characterization of the initial states of flight, we present the indicator flying speed. The value of the indicator flying speed is connected with the velocity head, to whose variation actuates the conventional speed indicator installed on the aircraft. If we assume that this instrument has no instrument errors and that there is no influence of the aircraft on the flow around the velocity pickup, then, in flight under sea-level conditions (760 mm Hg and 15° C), the indicator speed will exactly coincide with the speed shown by the instrument.

As indicated in Table 8.7, a change of attitude has relatively little effect on the value of the coefficient of the characteristic equation a_1 . Even if we allow for the influence of the compressibility of air on the coefficients m_2^w and m_2^d , the values of the coefficient a_1 vary relatively little.

The coefficient a_2 varies with the attitude to a somewhat greater extent than does the coefficient a_1 . The variation of a_2 is due primarily to the variation in the coefficient of stability m_2^a , the coefficient of damping m_2^d , the coefficient of moment due to lag of downwash at the tail m_2^a , and, finally, to the value of C_{Lc}^a .

The coefficients a_3 and a_4 , in contrast to the coefficients a_1 and a_2 , vary strongly in absolute value and even change their sign. The variation of a_3 and a_4 is mainly connected with the influence of the compressibility of air on C_D and on the coefficient of static stability m_2^x and m_{2c}^y ; the value of the generalized coefficient of drag of the aircraft C_{Dx} also exerts a substantial influence.

Approximate Formulas for Determining the Coefficients of the Characteristic Equation

Approximate formulas have been worked out for determining the coefficients of the characteristic equation. To obtain these approximate formulas, we must reject the terms of second-order value in the corresponding exact formulas of the preceding Chapter. The possibility of considerable simplifications of the formulas, in particular, is shown by the numerical examples presented in Tables 8.2 to 8.6. We

POOR ORIGINAL

now will set up these approximate formulas.

According to eqs.(7.17) and (7.18) of the preceding Chapter C_{Dc} and C_{Lc} are expressed by the formula

$$C_{Dc} = C_D - \frac{2P \cos \alpha}{S_b V^2};$$

$$C_{Lc} = C_L + \frac{2P \sin \alpha}{S_b V^2}.$$

In the states of flight most used in actual operations, the angles of attack generally do not exceed 10° . For this reason we may take $\cos \alpha \approx 1$ and neglect the summand $\frac{2P \sin \alpha}{S_b V^2}$ in the formula for C_{Lc} , i.e., we assume that $C_{Lc} = C_L$. If, starting from the equation of steady rectilinear flight

$$C_D S_b V^2 = G \cos \theta$$

we replace $\frac{2}{S_b V^2}$ by $\frac{C_L}{G \cos \theta}$, and take $\cos \theta \approx \cos \alpha \approx 1$, then we obtain the following approximate formula for C_{Dc} :

$$C_{Dc} = C_D - C_L \frac{P}{G}.$$

As confirmed by Table 8.2, we may consider that

$$C_{Dc}^N = C_D^N; \quad C_{Lc}^N = C_L^N; \quad C_{Lc}^N = C_L^N.$$

In eq.(7.21) we can neglect the summand $\frac{2P^V \cos \alpha}{S_b V^2 M_z}$, and use the following formula for C_{Dc}^N :

$$C_{Dc}^N = C_D^N + \frac{2P^V}{M_z} \frac{P}{G}.$$

In the formula for m_{zc}^V , we can neglect the summand $\frac{2P^V y_p}{S_b A_0 V^2 M_z}$ and write

$$m_{zc}^N = m_z^N + \frac{2P^V y_p}{S_b A_0} \frac{P}{G}.$$

On considering, analogously, the separate significance of each summand in the expressions for the coefficients of the characteristic equation, we obtain the

POOR ORIGINAL

following approximate formulas*:

$$a_1 = c_1^M - \frac{m_1^M + m_2^M}{T_1};$$

$$a_2 = - \frac{\mu m_1^M + c_1^M m_2^M}{T_1};$$

$$a_3 = -2(k_1 c_{o,c}^M + k_2 c_{o,c}^M - k_1 c_{o,c}^M + k_2 c_{o,c}^M) \frac{m_2^M}{T_1} -$$

$$-2(k_1 c_{o,c}^M + k_2 c_{o,c}^M) \frac{m_2^M}{T_1} - (1 + 2k_1) c_{o,c}^M \frac{\mu m_2^M}{T_1} + M c_{o,c}^M \frac{\mu m_2^M}{T_1};$$

$$a_4 = -2(k_1 c_{o,c}^M + k_2 c_{o,c}^M) \frac{\mu m_2^M}{T_1} + (c_{o,c}^M + c_{o,c}^M) M \frac{\mu m_2^M}{T_1},$$

where the coefficients $c_{o,c}^M$, $c_{o,c}^M$, m_1^M , m_2^M , k_1 , and k_2 are determined by the approximate formulas given below:

$$\left. \begin{aligned} c_{o,c} &= c_o - c_c \frac{P}{O} \\ c_{o,c}^M &= c_o^M + \frac{x_c}{M} \frac{P}{O} \\ m_{1,c}^M &= m_1^M + \frac{x_c}{M} \frac{y_p}{b_c} \frac{P}{O} \\ k_1 &= 1 + \frac{c_{o,c}^M M}{2c_{o,c}} \\ k_2 &= 1 + \frac{c_{o,c}^M M}{2c_c} \end{aligned} \right\}$$

Hereafter, in writing analytical formulas and expressions we will frequently drop the subscript "c" for the aerodynamic coefficients, considering them, however, to be taken in the general form ("generalized").

* As shown below, only the characteristics of dynamic stability which are connected with the coefficients of the characteristic equations a_1 and a_2 are of great practical importance.

POOR ORIGINAL

In order to evaluate the error due to use of the approximate equations (8.3) and (8.4), we present in Table 8.8 a comparison of the values of the coefficient of the characteristic equation calculated by the exact formulas and by the approximate ones for the four initial states of flight taken above.

Table 8.8

Exact and Approximate Values of the Coefficient
of the Characteristic Equation

Flight Conditions	a_1		a_2		a_3		a_4	
	Exact	Approximate	Exact	Approximate	Exact	Approximate	Exact	Approximate
<i>Glide at zero thrust</i>								
$c_L = 0.4$	14.30	14.21	115.58	116.4	10.54	10.54	27.6	27.6
<i>Flight at full engine thrust</i>								
$c_L = 0.4$	14.26	14.21	115.5	116.4	6.65	6.65	30.6	30.6
$c_L = 0.1$	14.08	14.77	94.72	93.0	9.50	9.47	-4.73	-4.73
$c_L = 0.05$	14.91	13.85	172.5	159.5	147.10	145.7	0.65	0.47

It follows from Table 8.8 that, in the region where the influence of the compressibility of air on the aerodynamics of the aircraft is relatively small, the difference between the exact and approximate values of all coefficients of the characteristic equation does not exceed 2%. Taking into account the known inaccuracies in the determination of the initial data for the calculation of the coefficients a_1 , a_2 , a_3 , and a_4 , we may consider this difference to be entirely allowable.

In diving at high speeds, when the altitude and, consequently, also the density of the air vary rapidly with time, the possibility of assuming constant density

POOR ORIGINAL

of air ($\rho = \text{const}$) which is adopted in the ordinary theory of dynamic stability, becomes questionable. It is entirely possible that the variation in density of the air with altitude, on consideration of a steep dive, may yield a much greater difference than the difference between the calculations by the exact formulas and those by the approximate ones.

Finding the Root of the Characteristic Equation

It is rather complicated and laborious to find the roots of biquadratic equation by the aid of exact algebraic methods. Various approximate methods are therefore ordinarily used to find the roots, which considerably shortens the time required for finding the roots and yields adequate accuracy, particularly when the possible errors in the determination of the original coefficient of the equation are taken into account.

In calculating the dynamic stability of aircraft, the method described below is convenient for finding the roots of the characteristic equation.

As pointed out in Chapter VII, the fourth-degree equation $F(\lambda) = 0$ may be presented in the form:

$$F(\lambda) = \lambda^4 + a_3\lambda^3 + a_2\lambda^2 + a_1\lambda + a_0 = (\lambda - \lambda_1)(\lambda - \lambda_2)(\lambda - \lambda_3)(\lambda - \lambda_4) = 0 \quad (8.5)$$

where $\lambda_1, \lambda_2, \lambda_3,$ and λ_4 are the required roots of the equation. In the general case, the four roots differ in absolute value, and the subscripts denote the roots in decreasing order of absolute value.

For the characteristic equation of longitudinal stability, in practice, the first two roots considerably exceed the last two roots in absolute value (as will be plain from the example presented). For this reason we may write

$$|\lambda_1| > |\lambda_2| > |\lambda_3| > |\lambda_4| \quad (8.6)$$

If, in eq.(8.5), we take the product $(\lambda - \lambda_1)(\lambda - \lambda_2)$ and the product $(\lambda - \lambda_3)(\lambda - \lambda_4)$ we obtain

$$F(\lambda) = (\lambda^2 + a_3\lambda + a_2)(\lambda^2 + a_1\lambda + a_0) = 0 \quad (8.7)$$

POOR ORIGINAL

where

$$\begin{aligned} A &= -(\lambda_1 + \lambda_2); & B &= \lambda_1 \lambda_2 \\ m &= -(\lambda_1 + \lambda_3); & n &= \lambda_1 \lambda_3 \end{aligned} \quad (8.8)$$

On the other hand, if we perform the multiplication in eq.(8.7) and equate the coefficients of the same powers of λ , we obtain the following four equations in four unknowns A, B, m and n:

$$\begin{aligned} a_1 &= A + m; \\ a_2 &= B + Am + n; \\ a_3 &= An + Bn; \\ a_4 &= Bn. \end{aligned}$$

If we then use these equations, for determining the values of A, B, m and n, and separately solve the two quadratic equations (8.7), it is easy to find all the values of the roots of the characteristic equations as well. The values of A, B, m, and n are found by calculation, according to the method of successive approximations. For this purpose, we write the last four equations in the following form:

$$\left. \begin{aligned} A &= a_1 - m; & B &= a_2 - Am - n; \\ n &= \frac{a_4}{B}; & m &= \frac{a_3 - An}{B}. \end{aligned} \right\} \quad (8.9)$$

In consequence of the fact that λ_2 and λ_4 are considerably greater in absolute value than λ_1 and λ_3 , it follows eq.(8.8) that A and B must be considerably greater than m and n. We may thus take the values as our first approximation for the values of A and B.

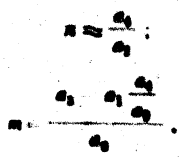
$$A \approx a_1; \quad B \approx a_2$$

On substituting these values of A and B in the expressions of eq.(8.9) for n and m, we obtain their approximate values.

By substituting these values of m and n in the first two expressions of eq.(8.9) we obtain the second approximations for the values of A and B, and then the second approximations for the values of m and n.

STAT

POOR ORIGINAL



This process of successive approximation is repeated until, within the required accuracy of calculation, A, B, m, and n of the preceding approximation coincide with those of the following one. It is convenient to perform the calculations by using the form given in Table 8.9.

After the coefficients A, B, m, and n have been calculated, the roots are determined by the formulas

$$i_{1,2} = -\frac{A}{2} \pm \sqrt{\frac{A^2}{4} - B}$$

$$i_{3,4} = -\frac{m}{2} \pm \sqrt{\frac{m^2}{4} - n}$$

Table 8.9

Horizontal Flight at $C_L = 0.1$,

$a_1 = 14.90$; $a_2 = 94.72$; $a_3 = 9.50$; $a_4 = -4.75$

N of approximation	$A = a_1$	m	A_m	$B = \frac{a_2 - a_1}{A_m - m}$	$n = \frac{a_3}{B}$	A_n	$a_4 - A_n$	$n = -\frac{a_4 - A_n}{B}$
1	14.90	0	94.7	-0.0601	-0.766	10.25	0.1023	
2	14.79	1.60	93.17	-0.0610	-0.756	10.25	0.100	
3	14.79	1.63	93.16	-0.0610	-0.756	10.25	0.100	
4	14.79	1.63	93.16	-0.0610	-0.756	10.25	0.100	
		$i_{1,2} = -7.395 \pm 0.21$		$i_3 = -0.2025$		$i_4 = -0.1725$		

STAT

POOR ORIGINAL

In most of the practical cases, $\frac{A^2}{L} < B$ and $\frac{m^2}{L} < n$. For this reason, we usually obtain complex and pairwise mutually conjugate values for the roots, as remarked before.

As will be seen from Table 8.9, the calculation of the roots of the characteristic equation by the above method requires only a short time. Usually two or three approximations are entirely sufficient. The number of approximations necessary for the exact calculation of the roots increases if the difference between the absolute values of all four roots decreases.

In solving most problems of any practical importance, we may, in first, approximation, replace the characteristic equation of the fourth degree by two quadratic equations, namely

$$\left. \begin{aligned} \lambda^2 + a_1\lambda + a_2 &= 0 \\ \lambda^2 + \frac{a_1a_2 - a_3a_4}{a_2}\lambda + \frac{a_4}{a_2} &= 0. \end{aligned} \right\} \quad (8.10)$$

Determination of the Period and Coefficient of Damping

As pointed out in the preceding Chapter, the disturbed motion of the aircraft after its random deviation from its initial state of flight consists of various partial forms of motion superposed on each other.

These partial motions may be represented with graphic clarity if we determine the oscillation periods T and the time of reduction or increase of the initial deviation (amplitude) to reach a definite value. The latter parameter characterizes the rate of damping or growth of the oscillation. It is customary to determine the time of increase or decrease of the initial deviation by a factor of two (t_2). The values of T and t_2 are determined from the roots of the characteristic equation.

As already stated, to each pair of mutually conjugate complex roots of the characteristic equation

POOR ORIGINAL

$$\lambda_{1,2} = a \pm bi$$

there corresponds a particular solution of the differential equations of motion of the formula

$$\Delta V = Ae^{at} \sin(bt + \psi)$$

If the value of a is negative, then the increment of each parameter of motion (ΔV , Δa , etc.) will have an amplitude Ae^{at} , decreasing with time. To determine the value of t_2 , we write the equation

$$Ae^{at} = \frac{A}{2}$$

On dividing both sides of this equation by A , and then taking the logarithms, we obtain the following formula for t_2 :

$$t_2 = -\frac{\ln 2}{a} = -\frac{0.693}{a} \quad (8.11)$$

To determine the period of oscillation in dimensionless time, we make use of the formula

$$T = \frac{2\pi}{b} \quad (8.12)$$

If the real part of the complex root is positive ($a > 0$), then the corresponding vibrations of the aircraft will take place at an increasing amplitude Ae^{at} . In this case, for determining the time required for the initial amplitude to double, we make use of the formula

$$t_2 = \frac{0.693}{a} \quad (8.13)$$

The partial solution of the differential equation, corresponding to a pure real root of the characteristic equation $\lambda = a$ will have the formula

$$\Delta V = Ae^{at}$$

STAT

POOR ORIGINAL

Depending on the sign of the quantity a , we can use the same formulas (eq.(8.11) or eq.(8.13)) to determine the value of \bar{t}_2 in the case of a periodic motion.

The above expressions for \bar{T} and \bar{t}_2 determine the dimensionless values of the period and time of damping of the disturbed motion. In determining the dimensional values T and t_2 we must use the formulas

$$\begin{aligned} T &= \bar{T} \cdot \frac{2\pi}{\rho}; \\ t_2 &= \bar{t}_2 \cdot \frac{0.693}{\rho}. \end{aligned} \quad (8.14)$$

Table 8.10 gives data on the period of damping to half-amplitude for the above examples of disturbed motion.

The Two Types of Disturbed Motion of the Aircraft

By comparing the values of the roots of the characteristic equation given in Table 8.10*, we see that the roots λ_1 and λ_2 considerably exceed the roots λ_3 and λ_4 in absolute value.

According to the above-indicated difference in the roots, it is of substantial importance to differentiate between the oscillation period, intensity of decay or increase in deviation of the parameters of motion and their values corresponding to the initial state of flight.

This difference in the roots is not random but is a typical characteristic property of all aircraft. The physical causes of this difference will be considered below.

The disturbed motion corresponding to the larger roots λ_1 and λ_2 is characterized by a period measured in seconds, while the oscillation period corresponding to the roots λ_3 and λ_4 (in the case where these roots are complex) is expressed in

* The amplitude doubles.

POOR ORIGINAL

Table 8.10

Periods and Time of Decay to Half Amplitude

	Gliding $c_L = 0.4; P = 0$		Diving at full thrust $c_L = 0.05$		
	$\lambda_{1,3}$	$\lambda_{2,4}$	$\lambda_{1,3}$	λ_2	λ_4
Roots of the dimensionless equation	-7.12 ± 0.1	0.0311 ± 0.0071	-7.395 ± 0.21	-0.2895	0.1795
Dimensionless period of oscillations (T)	0.785	12.9	1.013	—	—
Dimensionless time of decay to half amplitude (or doubling) (t_2)	0.0874	22.3	0.0837	2.4	3.86°
Value of $\tau = \frac{2m}{\lambda V}$	8.1	5.1	2.545	2.545	2.846
Dimensional period of oscillations (T) in sec.	4	65.7	3.68	—	—
Time of decay to half amplitude (or increase to double amplitude) (t_w) in sec.	0.496	113.5	0.22	6.1	9.82°
Ratio t_2 / T t_2 / T	0.124	1.73	0.0726	—	—

tens of seconds or longer. The difference in the intensity of the decrease or increase of the initial deviation (amplitude) is likewise great between these two types of roots. The quantity t_2 , corresponding to the roots λ_1 and λ_2 , is expressed in tenths of a second, while the value of t_2 for the roots λ_3 and λ_4 is expressed in tens or even hundreds of seconds. The roots λ_1 and λ_2 thus correspond to the sharp motion of the aircraft with a short period and very rapid damping of the in-



POOR ORIGINAL

initial amplitude, while the roots λ_3 and λ_4 correspond to the slow disturbed motion with a long period and weak extinction or growth in amplitude. These two types of disturbed motion are customarily termed: the former, short-period motion; the latter, long-period motion. The latter type of motion is often also termed phugoid oscillations, or phugoid motion. Phugoid oscillations were also investigated by N.Ye. Zhukowski (Zhukovskiy) and later by Professor V.P. Vetchinkin.

We note that the above terms for longitudinal disturbed motion reflect the fact that this is an oscillatory motion of both types typical for most cases. A combination of oscillatory and aperiodic motion for the most common conditions of flight occur only rarely. Still less frequent is the case when all the disturbed motion consists entirely of four purely aperiodic motions superimposed on each other. Such cases arise in the absence of static stability of the aircraft ($\mu_0 > 0$).

A Characteristic Example of Disturbed Motion

To give a graphically clear idea of disturbed motion, we present a characteristic example in which all the calculations have been carried to the end, and the results of the calculations are represented graphically.

Let us investigate a fighter with the following parameters: weight about 3000 kg, specific wing loading about 180 kg/m^2 , wing chord (MAC) about 2m, and coefficient of static longitudinal stability μ_0 , about 0.05.

As the initial state of rectilinear flight, we will take steady gliding with a windmilling propeller ($P = 0$) at an altitude of 1000 m and a velocity of 450 km/hr along the flight path ($C_L \approx 0.2$).

We will omit the values of the individual parameters and give no intermediate calculations, directly giving the roots of the characteristic equation in the dimensionless formula for this flight condition:

$$\begin{aligned} \lambda_{1,2} &= -6.6 \pm 5.12i; \\ \lambda_{3,4} &= -0.0387 \pm 0.224i. \end{aligned}$$



POOR ORIGINAL

The flight conditions used for this calculation corresponds to the values:

$$\rho = \frac{2m}{rS\Delta} = 167; \quad \tau = \frac{2m}{rSV} = 2.58.$$

We will assume that the disturbed motion of the aircraft was caused by a uniform ascending air stream with a vertical velocity of 5 m/sec. To simplify the calculations we assume that the aircraft instantaneously enters this ascending current. In that case, the initial values of the parameters at $t = 0$, required for the complete solution of the equations of disturbed motion, will be

$$\Delta\alpha_0 = \frac{5 \cdot 57.3 \cdot 3.6}{460} = 2.39^\circ;$$

$$\Delta V_0 = \Delta\theta_0 = 0.$$

The disturbed motion of the aircraft in the example taken is characterized by following the laws adopted for the time variation of the (dimensional) parameters of motion:

$$\begin{aligned} \Delta\alpha^\circ &= 2.61e^{-1.22t} \cos(1.985t + 0.414) - \\ &\quad - 0.0336e^{-0.0868t} \cos(0.0868t + 1.54); \\ \Delta V &= 0.0384e^{-1.22t} \cos(1.985t + 1.68) + \\ &\quad + 1.65e^{-0.0868t} \cos(0.0868t + 1.509); \\ \Delta\theta &= 1.68e^{-1.22t} \cos(1.985t + 0.89) - \\ &\quad - 1.071e^{-0.0868t} \cos(0.0868t + 0.115); \\ \Delta\omega_z &= \frac{d\Delta\theta}{dt} = -0.1224e^{-1.22t} \cos(1.985t + 1.569) + \\ &\quad + 0.0021e^{-0.0868t} \cos(0.0868t + 1.514). \end{aligned} \tag{8.15}$$

In eq.(8.15) the angles of attack and of pitching are given in degrees, the angular velocity in radians per second, and the velocity along the flight path in meters per second. The arguments of the cosines are given in radians. Figure 8.9 gives the graphs of the variation in ΔV , $\Delta\alpha$, $\Delta\theta$ and $\Delta\omega_z$ with time, with the disturbed motion considered lasting for one minute, while Fig.8.10 shows this motion



POOR ORIGINAL

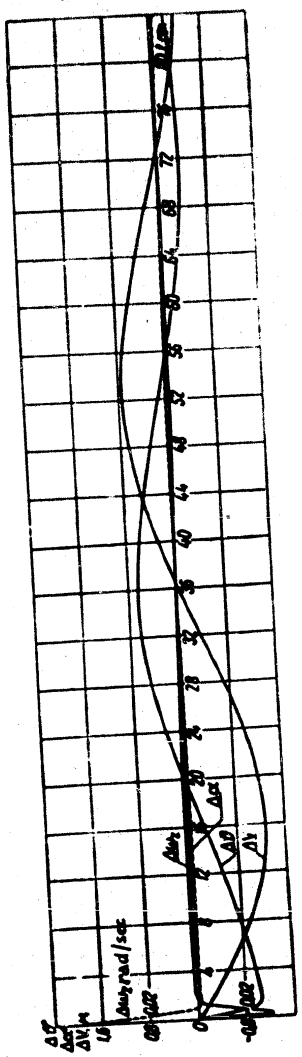


Fig. 8.9 - Variation with Time of the Increments of the Parameters of Position ΔV , $\Delta \alpha$, $\Delta \delta$, and $\Delta \omega_2$ with the Aircraft, Suddenly Entering an Ascending Air Current (Initial Disturbance of the Angle of Attack)



POOR ORIGINAL

on a large scale with respect to time during the first three seconds after the initial disturbance.

Equation (8.15) and Figs.8.9 and 8.10 clearly show the resolution of the disturbed motion of the aircraft into a short-period and a long-period motion. The short-period motion with the period $T = \frac{2\pi}{1.985} = 3.16$ sec decays with extraordinary rapidity. During the first 1 - 1.5 sec, the surrnanis in the increments ΔV , $\Delta \alpha$, $\Delta \theta$, and $\Delta \omega_z$ connected with the pair of large roots, practically vanish. As a result of

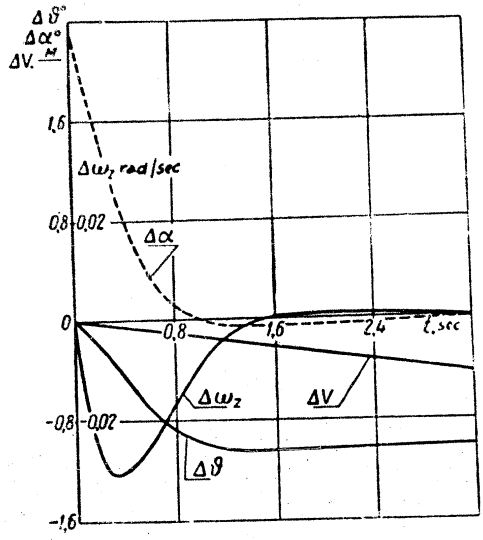


Fig.8.10 - Variation with Time of ΔV , $\Delta \alpha$, $\Delta \theta$, and $\Delta \omega_z$ during the First Stage of Disturbed Motion

the rapid decay, the oscillatory character of the short-period motion is masked and it is very similar to an aperiodic motion. This explains the fact that pilots in flight do not feel the oscillatory character of the motion. The long-period oscillatory motion with a period of $T = \frac{2\pi}{0.0868} = 72.3$ sec decays slowly. The pilot in



POOR ORIGINAL

flight is able to observe these oscillations very distinctly. The long-period oscillations can be simply recorded during flight, for example, by means of a velocity recorder, a pitch-angle recorder, or a load-factor recorder.

We observe that the resolution of the longitudinal disturbed motion into a short-period and a long-period motion is characteristic for all aircraft, even those that differ substantially in construction and in design parameters.

Physical Causes Responsible for the Resolution of
Disturbed Motion into Two Types

The resolution of longitudinal disturbed aircraft motion into two types of sharply differing character is explained by the fact that the angle of attack and the flying speed on which the aerodynamic forces and moments depend, greatly vary with time on any disturbance in the initial state of motion of the aircraft. The angle of attack of the aircraft varies rapidly, while the flying speed varies relatively slowly. To prove this, it is sufficient to take any numerical example and calculate the value of the angular acceleration of rotation of the aircraft about its transverse axis as well as the value of the linear acceleration along the flight path. For example, let us take the same aircraft as in the preceding section. Let the initial state of horizontal flight be characterized by the following values of the parameters:

$$v = 450 \text{ km/hr}; C_{Cl} = 0.2; q = \frac{\rho V^2}{2} = 900 \text{ kg/m}^2$$

$$m_z C_L = -0.06; C_L^\alpha = 4.2; m_z^\alpha = m_z C_L C_L^\alpha = -0.252; C_D^\alpha = 0.12$$

(in determining the derivatives, C_L^2, m_z^2, c_x^2 the angle of attack α is taken in radians). Let us take the following values for the mass of the aircraft and the moment of inertia with respect to the lateral axis, which we need to know in calculating the accelerations:

POOR ORIGINAL

$$m = 300 \text{ kg-m/sec}^2; \quad I_z = 900 \text{ kg-m/sec}^2$$

Let us assume further that the aircraft suddenly enters the zone of a rising air current, at a vertical velocity such that the angle of attack of the aircraft instantaneously changes by 2° . To calculate the accelerations of the aircraft in the first instant of disturbed motion we may use, together with the system of equations (7.14) of the preceding Chapter, the following two equations:

$$m \frac{dV}{dt} = -X_z^a;$$

$$I_z \frac{d\alpha}{dt} = M_z^a.$$

By substituting $X_z^a = c_x^a \rho v^2$ and $M_z^a = m_z^a S c_b \Delta$, using the approximate formulas $c_x^a \approx c_x^0$ and $m_z^a = m_z^0$, and substituting the numerical values, we obtain:

$$\begin{aligned} \frac{dV}{dt} &= -\frac{c_x^0 \rho}{m} \Delta z = -\frac{0.12 \cdot 16.5 \cdot 900}{300} \frac{2}{57.3} = -0.2 \text{ m/sec} \\ \frac{d\alpha}{dt} &= \frac{d\omega_z}{dt} = \frac{m_z^0 S c_b \Delta}{I_z} \Delta z = -\frac{0.252 \cdot 16.5 \cdot 900 \cdot 2}{900} \frac{2}{57.3} \\ &= -0.29 \text{ 1/sec} = -16.6 \text{ degree/sec} \end{aligned}$$

On the basis of the values so obtained the conclusion can be obtained that, in the first instant of disturbed motion, the rotation of the aircraft will be incomparably more intense than the increase or decrease in flying speed, as distinctly visible from Figs. 8.9 and 8.10. Analogously, the motion of the aircraft will be resolved into two types, even with a sharp deflection of the elevator.

When disturbances act on the aircraft, for example, when the pilot changes the position of the control surfaces, the motion of the aircraft varies in the following sequence: the disturbed equilibrium of aerodynamic moments produces a rotation of the aircraft with respect to its transverse axis. This rotation of the aircraft leads to a variation in angle of attack and, consequently, also to a change in the

POOR ORIGINAL

lifting force. As a result of the relatively high inertia of the aircraft, the flying speed during this time varies relatively slowly (cf. Figs. 8.9 and 8.10) and during the first 2-3 sec after the action of the disturbance, the flying speed may be considered equal to the initial speed. If in the initial state of flight, the lift was approximately equal to the weight of the aircraft ($Y = G \cos \theta$) then, after the disturbance, the excess or deficit of lift by comparison with the weight causes a curvature of the flight path. The extent of the curvature of the flight path $\frac{d}{dt}$ is determined by the value of the difference $Y - G \cos \theta$ at each instant of time.

The rotation of the aircraft and the curvature of the flight path, with oscillations due to the inertia of the aircraft, take place in a direction such that the angle of attack of the aircraft corresponds to the condition that the total aerodynamic moment vanishes under the action of a vertical air current, a stable aircraft will tend to return to its original angle of attack, while on deflection of the elevator the aircraft will establish a new angle of attack corresponding to a steady flight in the new position of the control surface. These stages correspond to the short period of motion of the aircraft. As a result of the high damping, such motion ends during the first 1-3 sec. However, as indicated in Figs. 8.9 and 8.10, as a result of the short-period motion, the angle of pitch and the angle of inclination of the flight path, $\theta = \theta - \alpha$ will not return to their "equilibrium" values corresponding to the initial state of flight. As a result, the equilibrium of the external forces (thrust, drag, and projection of the aircraft weight) along the tangent to the flight path is still not attained, while the equilibrium of the moments with respect of the transverse axis of the aircraft is, on the whole, already realized. The next motion of a stable aircraft will be a long-period motion and will continue until the equilibrium of forces is attained simultaneously along the normal to the flight path and along the tangent to it (provided the pilot leaves the aircraft to itself). In long-period motion, the flying speed, the angle of pitch

STAT

POOR ORIGINAL

of the aircraft, and the angle of inclination of the flight path to the horizon are the principal parameters that change, while the angle of attack and the angular velocity vary very little.

In this way, all the disturbed motion of the aircraft may be roughly and schematically divided into two stages. The first stage, that of a rapidly damped short-period motion, is connected primarily with the restoration of the equilibrium of the longitudinal moments. The second stage is that of long-period motion mainly due to the restoration of equilibrium of the forces along the tangent to the flight path. In reality, of course, these two motions are intimately interwoven, so that this schematic treatment can merely indicate their relative importance at the various stages of the total disturbed motion.

Practical Significance of the Two Types of the
Disturbed Motions

Before giving a further analysis of disturbed motion, let us discuss the practical significance of the characteristics of aircraft stability and of the above-described characteristics of the two types of disturbed motion. We will consider this question from two points of view: with respect to the maintenance of the state of flight assigned by the pilot for the aircraft, and with respect to the aircraft's response to the actions of the pilot, in other words, with respect to the controllability of the aircraft.

The deflections of the elevator performed by the pilot during execution of various maneuvers as well the purely random atmospheric influences, must be regarded as definite disturbing causes. Of course, the phenomena taking place under the action of atmospheric disturbances on the aircraft are not the same as those taking place when the elevator is deflected. For this reason, the requirements to be met by the characteristics of aircraft stability in each of these cases differ in principle.

The general requirements to be met by the behavior of the aircraft are stable

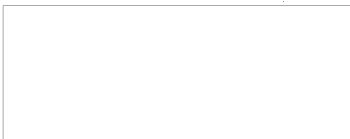
POOR ORIGINAL

0 maintenance of the attitude assigned by the pilot and simplest possible execution by the aircraft of the motion or maneuvers which the pilot intentionally performs.

As shown by studies, the role of the short-period and long-period motion, with respect to satisfaction of these requirements, and to evaluation of the so-called flying qualities of an aircraft differ substantially. Over 10 years ago, special flight tests were made with the purpose of studying the influence of the stability characteristics in the process of the long-period motion on the flying qualities of aircraft (Bibl.12). In these investigations, recording instruments were used to determine the period of phugoid oscillations and of their decay or growth was determined; at the same time the pilots made comments on the behavior and controllability of the aircraft. Aircraft of various types with widely differing characteristics of long-period disturbed motion were examined. These showed oscillations decreasing or increasing in amplitude, and also aperiodic deviations of the aircraft (aperiodic instability) from the initial state of flight.

A careful comparison of the pilots' comments with the quantitative characteristics so obtained led to significant conclusions which, at that time, were rather unexpected. It was found that with respect to the long-period motion, pilots require only that this motion must not be aperiodically unstable, when the aircraft leaves the initial state of flight with an intensity that increases with time. The oscillation period as well as the value of the decrease or increase in amplitude of the phugoid oscillations was not correlated with the comments of the pilots on the aircraft behavior. It was found that some aircraft with free long-period oscillations of increasing amplitude, i.e., aircraft with an oscillatory instability, received an excellent rating by the pilots. Even more than that, it was found that the pilots failed to suspect, prior to these tests, that a number of aircraft actually had oscillatory instability, although they had flown a good deal on such aircraft before.

How can such a result be explained?



POOR ORIGINAL

In the first place, by the fact that the long-period motion is manifested over such long time intervals that the pilot does not leave the aircraft to itself without intervening in its control. The period of these oscillations is usually not shorter than 20 sec. In the examples given above, the period was 60-70 sec. At such a slow rate of development of a disturbed motion, the pilot has enough time to note the deviation of the aircraft from the initial attitude and to react in time to it by proper manipulation of the control surfaces.

As aperiodic instability, the deviation of the aircraft from the initial attitude takes place more energetically and already becomes perceptible to the pilot and unpleasant. Table 3.10 indicates that while, in a dive at $\beta_1 = 0.65$, the aircraft is aperiodically unstable ($\lambda_1 > 0$) and the time of doubling the initial deviation (t_2) amounts to about 10 seconds, the time required for the oscillation amplitude in a state of gliding at $\beta_1 = 0.4$ to lag to half-value already amounts to 113.5 sec.

Thus, in consequence of the relatively rapid deviation of the aircraft from the initial state of flight, its aperiodic instability becomes unacceptable in flight. If however the aircraft has stability, then the quantitative difference of the characteristics of the long-period motion is not a substantial element in the evaluation of the flying qualities of the aircraft.

In contrast to long-period oscillations, the short-period oscillations cannot be directly detected by the pilot as "oscillations". The cause of this, as already stated, is the intense damping of such oscillations. The characteristics of these oscillations, however, are of substantial importance both from the point of view of behavior and stability of the aircraft in flight through a disturbed atmosphere ("bump") and in the execution of various maneuvers. The effect of short-period oscillations in flight through a bump are manifested in the susceptibility of the aircraft to bumps. In executing maneuvers, the characteristics of the short-period oscillations are manifested in the lag with which the aircraft responds to the

POOR ORIGINAL

force applied by the pilot to the stick or control wheel, and in the relation between the magnitudes of these forces or elevator deflections to the aircraft reactions. The latter properties may be combined in the concept of "response of the aircraft to the stick" which will be considered in more detail in Chapter X.

The characteristics of short-period oscillations are of basic and decisive importance for the controllability of the aircraft and its susceptibility to external disturbances. For this reason, we will consider the influence of the basic design and aerodynamic parameters of the aircraft on precisely these characteristics. Considerably less attention will be paid to the long-period oscillations.

Simplified Theory of the Short-Period Motions of an Aircraft

As stated above, during the first stage of disturbed motion, the velocity along the flight path does not undergo marked changes by comparison with the velocity of the initial steady flight condition. For this reason, for the first stage, i.e., for the short-period motion, the velocity increment ΔV may be considered equal to zero. In particular, the example given in Fig. 8.10 shows that, during the first 1.5 sec, the quantity ΔV increased from zero to 0.2 m/sec. At an initial flying speed of 125 m/sec, this amounts to less than 0.2%. At the same time, during the course of 1.5 sec, the short-period motion in this example is almost completely damped.

If we assume $\Delta V = 0$, we may, instead of the complete system of three differential equations of motions, take only two: the equation of the forces along the normal to the flight path and the equation of moments. Taking these two equations in the dimensionless form of system (7.24) of the preceding Chapter and substituting $\Delta V = 0$ in them, we will have

$$\frac{d\Delta\alpha}{dt} - \frac{d\Delta\beta}{dt} - (c_1' + c_{\alpha'}) \Delta\alpha + c_{\beta'} \Delta\beta = 0;$$

$$\frac{c_{\alpha'} \Delta\alpha}{r_1'} - p \frac{m_2'}{r_2'} \Delta\alpha - \frac{m_1'}{r_1'} \frac{d\Delta\alpha}{dt} - \frac{m_2'}{r_2'} \frac{d\Delta\beta}{dt} = 0.$$

POOR ORIGINAL

For further simplification, let us assume that the initial state of flight is one of horizontal flight. For steady horizontal flight, the coefficient C_{Dx} vanishes, as follows from eq.(7.16) of the last Chapter.

For this case, we will have the following two equations:

$$\left. \begin{aligned} \frac{d\Delta v}{dt} - \frac{d\Delta v}{dt} - c_2 \Delta v &= 0; \\ \frac{d^2 \Delta v}{dt^2} - \mu \frac{m_2^2}{r_2^2} \Delta v - \frac{m_2^2}{r_2^2} \frac{d\Delta v}{dt} - \frac{m_2^2}{r_2^2} \frac{d\Delta v}{dt} &= 0. \end{aligned} \right\} \quad (8.16)$$

By determining, from the first of these equations, $\frac{d\Delta v}{dt}$ as a function of Δv and substituting in the second equation (of moments) we finally obtain

$$\frac{d^2 \Delta v}{dt^2} + a_1 \frac{d\Delta v}{dt} + a_2 \Delta v = 0, \quad (8.17)$$

where

$$\left. \begin{aligned} a_1 &= c_2 - \frac{m_1^2 + m_2^2}{r_2^2}; \\ a_2 &= -\frac{\mu m_2^2 + c_2^2 m_1^2}{r_2^2}. \end{aligned} \right\} \quad (8.18)$$

In order to find the solution of the differential equation (8.17), as usual, we put

$$\Delta v = C e^{\lambda t}.$$

After substitution in eq.(8.17), we obtain a characteristic equation of the second degree

$$\lambda^2 + a_1 \lambda + a_2 = 0. \quad (8.19)$$

On comparing eq.(8.18) with the approximate expressions (8.3) for the coefficient of the characteristic equation of the fourth degree, corresponding to the exact solution, we see that the coefficients of a_1 and a_2 in the two cases exactly coincide.

From the latter equation we find



POOR ORIGINAL

$$\lambda_1 = -\frac{a_1}{2} + i\sqrt{a_2 - \frac{a_1^2}{4}}$$

$$\lambda_2 = -\frac{a_1}{2} - i\sqrt{a_2 - \frac{a_1^2}{4}}$$

We note that, formally, eq.(8.19) may be obtained by resolving the general equation of the fourth degree into two quadratic equations in the above-described manner [cf. eq.(8.10)].

If the roots λ_1 and λ_2 are real, then the general solution for $\Delta\alpha$ will have the form

$$\Delta\alpha = C_1 e^{\lambda_1 t} + C_2 e^{\lambda_2 t}.$$

If, however, the roots λ_1 and λ_2 are mutually conjugate complex numbers, as is usually the case in practice, then the general solution may be represented in the form

$$\Delta\alpha = A e^{\nu t} \cos(\omega t + \phi)$$

or in the form

$$\Delta\alpha = A e^{\nu t} \sin(\omega t + \phi).$$

where

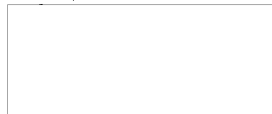
$$\nu = -\frac{a_1}{2}; \quad \omega = \sqrt{a_2 - \frac{a_1^2}{4}}.$$

The constants C_1 , C_2 or A , ν , and ϕ are determined by conventional methods from the assigned initial conditions at the time $t = 0$.

After finding the solution for $\Delta\alpha$, we then determine, from the first equation of the system (8.16), the solution for $\frac{d\Delta\theta}{dt}$:

$$\frac{d\Delta\theta}{dt} = \frac{d\Delta\alpha}{dt} + c_2 \Delta\alpha.$$

We find the variation of the angle of pitch $\Delta\theta$ by integrating the equation:



POOR ORIGINAL

$$\Delta\theta = \int \frac{d\Delta\theta}{dt} dt + \int c_i \Delta\alpha dt + C.$$

Finally, we determine the variation in the angle of inclination of the flight path by the formula

$$\Delta\theta = \Delta\theta - \Delta\alpha.$$

Thus, by using the above simplified theory, the parameters of aircraft motion in the first few moments after action of the disturbance may be determined in a simple manner. These simplified equations and formulas permit ready determination of the influence of the flight conditions (speed, altitude), of the design parameters of the aircraft (specific mass loading, dimensions of the aircraft, relative length of the aircraft, etc) and the influence of longitudinal static stability on the characteristics of the short-period disturbed motion (cf. Chapter X).

An analysis of the influence of the above factors on the characteristics of the long-period disturbed motion is considerably more complicated. As stated above, it is not of substantial practical importance.

The most important parameter that affects the characteristics of dynamic stability during the process of short-period motion as well as during the process of long-period motion, is the degree of static stability of the aircraft. It is precisely by means of varying the degree of static stability, which is directly connected with balancing of the aircraft, that the designer can best influence the dynamic stability and the controllability of the aircraft. Before analyzing the role of static stability, however, it will be advisable to recall the earlier statements as to the influence of the compressibility of air on static stability. In addition, it is useful to subdivide the general concept of static longitudinal into the concepts of static stability with respect to speed and static stability with respect to overload.

STAT

POOR ORIGINAL

Influence of the Compressibility of Air on the
Longitudinal Moment

The variation in the coefficient m_z with any variation in the angle of attack and the lift coefficient C_L depends, in the general case, on the flying speed of the aircraft or on the velocity of the flow at which the aircraft or its model is being tested in the wind tunnel. If we run wind-tunnel tests at various velocities of flow, then in the general case we obtain a family of curves $m_z = f(C_L)$ (Fig.8.11). The Mach number is usually the parameter of this family.

As shown in Fig.8.11, with varying Mach number not only the slope of the curve $m_z = f(C_L)$ varies but also the value of C_L at which the aircraft is balanced with respect to the moment ($m_z = 0$).

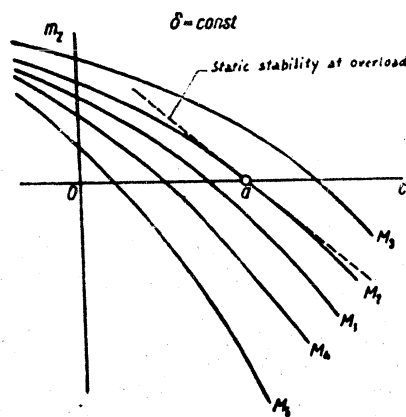
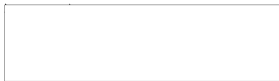


Fig.8.11 - Diagram of Variation of $m_z = f(C_L)$
for Various Mach Numbers



POOR ORIGINAL

Formerly, when flights were made at relatively low Mach numbers (up to $M = 0.6$) and the influence of the compressibility of air was slight, there was no need of making wind-tunnel tests for stability at various rates of flow. The curves $m_z = f(\alpha)$ or $m_z = F(C_L)$, obtained from model wind-tunnel tests of the aircraft at varying rates of flow, coincided with each other.

In evaluating the longitudinal static stability on passing from wind-tunnel tests to actual flight, it must be borne in mind that in flight, any variation in angle of attack or lift coefficient, in the general case, is accompanied by a variation in the Mach number. For example, in various states of steady rectilinear flight at a definite and constant altitude, a definite Mach number will correspond to each value at C_L . The correlation between the Mach number and the coefficient C_L in this case may be found from the solution of the equation of steady rectilinear flight (cf. eq.(7.11) of the last Chapter).

For the case of an unsteady maneuver in the vertical plane by the aircraft, assigned, for example, by the law of variation in overload with time $n = f(t)$, the relation between α and n may be found in the equations of the forces for the unsteady motion of the aircraft.

Static Stability with Respect to Overload
and with Respect to Flying Speed

Depending on the maneuvers performed in flight, C_L and M will vary according to different laws. In other words, in flight, widely varying relations exist between the variation in C_L and the variation in Mach number. It was found useful to segregate the two characteristic extreme cases from this multiplicity of relations. The first case arises when the variation in C_L and the flying speed, and, consequently, the Mach number are correlated with the condition of constant overload

POOR ORIGINAL

$n = 1^*$. The second case arises when C_L varies at constant speed (Mach number), due to the variation in the resultant load factor n . As stated in Chapter V, the former case corresponds to states of steady rectilinear flight at various speeds, while the latter case corresponds to the sudden entry of the aircraft into a rising or falling vertical air current, and likewise to the initial motion of the aircraft in executing maneuvers involving a sharp increase in overload when the flying speed may, in practice, be considered constant. In accordance with this, it has been found expedient to subdivide the concept of longitudinal static stability of aircraft into static stability^{**} with respect to flying speed and static stability with respect to overload.

Next we will give the physical interpretations of these concepts, starting from the curve m_z (Fig. 8.11). Let us agree to consider the above two forms of static stability under the condition that, in both cases, the initial state of motion of the aircraft must be rectilinear steady flight.

Let in Fig. 8.11, the Mach number and the value $(C_L)_a$, both determined by the point of intersection of the curve m_z at $M_2 = \text{const}$, with the abscissa, correspond to this state of flight. The lift $(Y)_a = (C_L)_a Cq$, corresponding to the state of flight "a", is approximately equal to the weight of the aircraft, and the load factor is equal to unity. Let us assume that the pilot executes a sharp maneuver, at the beginning of which the velocity along the flight path remains practically con-

* From the point of view of strictness of the subsequent reasoning, we must understand the load factor n to mean the ratio of the resultant of the aerodynamic horizontal flight, when the thrust $P \approx Q$ and $n = Y/G = 1$. For any other state of rectilinear steady flight, the load factor n is likewise equal to unity, since in this case R is always equal to G . In practice the limit load factor is often determined approximately as the ratio of the lift to the weight of the aircraft ($n = Y/G$).

** Hereafter we must be aware that the term "static stability" is a conventional one, as was pointed out in the introduction to this book.

POOR ORIGINAL

stant, and only the angle of attack varies. Accordingly, the variation of moments, due to the variation in angle of attack and in coefficient C_L will be characterized by the curve m_z , at $M = M_2$. Due to the variation in C_L , the lift and load factor will also vary.

The degree of variation of the coefficient m_z with any variation in C_L , under the condition that $M = \text{const}$, will be characterized by the derivative

$$\frac{dm_z}{dC_L} = m_z^c.$$

As already pointed out, in flight such a variation in C_L will correspond to the stage of maneuvers at which the load factor of the aircraft varies, while the ve-

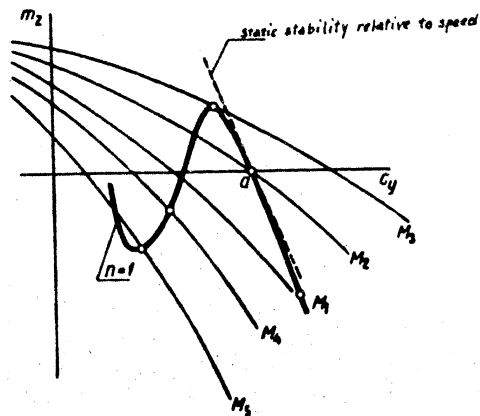


Fig.8.12 - Curves Characterizing the Variation in m_z with $M = \text{const}$ and $n = 1 = \text{const}$, Corresponding to the Concepts of Static Longitudinal Stability with Respect to Overload and with Respect to Flying Speed

locities and Mach number remain practically the same. For this reason, we agreed in Chapter V to denote the derivative $m_z^{C_L}$, used for the initial state of equilibrium,

POOR ORIGINAL

as the coefficient of static longitudinal stability with respect to overload.

Let us assume that the aircraft changes from the initial state of steady rectilinear flight to another state, again being steady and rectilinear. In such a transition, of course, the speed, angle of attack, and coefficient C_L will vary, but the load factor n will remain constant. As already pointed out, the variation in C_L and M in this case is found by solving the equations of steady flight [cf. eq.(7.11)] in Chapter VII. Having the relation between C_L and M for such states of rectilinear flight, let us determine from the diagram in Fig.8.12, for the values of M_1, M_3, M_4 , etc; the corresponding values of C_{L1}, C_{L3}, C_{L4} , etc. Through the points corresponding to each individual pair of values $M_1, C_{L1}; M_3, C_{L3}$ (cf. Fig.8.12) let us draw a curve. The load factor $n = 1$ will correspond to all points of this curve.

The total derivative of m_z with respect to C_L , determined in the state of aircraft balancing "a" ($m_z = 0$) under the condition $n = 1$ (the heavy line in Fig.8.12), i.e., at a change in flying speed and a constant load factor, is called the coefficients of static longitudinal aircraft stability with respect to velocity, and

denoted by $\frac{dm_z}{dC_L}$:

$$\frac{dm_z}{dC_L} = \frac{\partial m_z}{\partial C_L} + \frac{\partial m_z}{\partial M} \left(\frac{dM}{dC_L} \right)_{n=1}$$

Thus, the coefficient of static stability with respect to overload is characterized by a variation in the coefficient of longitudinal moment, as a function of the parameter C_L (or angle of attack) alone, under the condition that $V = \text{const}$ ($M = \text{const}$), while the coefficient of stability with respect to speed is characterized as a function of the parameter C_L and the parameter M , the variations in C_L and M in this case being rigidly connected with the condition $n = 1$.

For determining the coefficients of stability with respect to speed and overload at other initial states of flight, the curves m_z (cf. Fig.8.11) should be taken at another position of the elevator and a state of balance corresponding to

POOR ORIGINAL

the ratio of C_L and M under conditions of rectilinear steady flight, after which the operations described above must be repeated.

The Role and Place of Static Stability in the Dynamic

Stability of the Aircraft

A study of the coefficients a_1 and a_2 of the characteristic equation (eq.8.3 and eq.7.36) which define the decay and period of the short-period oscillation of the aircraft, shows that the coefficient a_1 does not depend on the degree of static stability, while the coefficient a_2 does depend on it linearly. According to the approximate formulas of eq.(8.3), we have

$$\left. \begin{aligned} a_1 &= c_1 - \frac{1}{T_2^2} (m_1^2 + m_2^2); \\ a_2 &= -\frac{1}{T_2^2} (\mu m_1^2 + c_1^2 m_2^2). \end{aligned} \right\}$$

The quantity m_2^a represents the coefficient of static stability with respect to overload since, as follows from Chapter VII, the derivative m_2^a is taken under the condition $K = \text{const}$.

In the expression for a_2 , instead of m_2^a it is easy to introduce the generally adopted coefficient of stability with respect to overload. In fact,

$$m_2^a = \frac{\partial m_2}{\partial x_1} = \frac{\partial m_2}{\partial x} \frac{\partial x}{\partial x_1} = \frac{m_1^2}{c_1^2},$$

and then

$$a_2 = -\frac{c_1^2}{T_2^2} (\mu m_1^2 + m_2^2). \quad (2.20)$$

The roots of the characteristic equation for short-period disturbed motions, as we know, are determined from the expression

$$\lambda_{1,2} = -\frac{a_1}{2} \pm \sqrt{\frac{a_1^2}{4} - a_2}. \quad (2.21)$$

POOR ORIGINAL

On analyzing the influence of the degree of static stability on the dynamic stability of an aircraft in the process of short-period motion, two cases must be considered.

The first case corresponds to the values

$$a_1 > \frac{a_2}{4}$$

i.e., to the case of the imaginary root

$$\sqrt{\frac{a_2}{4} - a_1}$$

In this case, as follows from eq.(8.3), the variation in static stability has no influence on the coefficient of damping of the short-period oscillations $h = -\frac{a_1}{2}$, but affects only the period of these oscillations, which is equal to

$$T = \frac{2}{\sqrt{\frac{a_2}{4} - a_1}} \quad (8.23)$$

With increasing static stability, the coefficient a_2 increases, so that the period of short-period oscillations diminishes.

The second case corresponds to the condition

$$\frac{a_2^2}{4} > a_1 > 0 \quad (8.24)$$

In this case, the short-period disturbed motion is no longer oscillatory but consists of two mutually superposed aperiodic damped motions. In the given region, the variations of static stability already affect the damping of the short-period motion; the damping of one of the partial aperiodic motions increases with increasing static stability while that of the second decreases*.

* The term short-period motion is not an entirely fortunate choice, since this motion is not always oscillatory. But this term is generally accepted and will, therefore, be used in the following.

POOR ORIGINAL

Accordingly, an aircraft will be dynamically stable in short-period motion even when there is a definite static instability with respect to overload; the maximum static instability here is determined by the condition

$$a_2 < -a_1.$$

Formally, it would be possible to consider still another case, corresponding to the condition

$$a_2 < 0 \quad (8.25)$$

Detailed analysis shows, however, that at small values of a_2 , it already is impossible to neglect the variation of $\Delta \bar{V}$, so that the resolution of the motion into two motions, a short-period and a long-period, becomes inaccurate.

This case can be considered only on the basis of the total equations of motion and of the characteristic equation of the fourth degree.

Since the coefficient $\frac{da_2}{dU}$ does not enter into eq.(8.3) for a_1 and a_2 , this is evidence that the static stability with respect to speed exerts practically no influence on the short-period disturbed motion.

Let us then analyze the influence of static stability on the long-period disturbed motion. This analysis will be performed by means of the approximate formulas for the coefficients of the quadratic characteristic equation defining that motion.

According to eq.(8.10), this equation can be represented in the form

$$\lambda^2 + b_1 \lambda + b_2 = 0 \quad (8.26)$$

where

$$b_2 = \frac{a_1 a_2 - a_1 a_3}{a_1^2}; \quad (8.27)$$

$$b_1 = \frac{a_2}{a_1}.$$

STAT

POOR ORIGINAL

The roots of the characteristic equation for the long-period motion will be defined by the expression

$$\lambda_{1,2} = -\frac{b_1}{2} \pm \sqrt{\frac{b_1^2}{4} - b_2}$$

Formally, the coefficients b_1 and b_2 in this case play the same role as the coefficients a_1 and a_2 in the characteristic equation of the short-period disturbed motion.

As mentioned above, the difference in the degree of damping of long-period disturbed motion, provided that this motion is unstable and oscillatory, exerts no substantial influence on the flying qualities of the aircraft. For this reason, the coefficient b_1 , defining this damping, will be disregarded in this analysis. We will consider only the coefficient b_2 , defining the transition (unpleasant for the pilot) to unstable aperiodic motion.

Let us further simplify the problem by considering only the sign of the coefficient of b_2 and its connection with the static stability of the aircraft. As will be demonstrated above, the boundary of the transition of the aircraft into the region of unstable aperiodic motion will be defined by the condition

$$b_2 = 0 \quad (8.28)$$

To adapt the calculation to the actual characteristics of the aircraft, which, as a rule, exhibit static stability with respect to overload, it will be assumed in the further analysis that the coefficient a_2 is a positive quantity. Then, the sign of the quantity b_2 will be determined from the sign of the coefficient of a_4 , while the condition (8.28) may be replaced by the condition

$$a_4 = 0 \quad (8.29)$$

In this case the statements made for the case of small values of a_2 must be taken into consideration.

POOR ORIGINAL

We will demonstrate next that the quantity a_4 is directly proportional to the coefficient of longitudinal static stability with respect to speed.

For the conditions of various steady states of rectilinear flight, the coefficients of longitudinal moment on the diagrams of the type shown in Fig.8.2 will be a function of two parameters, the coefficient C_L and the correlated Mach number or the angle of attack α and the Mach number. Let us take the derivative of the function

$$M_z = f(\alpha, M)$$

with respect to the angle of attack; obviously

$$\frac{dM_z}{d\alpha} = \frac{dM_z}{d\alpha} + \frac{dM_z}{dM} \frac{dM}{d\alpha} \tag{8.29}$$

The derivative $\frac{dM}{d\alpha}$ can be determined from the equation of steady rectilinear flight.

Starting from eq.(7.11) of the preceding Chapter, we write

$$\left. \begin{aligned} \frac{c_{D0} \rho^2 M^5}{2} &= -G \sin \theta \\ \frac{c_L \rho^2 M^5}{2} &= G \cos \theta. \end{aligned} \right\} \tag{8.31}$$

where a is the velocity of propagation of sound in air.

By differentiating eq.(8.31), we obtain

$$\begin{aligned} c_{D0}' \frac{\rho^2 M^5}{2} d\alpha + c_{D0}^n \frac{\rho^2 M^5}{2} dM + c_{D0} \rho^2 M^5 dM &= -G \cos \theta d\theta \\ c_L' \frac{\rho^2 M^5}{2} d\alpha + c_L^n \frac{\rho^2 M^5}{2} dM + c_L \rho^2 M^5 dM &= -G \sin \theta d\theta. \end{aligned}$$

On dividing both sides of the latter equations by $\frac{\rho a^2 M^2}{2}$, using the notation of eqs.(8.4) and (8.31), we have



POOR ORIGINAL

$$c_{D_0} \dot{M} + b_1 \frac{2v_0 c}{M} \dot{M} = -c_1 \dot{M}$$

$$c_2 \dot{M} + b_2 \frac{2v_0 c}{M} \dot{M} = c_0 \dot{M}$$

On eliminating the quantity \dot{M} from these last two equations, we obtain finally the following expression for $\frac{dM}{dt}$:

$$\frac{dM}{dt} = -\frac{c_0 c_1 c_0 + c_1 c_2}{b_1 c_0 c_1 + b_2 c_2} M \quad (8.33)$$

On substituting in eq.(8.30), we get

$$\frac{dm_2}{dt} = m_2 \left[-\frac{M}{2} \frac{c_0 c_1 c_0 + c_1 c_2}{b_1 c_0 c_1 + b_2 c_2} - m_1 \right] \quad (8.33)$$

The value of the coefficient of static stability with respect to speed is connected with the derivative $\frac{dm_2}{d}$ by the relation:

$$\frac{dm_2}{d} = \frac{dm_2}{dM} \cdot \frac{dM}{d} \quad (8.34)$$

Taking eq.(8.3) for the coefficient of a_4 it is not difficult to obtain

$$a_4 = -\frac{2v_0}{f_1} (b_1 c_0 c_1 + b_2 c_2) \left[m_1 - \frac{M}{2} \frac{c_0 c_1 c_0 + c_1 c_2}{b_1 c_0 c_1 + b_2 c_2} m_2 \right]$$

From this, taking account of eqs.(8.33) and (8.34), we finally have

$$a_4 = -\frac{2v_0}{f_1} \frac{dM}{d} (b_1 c_0 c_1 + b_2 c_2) \frac{dm_2}{dM} \quad (8.35)$$

Let us consider the influence of static stability with respect to speed on the dynamic stability of an aircraft, first at states of flight where the influence of compressibility on the coefficients C_D and C_L may be disregarded.



POOR ORIGINAL

In this case, the coefficient k_1 and k_2 will be equal:

$$k_1 = k_2 = 1$$

The quantity $\frac{dC_L}{d\alpha}$ will be equal to the quantity $\frac{C_L}{\alpha}$, which we will abbreviate as C_L^2 . As is well known, in the region of angles of attack less than the angle corresponding to C_{Lmax} , we have

$$C_L^2 > 0$$

Then the quantity a_4 can be represented by the expression

$$a_4 = -A^2 \frac{dm_z}{dC_L} \quad (8.36)$$

with the coefficient A^2 being a quantity of positive sign. Thus, in the field where the influence of the compressibility of the air on the coefficients C_D and C_L may be neglected, one of the conditions for dynamic stability, namely

$$a_4 > 0$$

is equivalent to the condition of the presence of static stability with respect to speed ($\frac{dm_z}{dC_L} < 0$).

In the region where the influence of compressibility on the coefficients C_D and C_L cannot be disregarded, it is impossible to make so definite a conclusion as to the relation between the coefficients a_4 and $\frac{dm_z}{dC_L}$, and an additional analysis is necessary.

Bearing in mind eq.(8.32), we obtain

$$\frac{da_4}{dC_L} = -A^2 \frac{d}{dC_L} \left(\frac{dm_z}{dC_L} \right) \quad (8.37)$$

On substituting the resultant eq.(8.37), in eq.(8.35), we have

POOR ORIGINAL

$$a_4 = -\frac{2\pi}{\rho_i} \frac{dm_i}{dx_i} \left[c_i (k_1 c_o^2 + k_2 c_i^2) - c_o^2 \frac{M}{2} (c_o c_o^2 + c_i c_i^2) \right].$$

On transforming this expression, replacing k_1 and k_2 by their expressions according to eq.(8.24), we get

$$k_1 = 1 + \frac{c_o^2 M}{2\alpha c};$$

$$k_2 = 1 + \frac{c_i^2 M}{2\alpha c}.$$

After simple transformations we obtain

$$a_4 = -\frac{2\pi}{\rho_i} \frac{dm_i}{dx_i} \left[c_i (c_i^2 + c_o^2) - c_o c \frac{M}{2} (c_i^2 c_o - c_o^2 c_i) \right]. \quad (8.38)$$

In absence of the influence of compressibility ($C_D^M = C_L^M = 0$) the subtrahend in the brackets vanishes, and eq.(8.38) takes the following form:

$$a_4 = -\frac{2\pi}{\rho_i} \frac{dm_i}{dx_i} c_i (c_i^2 + c_o^2) = -A^2 \frac{dm_i}{dx_i},$$

as mentioned above.

In presence of the influence of the compressibility of the air on the aerodynamic characteristics of the aircraft ($C_D^M \neq 0, C_L^M \neq 0$), then in the general case the subtrahend in the brackets of eq.(8.38) vanishes. The difference

$$D = c_i (c_i^2 + c_o^2) - c_o c \frac{M}{2} (c_i^2 c_o - c_o^2 c_i)$$

as a rule, may be either positive or negative, depending on the ratio of the values of the individual terms entering into them.

To satisfy the condition $a_4 > 0$, which is necessary to secure stability, it is now necessary to satisfy the inequality

$$\frac{dm_i}{dC_L} D < 0$$



POOR ORIGINAL

If (for example) in any special case, $D < 0$, then the following condition must be satisfied to secure stability

$$\frac{dm_z}{dC_L} > 0$$

The limiting case of the neutral aircraft corresponds to the equation

$$a_4 = 0$$

This equality is possible, if

$$1) \quad \frac{dm_z}{dC_L} = 0$$

i.e., if, as in the absence of the influence of compressibility, the coefficient of stability with respect to speed vanishes, or if

$$2) \quad D = c_x(c_x^2 + c_y^2) - c_z \left[\frac{M}{2} (c_x^2 c_z - c_y^2 c_z^2) \right] = 0. \quad (8.39)$$

In the special case of horizontal flight, we have

$$C_{Dc} = 0$$

so that eq.(8.39) cannot be satisfied since

$$C_L^2 > 0, \quad C_L^2 + C_{Dc}^2 > \text{ and } D > 0$$

will always be true. Consequently, in horizontal flight the condition of stability of an aircraft, if the compressibility has any influence, will have the same form as in the absence of that influence:

$$\frac{dm_z}{dC_L} < 0$$

If the flight path of the aircraft is not horizontal (gliding, gaining altitude), then $C_{Dc} \neq 0$ with eq.(8.39) is possible. In this case, as follows from eq.(8.39), we have



POOR ORIGINAL

$$c_{Dc} = \frac{c_L^2 (c_L^2 + c_{Dc}^2)}{c_L^2 c_{Dc} - c_L^2 c_{Dc}^2} \frac{1}{M}$$

If $C_L^M > 0$ (for example, at subcritical Mach numbers), and C_D^M is small, then the equality $D = 0$ might theoretically be obtained during gliding, since in this case $C_{Dc} > 0$. In the case $C_L^M < 0$ (at Mach numbers above critical), C_{Dc} becomes negative, which corresponds to gaining altitude. In the general case, this means that the negative sign of the coefficient of static stability with respect to velocity, $\frac{dm_z}{dC_L}$, is not a necessary condition for the dynamic stability of the aircraft.

In such a case, however, the derivative $\frac{dm_z}{dC_L}$ loses its physical meaning, so that it is more correct to consider the derivative $\frac{dm_z}{dM}$.

Now, by means of the expression

$$\frac{dc_L}{dM} = c_L^M + c_L^c \frac{dc_L}{dM}$$

and of eqs.(8.32) and (8.34), eq.(8.38) can be put into the form

$$a_4 = \frac{r}{r^2} (c_{Dc} c_{Dc}^c + c_L c_L^c) M \frac{dm_z}{dc_L} \frac{dc_L}{dM} = \frac{r}{r^2} (c_{Dc} c_{Dc}^c + c_L c_L^c) M \frac{dm_z}{dM} \quad (8.38')$$

The equality $a_4 = 0$ may be obtained only if one of the following two conditions is satisfied:

- 1) $c_{Dc} c_{Dc}^c + c_L c_L^c = 0;$
- 2) $\frac{dm_z}{dM} = 0.$

The former condition cannot be satisfied in practice for an aircraft, since in this case we would have

$$c_{Dc} c_{Dc}^c = -c_L \frac{c_L^c}{c_{Dc}^c},$$

while the expression



POOR ORIGINAL

$$c_o = c_{o0} + \frac{c_i^2}{2\lambda}$$

yields

$$c_o = \frac{2\lambda}{\lambda} c_i; \quad \frac{c_i^2}{c_o} = \frac{\lambda}{2c_i}$$

so that

$$c_{o0} = -\frac{\lambda}{2}$$

According to eq.(8.4) we have

$$-\frac{\lambda}{2} = c_o - \frac{P}{Q} c_i$$

whence

$$\frac{P}{Q} = \frac{c_o + \frac{\lambda}{2}}{c_i}$$

For the values of C_D , C_L , and λ met in practice, the values of the thrust necessary to satisfy the first condition are many times greater than the weight of the aircraft, a fact that does not occur in aviation.

Thus in practice the sum $C_{Dc} c_D^2 + C_L c_L^2$ is always positive, and the only condition of stability is that of

$$\frac{dm_z}{dH} > 0$$

In other words it is necessary for the stability of the aircraft that, at increasing Mach numbers (or flying speed) a moment causing the aircraft to climb will arise.

On comparing eqs.(8.38) and (8.38'), we conclude that

POOR ORIGINAL

$$D = -\frac{M}{2} (c_0 c_0' + c_1 c_1') \frac{dc_L}{dM}$$

Consequently, the condition $D = 0$ is equivalent to the condition $\frac{dc_L}{dM} = 0$, and at the same time to the condition $a_4 = 0$. But since, according to eq.(8.38'), the equality $a_4 = 0$ can be true only if $\frac{dm_2}{dM} = 0$, it follows that

$$\frac{dm_2}{dc_L} = \frac{\frac{dm_2}{dM}}{\frac{dc_L}{dM}} = \frac{0}{0}$$

Thus in the case under consideration, the coefficient $\frac{dm_2}{dc_L}$ becomes indeterminate and loses its physical meaning, while $\frac{dm_2}{dM}$ has a definite value and a definite meaning.

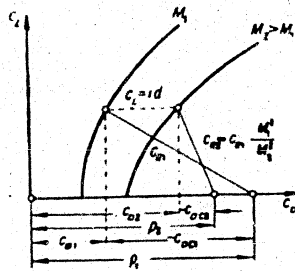


Fig.8.13 - Geometric Interpretation of the Case $\frac{dC_L}{dM} = 0$

The case $\frac{dC_L}{dM} = 0$ is geometrically interpreted by Fig.8.13. It follows from eq.(8.31) that

$$\sqrt{c_0^2 + c_1^2 M^2} = \frac{20}{M^2} = \text{const.}$$

POOR ORIGINAL

According to eq.(7.17), we have

$$C_{Dx} = C_D - P_x$$

When the Mach number increases from M_1 to M_2 , the vector $c_R = c_{Dc}^2 + c_L^2$ decreases in the ratio $\frac{M_1^2}{M_2^2}$; at the same time, C_{Dc2} strongly decreases, while C_L remains unchanged, so that $\frac{dC_L}{dM} = 0$, as will be seen from Fig.8.13.

POOR ORIGINAL0
2
4
6
8
10
12
14
16
18
20
22
24
26
28
30
32
34
36
38
40
42
44
46
48
50
52
54
56
58

CHAPTER IX

STABILITY, CONTROLLABILITY, AND MANEUVERABILITY OF AIRCRAFT

Elements of Maneuvers Performed in Flight

In order to distinguish the most characteristic of the numerous maneuvers performed by aircraft, let us consider a few instrument records made during the flight by one of our trainers. Figure 9.1 shows the records of variation in flying speed, overload with respect to the normal axis of the aircraft, angles of elevator deflection with time, at the beginning of a simulated aerial combat for training purposes. The records correspond to the interval of time during which, after receipt of the signal for starting the aerial combat, the pilot performed the so-called tactical maneuver* to intercept the "enemy" and to gain altitude. Within 1.5 to 2 sec. after starting the tactical maneuver, the aircraft attained the maximum load factor $n = 5.6$, which then diminished relatively smoothly to $n = 3.3$ in the 15th second, when gaining altitude had been completed and the pilot had brought the aircraft into a horizontal turn.

Figure 9.2 shows the part of the record on focusing and "aiming" the camera gun at the "enemy". In this case the aircraft executed a curvilinear flight (turn) almost in a horizontal plane. A characteristic feature are the oscillatory motions of the control surfaces and the fluctuations in the overload particularly during the maneuver for a rapid 180° change in direction of flight, at a simultaneous gain in altitude, is called a tactical maneuver.

POOR ORIGINAL

0 first stage of this motion (while aiming).

2 Figure 9.3 shows the instrument records during the relatively sharp transition
 4 from the glide at an initial indicated speed of 425 km/hr. Besides the records of
 6

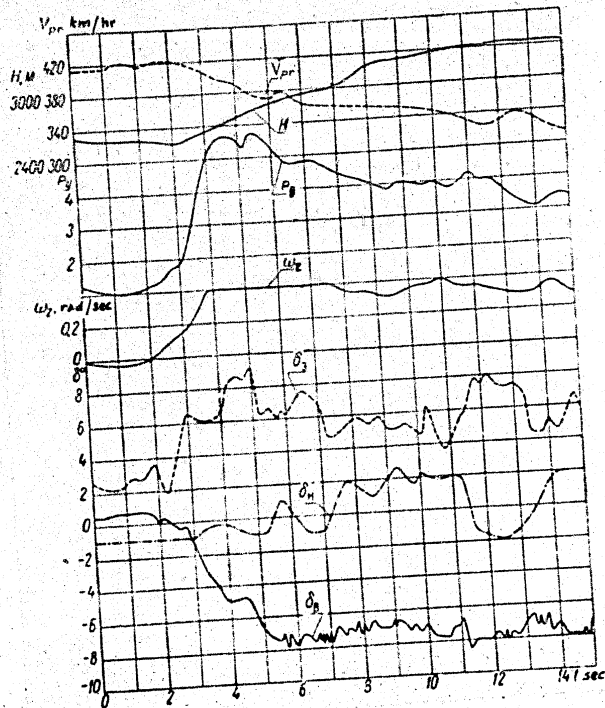


Fig.9.1 - Parameters of Aircraft Motion at the Beginning of
 an Aerial Training Combat between Two Fighter Planes (Example)

the elevator deflection, this diagram also shows a record of the stick force.

52 Figure 9.4 gives the instrument records on landing. Here again, oscillatory
 54 motions of the elevator and corresponding oscillations of the stick force
 56

POOR ORIGINAL

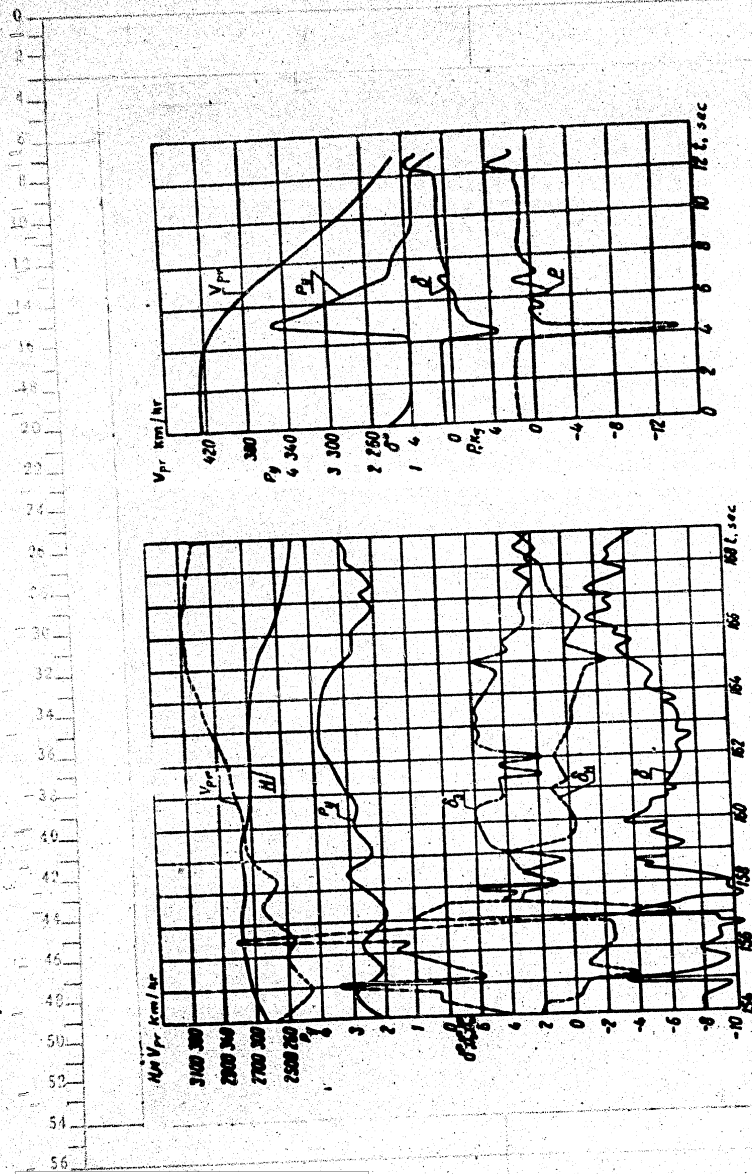


Fig. 9.3 - Instrument Records when Aircraft is Pulling Sharply out of a Dive

Fig. 9.2 - Parameters of Aircraft Motion during Aiming and "Firing" of a Camera Gun in a Training Aerial Combat between Two Fighter Planes (Example)

POOR ORIGINAL

occur*. These oscillations take place with respect to certain mean lines characterizing the deflection on the elevator "upward" and a certain increase of the stick

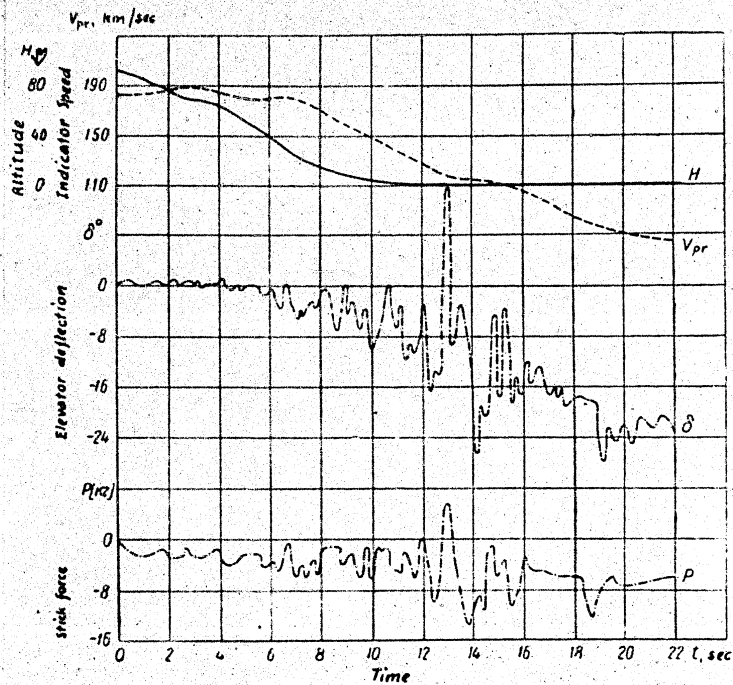


Fig.9.4 - Instrument Records during Landing

* These oscillatory elevator motions of small amplitude can, to a certain extent, be explained by the violent vibration of the aircraft and by the deflections of the elevator due to rough weather (in flight through a bump). However, as shown by the example of high-amplitude elevator motions, during landing the pilot may actually make rather sharp motions of the stick with a frequency of the order of two cycles per second, i.e., with a period of about 0.5 sec for the oscillatory motions.

POOR ORIGINAL

force in the direction "towards the pilot".

For an analysis of the longitudinal controllability of the aircraft (its capacity to "follow the stick") let us chematize this phenomenon and take, as the

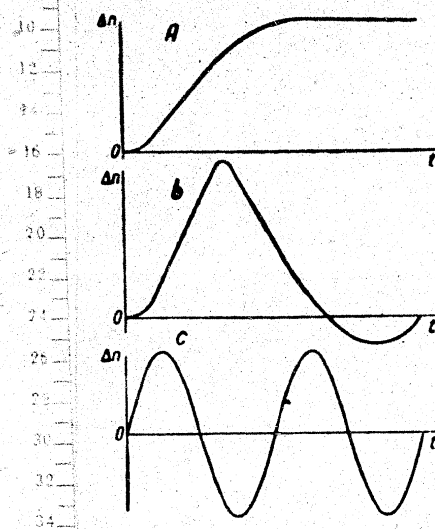


Fig.9.5 - Variation in Overload during Three Characteristic Types of Maneuvers

a - Leaving an assigned overload;
 b - Rapid change in overload; c - Vibrations of aircraft, produced by pilot

of the force applied to the stick in performing these elementary maneuvers as a function of the degree of longitudinal static stability with respect to overload

most characteristic, the three maneuver elements shown in Fig.9.5. Let maneuver element A be the removal of the aircraft from an assigned overload; maneuver element B, the rapid variation in overload; and maneuver element C, the small vibrations of the aircraft produced by the pilot. In considering the controllability, we will assume approximately that the flying speed during these maneuvers remains constant ($V = C$) since, for these three types of maneuver, it is the variation in overload rather than the variation in speed that is of primary importance.

These three maneuver elements must be supplemented by a fourth one, the smooth variation in flying speed at practically constant load factor.

In analyzing the controllability of aircraft we will consider the deflection of the stick in time and the variation

POOR ORIGINAL

and at various combinations of other design parameters.

Angle of Elevator Deflection during Maneuver

For simplicity of the following calculations, we assume that, before the beginning of the maneuver, the aircraft was in a horizontal steady flight. Desiring to execute a maneuver, the pilot changes the elevator setting, deflecting it through the additional angle $\Delta\delta$. As a consequence, an angular acceleration appears, together with a variation of all the parameters of motion. Using the method of small perturbations, as before, the equation of moments in disturbed motion may be represented in the following form:

$$I_z \frac{d^2 \Delta\delta}{dt^2} - M_z^{\delta} \Delta c_i - M_z^V \Delta V - M_z^{\omega} \frac{d\Delta\theta}{dt} - M_z^{\dot{\omega}} \frac{d\Delta\dot{\omega}}{dt} = M_z^{\delta} \Delta\delta. \quad (9.1)$$

where M_z^L , M_z^V , M_z^{ω} , $M_z^{\dot{\omega}}$, M_z^{δ} are the partial derivatives of the aerodynamic moment, taken with respect to the corresponding parameters.

To perform the subsequent analysis it is convenient to use dimensionless quantities, for which purpose we introduce as before the concepts of the relative density $\rho = \frac{2m}{\rho S b_A}$, the time ratio $\tau = \frac{2m}{\rho S V}$, and the dimensionless radius of inertia $\bar{r}^2 = \frac{I_z}{m b_A^2}$. Using these symbols, and dividing both sides of eq.(9.1) by $\frac{\rho^2 S^2 V^2}{4m}$ we will have, after simplification,

$$\frac{\bar{r}^2 d^2 \Delta\delta}{\tau^2} - \frac{\rho M_z^{\delta}}{\tau^2} \Delta c_i - \frac{\rho M_z^V}{\tau^2} M \Delta V - \frac{\rho M_z^{\omega}}{\tau^2} \frac{d\Delta\theta}{dt} - \frac{\rho M_z^{\dot{\omega}}}{\tau^2} \frac{d\Delta\dot{\omega}}{dt} = \frac{\rho M_z^{\delta}}{\tau^2} \Delta\delta.$$

From this we determine the necessary angle of deflection of the elevator, and find it to be

$$\Delta\delta = \frac{1}{\bar{r}^2} \left(\frac{\tau^2 \rho \Delta\theta}{\rho} - \rho M_z^{\delta} \Delta c_i - \rho M_z^V M \Delta V - \frac{\rho M_z^{\omega}}{\tau} \frac{d\Delta\theta}{dt} - \frac{\rho M_z^{\dot{\omega}}}{\tau} \frac{d\Delta\dot{\omega}}{dt} \right). \quad (9.2)$$

POOR ORIGINAL

Obviously, the magnitude of the elevator deflection required for the maneuver at each instant of time will be determined by the moment of inertia $\left(\frac{I_x}{\mu} \frac{d^2 \Delta \theta}{dt^2}\right)$ of the moment connected with the static stability $(m_z^L \Delta C_L + m_z^M M \Delta \bar{V})$, the damping moment $\left(\frac{m_z^W}{\mu} \frac{d \Delta \theta}{dt}\right)$, and the moment due to the lag of the downwash $\left(\frac{m_z^a}{\mu} \frac{d \Delta \alpha}{dt}\right)$.

Thus, if we know the characteristics of the aircraft and assign a definite maneuver, we may determine the deflection of the elevator or stick necessary to perform this maneuver, as a function of time.

To define any maneuver, it is sufficient to assign the law of variation with time of one of the parameters of aircraft motion. According to our earlier discussion, we have three independent differential equations of motion: one equation of moments and two equations of forces. These three equations contain the four variables

3a, 3V, 30 and 32

It is therefore sufficient to assign one of these variables in the form of a definite function of time in order to determine the remaining variables.

Relation between the Variation in Angle of Attack, Angular Velocity, and Angular Acceleration of the Aircraft, with any Variation in Speed and Overload

If, in eqs.(9.1) and (9.2), the increment C_L is expressed as a function of the increments of the angle of attack and the Mach number, then it will become obvious that the elevator deflection, in executing the maneuver, is connected with a change in the three parameters of the plane aircraft motion; the flying speed, the angle of attack, and the angular velocity of pitching, and with their derivatives with respect to time. It is more convenient to replace these three parameters by the following two: flying speed and overload. Mathematically, the transition from the former three variables to the latter two is performed by the transition of the equations of aircraft motion.

POOR ORIGINAL

The selection of speed and overload as the principal parameters is the most convenient. When using these parameters, it is considerably simpler to compare the results of theoretical studies and calculations with the results of flight tests. In flight, the pilot distinctly and directly feels the changes in speed and overload, while the variations in angle of attack are not noted directly by the pilot. The pilot usually relates his reports on the behavior of the aircraft in the air to overload and flying speed.

Structural stress analysis of the aircraft is also based on flying speed and load conditions. The problems of stability and controllability are also related to questions of structural strength, and to the conditions for flight safety. Finally, the choice of the speed and overload as the variables is also advantageous in connection with the fact that these quantities during flight can be readily registered by means of speed and overload recorders.

Let us express the quantities $\frac{d\Delta\theta}{dt}$, $\frac{d^2\Delta\theta}{dt^2}$, ΔC_L and $\frac{d\Delta\alpha}{dt}$, which enters the equation in terms of the velocity increment ΔV and load increment Δn , and of their derivatives with respect to time.

Let us represent the lift of the aircraft in the form $Y = C_L S \frac{\rho V^2}{2} \approx nG$ and let us assume that the coefficient of lift C_L and the velocity V vary by ΔC_L and ΔV , respectively. Then, taking ΔC_L and ΔV as small quantities, neglecting terms of the second order of smallness, remembering that, by hypothesis, $n = 1$ in the initial state of flight, and putting $\Delta \bar{V} = \frac{\Delta V}{V}$, we have

$$\begin{aligned}
 n = 1 + \Delta n &= \frac{1}{G} \left(c_L S \frac{\rho V^2}{2} + \Delta c_L S \frac{\rho V^2}{2} + c_L S \rho V \Delta V \right) = \\
 &= 1 + \frac{\Delta c_L}{c_L} + 2\Delta \bar{V}, \text{ neglecting:} \\
 \Delta c_L &= c_L (2\Delta \bar{V}),
 \end{aligned} \tag{9.3}$$

Let us now determine the value of the variation in the angle of attack during the maneuver $\Delta\alpha$. In the general case, $C_L = C_L(\alpha, M)$ and obviously

POOR ORIGINAL

$$\frac{dc_l}{da} = \frac{dc_l}{da} + \frac{dc_l}{dM} \frac{dM}{da} = c_l^* + c_l^* \frac{dM}{da} \frac{dc_l}{dc_l}$$

whence

$$\frac{dc_l}{da} = \frac{c_l^*}{1 - c_l^* \frac{dM}{da}} = \frac{c_l^*}{1 - c_l^* \frac{\Delta M}{\Delta c_l}}$$

It is obvious that the change of the angle of attack is equal to

$$\Delta \alpha = \frac{\Delta c_l}{dc_l} = \frac{\Delta c_l}{c_l^*} \left(1 - c_l^* \frac{\Delta M}{\Delta c_l} \right) = \frac{1}{c_l^*} (\Delta c_l - c_l^* \Delta M)$$

On substituting in this equation the expression for Δc_l by eq.(9.3) and noting that

$$\Delta M = \frac{\Delta V}{a} = \frac{\Delta V}{V} M = \Delta \bar{V} M,$$

we get

$$\Delta \alpha = \frac{1}{c_l^*} [c_l (\Delta \alpha - 2\Delta \bar{V}) - c_l^* M \Delta \bar{V}] = \frac{c_l}{a} (\Delta \alpha - 2k_2 \Delta \bar{V}), \quad (9.4)$$

in which

$$a = c_l^* \text{ AND } k_2 = 1 + c_l^* \frac{M}{2c_l}$$

k_2 being the coefficient encountered in Chapter VII.

In this way, we have expressed the change in the angle of attack in terms of the change of flying speed and in overload.

Taking the derivative of eq.(9.4) with respect to the dimensionless time \bar{t}

we obtain

$$\frac{d\Delta \alpha}{d\bar{t}} = \frac{c_l}{a} \left(\frac{d\Delta \alpha}{d\bar{t}} - 2k_2 \frac{d\Delta \bar{V}}{d\bar{t}} \right). \quad (9.5)$$

POOR ORIGINAL

Let us further express the angular velocity Δn and ΔV in terms of $\omega_z = \frac{d\Delta\theta}{dt}$

$$\frac{d\Delta\theta}{dt} = \frac{d\Delta n}{dt} + \frac{d\Delta\alpha}{dt}.$$

From the equation of equilibrium of the projections of the forces onto the normal to the flight path, we have

$$mV \frac{d\Delta\theta}{dt} = Y - G \cos \theta \approx G(n-1) = G\Delta n,$$

since the angle θ , by hypothesis, is assumed to be small, and $\cos \theta = 1$. By using the dimensionless time $\bar{t} = \frac{t}{\tau} = \frac{\rho S V}{2m} t$, we find

$$\frac{d\Delta n}{d\bar{t}} = \frac{\gamma G}{\rho S V^2} \Delta n = c_1 \Delta n.$$

Thus

$$\frac{d\Delta\theta}{d\bar{t}} = \frac{c_1}{a} \left(\frac{d\Delta n}{d\bar{t}} - 2k_1 \frac{d\Delta V}{d\bar{t}} \right) + c_1 \Delta n \quad (9.4)$$

Whence

$$\frac{d^2\Delta\theta}{d\bar{t}^2} = \frac{c_1}{a} \left(\frac{d^2\Delta n}{d\bar{t}^2} - 2k_1 \frac{d^2\Delta V}{d\bar{t}^2} \right) + c_1 \frac{d\Delta n}{d\bar{t}}. \quad (9.7)$$

If we now substitute eqs.(9.3), (9.5), (9.6), and (9.7) in eq.(9.2), and combine all similar terms, we obtain

$$\Delta \delta = \frac{c_1}{m_1^2} \left\{ \frac{\gamma^2}{\rho^2} \Delta n + \frac{1}{\rho} \left(\gamma^2 - \frac{m_1^2 + m_2^2}{a} \right) \Delta n - \left(m_1^2 + \frac{m_2^2}{\rho} \right) \Delta n + 2 \left(m_1^2 - \frac{m_2^2}{2} M \right) \Delta V \right\}. \quad (9.8)$$

where, for brevity, we put

$$\frac{d\Delta n}{d\bar{t}} = \Delta \dot{n}, \quad \frac{d^2\Delta n}{d\bar{t}^2} = \Delta \ddot{n}.$$

POOR ORIGINAL

0 It is obvious that the terms M_{zL} and $m_{zL} = \frac{M}{2C_L} K = \frac{d^2 z}{dC_L^2}$ are measures of the
 2 longitudinal static stability with respect to overload and flying speed.

4 In eq.(9.8) we neglected the summands with \bar{V} and \bar{V} . Detailed calculations
 6 show that, in the analysis of the longitudinal stability and controllability of
 8 aircraft, it is possible to neglect, in view of their smallness, the summands con-
 10 nected with the first and second derivatives of the increments of velocity with
 12 respect to time in various analytic expression and formulas. We will neglect all
 14 such summands without making special reservations to that effect.

16 Deflection of Stick during Maneuver

18 As stated above, the parameters of aircraft motion are quantities characterizing
 20 the motion of the center of gravity and the position of the aircraft in space: the
 22 speed of flight along the flight path, the angle of attack, the angle of inclination
 24 of the flight path to the horizon, the components of the linear and angular veloci-
 26 ties with respect to the body axes of the aircraft, the altitude of flight, etc.
 28 The pilot, by changing the position of the control levers, is able to change the
 30 parameters of motion in such a way as to perform the desired turn or maneuver. For
 32 this reason the fundamental task of the theory of longitudinal aircraft stability is
 34 to define the laws governing the most rational connection between displacements of
 36 the stick, as well as the forces applied to it, and the variation in the parameters
 38 of aircraft motion.

40 To evaluate the controllability we might have taken the deflection of the
 42 elevator itself instead of the displacement of the control stick. It is more
 44 correct, however, to start from the displacements of the stick, since the pilot
 46 directly senses the displacement of the stick, but does not sense the angle of
 48 elevator deflection. The relation between the displacements of the stick and the
 50 deflection of the elevator is given by the equation

$$52 \Delta x_p = \frac{\Delta \delta^e}{\delta^e} \cdot \Delta x_p \quad (9.10)$$

POOR ORIGINAL

On substituting the expression for $\Delta\delta$ by eq.(9.8), we get

$$\Delta x_p = -x_p^x \left\{ \frac{\bar{r}_z^2}{\rho a} \Delta \bar{n} + \frac{1}{\rho} \left(\bar{r}_z^2 - \frac{m_z^2 + m_i^2}{a} \right) \Delta \bar{n} - \left(m_z^2 y + \frac{m_i^2}{\rho} \right) \Delta \bar{n} + 2 \frac{dm_z}{dy} \Delta V \right\}, \quad (9.11)$$

where

$$x_p^x = - \frac{c_y}{m_z^2 \frac{d\bar{n}}{dy}} = - \frac{c_y}{S \bar{c}_z^2 \frac{d\bar{n}}{dy}} \quad (9.12)$$

(x_p^x is the coefficient of transmission from the elevator to the stick - of. Chapter V.)

The coefficient x_p^x characterizes the deflection of the stick necessary to maintain the state of flight by displacement of the centering alone (by the value of the MAC) along the longitudinal axis of the aircraft, and is in this sense analogous to the coefficient P^x (of. Chapter V).

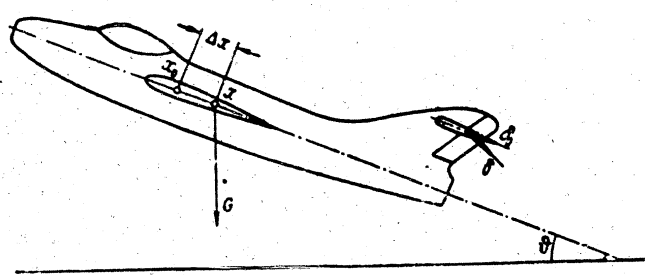


Fig.9.6 - Change of Position of Elevator for Maintaining the Previous State of Flight when the Centering is Changed



POOR ORIGINAL

Now, during flight, as a result of movements of the crew, passengers, or cargo, let the centering of the aircraft vary by the quantity x_T (Fig.9.6). Then, with respect to the initial position of the center of gravity x_0 , the force of the weight of the aircraft produces a moment equal to

$$Gx_T \cos \theta$$

In order for the aircraft in this case to be balanced in the previous state of flight, the elevator must be deflected by the quantity $\Delta\delta$, to which the stick deflection Δx_p will correspond. Under these conditions,

$$G \cos \theta \Delta x_T = -m_z^2 q S b_A \Delta\delta^2 = -m_z^2 \frac{d\delta}{dx_p} S b_A q \Delta x_p$$

Since $\frac{G \cos \theta}{S q} \approx c_L$, while $\frac{\Delta x_T}{b_A} = \Delta \bar{x}_T$, we obtain

$$\Delta x_p = -c_L \frac{\Delta \bar{x}_T}{m_z^2 \frac{d\delta^2}{dx_p}} = -\frac{c_L}{m_z^2 \frac{d\delta^2}{dx_p}} \frac{\Delta x_p}{\Delta x_T} = x_p^x \quad (9.13)$$

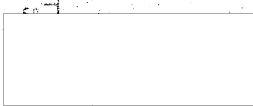
Force On the Stick During Maneuver

The force on the stick in the general case, when the overload is not equal to unity, may be determined (cf. Chapter V) by the formula

$$P = -k_n M_n - n P_w - P_{sp} \quad (9.14)$$

where n is the overload acting on the aircraft, and P_w and P_{sp} are the forces on the stick due to the presence of weights and springs in the system of longitudinal control of the aircraft.

The quantities P_w and P_{sp} are considered positive if the springs and weights tend to depress the elevator or to deflect the stick forward.



POOR ORIGINAL

Replacing M_h by its developed expression (cf. Chapter V) we shall have

$$P = -k_h m_h S_e b_e \frac{V^2}{2} k - n P_w - P_{Sv} \quad (9.15)$$

At a small deviation of the aircraft from its initial state of flight, i.e., considering the increments of the coefficient of the elevator hinge moment Δm_h , of the flying speed ΔV , and of the overload Δn to be small, and retaining only the terms of the first order of smallness, we obtain the following expression for the change of the stick force

$$\begin{aligned} \Delta P &= -k_h S_e b_e \frac{V^2}{2} (2m_h^0 \Delta V + \Delta m_h V_0^2) - P_w \Delta n = \\ &= -\frac{P_w m_h^0}{c_{10}} \left(2 \frac{m_h^0}{m_h^0} \Delta V + \frac{\Delta m_h}{m_h^0} \right) - P_w \Delta n, \end{aligned} \quad (9.16)$$

where the index "0" means that the corresponding quantities are taken in the initial state of flight, and (cf. Chapter V)

$$P_w = \frac{k_h m_h^0 S_e b_e \rho}{m_h^0} \frac{V^2}{2}$$

The coefficient of elevator hinge moment in the absence of the influence of compressibility, is a function only of the angle of attack of the horizontal tail surface and the angle of deflection of the elevator.

Considering that $m_h = f(\alpha_{h.t.}, \delta)$, i.e., disregarding the dependence of M_h on the Mach number, we obtain

$$\Delta m_h = m_h^\alpha \Delta \alpha_{h.t.} + m_h^\delta \Delta \delta$$

Here m_h^α and m_h^δ denote the derivatives of the hinge moment with respect to the angles of attack of the tail and with respect to the angle of deflection of the elevator, respectively.

We already obtained the expression for $\Delta \delta$ above, so that to establish the



POOR ORIGINAL

relation of ΔP with $\Delta \alpha$ and ΔV , it remains only to find the expression for $\Delta \alpha_{h.t.}$.

We have seen above that the angle of attack of the horizontal tail surfaces depends on the lift coefficient and on the angle of attack of the wings, on the angular velocity of rotation of the aircraft, and on the lag of the downwash. Thus we may write*

$$\Delta \alpha_{h.t.} = \Delta \alpha - D \Delta \alpha_i + D a \frac{L_{h.t.}}{V^2} \frac{d\alpha}{dt} + \frac{L_{h.t.}}{V^2} \frac{d\delta}{dt}$$

Passing to the dimensionless time, we will have

$$\Delta \alpha_{h.t.} = \Delta \alpha - D \Delta \alpha_i + D a \frac{L_{h.t.}}{V^2 b^2} \frac{d\alpha}{dt} + \frac{L_{h.t.}}{V^2 b^2} \frac{d\delta}{dt}$$

On substituting in this formula the expressions for $\Delta \alpha$ (9.4), for $\Delta \alpha_i$ (9.3), for $\frac{d\alpha}{dt}$ (9.5) and for $\frac{d\delta}{dt}$ (9.6), then after collecting the corresponding terms we have

$$\Delta \alpha_{h.t.} = \frac{c_l L_{h.t.}}{V^2 b^2} (D a + 1) \Delta \alpha + \frac{c_l}{V} \left(1 - D a + \frac{a L_{h.t.}}{V^2 b^2} \right) \Delta \alpha - 2 \frac{c_l}{V} (k_2 - D a) \Delta \bar{V}. \tag{9.17}$$

On substituting in the general expression for $\Delta m_{h.t.}$, the expression for $\Delta \alpha_{h.t.}$ and $\Delta \delta$ by eq.(9.17) and combining the corresponding terms, we have

$$\begin{aligned} \Delta m_{h.t.} = & \frac{c_l \bar{r}_i^2}{V} \frac{m_1^2}{m_2^2} \Delta \alpha + \frac{c_l}{V} \frac{m_1^2}{m_2^2} \left[\bar{r}_i^2 - \frac{m_1^2 + m_2^2}{V} + \right. \\ & \left. + \frac{L_{h.t.}}{V^2 b^2} m_1^2 \frac{m_2^2}{m_1^2} (D a + 1) \right] \Delta \alpha + c_l \frac{m_1^2}{m_2^2} \left[\frac{m_1^2}{V} \frac{m_2^2}{m_1^2} \times \right. \\ & \left. \times \left(1 - D a + \frac{a L_{h.t.}}{V^2 b^2} \right) - \left(m_1^2 + \frac{m_2^2}{V} \right) \right] \Delta \alpha + 2 c_l \frac{m_1^2}{m_2^2} \times \\ & \left. \times \left[\frac{m_1^2}{V} - m_1^2 \frac{m_2^2}{m_1^2} \frac{k_2 - D a}{V} \right] \Delta \bar{V}. \tag{9.18} \end{aligned}$$

* Neglecting the influence of the compressibility of the air on the downwash, i.e.

setting $\Delta D = \frac{dD}{dM} \Delta M$ as equal to zero.



POOR ORIGINAL

To explain the physical meaning of the elevator hinge moment necessary for execution of the maneuver, let us consider the stick-free motion of the aircraft. In view of the fact that, in this case, the stick force is equal to zero, we may write, on the basis of eq.(5.25) of Chapter V:

$$m_{z_{co}} = m_{z_{co}} - m_{z_{co}}^h \frac{\partial h_{c,t}}{\partial \delta} - m_{z_{co}}^h \frac{\partial h_{c,t}}{\partial \delta} \times \left(c_1 P_1 + \frac{q}{V} P_w \right).$$

Taking the partial derivatives of this expression with respect to the corresponding variables, we will have

$$m_{z_{co}}^c = \frac{\partial m_{z_{co}}}{\partial \delta} = m_{z_{co}}^c - m_{z_{co}}^h \frac{\partial h_{c,t}}{\partial \delta}.$$

However,

$$\frac{\partial h_{c,t}}{\partial \delta} = \frac{\partial h_{c,t}}{\partial V} = \frac{\partial h_{c,t}}{\partial V} \frac{dV}{dt} = \frac{\partial h_{c,t}}{\partial V} \frac{1}{\mu} \frac{dV}{dt},$$

so that

$$\frac{\partial h_{c,t}}{\partial \delta} = \frac{L_{h,t}}{V k b_A}$$

and

$$m_{z_{co}}^c = m_{z_{co}}^c - m_{z_{co}}^h \frac{L_{h,t}}{V k b_A}.$$

Analogously

$$\left. \begin{aligned} m_{z_{co}}^c &= m_{z_{co}}^c - m_{z_{co}}^h \frac{D \alpha}{V k b_A} \frac{L_{h,t}}{V k b_A} \\ m_{z_{co}}^c &= m_{z_{co}}^c - m_{z_{co}}^h \left(\frac{1}{s} - D \right) \frac{P_w}{P^2} \end{aligned} \right\} \quad (9.19)$$

(the latter result was already obtained in Chapter V). On taking the total derivative of $m_{z_{co}}$ with respect to C_L under the condition $n = 1$, we will have

POOR ORIGINAL

$$\left(\frac{dm_z}{dc_L}\right)_m = \frac{dm_z}{dc_L} - m_z^2 \frac{m_h^2}{m_h^2} \frac{da_{h,t}}{dc_L} - \frac{P_N + P_{SP}}{P^2} \quad (9.20)$$

However,

$$\frac{da_{h,t}}{dc_L} = \frac{da}{dc_L} - D.$$

We have seen above that

$$\frac{dc_L}{da} = \frac{a}{1 - c_L^2 \frac{dM}{dc_L}}$$

At $n = 1 = \text{const.}$

$$c_L S q_0 M^2 \approx G,$$

where $q_0 = \frac{\rho a^2}{2}$, and a is the velocity of sound.

Hence, $\frac{dM}{dc_L} = \frac{M}{2c_L}$ and $\frac{dc_L}{da} = \frac{a}{1 + \frac{M}{2c_L} c_L^2} = \frac{a}{k_2}$. Consequently, $\frac{da_{h,t}}{dc_L} = \frac{k_2}{a} - D$

so that, taking into consideration eqs.(9.19) and (9.20), eq.(9.18), after a few simplifications, may be rewritten in the following form

$$\Delta m_h = c_L \frac{m_h^2}{m_z^2} \left\{ \frac{r_z^2}{r_0^2} \Delta n + \frac{1}{r} \left[r_0^2 - \frac{m_z^2 m_h^2}{m_z^2} \right] \Delta n - \left[\frac{m_z^2 c_L^2}{a^2} + m_z^2 c_L + \frac{P_N}{P^2} \right] \Delta n + 2 \left[\left(\frac{dm_z}{dc_L} \right)_m + \frac{P_N + P_{SP}}{P^2} \right] \Delta V \right\} \quad (9.18)$$

In this way, for an assigned maneuver, i.e., at known values of $n = f(t)$ and $V = \varphi(t)$, the necessary change in the hinge moment of the elevator produced by the pilot will depend on the values of c_L and V characterizing the initial state of flight: on the design parameters of the aircraft $r_z^2, \mu, G/S$, on the aerodynamic parameters m_z^2 , the coefficient of elevator efficiency $\frac{d m_z^2 c_L}{dc_L}$ and, $m_z^2 c_L$, the coefficients of static stability of the aircraft and, finally, on the design para-



POOR ORIGINAL

0 meters of the system of longitudinal control P^x , P^y , and P^{sp} .

2 Bearing in mind eq.(9.18), and substituting, on the basis of eq.(9.15) under
 4 the condition $P = 0$, $\frac{m_{sp}}{m} = -\frac{P_b + P_{sp}}{P^x m_2^0}$, we may now replace eq.(9.16) by

$$\begin{aligned} \Delta P = & - \left(\frac{2m_{sp}}{m} \Delta V + \frac{\Delta m_{sp}}{m} \right) \frac{P^x m_2^0}{c_{L_1}} - P_c \Delta \delta = \\ & - P^x \left(\frac{r_2^0}{a} \Delta \delta + \frac{1}{\mu} \left(\gamma_2^0 - \frac{m_{2c}^0 + m_{1c}^0}{a} \right) \Delta \delta - \right. \\ & \left. - \left(m_{1c}^0 + \frac{m_{2c}^0}{\mu} \right) \Delta \delta + 2 \left(\frac{dm_1}{dc_L} \right) \Delta V_{sp} \right). \end{aligned} \quad (9.21)$$

15 We then write eqs.(9.11) and (9.21) in the more concise form:

$$\begin{aligned} \Delta x_1 = & x_1^0 \Delta \delta + x_2^0 \Delta \delta + x^0 \Delta \delta + x^v \Delta V; & (9.22) \\ \Delta P = & P_2^0 \Delta \delta + P_1^0 \Delta \delta + P^x \Delta \delta + P^v \Delta V. & (9.23) \end{aligned}$$

20 where

$$\begin{aligned} x_2^0 = & -x_1^0 \frac{r_2^0}{a}; \\ x_1^0 = & -\frac{x_2^0}{\mu} \left(\gamma_2^0 - \frac{m_{2c}^0 + m_{1c}^0}{a} \right). \end{aligned} \quad (9.24)$$

$$x^0 = x_1^0 \left(m_{1c}^0 + \frac{m_{2c}^0}{\mu} \right); \quad x^v = -2x_1^0 \frac{dm_1}{dc_L}; \quad x_2^v = -\frac{c_L}{57.3 k_{m_1}}; \quad (9.25)$$

and

$$\begin{aligned} P_2^0 = & -P^x \frac{r_2^0}{a}; & P_1^0 = & -\frac{P^x}{\mu} \left(\gamma_2^0 - \frac{m_{2c}^0 + m_{1c}^0}{a} \right); \\ P^x = & P^x \left(m_{1c}^0 + \frac{m_{2c}^0}{\mu} \right); & P^v = & -2P^x \left(\frac{dm_1}{dc_L} \right)_{c_0}; \\ P^x = & \frac{m_1^0}{m_1} k_{m_1} S_{\delta} b \frac{Q}{S}. \end{aligned} \quad (9.25)$$

54 As indicated by eqs.(9.22) - (9.25), the formulas for calculating the stick
 56 force and the stick deflections are entirely analogous to each other, with the

POOR ORIGINAL

single difference that the expressions for the deflections of the stick contain the derivatives of the fixed-rudder aerodynamic coefficients, while the equations for the stick force contain the same derivatives for the stick-free case. For this reason, we will hereafter analyze only the forces applied by the pilot to the stick or the control wheel. By making use of this analogy, the reader will easily be able to extend the corresponding deductions and conclusions of the analysis of the forces to the displacements of the control stick.

In the analysis of aircraft controllability, the coefficients P_2^0 , P_1^0 , P_0^0 , P_4 play a substantial role, and will be encountered often in this book. Therefore, it is of importance to obtain a clear idea of their physical meaning.

The coefficient P_2^0 characterizes the value of the force necessary for balancing the change in moments which take place as a result of the passage of the aircraft from the original steady state of flight at $n = 1$, to the conventional steady state of curvilinear flight in the vertical plane at constant load $n = 2$, i.e., at $|\Delta n| = 1$, and at the same flying speed as in the initial state of flight. Such a strictly steady state of curvilinear flight could be obtained by us if the pilot or a special automatic device were to regulate the engine thrust during flight in such a way that, at each instant of time, the projection of the engine thrust onto the direction of the flying speed were equal to the algebraic sum of the drag of the aircraft and the projection of the weight of the aircraft onto the direction of the speed of flight. It may be considered approximately true that a steady state of curvilinear flight in the vertical plane at $n = \text{const}$ may be obtained 1-2 sec after the beginning of the maneuver, when the flying speed may still be taken as equal to the flying speed in the initial steady state ($V = 0$). As shown in Fig.9/5, we may consider that the steady curvilinear flight indicated corresponds only to that segment of the curve of the maneuver A where $n = \text{const}$.

At $\Delta V = 0$ and $\Delta n = \text{const}$, the variation of the stick force, as will be seen from eq.(9.23), will be determined by the expression



POOR ORIGINAL

$$\Delta P = P^{\text{II}} \Delta n$$

In accordance with the above, we shall term the quantity P^{II} the coefficient of consumption of force on the load factor.

Let us evaluate the order of the quantity P^{II} for fighters and dive bombers. Taking $\epsilon_{\text{locB}}^{\text{CL}} = -0.10$, $\epsilon_{\text{locB}}^{\text{W}} = -6$, and the quantity $P^{\text{K}} = 30-100$ kg (if the change in centering is measured in percent of the mean aerodynamic chord instead of in fractions of it, the indicated range of values of P^{K} will correspond to the change in stick force from 0.3 to 1 kg at a $1\frac{1}{2}$ MAC, for a variation in the centering of the aircraft by $1\frac{1}{2}$ MAC) and $\mu = 300 - 400$, we get

$$P^{\text{II}} = -3 + -12 \mu g$$

For heavy aircraft, the value of P^{II} may exceed 50 kg in absolute value.

The quantities P_1^{II} and P_2^{II} , as follows from eq.(9.23), affect only those segments of the unsteady aircraft motion where Δn and Δn do not vanish.

As confirmed by the records of aircraft maneuvers made during flight (cf. Figs.9.1-9.4), the motion of the aircraft is, on the whole, unsteady. For this reason, the quantities P_1^{II} and P_2^{II} play no less important a role in the controllability of the aircraft (as will be shown in more detail) than the quantity P^{II} , the coefficient of expenditure of force on the load.

Let us now imagine that the pilot deflects the elevator so slowly that the aircraft smoothly changes its attitude at a practically constant load, equal to unity. In that case the variation in force will be connected only with the variation in flying speed, so that eq.(9.23), can be replaced by

$$\Delta P = P^{\text{V}} \Delta \bar{V}$$

The quantity P^{V} , which we will denote as the coefficient of expenditure of force on speed, characterizes the variation in stick force with the flying speed, which

STAT

POOR ORIGINAL

is customarily represented in the form of the balancing curve $P = f(V)$ (Fig.9.7).

If the variation in the derivative P^V is assigned as a function of the flying speed, we can determine the balancing curve $P = f(V)$; conversely, if we have the balancing curve it is not hard to calculate the value of P^V for any initial state of flight.

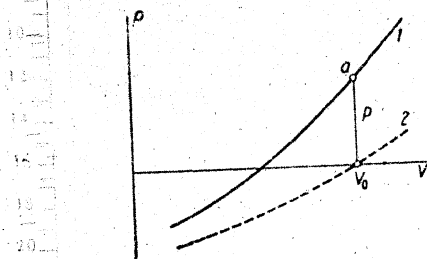


Fig.9.7 - Balancing Curve $P = f(V)$
at Constant Elevator Position
and the quantity P

As seen from eq.(9.25), the quantity P^V is proportional to the coefficient of static stick-free stability with respect to speed $\left(\frac{d\bar{m}_z}{dC_L}\right)_{CB}$.

To evaluate P^V , let us take $\left(\frac{d\bar{m}_z}{dC_L}\right)_{CB} = 0.10$ (10% stability reserve) and the quantity P^V for light aircraft equal to 30-100 kg.

We shall then obtain $P^V = 6 - 20$ kg.

For heavy aircraft, P^V may reach 100-200 kg.

By definition,

$$P^V = V \frac{\partial P}{\partial V} = \frac{\partial P}{\partial \bar{V}}.$$

It follows that the quantity P^V characterizes the force that must be applied by the pilot to the stick in order to change the relative speed \bar{V} of steady flight by unity. Starting from the figures given above for P^V , we find that in light aircraft a force of 0.06-0.2 kg must be applied to the stick in order to make a 1% change in the speed by comparison with the speed in the initial state of flight, and up to 1-2 kg in heavy aircraft.

POOR ORIGINALRelation between Stick Force during a Maneuver and StickDisplacement

On comparing the expression for x_p (9.11) and for P (9.21), we found that, formally, these two expressions are analogous and differ only by the factor in front of the braces, and by the fact that all terms in eq.(9.11) correspond to stick-fixed flight, while those in eq.(9.21) correspond to stick-free flight.

If the conditions

$$m_{z_{cb}}^{c_A} = m_{z_{cb}}^{c_A}; \quad \left(\frac{dm_z}{dc_z}\right)_{cb} = \frac{dm_z}{dc_z}; \quad m_{z_{cb}}^w = m_z^w; \quad m_{z_{cb}}^2 = m_z^2, \quad (9.26)$$

are satisfied, then the following relation will exist between the deflection of the stick and the force applied to it:

$$\Delta P = \frac{P^2}{x_p^2} \Delta x_p = - \frac{57.3 P^2 B_{cb}^2}{c_z} \Delta x_p, \quad (9.27)$$

Since for the case of horizontal flight, which is the state for which we obtained the expression x_p^x

$$c_z = \frac{0}{S_0}.$$

Then,

$$\frac{\Delta P}{\Delta x_p} = - \frac{P^2 B_{cb}^2}{0} g. \quad (9.28)$$

As we see, the relation $\frac{\Delta P}{\Delta x_p} = \frac{dP}{dx_p}$, which plays an important role in the calculation and analysis of stability and controllability, is found to be directly proportional to the velocity head and does not depend on the load conditions. If the conditions of eq.(9.26) are satisfied, the control of the aircraft has the property of full balance of stick force and stick displacement. This property consists in that, on performing maneuvers at $V \approx \text{const}$, the force applied to the stick is proportional to its deflection and has the same sign as the deflection of the stick, regardless of the instant of time being considered. If, for example, the

POOR ORIGINAL

stick is pushed away from the pilot during a maneuver, then the pilot's effort is directed inwards toward him. In aircraft designing, efforts should be made to satisfy the conditions of eq.(9.26).

Selection of Weights and Springs Installed in the System of Longitudinal Control

The conditions (9.26), taking into account eqs.(9.19) and (9.20), can be represented in the following form:

$$\begin{aligned}
 -m_i \frac{m_h^2}{m_h} \left(\frac{1}{s} - D \right) &= \frac{P_v}{P^2} \quad (\text{CONDITION } m_i^2 = m_{i,eq}^2); \\
 m_h^2 &= 0 \quad (\text{CONDITIONS } m_i^2 = m_{i,eq}^2; m_h^2 = m_{h,eq}^2); \\
 -m_i \frac{m_h^2}{m_h} \left(\frac{h_2}{s} - D \right) &= \frac{P_v + P_{SP}}{P^2} \quad \left[\text{CONDITION } \left(\frac{dm_z}{dc_L} \right) = \left(\frac{dm_z}{dc_L} \right)_0 \right].
 \end{aligned}$$

These conditions can be exactly satisfied by putting $m_h^2 = 0$ and not introducing springs or weights into the control system. In practice, however, it is difficult to realize $m_h^2 = 0$. For this reason, we must proceed to a partial satisfaction of the conditions (9.26), and maintain only the equalities $m_i^2 = m_{i,eq}^2$. And $\frac{dm_z}{dc_L} = \frac{dm_z}{dc_L} \cdot c_B$, by selecting the corresponding springs and weights at assigned m_h and m_h^2 . In this case, strictly speaking, the conditions of harmony will not be satisfied, but in practice the deviations from eq.(9.26) will be small, since the aerodynamic moments connected with static stability will play the major role in determining the stick force and stick displacements.

It is rather obvious that

$$\left. \begin{aligned}
 P_v &= -P^2 m_i \frac{m_h^2}{m_h} \left(\frac{1}{s} - D \right); \\
 P_{SP} &= -P^2 m_i \frac{m_h^2}{m_h} \frac{h_2 - 1}{s} = -P^2 m_i \frac{m_h^2}{m_h} \frac{M_{zL}^A}{2ac_L}.
 \end{aligned} \right\} \quad (9.29)$$

POOR ORIGINAL

It follows from this last expression that a spring selected for some definite state of flight will not be optimum, from the point of view of harmony of control, in other states of flight. In exactly the same way, since the derivative $\frac{\partial C_L}{\partial a}$ depends on the Mach number, and consequently will differ in different states of flight, a weight selected by any state of flight will not be optimum in any other states. The selection of weights and springs must therefore be made for the principal rated state of flight.

In practice, in the final adjustment of aircraft controllability during flight tests, the springs and weights are often selected on the basis of the conditions of obtaining the required values for the coefficients of expenditure of force on the load factor P^n and on the speed P^v , without changing the aerodynamic compensation of the elevator. For this case, starting from eqs.(9.25), (9.19), and (9.20), we obtain the following formulas:

$$\left. \begin{aligned} P &= P_0^n - P_w \\ P^v &= P_0^v + 2(P_w + P_{sp}) \end{aligned} \right\} \quad (9.30)$$

where P_0^n and P_0^v denote, respectively, the coefficients of expenditure of force without springs and weights in the system of elevator control. From eq.(9.30), it is easy to define what weights and springs to install in the longitudinal control of the aircraft.

We note that, according to eq.(9.29), no springs should be installed ($P_{sp} = 0$) in aircraft in which the influence of the compressibility of the air on the coefficients C_L may be neglected ($C_L^M = 0$). However, if the influence of the compressibility of the air or the influence of the deformation of the elevator tab, related to the flying speed, on the elevator hinge moment are taken into account, then terms with the coefficients $m_h^M = \frac{\partial m_h}{\partial M} \neq 0$ will appear in the corresponding formulas for the stick force. In that case, to satisfy the conditions (9.26) and to obtain the desired values of P^n and P^v , it is necessary in the general case to install both

POOR ORIGINAL

weights and springs.

Bringing the Aircraft to Assigned Overload

We have considered above the case of the variation in velocity at constant load $n = 1$.

Let us now consider the remaining typical elementary maneuvers, mentioned at the beginning of this Chapter and schematically represented in Fig. 9.5.

In order to give a clearer and more graphic representation by analytic expressions of the physical nature of the phenomena being considered, we will use the dimensional time t . Then, bearing in mind that we have agreed to consider $\Delta V = 0$, we will have

$$\Delta P = cP_1 \frac{dV}{dt} + cP_2 \frac{d\gamma}{dt} + P_{12} \quad (9.31)$$

where

$$\left. \begin{aligned} c &= \frac{m}{S V} \\ P_2 &= -P \frac{\gamma}{\alpha} \\ P_1 &= \frac{P}{\alpha} (m_{\gamma_{\alpha}} + m_{\gamma_{\omega}} - \alpha V^2) \\ P &= P \left(m_{\gamma_{\alpha}} + \frac{m_{\gamma_{\omega}}}{V} \right) \end{aligned} \right\} \quad (9.32)$$

For the examples given below, let us take an aircraft with the following data:

$$\begin{aligned} G &= 4000 \text{ kg}; & \frac{G}{S} &= 200 \text{ kg/m}^2; & \gamma_0 &= 2 \text{ m}; \\ \alpha &= 0.2; & m_{\gamma_{\alpha}} &= -6; & m_{\gamma_{\omega}} &= -2; & \gamma_0 &= 1.2 \end{aligned}$$

We will assume, in first approximation, that at any change in the selection of the initial steady state of flight, the parameters will remain constant, except for cases where specifically stated otherwise.

Let us take an altitude of flight of 5000 m for the calculations. Then, the



POOR ORIGINAL

coefficients of relative density of the aircraft will be

$$\mu = 271$$

With the above data we obtain the following computation formulas for P_2^1 , P_1^1 , and P^1 :

$$\left. \begin{aligned} P_2^1 &= -0,00106P^x \\ P_1^1 &= -0,0117P^x \\ P^1 &= (m_{z, \delta}^1 - 0,0222)P^x \end{aligned} \right\} (9.32)$$

To simplify the calculation, the maximum variation in overload will be taken as $\Delta n_{max} = 1$. For other values of Δn , all the forces must be varied in proportion to Δn .

As the initial values for P^1 and P^x let us take

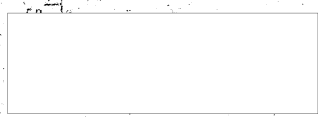
$$P^1 = -3 \text{ kg and } P^x = 41.5 \text{ kg}$$

The flying speed along the flight path in the initial state of flight will be taken as equal to 150 m/sec, which corresponds to an indicator speed of 418 km/hr at an altitude of 3000 m. In accordance with the initial data we then have

$$\tau = 2.6 \text{ sec; } \tau^2 = 13.0 \text{ sec}^2$$

Figure 8.9 shows, as a function of time, the variations in the overload and forces necessary to execute the assigned maneuver at various degrees of static stability and at constant value of the coefficient of expenditure of force $P^x = 41.5 \text{ kg}$, i.e., at constant aerodynamic compensation of the elevator.

As indicated by these curves, the forces increase sharply with increasing stability. At $m_{z, \delta}^1 = 0$, i.e., for a statically neutral aircraft (in the sense of stability with respect to load conditions), the force necessary for balancing the aerodynamic moments acting on the aircraft, at a variation in the load conditions constant with time (after 1.6 sec), is very small and amounts to $P = P^x = -0.92 \text{ kg}$.



POOR ORIGINAL

As shown by actual flight tests, at such a value of P_n the pilot will easily be able to produce an inadmissibly high overload on the aircraft. On the other hand, at $m_{zch}^{C_1} = -0.30$, i.e., at very great stability of the aircraft, the forces required to balance the aircraft in curvilinear flight are inadmissibly large and amount to 13.4 kg per unit of variation of n . At such a large value of P_n^0 , the aircraft is too difficult to control. For example, it will be impossible to bring the aircraft up to a load factor $n = 4-5$, possibly required in aerial combat (cf. Fig. 9.3), since the stick force required for this purpose will amount to 40-50 kg.

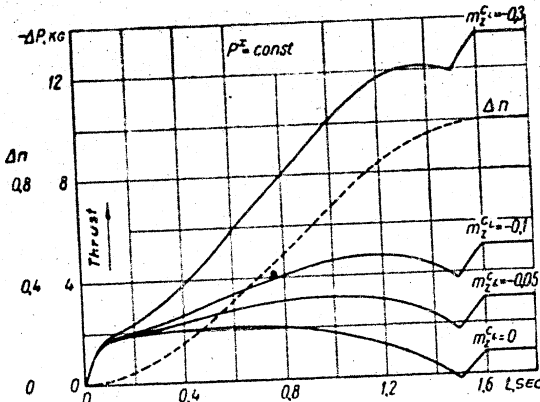


Fig. 9.3 - Representation of the Stick Force Necessary to Bring the Aircraft to Assigned Load Conditions as a Function of Time, for Various Degrees of Static Stability, in Stick-Free Flight, at Constant Aerodynamic Compensation of the Elevator ($P_n^0 = 41.5$ kg)

Attention should be paid to the presence of a forward and rearward travel of the stick forces at low degrees of stability, in spite of the smooth rise in load. The pilot at first must apply considerably more force to the stick (in the direction



POOR ORIGINAL

0 "toward himself") than would be needed to balance the aircraft in steady curvilinear
 1 flight at $n = \text{const}$. Before reaching the assigned load conditions, the pilot must
 2 reduce the stick force in the direction "toward himself" so as to stop the increase
 3 in load by means of the corresponding deflection of the elevator.

4
 5
 6
 7
 8 If follows from Fig.9.8 that, if the aerodynamic rudder balance is selected
 9 regardless of the degree of stability ($p^x = \text{const}$), less stable aircraft will re-
 10 quire stick forces of smaller absolute value in piloting.

11
 12
 13
 14
 15
 16
 17
 18
 19
 20
 21
 22
 23
 24
 25
 26
 27
 28
 29
 30
 31
 32
 33
 34
 35
 36
 37
 38
 39
 40
 41
 42
 43
 44
 45
 46
 47
 48
 49
 50
 51
 52
 53
 54
 55
 56

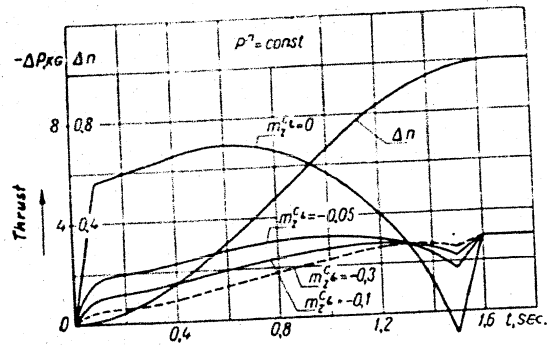


Fig.9.9 - Stick Force Necessary to Bring the Aircraft to an Assigned Load, as a Function of Time, for Various Degrees of Stability with Free Stick, and at Various Values of Aerodynamic Elevator Balance ($p^x = -3 \text{ kg}$)

It is clear from Fig.9.9 that, at $p^x = \text{const}$, the forces necessary to execute the first stage of the maneuver under consideration will decrease with increasing stability; the relative significance of the summands $\Delta P_1 = \tau p^x \frac{d\Delta n}{dt}$ and $\Delta P_2 = \tau^2 p^x \frac{d^2\Delta n}{dt^2}$ will diminish with increasing m_{zGB}^c , because of the decrease in the



POOR ORIGINAL

coefficient P^X , to which the quantities P_1^H and P_2^H are proportional.

Rapid Variation in Overload

Rapid variation in overload are more characteristic at high flying speeds. For this reason, let us take as the initial value $V_1 = 250$ m/sec, corresponding to an indicator value $V_1 = 700$ km/hr at an altitude of 5000 m. In accordance with the initial data adopted, we will then have

$$\tau = 2.16 \text{ sec}; \tau^2 = 4.65 \text{ sec}^2$$

Figure 9.10 shows the variations in load factor and stick force necessary to execute an assigned maneuver at various values of m_{zcb}^{CL} , a constant value of P^X , and a variable value of P^Z , while Fig. 9.11 shows the same at constant value of P^H and variable value of P^X .

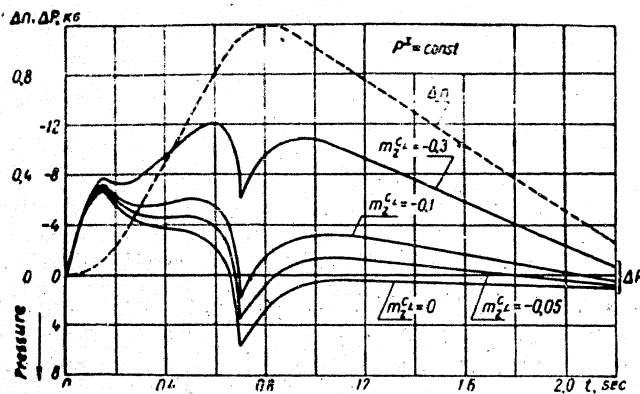


Fig. 9.10 - Stick Forces Necessary to Obtain a High Load at Various Values of m_{zcb}^{CL} , at Constant Aerodynamic Elevator Balance ($P^X = 41.5$ kg)

It will be seen that at constant value of the coefficient P^X , the stick forces increase with increasing stability, while at constant value of P^H , the stick forces on the whole decline with increasing stability.



STAT

POOR ORIGINAL

It must be noted that the instants of time corresponding to the maximum value of the stick force in the direction "toward the pilot" do not coincide with n_{max} , but considerably exceed it.

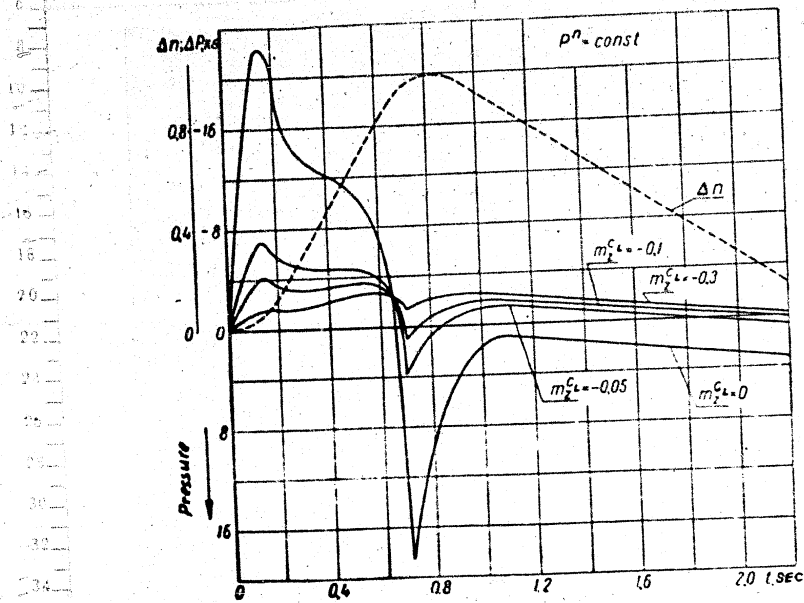


Fig.9.11 - Stick Force Necessary to Obtain a High Load at Various Values of m_{zcB}^c and at Various Corresponding Values of the Aerodynamic Elevator Balance ($P^0 = -3 \text{ kg}$)

In other words, there is a considerable lag in the variation of the load with respect to the variations of the stick force.

Stability and Controllability at High Flying Speeds

When the aircraft is not well designed and its structure is insufficiently rigid, there may be variations in the longitudinal moments, leading to a number of



POOR ORIGINAL

0 unpleasant phenomena with respect to longitudinal controllability, in particular:
 2 pulling the aircraft into a dive, so-called wedging of elevator, accidentally ex-
 4 ceeding the permissible overload sufficient to cause structural failure, and exces-
 6 sively high stick force for balancing the aircraft at high flying speeds.

8 An analysis of these phenomenon reveals the great "sensitivity" of the aircraft
 10 controllability to variations in the longitudinal moments in the region of high
 12 flying speeds.

14 Now, the value of the control-surface deflection required for counteracting the
 16 change in Δm_z is determined by the equation

$$\Delta m_z = -m_1^i \Delta \delta,$$

22 whence

$$\Delta \delta = -\frac{\Delta m_z}{m_1^i}.$$

26 The corresponding stick force at constant position of the stabilizer and eleva-
 28 tor tab is equal to

$$\Delta P = -k_h S_b k q m_1^i \Delta \delta = k_h S_b k q \frac{m_1^i}{m_1^i} \Delta m_z,$$

32 In this case, we assume for simplicity that $m_{11}^i = 0$. We assume further that
 34 the coefficient k , m_1^i and m_2^i are constant quantities, independent of the initial
 36 values of C_L and M under consideration. Then, ΔP may be represented by the formula

$$\Delta P = A q \Delta m_z, \quad (9.34)$$

42 where A is a constant quantity.

44 With Δm_z , the corresponding stick forces, according to eq. (9.34) will
 46 be proportional to the velocity head or to the square of the flying speed if the
 48 flying speed remains constant.

50 If, for example, at a speed of $V = 250$ km/hr, the stick force necessary for
 52 counteracting a certain value of $\Delta m_z = \text{const}$, amounts to 3 kg, then the stick force
 54
 56

POOR ORIGINAL

0 increases to 27 kg at a speed of $V = 750$ km/hr and to 75 kg at speed of 1250 km/hr.

2 Let us continue our analysis of the variations in stability and controllability
4 in the region of high flying speeds. To carry out this analysis it is necessary to
6 know the relation between the variations in C_L and the Mach number under the condi-
8 tions of steady rectilinear flight at various speeds and at various initial states
10 of engine operation.

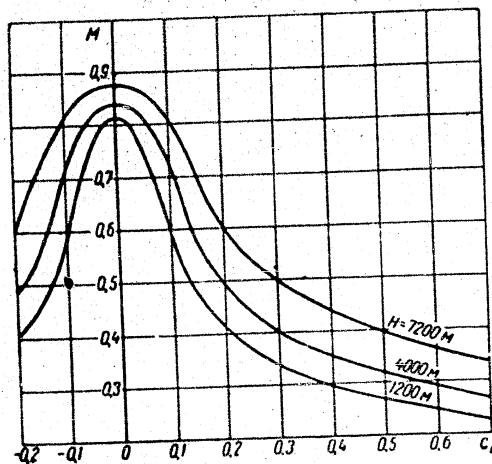


Fig.9.12 - Relation between C_L and M for Steady Rectilinear Flight, Engine Off ($P = 0$) at Three Altitudes

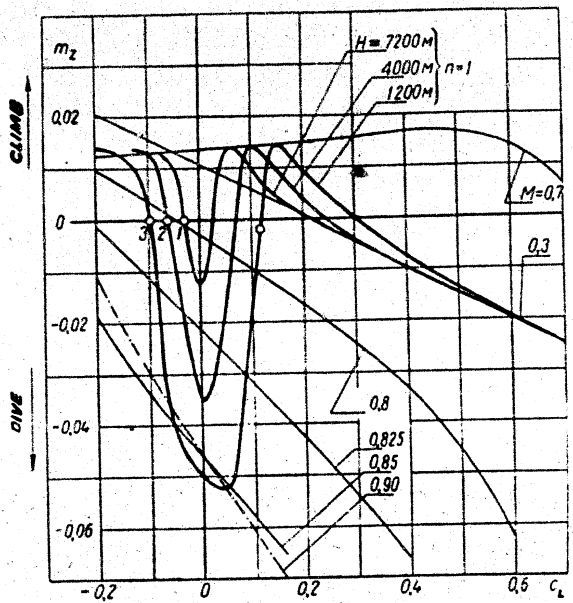
As an example, Fig.9.12 shows the relation between M and C_L for the condition of steady rectilinear gliding flight at three altitudes. On determining $M = f(C_L)$ for horizontal rectilinear flight, we obtain a curve tending toward infinity upward, with the ordinate axis as asymptote, as follows from the equation of the forces along the normal to the flight path:

$$C_L S \frac{\rho a^2 M^2}{2} = G$$

POOR ORIGINAL

0 Making use of the relation $M = f(C_L)$ in Fig.9.12 and considering that, the air-
 2 aircraft under consideration corresponds, for example, to the curves $m_z = f(C_L)$
 4 at $M = \text{const}$ in Fig.9.13, as already stated in Chapter VIII, the curves $m_z = f(C_L)$,
 6 corresponding to $n = 1$, can be obtained.

8 These curves are shown in Fig.9.13 by heavy lines and, as already stated above,
 10 characterize the degree of static longitudinal stability of the aircraft with respect
 12 to flying speed.



44 Fig.9.13 - Curves of Static Longitudinal Stability with
 46 Respect to Overload and with Respect to Flying Speed

48 Pulling the Aircraft into a Dive

50 In some cases, as mentioned several times, an aircraft manifests a tendency to
 52 go into a dive spontaneously during flight at high speeds, due to the influence of
 54 the compressibility of the air on the aerodynamic characteristics of the aircraft.
 56



POOR ORIGINAL

Let us attempt to elucidate the causes of this phenomenon.

In order to pass from the variation in longitudinal moments to the characteristics of controllability, we must consider the deviation of the airplane balancing both in rectilinear flight and when the load is built up. Figure 9.14 shows, as an example, the result of a calculation from the plots presented in Fig. 9.13, under the condition of $m_{fl}^{\delta} = -0.01 = \text{const}$, indicating the linear displacements of the stick necessary for balancing the aircraft in rectilinear gliding flight (at a thrust of $P = 0$). The displacements of the stick are plotted as a function of indicated speed, which, neglecting the corrections, may be considered equal to the speed shown by the ordinary instrument in the pilot's cabin.

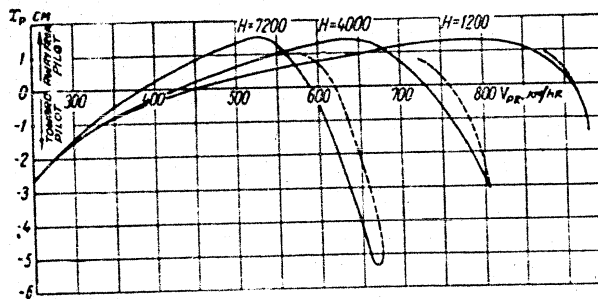


Fig. 9.14 - Balancing Curves $x_p = f(V_i)$ for Steady Rectilinear Flight at Three Altitudes with Engines Operating at Low Speed.

The balancing curves of the stick forces constructed from the plots presented in Fig. 9.13 at $m_{fl}^{\delta} = \text{const}$ and $m_{fl}^{\alpha} = 0$ and the absence of spring and weight balance of the longitudinal control, are shown in Fig. 15*. The values of m_{fl}^{δ} and the dimensions of the elevator taken in this case correspond to an aircraft with a flying weight of about 6000 kg.

* The calculation of the elevator deflection and stick forces under the above assumptions may be performed from the formulas given in the preceding Section.

POOR ORIGINAL

Let us assume, for example, that the pilot, attempting to obtain a higher flying speed, has brought the aircraft into the region of loss of stability with respect to speed and of the appearance of longitudinal diving moments.

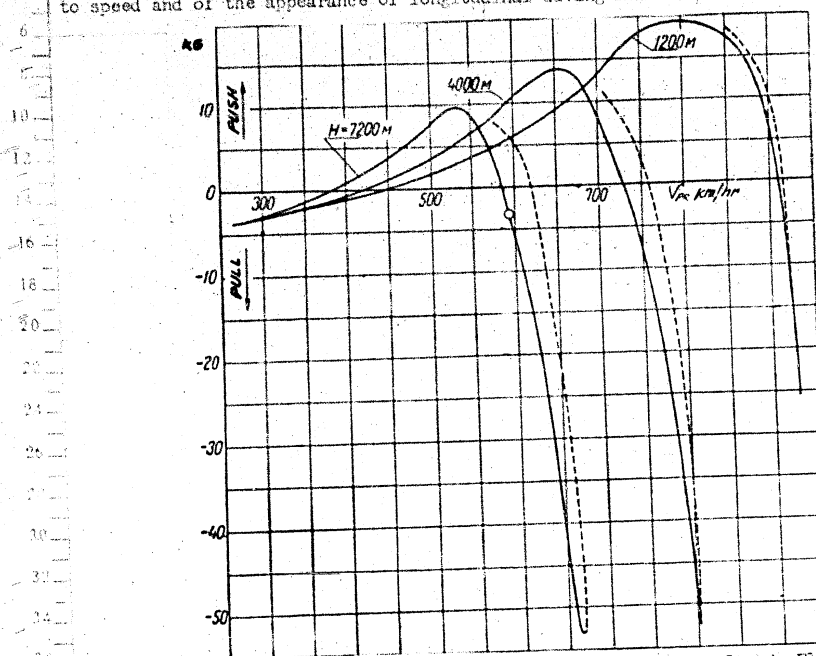


Fig.9.15 - Balancing Curves $P = (V_1)$ for Rectilinear Steady Flight at Three Altitudes with Engines Operating at Low Speed

The balancing stick forces for the example taken change their sign in this region and become "pulling" forces. If the pilot accidentally releases the stick or his strength is insufficient to overcome the diving moments, the aircraft will continue its flight at low or even negative values of C_L determined by the balancing states with respect to the moments ($m_{zCB} = 0$ and, correspondingly, $P = 0$) in the region of high static stability with respect to flying speed. These states of flight in our example on Fig.9.13, correspond to the points 1, 2, 3, in Fig.9.13 and the points of intersection of the broken curves with the abscissa in Fig.9.15.

POOR ORIGINAL

0 The stable balancing states of aircraft at small value of C_L and, even more so,
 2 at negative values, cause a steady downward curvature of the flight path $\frac{d\theta}{dt} < 0$
 4 until the lift becomes greater in value than the projection of the force of the
 6 aircraft weight onto the normal to the flight path.

8 Indeed, from the equations of motion of the aircraft (7.4), if we neglect the
 10 projection of the thrust onto the normal to the flight path, it follows that

$$Y = G \cos \theta + mV \frac{d\theta}{dt}.$$

12 In the case that

$$Y < G \cos \theta, \text{ to } \frac{d\theta}{dt} = \frac{1}{mV} (Y - G \cos \theta) < 0.$$

14
 16
 18
 20 In order to bring the aircraft out of the dive, the pilot must apply a force that
 22 is greater in absolute value than the maximum pulling force corresponding to the
 24 vertex of the balancing curve $P = f(Y)$ (cf. Fig.9.15) in the region of negative
 26 values of P . For the example presented in Fig.9.15, in the altitude range
 28 of 7000 - 4000 m, the pilot must apply a stick force (toward him) of more than 53 kg
 30 in order to pull the aircraft out of the this type of a dive.

32 If the pilot's physical strength is not sufficient to produce such large stick
 34 forces, we shall have the dangerous case of complete loss of control of the air-
 36 craft. Because of the large stick forces necessary to pull the aircraft out of a
 38 dive, the pilot may get the wrong impression that the elevator is "wedged", as
 40 though caused by a structural failure.

42 To get a general idea as to the character of motion of an aircraft during an
 44 uncontrolled change into a dive, Fig.9.16 shows as an example plots of the time
 46 variations in angle of inclination of the flight path, of the true and indicator
 48 flying speed, of the Mach number, the altitude and the load factor. These data
 50 were obtained by calculation, using the characteristics of static stability shown
 52 in Fig.9.13 as the initial data.

54 We observe that the principal cause of going into a dive is the displacement
 56

POOR ORIGINAL

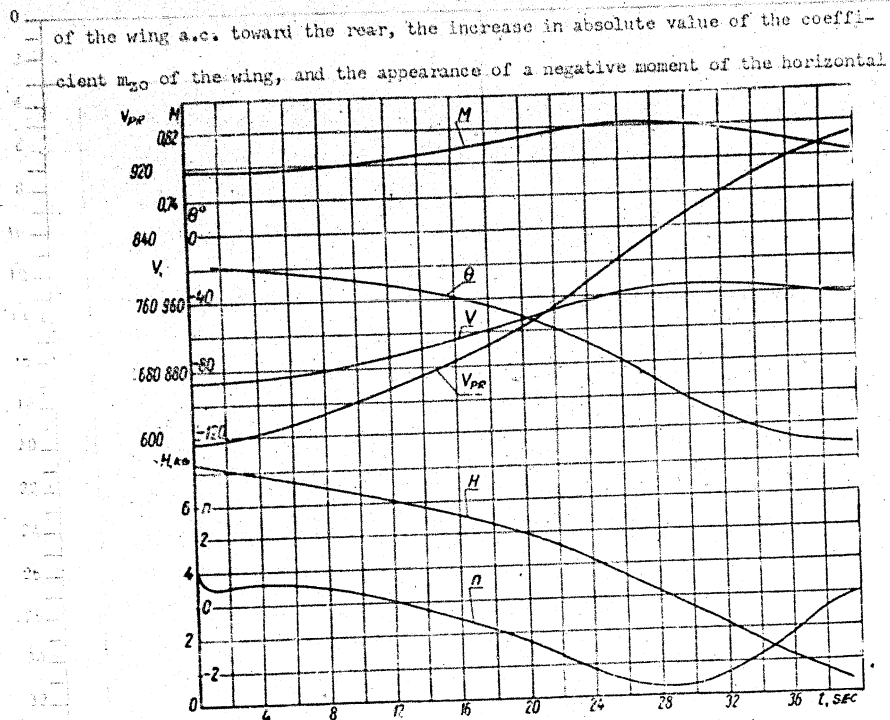


Fig.9.16 - Characteristics of the Uncontrolled Motion

of an Aircraft when Pulled into a Dive

tail, as already discussed in Chapters II and III. The inadequate rigidity of individual structural elements of the aircraft may also exert an unfavorable influence (cf. infra, Chapter XI).

The Possibility of Obtaining High Overloads

The influence of the compressibility of air and of structural deformation on the aircraft stability may also show in an increase in climbing moments at high flying speeds. Such phenomena may occur if an aircraft has sweptback wings and is improperly designed. The large aerodynamic moments may result in making great stick forces necessary for balancing the aircraft in rectilinear flight at high speed.



POOR ORIGINAL

The increase of stick force in the direction "away from the pilot" to counteract the climbing moments may in a number of cases, be increased still more because of the variations in the elevator hinge moments at high speeds and the deformations of the elevator tab (cf. infra, Chapter XI).

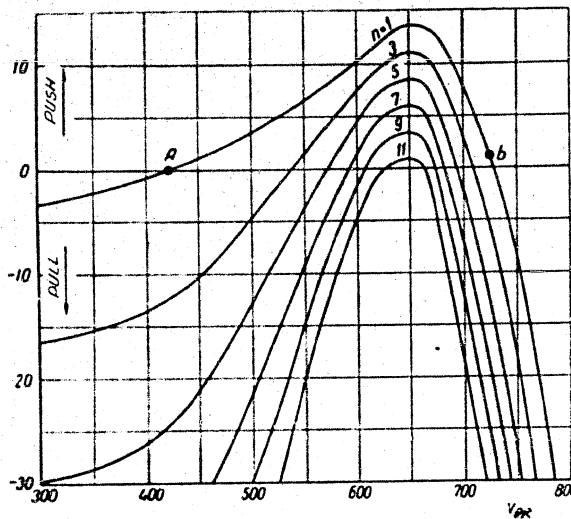


Fig.9.17 - Balancing Force on Stick in Steady Rectilinear Flight ($n = 1$) and in Steady Curvilinear Flight, at Various Values of Overload

The increase in climbing moments and the decrease in static stability with respect to the load at high speeds may be the cause of easy or even accidental production of high loads on the aircraft.

To give a more graphic and clear idea of this, let us look at Fig.9.17 showing the balancing curve of the stick forces for steady rectilinear flight and for steady curvilinear flight, at various values of the load factor $n = \text{const}$. The curves shown in Fig.9.17 were obtained by calculation, starting from the variation in

POOR ORIGINAL

static stability with respect to flying speed and load conditions shown in Fig.9.13, and under the above assumptions that the coefficients $m_{\dot{\omega}}^{\delta}$ and $m_{\dot{\omega}}^{\delta}$ are constant and that $m_{\dot{\omega}}^{\alpha} = 0$; the coefficient of damping moment $m_{z\dot{\omega}}^{\alpha}$ was likewise taken as constant and independent of the Mach number.

Let us now imagine that the pilot, being in a state of rectilinear flight Γ (Fig.9.17), for some reason releases the stick. Since, in the initial state of flight Γ , the pilot pushes the stick forward, it will deflect toward the pilot when released. Accordingly, the elevator will be deflected upward, producing a longitudinal moment tending to turn the aircraft into the stable balancing state A .

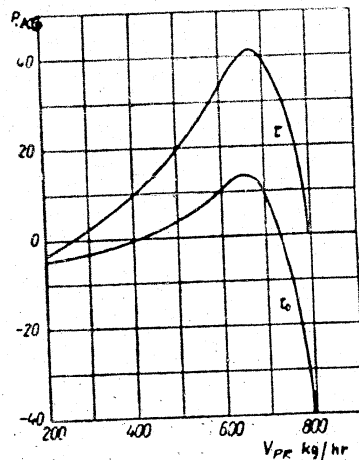


Fig.9.18 - Balancing Curves of Stick Forces at Two Positions of the Elevator Tab

As follows from Fig.9/17, in this example, the value of the overload obtained at such a motion of the aircraft, in stick-free flight ($P = 0$), may attain the maximum $n_{\max} = 11-12$ in the field of maxima on the curves $P = f(V)$. The second dangerous case of obtaining a destructive load factor may arise

POOR ORIGINAL

0 when the aircraft is pulled up out of an "induced" dive by the aid of the elevator
 2 tab or the stabilizer control during flight. Let us assume that the pilot, not
 4 being able to direct action on the stick alone to pull the aircraft out of the
 6 dive, makes use for this purpose of a deflection of the tab or stabilizer. By
 8 changing the position of the latter control surfaces, the pilot is able to produce
 10 a moment sufficient to pull the aircraft out of the dive without excessive stick
 12 forces, but the pilot will then be unable to cope with the climbing moments, even
 14 those caused only by the deflection of the tab or stabilizer for pulling out of
 16 the dive (Fig. 9.16).

18 In order to exclude these dangerous cases of loss of control, the character-
 20 istics of stability and controllability of the aircraft must be carefully investi-
 22 gated while it is being designed. Correct layout of the aircraft and proper selec-
 24 tion of wing and tail profiles should exclude any considerable variation in longi-
 26 tudinal moments (m_x) in the region of high Mach numbers.

POOR ORIGINAL

CHAPTER X

METHODS OF SELECTING THE DEGREE OF STABILITY OF AN AIRCRAFT

General Remarks

The selection of the degree of longitudinal static stability of an aircraft and of the corresponding design parameters is determined by the necessity of satisfying a number of demands made on the behavior of the aircraft in rough air, on its controllability in maneuvers, on an adequate elevator reserve for landing, pulling out of a tail spin, etc. In addition, the industrial facilities available for accurate realization of the corresponding design parameters (for example, the aerodynamic elevator balance) must also be taken into account in selecting the stability. These conditions must be considered together; the method of selecting the degree of stability must permit determination of the most expedient combination of structural design parameters (tail area, centering of aircraft, value of aerodynamic elevator balance, etc.) satisfying these conditions.

Before considering the possible methods of selecting the degree of stability, it is necessary to analyze in detail the individual and determining conditions. These basic conditions might include the behavior of the aircraft in bumpy flight ("steady march" of the aircraft) and the aircraft's ability to "follow" the stick (controllability of the aircraft in maneuvers).

Behavior of the Aircraft in Bumpy Flight

When external atmospheric disturbances act on the aircraft (in flight through

POOR ORIGINAL

0 a "bump"), it is desirable to have the aircraft deviate as little as possible from
2 the original state of flight and to have the pilot intervene as little as possible
4 in the control to restore the aircraft to the original state of flight. To evaluate
6 the behavior of the aircraft in bumpy flight, pilots use the expression "firmness of
8 seating" of the aircraft in the air, or "firmness of travel" of the aircraft.
10
12
14
16
18
20
22
24
26
28
30
32
34
36
38
40
42
44
46
48
50
52
54
56

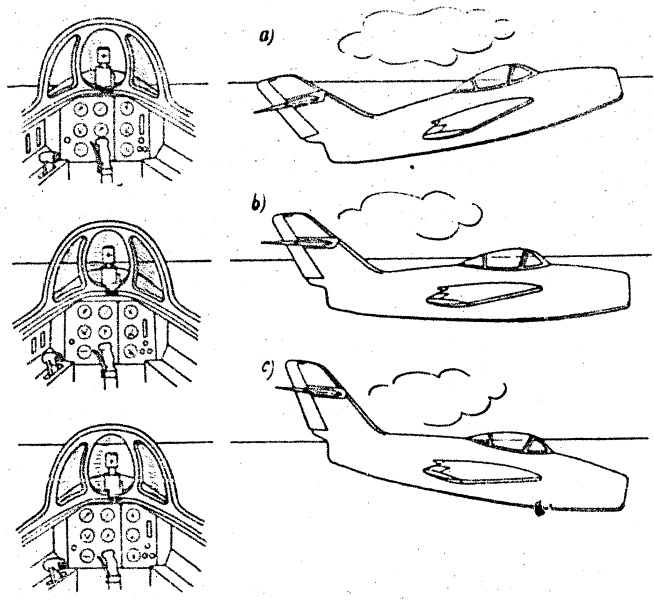
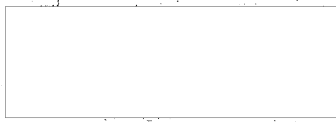


Fig.10.1 - Position of Aircraft Engine Nacelle with Respect to the
Horizon in Various States of Flight
a - Low Speed; b - Cruising speed; c - Dive

In theoretical studies, as an index of the "firmness of seating" of the aircraft, the degree of variation of the angle of pitch ($\Delta \theta$) under the influence of the action of atmospheric disturbances is commonly used. The less the variation in angle of pitch in flight through a bump, the more "firmly seated" in the air



POOR ORIGINAL

0 the airplane is considered to be.

2 The choice of the angle of pitch as the principal parameter for evaluating an
4 aircraft is based on the consideration that the pilot usually flies the aircraft by
6 orienting himself from the position of the engine nacelle with respect to the hori-
8 zon.

10 From the position of the nacelle with respect to the horizon, the pilot judges
12 the attitude and the deviations from this state (Fig.10.1). If the aircraft, under
14 the action of each individual disturbance, maintains a constant angle of pitch, then,
16 after the action of the disturbance has ended, the equilibrium of forces along the
18 normal and along the tangent to the flight path is not disturbed and the aircraft
20 will continue its flight in the earlier attitude.

22 It may be assumed that, in addition to the reaction of the engine nacelle, with
24 respect to the horizon, the change in the balancing of the aircraft on flight
26 through a bump, the load factors continuously acting on the aircraft, and other
28 factors, likewise exert an influence on the pilot's judgement as to the stability
30 of course.

32 A certain idea of the motion of the aircraft in a bump may be obtained by a
34 glance at the instrument records made during flight on an aircraft weighing 3000 kg,
36 as shown in Fig.1.3 (cf.1). The flight was made on a summer day at a wind speed
38 of about 4 m/sec (with gusts running up to 7 m/sec) and in the presence of vertical
40 displacement of air masses leading to the formation of cumulus clouds. The value
42 of the static stability of the aircraft was defined by the quantity $n_z^{C_L} = -0.08 +$
44 $+ -0.10$.

46 As follows from Fig.1.3, the aircraft continuously encountered atmospheric
48 disturbances. The intervals between the individual "shocks" of the bump varied
50 from 0.5 sec to 2.5 sec. The rise and fall of the load component n_y at each "shock"
52 occupied a definite time interval. The maximum values of the angular velocity of
54 pitch did not exceed 1.5-2.5% per second. The change in the angle of pitch did not
56

POOR ORIGINAL

0 exceed 1.5° . In rectilinear flight on an assigned course the pilot allowed a deviation
 2 of the flying speed from its mean value within the limits of 10 km/hr.

4 We remark that the structure of the air currents, i.e., their dimensions, directions,
 6 rections, and velocity distribution of the air motion in each of the individual
 8 currents vary and have not been much studied to date.

10 In the theoretical investigation of the aircraft motion through a bump, a
 12 number of simplifying assumptions are made in view of the complexity of the question.
 14 But the results of the theoretical analysis depends to a very great extent on the
 16 original assumptions on which it is based. The complexity and unfamiliarity of the
 18 phenomena under discussion lead to a rather considerable degree of arbitrariness in
 20 the selection of these assumptions and, consequently, also to a considerable degree
 22 of arbitrariness in the conclusions of the theory.

24 Modern theory does not take into consideration, for example, with sufficient
 26 accuracy, such factors as the nonstationary character of the aerodynamic process
 28 during flight in rough air, the structure of the air currents (disturbances), the
 30 entry of the aircraft into an air pocket (at first the wing and then the tail
 32 assembly), etc.

34 For this reason, an evaluation of the motion of aircraft in a bump will be
 36 based on the results of flying practice. Actual flight experience shows that the
 38 increase in static stability to substantial values favorably affects the behavior
 40 of the aircraft in a bump. According to the reports of pilots, the "firmness of
 42 travel" of an aircraft flying through a bump is increased with increasing static
 44 stability. In the consideration of aircraft of widely varying types it has been
 46 found that, according to the results of flying practice, no example can be cited
 48 of an aircraft with a high degree of longitudinal static stability that behaved
 50 unsatisfactorily in flight through a bump, due to large fluctuations of the angle
 52 of roll.

54 Two facts must be noted in the reports of pilots in this connection; first
 56

POOR ORIGINAL

0 a pilot senses any unsatisfactory behavior of an airplane in a bump if its degree
2 of stability is low; secondly, a pilot fails to note any substantial difference in
4 the behavior of aircraft with moderate and high longitudinal static stabilities in
6 flying through a bump.

8 Thus the experience of flight tests proves that it is desirable to increase
10 the degree of longitudinal static stability with respect to overload (n_{CL}), in order
12 to improve the behavior of an aircraft in rough air.

14 Theory does not give exact limits for the increase of static stability, but
16 flying experience indicates that a very high degree of stability is not essential
18 from this point of view.

20 We shall see from what follows that the remaining conditions enumerated at the
22 beginning of this Chapter do not allow the degree of longitudinal static stability
24 to be increased without limit; these conditions, however, give upper limits for the
26 increase in static stability.

28 To recapitulate, we will consider that the degree of longitudinal static stability
30 required by flight in rough air is covered by the other conditions. Consequently,
32 we will not introduce the condition of flight in rough air as a separate
34 matter for calculation in our practical selection of the degree of stability.

36 Controllability of the Aircraft during a Maneuver.

38 General Considerations

40 The influence of the degree of static stability on the controllability of an
42 aircraft during a maneuver will now be considered by analyzing the aircraft's ability
44 to "follow" the stick. This property may be characterized on the one hand by
46 the lag in the reaction of the aircraft to the deflection of the stick and to the
48 force applied to the stick, and on the other hand, by the relation between the
50 stick force or the stick deflection and the value of the change in the parameters
52 of aircraft motion produced thereby (load factor, angle of pitch, angular velocity,
54
56



POOR ORIGINAL

etc.) in executing various types of maneuvers. For the reasons given above (cf. Chapter IX), it is convenient, in analyzing the "following" of the stick by the aircraft, to select a single parameter, namely the overload, out of all the parameters of aircraft motion.

The ability of the aircraft to "follow" the stick is manifested most distinctly when we consider the relatively sharp maneuvers executed during a short time interval, so that the flying speed may be considered constant during its entire period. The relation between the variation of stick force and the variation in overload at $V = \text{const}$ is determined by eq.(9.31) of Chapter IX:

$$\tau P_2 \frac{d^2 \Delta P}{dt^2} + \tau P_1 \frac{d \Delta P}{dt} + P^0 \Delta P = \Delta P. \quad (9.31)$$

The physical meaning of the quantities P_2^n , P_1^n , and P^0 has already been considered in Chapter IX during our analysis of eq.(9.23), and we will therefore not discuss the question further.

Equation (9.31) is a second-order differential equation with constant coefficients and with a right-hand side which, in the general case, is an arbitrary function of time. Thus we know the values of τ , P_2^n , P_1^n , and P^0 ; on assuming the law of variation of ΔP with time, we can determine the corresponding time variation of the load and, consequently, using the general equations of motion, also the variation of all the other parameters of aircraft motion. To obtain the same reaction of two aircraft of different types to one and the same stick force ΔP (in other words, to obtain the same controllability), it is sufficient, as follows from eq.(9.31), that the values of $\tau^2 P_2^n$, τP_1^n , and P^0 are the same in both aircraft.

The quantity $\tau = \frac{2m}{\rho S V} = \frac{2G}{\rho g V S}$ is determined from the value of the relative wing loading $\frac{G}{S}$, the altitude (the parameter ρ), and the flying speed. For this reason, it is possible in actual flying to influence the characteristics of controllability of a specific aircraft by varying only the values of P_2^n , P_1^n , and P^0 . These values might be taken as criteria for evaluating longitudinal controllability. For

POOR ORIGINAL

0 the combined analysis of the actual (dynamic) stability and controllability of the
 2 aircraft, however, it is more convenient to take, as the criteria, the value
 4 of P^{η} and the quantities that determine the period and damping of the short-period
 6 oscillations of the aircraft. This can be proved by the example (given below) of
 8 the analysis of a schematized maneuver, that of vibration of an aircraft produced
 10 artificially by the pilot. In considering this maneuver, we will make a detailed
 12 analysis of the aircraft properties from the point of view of its "following" the
 14 stick.

The Initial Equations

16 Since any timewise variation of the stick force $P = f(t)$ may be approximately
 18 represented by a series of the form

$$\Delta P = \sum_{l=0}^{l=1} \Delta P_l \sin \omega_l t,$$

20 let us take an elementary schematized action of the pilot.

22 Let the pilot, beginning at the time $t = 0$, vary the stick force by the sine
 24 law

$$\Delta P = \Delta P_0 \sin \omega t$$

26 Then, instead of eq.(9.31), we may write

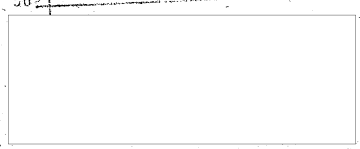
$$\rho^2 P_2^{\eta} \frac{d^2 \Delta \eta}{dt^2} + \rho P_1^{\eta} \frac{d \Delta \eta}{dt} + P^{\eta} \Delta \eta = \Delta P_0 \sin \omega t. \quad (10.1)$$

28 On dividing both sides of eq.(10.1) by $\rho^2 P_2^{\eta}$, we may write it in the form

$$\frac{d^2 \Delta \eta}{dt^2} + 2h \frac{d \Delta \eta}{dt} + k^2 \Delta \eta = q \sin \omega t, \quad (10.2)$$

30 where the constant quantities $2h$, k^2 , and q are defined by the formulas

$$2h = \frac{P_1^{\eta}}{\rho P_2^{\eta}} \quad (10.3)$$



POOR ORIGINAL

$$\left. \begin{aligned} k^2 &= \frac{P^2}{\sqrt{P_2^2}} \\ q &= \frac{M P_0}{\sqrt{P_2^2}} \end{aligned} \right\} (10.3)$$

Let us now find the relation between the coefficients $2h$ and k^2 and the coefficient of the characteristic equation for the short-period disturbed motion of the aircraft.

If we take the expanded expressions of eq.(9.32) for P_2^2 , P_1^2 , and P^2 , substitute them in eq.(10.3), and compare the result with eq.(8.17) or eq.(8.3), we may

$$\left. \begin{aligned} 2h &= \frac{a_1}{v} = \frac{1}{v} \left[a - \frac{m_{\dot{\alpha}}^2 + m_{\dot{\alpha}\alpha}^2}{T} \right] \\ h^2 &= \frac{a_2}{v^2} = -\frac{a}{v^2} \frac{m_{\dot{\alpha}}^2 + m_{\dot{\alpha}\alpha}^2}{T} \end{aligned} \right\} (10.4)$$

where a_1 and a_2 are the coefficients of the characteristic equation determining the short-period disturbed motion of the stick-free aircraft. This characteristic equation corresponds in this case to the dimensionless form of the equations of disturbed motion of the aircraft. It is not difficult to show that if, in setting up and solving the equations of disturbed longitudinal motion, the time is taken in the usual units (t in seconds), instead of in the dimensionless form ($\bar{t} = \frac{t}{T}$), then the coefficients of such a characteristic equation, a_1 and a_2 , will be equal respectively to the coefficients $2h$ and k^2 .

It follows from this that the controllability of the aircraft in executing sharp maneuvers ($v \approx \text{const}$) and, in particular, the aircraft's ability to "follow the stick" is determined by the very same parameters that determine the characteristics of the short-period disturbed motion.

This relation between the characteristics of aircraft controllability and the characteristics of the disturbed motion of the aircraft is not hard to understand, even on the basis of simple physical considerations.

POOR ORIGINAL

0 For example, let the pilot, in some steady state of flight, instantaneously
 2 deflect the elevator by a certain quantity of $\Delta\delta = \text{const}$ and then keep the new
 4 position of the elevator constant. The new position of the elevator there corre-
 6 sponds to a definite steady attitude which, with a stable aircraft, is established
 8 after a definite time interval has elapsed following this deflection of the eleva-
 10 tor. The transitional period between the initial and the following steady attitudes
 12 will be one of unsteady or disturbed motion, obeying the same laws as the disturbed
 14 motion due to any cause other than the deflection of the elevator, but under the
 16 same initial deviations of the parameters of aircraft motion. In the example under
 18 consideration, the initial deviations of each of the parameters of motion are re-
 20 presented by the difference between their values in the initial state of flight and
 22 the following steady state of flight.

24 The smooth motion of the control surface may be considered a continuous chain
 26 of individual instantaneous disturbances of infinitesimal duration*, acting on the
 28 aircraft. For this reason, the aircraft motion produced by the pilot will be re-
 30 presented as a special form of disturbed motion. The general solution of eq.(10.2)
 32 may be represented in the form

$$\Delta\delta = C_1 e^{\lambda_1 t} + C_2 e^{\lambda_2 t} + N \sin(\omega t - \gamma) \quad (10.5)$$

34 where λ_1 and λ_2 are the roots of the characteristic equation

$$\lambda_1 = -A + \sqrt{A^2 - B^2}$$

$$\lambda_2 = -A - \sqrt{A^2 - B^2}$$

36
 38
 40
 42
 44
 46
 48
 50 * We are here concerned with the short time interval following the deflection of
 52 the elevator. The flying speed may thus be considered to be approximately con-
 54 stant.
 56

POOR ORIGINAL

The values of N and γ are determined by means of the formulas

$$\left. \begin{aligned} N &= \frac{q}{\sqrt{(\lambda_1^2 - \omega^2)^2 + 4\lambda_1^2 \omega^2}} \\ \operatorname{tg} \gamma &= \frac{2\lambda_1 \omega}{\lambda_1^2 - \omega^2} \end{aligned} \right\} \quad (10.6)$$

The quantities C_1 and C_2 are arbitrary constants in the general solution of the differential equation (10.2) and are determined from the assigned initial conditions.

Next, we will describe the methods of finding the values of N , λ_1 , C_1 , and C_2 .

It is obvious that the expression

$$\Delta n_2 = N \sin(\omega t - \gamma) \quad (10.6')$$

is a particular solution of eq.(10.2). By finding the derivatives $\frac{d\Delta n_2}{dt}$ and $\frac{d^2\Delta n_2}{dt^2}$ by differentiating eq.(10.6') and substituting them in eq.(10.2), we will have

$$-\omega^2 N \sin(\omega t - \gamma) + 2\lambda_1 \omega N \cos(\omega t - \gamma) + \lambda_1^2 N \sin(\omega t - \gamma) = q \sin \omega t.$$

Setting $t = 0$, we have

$$\operatorname{tg} \gamma = \frac{2\lambda_1 \omega}{\lambda_1^2 - \omega^2}.$$

Setting $\omega t = \gamma$, and replacing $\sin \gamma$ by its expression in terms of $\operatorname{tg} \gamma$, we obtain

$$N = \frac{q}{\sqrt{(\lambda_1^2 - \omega^2)^2 + 4\lambda_1^2 \omega^2}}.$$

To determine the arbitrary constants C_1 and C_2 in eq.(10.5) let us, for example, assume that for $t = 0$, $\Delta n = \frac{d\Delta n}{dt} = 0$. Thus, we obtain

$$C_1 = \frac{N(\lambda_2 \sin \gamma + \omega \cos \gamma)}{\lambda_2 - \lambda_1};$$

$$C_2 = -\frac{N(\lambda_1 \sin \gamma + \omega \cos \gamma)}{\lambda_2 - \lambda_1}.$$

In this case,

$$\lambda_2 < \lambda_1.$$

Then the roots λ_1 and λ_2 will be complex and mutually conjugate. In this case, the

POOR ORIGINAL

0 general solution of eq.(10.2) can be represented (cf.Chapter VII) in the form

$$\Delta z = A e^{-\mu t} \sin(\omega t - \alpha) + N \sin(\omega t - \gamma) \quad (10.7)$$

2 where

$$\omega = \sqrt{P^2 - \mu^2}$$

4 while the quantities A and α are arbitrary constants determined from the initial

6 conditions.

8 In both solutions (10.5) and (10.7), the expressions

$$\Delta z_1 = C_1 e^{\mu t} + C_2 e^{-\mu t}$$

12 or

$$\Delta z_1 = A e^{-\mu t} \sin(\omega t - \alpha)$$

14 correspond to the motion of the aircraft due to the instantaneous initial disturb-

16 ance (such motions are considered above in Chapter VIII) or by the so-called proper

18 motion of the aircraft, which may be either aperiodic or oscillatory with frequen-

20 cy ω .

22 The expression

$$\Delta z_2 = N \sin(\omega t - \gamma)$$

24 corresponds to the so-called forced oscillations of the aircraft at a frequency ω ,

26 due to the existence of the right-hand side in eq.(10.1).

28 General Analysis of the Aircraft's Ability to "Follow" the Stick

30 Let us begin the general analysis of the aircraft's ability to "follow" the

32 stick with a specific example to enable the reader to get a clearer conception of

34 the reasoning that will follow.

36 Let us take an aircraft with the same structural and aerodynamic parameters

38 as that considered in Chapter IX. Let us assume that the pilot, beginning at a

POOR ORIGINAL

definite instant of time, varies the stick force by the law

$$\Delta P = -3 \sin \frac{2\pi}{4} t,$$

thereby deflecting, in a definite way, the control stick and the elevator. Let us further determine the time variation of the load, using the above equations and

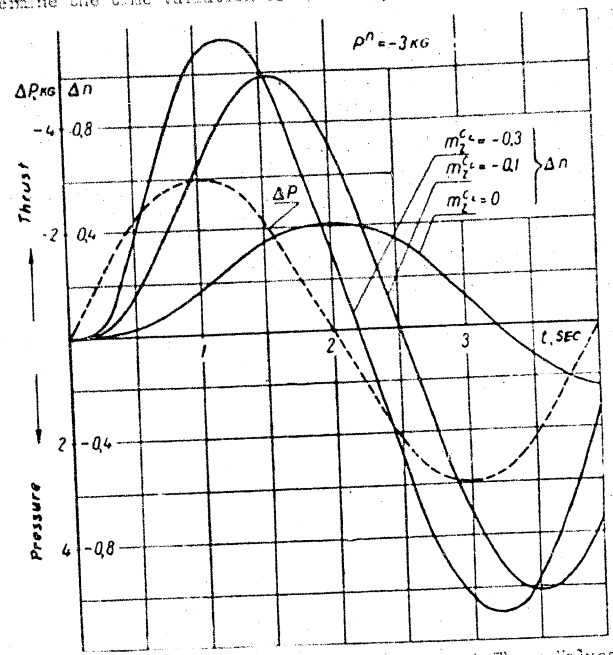


Fig. 10.2 - Variation in Overload with Time, at Three Values of the Coefficient of Stick-Free Static Stability, for p^n const, with the Stick Force Varying by the Law

$$\Delta P = -3 \sin \frac{2\pi}{4} t$$

three values of the coefficient of longitudinal static stability at overload (m_z^C) under the condition that the criterion in all cases is $p^n = -3 \text{ kg}$, in accordance with the above equation for P, having a period of variation of the stick force of $T_{\text{max}} = 4 \text{ sec}$.

Figure 10.2 shows the time variation of the overload as obtained by calculation.



POOR ORIGINAL

tion. Obviously, the reaction of the aircraft lags with respect to the variation in stick force. After a lapse of 0.1-0.2 sec from the beginning of the aircraft motion, the load conditions remain practically unchanged; the maximum values of n in absolute magnitude are obtained later than the maximum values of P . A further

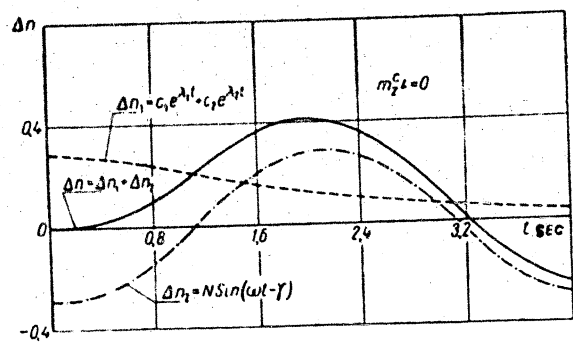


Fig.10.3 - The Two Summands and the Resultant Variation in Overload in a Fighter Plane, Neutral with Respect to Static Stability ($m_2^0 L = 0$), at the Beginning of the Forced Oscillation

analysis of the curves in Fig.10.2 shows that the lag of the reaction of the aircraft decreases very substantially with increasing static stability of the aircraft. In addition, even the absolute variations of the load factor differ substantially.

To evaluate the significance of the summands Δn_1 and Δn_2 , i.e., of the significance of the proper motion of the aircraft, and its forced motion, respectively, these summands are shown separately in Figs.10.3, 10.4, and 10.5 where their resultant $\Delta n = \Delta n_1 + \Delta n_2$ is also presented. From a consideration of these graphs, for example shows that if, at $t = 0$, the summands Δn_1 and Δn_2 are equal in absolute value, then the role of the component of proper motion declines rather rapidly; after the lapse of a definite time interval, the motion of the aircraft is determined by the component Δn_2 , i.e., by the motion of the aircraft forced by the

POOR ORIGINAL

elevator. We remark that, at increasing stability, the role of the proper motion of the aircraft declines; at $m_{\xi}^C L = -0.1$ and $m_{\xi}^C L = -0.3$, the summand Δn_1 may be, in practice, neglected after the lapse of about 0.8 sec from the beginning of motion.

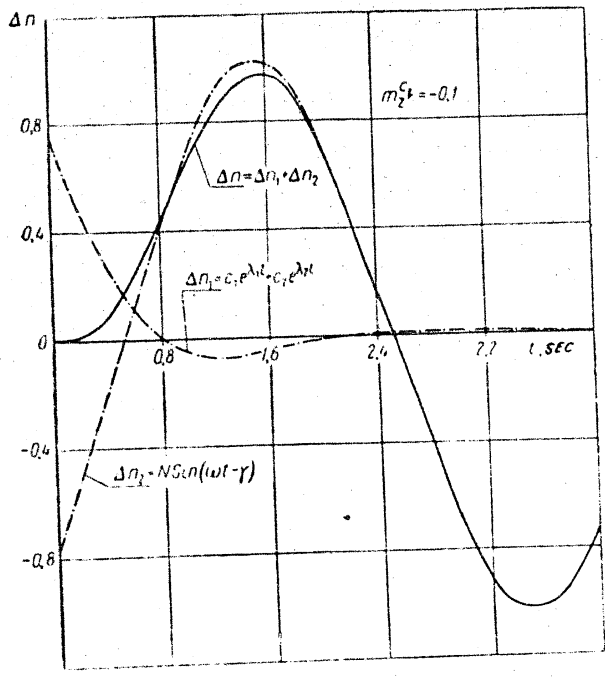
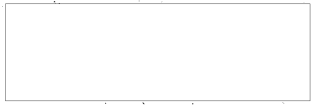


Fig. 10.4 - The Two Summands and the Resultant Variation in Overload in a Fighter Plane with a Coefficient of Static Stability $m_{\xi}^C L = -0.10$ at the Beginning of the Forced Oscillations

The example confirms the fact that the ability of the aircraft to respond to the actions of the pilot depends substantially on the design and aerodynamic parameters of the aircraft.

The theoretical analysis of the influence of these parameters on the proper



POOR ORIGINAL

0 motion of the aircraft is very complex in the general form. The quantities C_1 , C_2 ,
 2 A and α , which enter into the analytical expressions for the summand of the proper
 4 motion Δn_1 , are complex functions of the quantities λ_1 , λ_2 , h , k , and ω . We will
 6 therefore disregard this analysis and will confine the discussion to the general

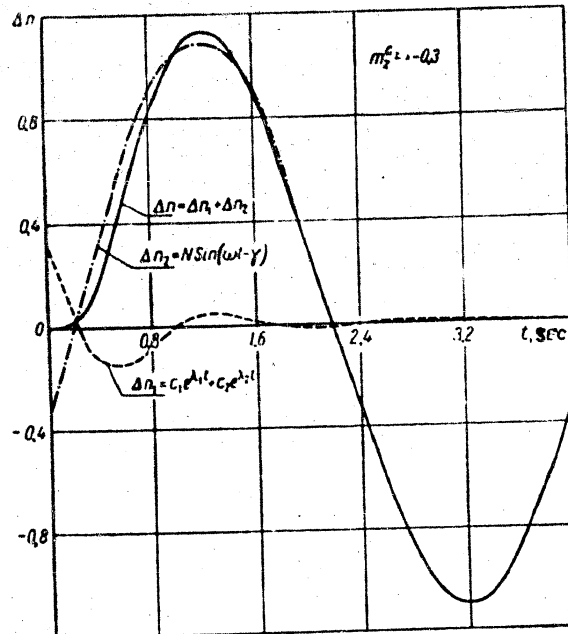


Fig. 10.5 - The Two Summands and the Resultant Variation of Load Factor
 in a Fighter Plane with the Coefficient of Static Stability $\bar{L} = -0.30$
 at the Beginning of the Constrained Oscillations

conclusion that the more rapidly the proper motion of the aircraft is damped, the
 more accurately the aircraft will "follow" the stick.

The damping of the proper motion of the aircraft is determined by the value
 of the coefficient of damping h . In designing a new aircraft, provision must be
 made for the necessary damping of the proper short-period disturbed motion of the

POOR ORIGINAL

aircraft.

Let us analyze the forced motion of the aircraft characterized by the particular solution of eq.(10.2)

$$\Delta n_2 = N \sin(\omega t - \gamma)$$

The quantity N characterizes the maximum variation in overload n_{\max} , which the aircraft will have under the assigned law of change in stick force:

$$\Delta P = \Delta P_0 \sin \omega t$$

while the quantity γ is the phase lag of the variation of load factor with respect to the variation of stick force.

If $\gamma = 0$, then, as shown by a comparison of the expressions for ΔP and Δn_2 , the load acting on the aircraft at each instant of time is directly proportional to the force applied by the pilot, i.e., the overload obeys the stick force with no lag whatever. The more γ differs from zero, the greater will be the lag of the overload with respect to the stick force.

For γ and N , the following expressions were obtained above

$$\left. \begin{aligned} \operatorname{tg} \gamma &= \frac{2h\omega}{k^2 - \omega^2}; \\ N &= \Delta n_{\max} = \frac{q}{\sqrt{(k^2 - \omega^2)^2 + 4h^2\omega^2}}. \end{aligned} \right\} \quad (10.4)$$

Making use of eq.(10.3), we can replace eq.(10.4) by

$$\left. \begin{aligned} \operatorname{tg} \gamma &= \frac{2r\psi}{1 - \psi^2}; \\ \Delta n_{\max} &= \frac{\frac{\Delta P_0}{P^0}}{\sqrt{(1 - \psi^2)^2 + 4r^2\psi^2}}. \end{aligned} \right\} \quad (10.5)$$

* The maximum value of the sine of any angle is equal to unity. For this reason

$$\sin(\omega t - \gamma)_{\max} = 1 \text{ and } \Delta n_{\max} = N.$$

POOR ORIGINAL

where

$$\left. \begin{aligned} \eta &= \frac{h}{k}, \\ \psi &= \frac{a}{k}. \end{aligned} \right\} \quad (10.9)$$

The quantities η and ψ are important parameters for analyzing the motion of the aircraft and its ability to "follow" the stick. We remark that these parameters are always used in technology in the analysis of phenomena, mathematically characterized by second-order differential equations with constant coefficients like our initial eq.(9.31).

The quantity ψ characterizes the relation of the coefficient of damping in the aircraft (mechanical or electromagnetic system) and the natural frequency of the aircraft (or system), as follows from eq.(10.4),

$$\psi = \frac{h}{k} = \frac{a_1}{2V a_2} = \frac{a \frac{m_1^2 + m_2^2}{r_1^2}}{2 \sqrt{-a \frac{\mu m_1^2 + m_2^2}{r_1^2}}}. \quad (10.10)$$

In the theory of dynamic stability, the period of oscillations T and the time t_2 in which the initial amplitude of the vibrations is damped to half its value, are considered as the characteristic quantities (cf. Chapter VIII). We remark that these quantities T and t_2 have a simple correlation with the parameters k and η . The period T of the natural short-period oscillations of the aircraft is determined by the formula

$$T = \frac{2\pi}{\omega} = \frac{2\pi}{\sqrt{k^2 - h^2}} = \frac{2\pi}{k\sqrt{1 - \eta^2}}.$$

Hence

$$k = \frac{2\pi}{T\sqrt{1 - \eta^2}}. \quad (10.11)$$

POOR ORIGINAL

The quantity ψ characterizes the ratio of the frequency of the forced oscillations to the natural frequency of the aircraft (or system) or the ratio of the period of the natural short period oscillations of the aircraft T_{nat} to the period of the forced oscillations T_{forced} . If we use the well-known relation between the period of oscillations and angular velocity, we may write

$$h = \frac{2\pi}{T_{nat}} \quad \text{AND} \quad \psi = \frac{2\pi}{T_{forced}}$$

Hence

$$\psi = \frac{h}{\lambda} = \frac{T_{nat}}{T_{forced}}$$

In this case, as follows from eq.(10.9), the natural frequency is arbitrarily taken without allowing for the damping ($h = 0$). The actual natural frequency of the aircraft will be equal to $m = k^2 - h^2$. Only at sufficiently high static stability will the actual natural frequency of the short-period oscillations of the aircraft be equal to its conventional natural frequency ($m \approx k$).

Symbols of "Following" the Stick

In order to analyze the ability of an aircraft to "follow" the stick, it is useful to define the symbols to be used for evaluating this ability.

It is convenient to take the quantity γ of the phase lag of the aircraft reaction to the pilot's action as one of such symbols.

Let us take as the second symbol for "following" the stick, the coefficient λ , which characterizes the ratio of the stick force (or stick displacement) necessary for changing the overload of the aircraft by unity ($\Delta n = 1$) under forced oscillations at finite frequency, to the stick force necessary for changing the overload by unity under static conditions. Here, the term static conditions means a very smooth transition at infinitesimal frequency from one steady state of flight, and in particular, from a rectilinear flight to another steady (curvilinear) state of

POOR ORIGINAL

0 flight at a different load but at the same flying speed for both states of flight.
 2 We will demonstrate that the quantity λ is a function only of the two param-
 4 eters η and ψ , just as is the case for the quantity γ .
 6

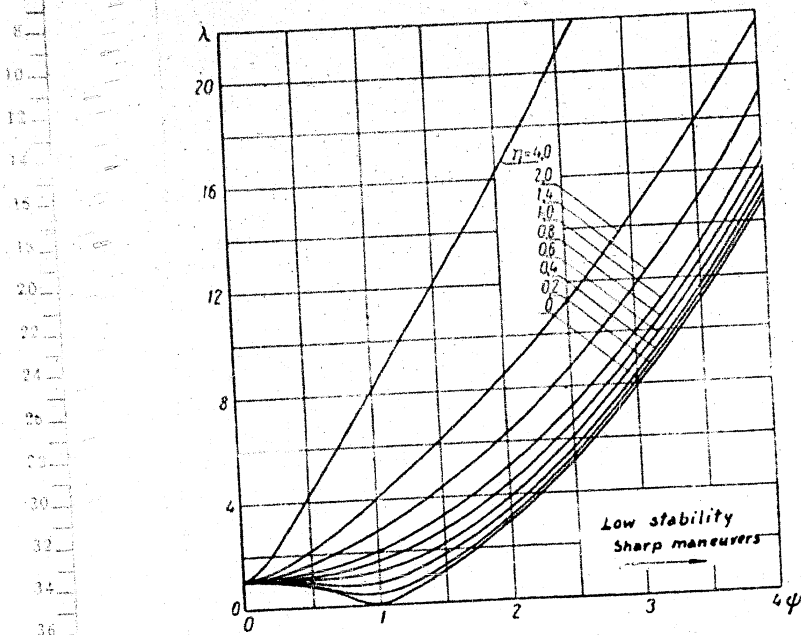


Fig.10.6 - Variation in the Coefficient of Dynamic Increase of λ as a Function of ψ at Various Values of η

Let us assume that, under forced oscillations, the value of $\Delta n_{max} = N = 1$.
 Corresponding to this condition, the value of the stick force ΔP_0 is found from eq.(10.8) to be as follows:

$$\Delta P_0 = \frac{N}{\sqrt{1 - \eta\psi + \eta^2\psi^2}} \quad (10.12)$$

The magnitude of the stick force necessary for changing the load under static conditions is determined from eq.(9.31), bearing in mind that, in this case,



POOR ORIGINAL

$$\frac{d^2 \Delta n}{dt^2} = \frac{D \Delta n}{dt} = 0 \text{ and } \Delta n = 1.$$

Then

$$P_{st} = p^n \quad (10.13)$$

On dividing eq.(10.12) by eq.(10.13), we obtain

$$\frac{\Delta P_0}{\Delta P_{cr}} = \lambda = \sqrt{(1 - \psi^2)^2 + 4\gamma^2 \psi^2}. \quad (10.14)$$

Making use of eq.(10.9), we may rewrite the expression for λ in the form

$$\lambda = \frac{\sqrt{(k^2 - \omega^2)^2 + 4\eta^2 \omega^2}}{k}. \quad (10.15)$$

The quantity λ will be denoted as the dynamic coefficient of stick force.

To give a more lucid idea on the variation of symbols "following the stick", as a function of the parameters η and ω , the corresponding curves are plotted in Figs.10.6 and 10.7.

Figure 10.7 is the conventional diagram of the family of curves characterizing the phase shift in the consideration of the classical problem of the theory of oscillations, at resonance. If λ is replaced by its reciprocal $\frac{1}{\lambda}$, we obtain the second classical diagram (Fig.10.8, cf. also Fig.10.6) of the ratio of amplitudes used in the analysis of resonant phenomena*. In the analysis of controllability, however,

* We recall that in the theory of oscillations, resonance represents a sharp increase in amplitude of the oscillations, where the frequency of the forced oscillations and that of the natural oscillations of the system coincide. In the presence of considerable damping, the case of coincidence of frequencies cannot be differentiated so that the corresponding curves in Figs.10.8 and 10.10 have a smooth course.

POOR ORIGINAL

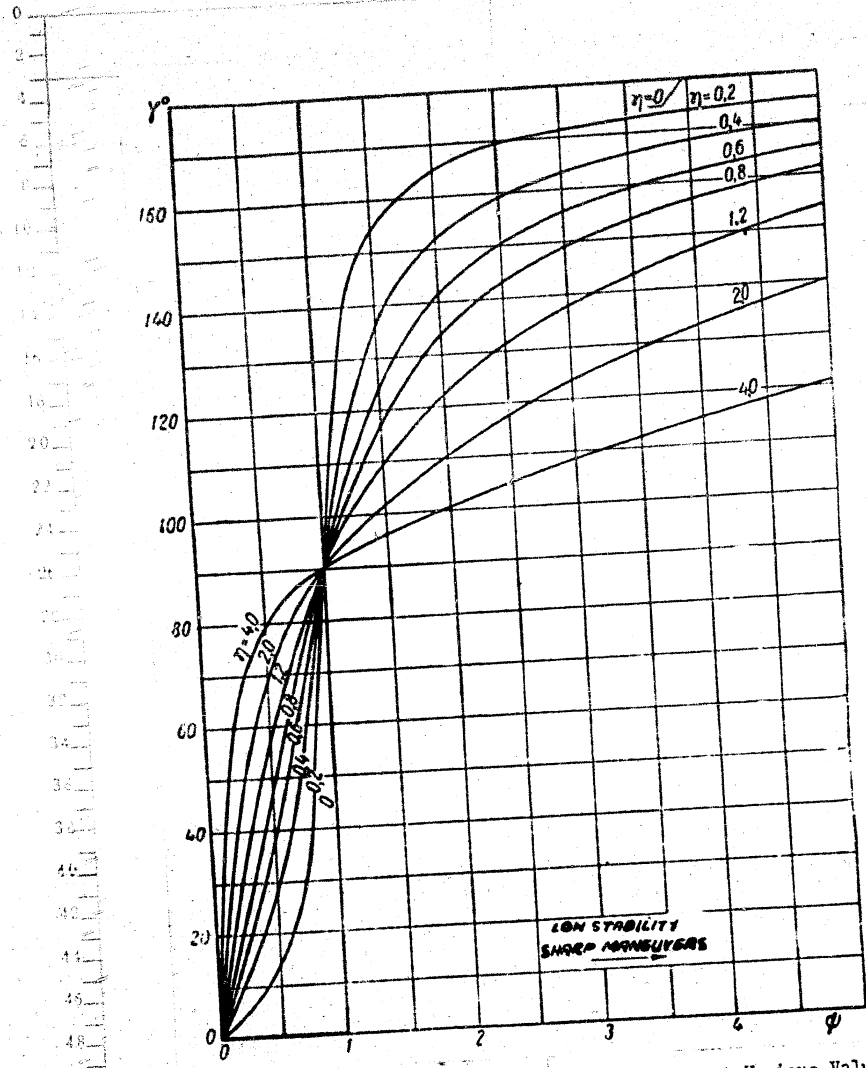


Fig.10.7 - Angular Phase Shift as a Function of ψ at Various Values of η



POOR ORIGINAL

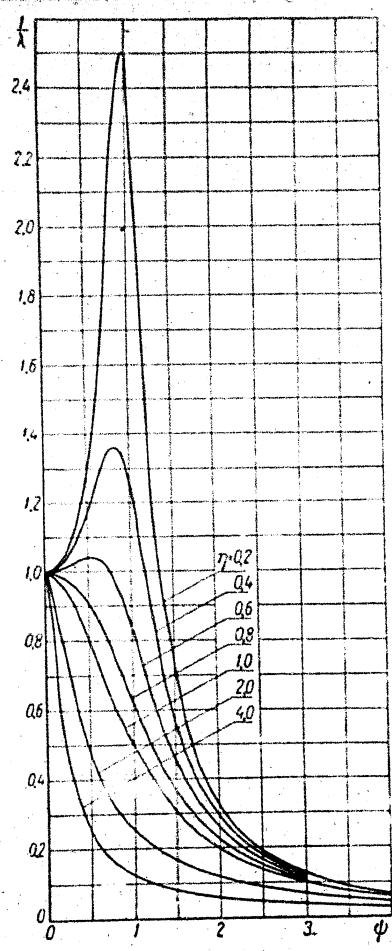


Fig.10.8 - Resonant Curve of Variation of Amplitude of Forced Oscillations of System at Various Values of η

it is more convenient to use the quantity λ instead of $\frac{1}{\lambda}$.

Let us now consider, in somewhat more detail, the influence of the basic design parameters and of the state of flight on the ability of the aircraft to "follow" the stick.

The limit for "following" the stick will be the point at which the overload follows the variation in stick force and the position of the stick with no lag whatever ($\lambda = 0$), while the value of the overload, at any instant of time, is strictly proportional to the values of ΔP and δx_p to which $\lambda = 1$ corresponds.

If these conditions are satisfied, $P_2^0 \approx P_1^0 \approx 0$ and eq.(9.31) are transformed into the simpler equation

$$\Delta P = P^0 \Delta n$$

Equation (9.25) shows that these conditions could be satisfied theoretically in two ways. The first way would be to give the aircraft an infinitely high static stability, an infinitely great elevator efficiency, and an infinitely great aerodynamic elevator balance, thus ensuring a value of the stick force that would

POOR ORIGINAL

be acceptable to the pilot. This latter condition can be realized with a constant stick force, necessary for the constant increase in overload, which is equivalent to the condition $pn = \text{const}$. The second way would be to design an aircraft with infinitesimal moment of inertia with respect to the lateral axis and with infinitesimal longitudinal damping moments ($m_2^u = 0$), as well as an infinitesimal moment due to the lag of the downwash at the tail ($m_2^d = 0$). It is obvious that it is in practice impossible to satisfy these conditions.

However, even from the point of view of controllability alone, without mentioning the design ratings and other flying qualities of the aircraft, a realization of the extreme degree of "following" the stick would evidently not be desirable.

Indeed, at a very high degree of static stability*, owing to the increase in the dimensions of the control surface and the very significant increase of its aerodynamic compensation that this would involve (given the usual system of longitudinal control), the stick force and the stick displacement necessary for producing a rotation of the aircraft and an acceleration of such rotation, would be too small. The aircraft might thus be made too sensitive to small motions of the pilot - often random ones. Because of the resultant excessively rapid reaction, the aircraft, as pilots say, will not "forgive" even insignificant errors of the pilot during piloting.

Controllability and Degree of Longitudinal Static Stability

We have seen that, at increasing longitudinal static stability with respect to overload, the ability of the aircraft to "follow" the stick is increased. Let us consider this influence of the degree of stability in a more concrete way, by using a numerical example.

* In these arguments we assume that the variation in the degree of static stability is effected by the forward displacement of the aircraft centering without change in the area of the horizontal tail surface.

POOR ORIGINAL

Let us take a fighter aircraft with the following data:

$$\frac{G}{S} = 175 \text{ kg/m}^2; \quad \frac{S_{hc}}{S} = S_{hc} = 0.20; \quad \frac{L_{hc}}{S_A} = L_{hc} = 2.7;$$

$$b_A = 1.9 \text{ m}; \quad \frac{S_o}{S_{hc}} = S_o = 0.36; \quad S_o = 1.23 \text{ m}^2; \quad b_o = 0.25 \text{ m};$$

$$k = 0.9; \quad k_h = 2.26 \text{ 1/m}; \quad r_1^2 = 0.76; \quad a = 4; \quad a_{hc} = 3;$$

$$m_1^a = -0.0153; \quad m_1^s = -5.2; \quad m_1^c = -2.6.$$

Let us assume that the flight takes place at an elevation of 3000 m at a speed of 92 m/sec or 333 km/hr.

Then we will have

$$\mu = 200; \quad t = 4.15 \text{ sec}$$

Let us assume, for the sake of simplicity, that the stability varies as a result of that variation in the disposition of the cargo in the fuselage, which leads to displacement of the centering but does not change the moment of inertia of the aircraft with respect to its lateral axis. We will also consider that the geometric dimensions of the aircraft (in particular, the wing area and the horizontal tail area) remain unchanged. Then, approximately, the quantities m_2^u and m_2^a will likewise remain constant.

Under these assumptions and initial data, we obtain the following formulas for determining the quantities P_2^u , P_1^u , and P^u :

$$P^u = (m_2^c - 0.026) P^s;$$

$$P_1^u = -0.01355 P^s;$$

$$P_2^u = -0.00095 P^s.$$

We remark that ordinarily, in designing an aircraft of some definite type or class, the value of the criterion P^u is considered to be assigned in advance and the choice of the design parameters of the aircraft must ensure satisfaction of this

POOR ORIGINAL

condition. We will, therefore, perform our calculations under the conditions:

$$p^x = -3 \text{ kg} = \text{const}$$

regardless of the degree of stability. Then, to each value of the coefficient of stability there will correspond its value of the coefficient of stick force P^x , as defined by the formula

$$P^x = \frac{3}{m_{z_{cs}}^{\epsilon} - 0.026}$$

From the value of P^x , at given values of m and of the geometric dimensions of the elevator, the required value of the moment coefficient of the elevator hinge can be found; by means of the appropriate calculation, the required value of the aerodynamic elevator balance $S_{ax.c} = \frac{S_{ax.c}}{S_B}$ may also be found.

Table 10.1

$m_{z_{cs}}^{\epsilon}$	P^x kg	k	γ_i	T_{NAT} SEC	m_h^{δ}	$\bar{S}_{ax.c}$
0	115	1,26	1,36	4,93	-0,0115	-
0,025	59	1,76	0,97	3,57	-0,0059	0,11
-0,05	39,5	2,16	0,80	2,90	-0,0039	0,18
-0,10	23,8	2,78	0,62	2,28	-0,0024	0,23
-0,15	17,0	3,28	0,52	1,91	-0,0017	0,25
-0,20	13,3	3,72	0,46	1,70	-0,0013	0,26
-0,30	9,2	4,46	0,38	1,41	-0,0009	0,27
-0,50	5,7	5,67	0,30	1,11	-0,0006	0,28
-0,80	3,6	7,11	0,24	0,88	-0,00036	0,285



POOR ORIGINAL

The results of such a calculation are represented in Table 10.1 and Figs.10.9 - 10.12.

As indicated in Table 10.1 and Fig.10.9, an increase in the static stability causes the period of natural oscillations T_{nat} , of the aircraft and the coefficient of relative damping η to decrease sharply in the region of small values of $m_z^* c_B$.

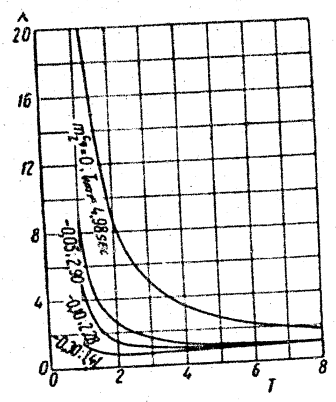
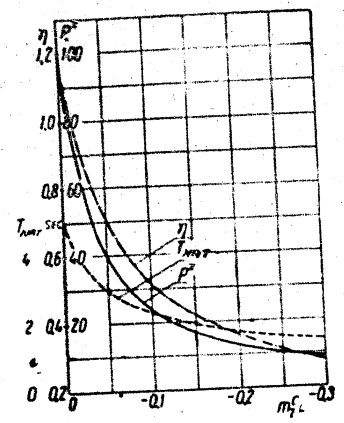


Fig.10.9 - Variation in the Period of Natural Oscillations of the Aircraft T_{nat} , the Coefficient of Stick Force P^x , and the Relative Coefficient of Damping η as Functions of the Coefficient of Stick-Free Static Stability under the Condition $p^0 = -3 \text{ kg} = \text{const.}$

Fig.10.10 - Variation in the Dynamic Coefficient of Stick Force as a Function of the Sharpness T_{forced} of a Maneuver at Various Values of $m_z^* c_B$

On increase of the static stability, the value of the coefficient of stick force P^x , necessary to satisfy the condition $p^0 = \text{const}$, rapidly decreases, which, with conventional control systems, requires a corresponding increase in aerodynamic balance of the elevator.

In the example taken, at $m_z^* c_B = -30$, the value of the axial dynamic compensa-

POOR ORIGINAL

tion amounts to about 27%. At such compensation, the deviations in the geometric shape of the elevator and tail that are possible in series production lead to inadmissibly great deviations of the actual values of the hinge moments from their required values. This fact may in practice make it difficult to realize the increase in the degree of longitudinal static stability of the aircraft that is desirable from the point of view of controllability.

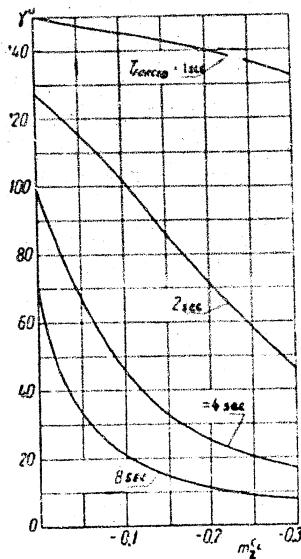


Fig.10.11 - The Angular Phase Shift between the Variations of the Stick Force (of the Stick Position) and the Overload, as a Function of the Quantities M_{zCB} and T_{forced}

It will be seen from Fig.10.10 that, at high static stability ($-m_{zCB} > 0.10$) and at $T_{forced} > 2.5 \text{ sec}$, the value of γ is practically constant and may be taken as equal to unity. In other words, under these conditions the relation between the stick forces (or stick displacements) and the change in load factor during a maneuver will be practically the same as under static conditions, i.e., will not depend on the sharpness of the maneuver.

On the other hand, at low stability, the value of the stick forces (or displacements) in executing a maneuver will be considerably greater than the value of the forces necessary for static balancing of the aircraft, at the same change in load for both cases.

It follows from the above that if we take two aircraft, with the same geometric

dimensions and weight and with the same values of P_n , but one being statically neutral ($m_{zCB} = 0$) and the other having rather good static stability, then the first

POOR ORIGINAL

aircraft will be considerably harder to control on executing unsteady maneuvers than the second one.

Figure 10.11 shows that another symbol of "following" the stick, the angle of phase shift, increases with decreasing stability and with increasing sharpness of maneuver (decrease of T_{forced}).

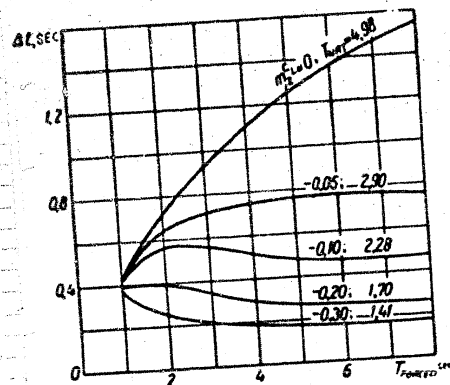


Fig. 10.12 - Time Lag between Changes in Stick Force (or Stick Position) and Overload, as a Function of the Quantities T_{forced} and m

airplane that is statically less stable. With increasing static stability, the ability, of the aircraft to "follow" the stick increases. In an aircraft with inadequate stability, the pilot, in performing a maneuver, must deflect the stick with a considerably longer time margin and must apply greater forces to it, than on an aircraft with adequate stability. In an aircraft with low stability it is harder for the pilot to adjust his manipulation of the elevator, and he is therefore compelled to further deflect the elevator to correct his earlier insufficiently precise actions.

It is possible to pass from the angle of phase shift to the quantity Δt (time lag of aircraft reaction) by means of the formula

$$\Delta t = \frac{I}{360} T_{forced}$$

Figure 10.12 shows the curves Δt as a function of T_{forced} at various values of m_{zcb} . As will be seen, at any value of T_{forced} the value of the lag in the aircraft reaction Δt decreases with increasing stability.

Thus, at the same values of P^H , it will be easier to control an airplane that is statically more stable than an

POOR ORIGINALInfluence of Flying Speed on Controllability

Let a flight take place at one and the same altitude, but at different velocities along the flight path. In considering the influence of flying speed on the "following" of the stick, we will assume, in first approximation, that the quantities $C_{l_{zcB}}, m_{zcB}, m_{icB}, P^X$, and a remain constant for all initial states of flight. It is not difficult to demonstrate that, with decreasing flight speed, the aircraft's ability to "follow" the stick decreases. Now, at a reduction in speed, the quantity

$$\tau = \frac{2m}{\rho S V}$$

will increase and, consequently, the stick forces and stick displacement, expended for overcoming the damping moments and for producing acceleration, as follows from eq.(9.3), will increase in comparison with the stick forces and displacements expended directly for the purpose of balancing the aircraft when the load conditions change. The impairment of the ability to "follow" the stick with decreasing flying speed is well illustrated by the sharp variations of oscillatory character in the stick force and stick position that occur during landing (cf. Fig.9.4) on any aircraft. This type of oscillatory motion of the elevator and of variation in the stick force are not characteristic of landing alone. They are observed to a greater or lesser extent in all cases where particularly exact piloting is required.

As shown above, the aircraft's ability to "follow" the stick improves with increasing static stability. For this reason, from the point of view of compensating the unfavorable influence of the reduction in flying speed on the "following" the stick, it is advantageous to design the aircraft as a high-wing monoplane in which the static stability usually increases with decreasing speed (cf. Chapter II).

Influence of the Dimensions of the Aircraft on its Controllability

In evaluating the influence of the dimension of the aircraft on its ability to "follow" the stick, we will assume that all linear dimensions of the aircraft are

POOR ORIGINAL

increased at one and the same ratio (geometric similitude). In addition, we will consider that the value of the specific loading and the distribution of masses (r_z^2) is constant. In that case, considering a flight at the same speed and same altitude, we get the result that the influence of the dimensions of the aircraft on the characteristics of controllability will be connected with the change of only a single parameter, the coefficient of relative density of the aircraft

$$\mu = \frac{2m}{\rho S b_A}$$

With increasing dimensions of the aircraft, the coefficient μ decreases. Equation (9.25) indicates that an increase in the dimensions of the aircraft will increase the value of P_2^H and P_1^H , i.e., will increase the percentage of stick forces and stick displacements expended in overcoming the damping moments and in the production of accelerations. In this way, at the same degree of static stability and same wing loading, a large aircraft will "follow" the stick less accurately than a small one.

The characteristics of "following" the stick during an assigned maneuver are determined by the quantities h and k . A study of eq.(10.4) shows that μ enters only as a factor in m_z^C . It follows that the influence of the variation in linear dimensions may be fully compensated by varying the degree of static stability, starting from the condition

$$\frac{C_L}{m_z^C} = \text{const.}$$

If, for example, we compare a fighter with the wing chord $b_A = 1.5$ m and $\frac{C_L}{m_z^C} = -0.15$ (15% reserve stability) with a bomber having a wing chord $b_A = 4.5$ m and the other parameters the same ($\frac{G}{S}$, m_z^w , r_z^2 , etc.), then to obtain the same indexes of "following" the stick (λ and γ), the coefficient of static stability of the bomber must be $\frac{C_L}{m_z^C} = -0.45$, i.e., the bomber must have a 45% excess stability. Such high degrees of stability for a bomber would be extremely difficult to realize

POOR ORIGINAL

0 in practice. For this reason, as a rule, large aircraft are considerably more inert
2 and follow the stick less accurately than small aircraft.

4
6 Method of Selecting Design Parameters for an
8 Aircraft during the Design

10 The major requirements for stability and controllability which must be satis-
12 fied by the designer are: to provide the required degree of "following" the stick,
14 to provide the required reserve in the elevator deflections on landing, and to pro-
16 vide definite values of the forces on the stick from the elevator, and likewise of
18 the stick displacements.

20 We have reached the conclusion that there is no good reason for introducing the
22 behavior of an aircraft in rough air as a separate case in calculating the selection
24 of the design parameters of an aircraft. It has also been noted above that the in-
26 crease in the degree of longitudinal static stability, which is desirable from the
28 point of view of controllability, may in a number of practical cases be limited by
30 the impossibility of effecting large aerodynamic compensation of the elevator with
32 the required degree of accuracy. In addition, the degree of variations in the stick
34 force on any change in the state of flight or on changes in the centering of the
36 aircraft must not go beyond definite limits. It is finally required that the degree
38 of stability of the aircraft, both rudder-fixed and rudder-free, be practically the
40 same. These requirements can be briefly summarized as follows: The designer has
42 to provide:

- 44 1. Adequate elevator reserve for landing (Δ_{max}^2);
46 2. Damping of the short-period disturbed motion (minimum allowable value of h);
48 3. Proper following the stick (limits of the parameter η);
50 4. Maximum possible aerodynamic compensation (minimum m_h^{δ});
52 5. Allowable limits of the stick force ($\frac{p_n}{p_n^{\min}}$);
54 6. Equal degree of stability, rudder-fixed and rudder-free ($m_{zCB}^{C_L} = m_1^{C_L}$)

POOR ORIGINAL

0 7. Allowable value for the derivative P^V .

2 This list can be supplemented by a number of less important requirements, for
4 example, the variation of aircraft balancing by forces on lowering the landing gear
6 and flaps, in performing a glide, etc.

8 The major design means, depending on the selection of the above requirements to
10 be simultaneously satisfied, are as follows: centering of the aircraft, area of
12 horizontal tail surface, arm of horizontal tail surface, dimensions of elevator;
14 magnitude of aerodynamic elevator balance; magnitude of transmission ratio from ele-
16 vator to stick, weight of balancers in control drive, and elastic force of springs
18 in control.

20 It is theoretically possible to imagine that if, in accordance with the number
22 of requirements, the same number of independent design parameters were taken, and
24 these requirements were expressed in the form of definite equations, then the exact
26 qualitative values of the corresponding design parameters could be found by solving
28 these equations. In this case, we would obtain an ideal solution of the problem.
30 Such a solution of the problem would be possible in practice, if the characteristics
32 of stability, the hinge moments, and also the requirements themselves, were all
34 maintained constant at any change in attitude of flight. However, this does not
36 take place in practice. The aerodynamic characteristics vary with speed and alti-
38 tude; the centering and the weight of the aircraft change with the fuel consumption.
40 In addition, a method of the above type would require complex and laborious calcula-
42 tions. For this reason, simpler and more convenient methods must be developed for
44 practical use. We will describe one of these methods, which may be called the meth-
46 od of boundary conditions.

48 In our calculations, the weight of the aircraft, the shape and area of the
50 wings, the dimensions of the landing flaps will be considered as already determined
52 by the tactical and technical requirements for maximum and landing speed, for lift,
54 for cargo capacity, etc. The length of the aircraft and the distribution of cargo
56

POOR ORIGINAL

0 along its longitudinal axis will likewise be considered assigned by the preliminary
 2 sketch plan. Consequently, we will assume the moment of inertia and the range of
 4 variation of the aircraft centering in flight to be known. The shape of the horizon-
 6 tal tail surface and the relative elevator area ($S_a = \frac{S_a}{S_{h.t.}}$) as well as the ex-
 8 tremes values of elevator deflection will be considered assigned on the basis of gen-
 10 eral recommendations. For the time being we will start from the assumption that,
 12 for satisfying the stability and controllability requirements, the following para-
 14 meters are available: x_T , centering of the aircraft; $S_{h.t.} = \frac{S_{h.t.}}{S}$, the tail area;
 16 m_h^0 , the value of the aerodynamic elevator balance; F_b , the weight in the control
 18 transmission; F_{sp} , the spring in the control transmission; and γ_{land} , the angle of
 20 stabilizer setting on landing.

22 As the principal design parameters to be determined and to be selected, the
 24 aircraft centering and the area of the horizontal tail surface will be used. The
 26 various controllability requirements will set definite limits for the possible vari-
 28 ations in $S_{h.t.}$ and x_T .

30 Having the above data on the aircraft, wing, and shape of tail, from the pre-
 32 liminary sketch plan, let us determine, by means of the methods described in
 34 Chapters II - VI, the quantities

$$36 \quad a, a_{h.t.}, k, k_{land}, D, \bar{x}_{F.b.h.t.}, \bar{m}_z k.p., \bar{l}_{h.t.} = \frac{l_{h.t.}}{b_A} \quad \text{etc.}$$

38 and then let us consider the above-listed seven requirements.

40 For greater conceptual clarity, let us consider a specific example. Assume
 42 that the fighter being designed has the following initial data:
 44
 46
 48
 50
 52
 54
 56

POOR ORIGINAL

$$\begin{aligned}
 G &= 3000 \text{ kg}; \quad S = 15 \text{ m}^2; \quad \chi = 35^\circ; \quad \delta_A = 1,5 \text{ m}; \\
 a &= 0,075 \frac{1}{\text{degree}}; \quad \epsilon_{\text{LAND}} = \epsilon_Y + \Delta \epsilon_Y^* = 1,4; \\
 \Delta \epsilon_Y^* &= 0,4; \quad \alpha_{\text{LAND}} = 12^\circ; \quad m_{\text{LND}}^* = -1,5; \quad \bar{x}_{\text{PAC}} = 0,20; \\
 L_{\text{ht}} &= 2,7; \quad \frac{dh}{dt} = D = 8^\circ; \quad \delta_{\text{ht}} = 4; \quad \alpha_{\text{ht}} = 0,06 \frac{1}{\text{degree}}; \\
 S_0 &= 0,35; \quad \delta_{\text{max}} = -30^\circ; \quad k = 0,95; \quad k_{\text{LAND}} = 0,95; \quad a = 0,53; \\
 \epsilon_{\text{LAND}} &= 4^\circ; \quad \epsilon_0 = 1^\circ; \quad m_{\text{LAND}} = m_{\text{st}} + \Delta m_{\text{st}} + \Delta m_{\text{res}} = -0,1; \\
 x_{\text{rh}} &= 0,20; \quad \frac{d\omega_2}{dt} = -0,6; \quad k_h = 1,75.
 \end{aligned}$$

The design altitude is $H = 3000 \text{ m}$.

Control Surface Reserve for Landing

In Chapter IV we established that the maximum angle of control-surface deflection necessary for balancing the aircraft at the landing angle of attack is obtained at extreme forward centering, and is equal to (eq.(4.8"))

$$\delta_{\text{LAND}} = - \frac{m_{\text{st}} \text{ DAT LAND}}{m_{\text{st}}} - \frac{1}{n} (\alpha_{\text{LAND}} - \epsilon_{\text{LAND}} - \epsilon_Y + \epsilon_{\text{LAND}}).$$

This angle must be less than the maximum allowable angle δ_{max} , since the pilot must have a definite reserve for overcoming the moment of inertia and for imparting an angular acceleration to the aircraft during the landing approach (the damping moment during landing is small and is usually neglected).

The value of the rudder deflection $\Delta \delta_{\text{res}}$, required to overcome the moment of inertia, may be found from the equation

$$I_s \frac{d\omega_2}{dt} = M_{\text{LAND}}^* \Delta \delta_{\text{res}}.$$

whence

$$\Delta \delta_{\text{res}} = \frac{I_s \frac{d\omega_2}{dt}}{M_{\text{LAND}}^* S \delta_{\text{LAND}}}.$$

POOR ORIGINAL

The graphs in Fig.9.4 show that the elevator deflections necessary for balancing the aerodynamic moments will correspond to the center line of the curve $\delta = f(t)$, on which the oscillatory deflections of the elevator $\Delta\delta$, used for counteracting the moment of inertia, are superimposed. The value of δ_{land} , for the example shown in Fig.9.4, can be determined by drawing the mean line $\delta_{mean} = f(t)$ and laying off the point corresponding to the instant of landing.

The maximum deflection of the elevator during landing at the most forward centering of the aircraft will be determined by the sum:

$$\delta_{max} = \delta_{land} + \Delta\delta_{res}$$

On taking the expanded expression for δ_{land} and $\Delta\delta_{res}$, we have

$$\delta_{max} = \frac{I_z \frac{d\omega_z}{dt}}{m_{z,land}^2 S_{h,t,land}^2} - \frac{m_{z,h,t,land}}{m_{z,land}^2} - \frac{1}{n} (\theta_{land} - \varphi_{land} - \psi_{land} + \chi_{land}). \quad (10.16)$$

Let us express the quantities $m_{z,land}^2$ and $m_{z,h,t,land}$ entering into this equation as functions of the variables $S_{h,t}$ and χ_T .

Equation (4.10), taking the statements in Chapter III into consideration, yields

$$m_{z,land}^2 = -a_{r,0} \bar{L}_{h,t} n k k_{land} \bar{S}_{h,t} = -0,0775 \bar{S}_{h,t}$$

From eq.(2.57'), taking eq.(2.60') into consideration, it follows that

$$m_{z,h,t,land} = m_{z0,land} - (\bar{x}_{F,h,t} - \bar{x}_T) c_L - (\bar{x}_{F,h} - \bar{x}_T) \Delta c_L = -0,38 + 1,4 \bar{x}_T$$

After substituting these expressions in eq.(10.16) and further calculating, considering that the angle of stabilizer setting on landing is $\varphi_{land} = 0$, we obtain

$$\bar{x}_T = 0,529 - 0,93 \bar{S}_{h,t}. \quad (10.17)$$

POOR ORIGINAL

If, for example, we assume $\varphi_{\text{land}} = -6^\circ$, we get

$$\bar{x}_T = 0.377 - 1.5 S_{h,t} \quad (10.18)$$

Equation 10.17 or eq.(10.18) determines, on a plane, the limits of permissible values of centering and tail area, under the condition of control-surface reserve

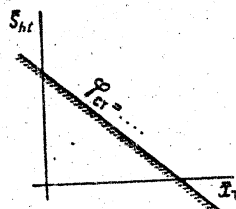


Fig.10.13 - Boundary of Allowable Values of Centering and Area of Horizontal Tail Surface under Conditions of Controllability of the Aircraft on Landing

for landing (Fig.10.13). Let us assume for example, that, without changing the tail area, we displace the centering of the aircraft forward. In order to counteract the diving moment, as the centering is shifted forward, the upward elevator deflection will increase. Along the boundary (cf. Fig.10.13), the extreme possible upward deflection of the elevator will be located. On further shifting of the centering forward the power of the elevator will be insufficient to balance the aircraft during landing. We may reason similarly with respect to the reduction of the horizontal tail area on unchanged balancing of the

aircraft.

Damping of the Short-Period Disturbed Motion

As follows from eq.(10.4), the characteristic quantity that determines the damping of the short-period motion is the quantity

$$\bar{h} = h = \frac{1}{2} \left(a - \frac{m_{z'ca}^2 + m_{z'ca}^2}{r_z^2} \right).$$

In our calculations we will assume, in first approximation, that the damping of the wing and the tail does not depend on the centering of the aircraft. The damping moment due to the wing will be calculated, allowing for the influence of the free

POOR ORIGINAL

elevator, which decreases the damping. According to eq.(9.19)

$$m_{zcs}^w = m_z^w - 57,3 m_z^{\delta} \frac{m_h^{\alpha} \bar{L}_{ht}}{m_h^{\delta} \sqrt{k}}$$

The value of the ratio $\frac{m_h^{\alpha}}{m_h^{\delta}}$ can be taken, in this calculation, as approximately equal to

$$\frac{m_h^{\alpha}}{m_h^{\delta}} = 0,15.$$

The value of the coefficient m_z^w will be determined from eq.(6.18), while we will assume m_{zcp}^w as equal to -1.5, regardless of the centering, so that

$$m_z^w = -1,5 - 1,2 \bar{L}_{ht} \sqrt{k} S_{ht}$$

We determine the value of m_{zcb} from the relation

$$m_{zcb}^{\delta} = \frac{d\varepsilon}{dz} m_{zcb,ht}^w = D a m_{zcb,ht}^w$$

We represent the value of m_z^{δ} by the equation

$$m_z^{\delta} = -a_{ht} \bar{I}_{ht} k n \bar{S}_{ht} = -0,0816 \bar{S}_{ht}$$

On substituting these expressions in the original formula for h, we have an equation of the form

$$\bar{h} = A + B \bar{S}_{ht}$$

This equation limits the area of the horizontal tail surface, allowing for the assigned value of the coefficient of damping of the short-period motion of the aircraft (Fig.10.14).

Let us assume, for example, that the minimum allowable value is $\bar{h} = 5$. Then, for our case, we obtain

$$\bar{S}_{ht} = 0.0965 \quad (10.19)$$

POOR ORIGINAL

"Following" the Stick

We have adopted above, as a basic parameter for evaluating the ability of the aircraft to follow the stick, the quantity (cf. eq.(10.10)) which is equal to

$$\eta = \frac{h}{k} = \frac{\frac{1}{2} \left(a - \frac{m_{zcb}^w + m_{zcb}^s}{r_z^2} \right)}{\sqrt{-\frac{a}{r_z^2} (\mu m_{zcb}^c + m_{zcb}^s)}} \quad (10.10)$$

The quantities m_{zcb}^w and m_{zcb}^s entering into this formula have been expressed in the form of functions of $\bar{S}_{h.t.}$.

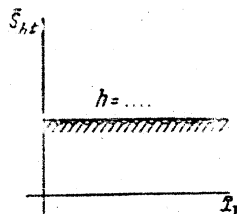


Fig.10.14 - Boundary Line $\bar{S}_{h.t.} = f(\bar{x}_T)$ under Conditions of Damping the Short-Period Oscillations of an Aircraft

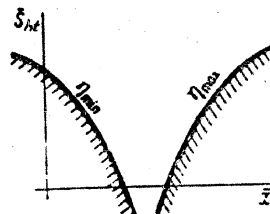


Fig.10.15 - Boundary Lines $\bar{S}_{h.t.} = f(\bar{x}_T)$ under Conditions of "Following" the Stick

From eq.(4.2), on substituting

$A = \bar{S}_{h.t.} \bar{L}_{h.t.}$ and since $m_{zcb}^{CL} = m_z^{CL}$ it follows that

$$m_{zcb}^c = -(\bar{x}_{Fbh.t.} - \bar{x}_T) - ka_{h.t.} \bar{L}_{h.t.} \left(\frac{1}{a} - D \right) \bar{S}_{h.t.} \quad (10.20)$$

After substituting the numerical values, we have

$$m_{zcb}^c = \bar{x}_T - 0,20 - 0,82 \bar{S}_{h.t.} \quad (10.21)$$

Taking the minimum allowable and maximum allowable values for η and substitut-

POOR ORIGINAL

ing in eq.(10.10), m_{zCB}^{CL} , m_{zCB}^{w} , and m_{zCB}^u , expressed in the form of functions of \bar{x}_T and $\bar{S}_{h.t.}$, we obtain two equations for the boundary lines (Fig.10.15) on the plane \bar{x}_T - $\bar{S}_{h.t.}$.

If, for example, we take $\eta_{min} = 0.4$ and $\eta_{max} = 0.7$ for our fighter, we obtain the following equations, respectively:

$$(\eta = 0.4) \bar{x}_T = 0.147 + 0.138\bar{S}_{h.t} - 2.05\bar{S}_{h.t}^2; \quad (10.22)$$

$$(\eta = 0.7) \bar{x}_T = 0.186 + 0.687\bar{S}_{h.t} - 0.669\bar{S}_{h.t}^2. \quad (10.23)$$

If we select $\bar{S}_{h.t.}$ and \bar{x}_T in such a way that the corresponding point will be located to the left of the boundary line (cf. Fig.10.15) η_{min} , then the degree of static stability will be too great and the aircraft will be too sensitive to the control in executing sharp maneuvers. If, conversely, we assume that $\bar{S}_{h.t.}$ and \bar{x}_T are located to the right of the line η_{max} , we will get an aircraft with too much inertness of the control.

Maximum Allowable Aerodynamic Elevator Balance

The initial condition, limiting the increase in static stability and in damping moment, is the maximum permissible value of the criterion P^* . According to eq.(9.25)

$$P^* = P^* \left(m_{i_{ca}}^{f_{ca}} + \frac{m_{i_{ca}}^u}{\mu} \right). \quad (10.24)$$

In accordance with the requirement that the degree of static stability, stick-fixed, be equal to that stick-free (cf. Chapter IX) as already stated above, we can assume that

$$m_{zCB}^{C_L} = m_z^{C_L}$$

The quantity $m_z^{C_L}$ is determined in its general form by eq.(10.20), but for our example by eq.(10.21).

Starting from eqs.(6.18) and (9.19), we have

POOR ORIGINAL

$$m_{z,ca}^w = m_{z,sp}^w - 1,2 \cdot 57,3 a_{ht} L_{ht}^2 \sqrt{k} S_{ht} - 57,3 m_{z,h}^w \frac{L_{ht}}{a_{ht} \sqrt{k}}$$

Considering $\frac{m_h^\alpha}{m_h^\delta} = 0.15$ and $m_{z,ekp}^w = 1.5$, we have for our example

$$m_{z,ca}^w = -1,5 - 27,4 S_{ht} \tag{10.25}$$

Let us assume that, as the maximum permissible value, we take the axial aerodynamic compensation $S_{ax.c.} \approx 0.26$, to which the value $m_h^\delta = -0.0015$ corresponds.

Making use of the initial data, let us express S_{PB} as a function of $\bar{S}_{h.t.}$.

Let us assume that the elevator span is 75% of the horizontal-tail span. Then,

$$S_e b_e = S_e \frac{S_e}{0,75 L_{ht}} = \frac{S_e^2}{0,75 \sqrt{L_{ht}} \sqrt{S_{ht}}} = \frac{S_e^2 S_{ht}^2}{0,75 \sqrt{L_{ht}}} = \frac{S_e^2 S_{ht}^2}{0,75 \sqrt{L_{ht}}}$$

Substituting the numerical values in the formulas, we obtain

$$P^x = 29 S_{ht}^{-0.5} \tag{10.26}$$

Taking $P^n = -4$ kg as the maximum allowable value of the criterion P^n in a fighter plane, and substituting in eq.(10.24) the expression for P^x , m_{zCB}^C and m_{zCB}^w in our example, we have the equation

$$\bar{x}_T = 0.205 - 0.138 S_{ht}^{-0.5} + 0.914 \bar{S}_{h.t.} \tag{10.27}$$

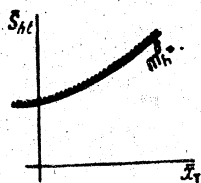


Fig.10.16 - Boundary Line $\bar{S}_{h.t.} = f(\bar{x}_T)$ under the Conditions of Extreme Aerodynamic Compensation

This equation will determine the boundary line on the plane $x_T \bar{S}_{h.t.}$, corres-

POOR ORIGINAL

0 ponding to the maximum permissible value of the aerodynamic compensation (Fig.10.16).
 2

4 Permissible Limits of Variation of the Stick Force

6 During operation, the balance of the aircraft may vary because of fuel consump-
 8 tion or variations in loading of the aircraft in different flights, which will lead
 10 to a change in the degree of static stability and, consequently, to a change in the
 12 stick force. In addition to this, when the initial state of flight of the aircraft
 14 varies, the degree of static stability may likewise vary, because of the shift in
 16 the aircraft aerodynamic center under the influence of the compressibility of air.
 18 This naturally results in the requirement that the variation in stick force on
 20 changes in the aircraft balance and on changes in attitude must not exceed definite
 22 limits. This type of limitation consists in a standardization of the maximum permis-
 24 sible values of the criterion P^{st} . Let us assume that, for a fighter plane, -4 kg is
 26 adopted as the maximum allowable value of P^{st} , and -2 kg as its minimum allowable
 28 value. If we consider the value of P^{st} to be constant over the entire range of atti-
 30 tudes and balance states of the aircraft, we may write

$$32 \frac{P_{\text{max}}^{\text{st}}}{P_{\text{min}}^{\text{st}}} = \frac{\mu (m_{zcB}^{\text{cl}} - \Delta \bar{x}_{FT}) + m_{zcB}^{\text{w}}}{\mu m_{zcB}^{\text{cl}} + m_{zcB}^{\text{w}}}, \quad (10.28)$$

34 where m_{zcB}^{cl} is the minimum value of the coefficient of static stability, which cor-
 36 responds to the condition of flight with the maximum rearward operational balance
 38 at an attitude at which the aircraft aerodynamic center occupies the most forward
 40 position, the quantity $\bar{x}_{FT} = \bar{x}_F + \bar{x}_T$, where \bar{x}_F is the maximum rearward shift of
 42 the a.c. and \bar{x}_T is the maximum forward shift of the centering.

44 After substitution of the corresponding expressions for m_{zcB}^{cl} and m_{zcB}^{w} as func-
 46 tions $\bar{S}_{h.t.}$ and \bar{x}_T we obtain a new boundary condition which limits the maximum per-
 48 missible rearward centering of the aircraft (Fig.10.17).

50 We assume that, for our fighter, $\Delta \bar{x}_{FT}$ has been found equal to

$$52 \Delta \bar{x}_{FT} = 0.12$$

STAT

POOR ORIGINAL



Then, for the above initial data, we will obtain the equation

$$\bar{x}_T = 0.085 + 0.914\bar{S}_{h.t.} \quad (10.29)$$

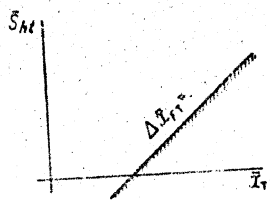


Fig.10.17 - Boundary Line $\bar{S}_{h.t.} = f(\bar{x}_T)$ under the Conditions of the Permissible

Ratio $\frac{P^n_{max}}{P^n_{min}}$

If, for example,

$$\Delta \bar{x}_T = 0.08$$

then we shall have the variation

$$\bar{x}_T = 0.125 + 0.914\bar{S}_{h.t.} \quad (10.30)$$

It follows from a comparison of eqs.(10.29) and (10.30) that, at smaller displacements of the a.c. and centering during flight, larger rearward operational balance of the aircraft is permissible for a given horizontal tail area.

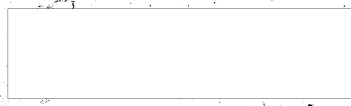
Equal Degree of Stability, Stick-Fixed and Stick-Free

This requirement may be satisfied at any aircraft centering and any horizontal tail area by installing the proper weight in the control system to produce an additional hinge moment of constant value or a constant stick force P_b .

The value of the weight is determined by condition (9.29):

$$P_b = -P^n_{max} \frac{a_1^2}{a_2^2} \left(\frac{1}{\sigma} - D \right) \quad (9.29)$$

In our case it is no longer possible to make use of the approximate value



POOR ORIGINAL

$\frac{m_h^a}{m_h^b} = 0.15$ which we adopted above. The values of m_h^a and m_h^b must be determined by starting from a selected horizontal tail area and centering, on the basis of the consideration of the entire group of all boundary conditions.

The Derivative of Stick Force with Respect to Speed

From the point of view of controllability, it is of importance to ensure a definite law of variation in stick force with variation in flying speed, instead of variation in the value of the static stability coefficient of the aircraft with respect to flying speed. The variation in the stick force with flying speed, as shown in Chapter IX, is characterized by the value of the criterion P^V , which is equal to (cf. eq.(9.25))

$$P^V = -2P^X \left(\frac{dm_x}{dx} \right)$$

The value of P^X is determined, as shown above, by the value of the static stability at an overload m_{icB} and by the value of the criterion P^N . For this, the required value of the criterion P^N may be obtained by installing an additional spring, producing a practically constant stick force P_{sp} (independent of the control-surface position). The value of P_{sp} is determined from eq.(9.30).

$$P^V = P_0^V + 2(P_b + P_{tail})$$

where P_0^V corresponds to the value of the criterion P^V without springs and weights in the elevator control transmission. The value of P_b , however, is determined, as stated above, by the conditions of assuring equality between the stick-fixed and stick-free degrees of static longitudinal stability of the aircraft with overload.

Selection of Horizontal Wing Area and of Aircraft Centering

In practice, all boundary lines obtained above, in accordance with the requirements posed for stability and controllability, must be plotted on a single diagram.

POOR ORIGINAL

Figure 10.18 gives such a diagram for our example. To give a clearer idea as to the significance of the influence of the variation in angle of stabilizer setting during landing, and of the variation in the aircraft a.c. and centering, Fig. 10.18 also gives, for our example, the boundary lines for two values of φ_{land} and two values of \bar{x}_{PT} .

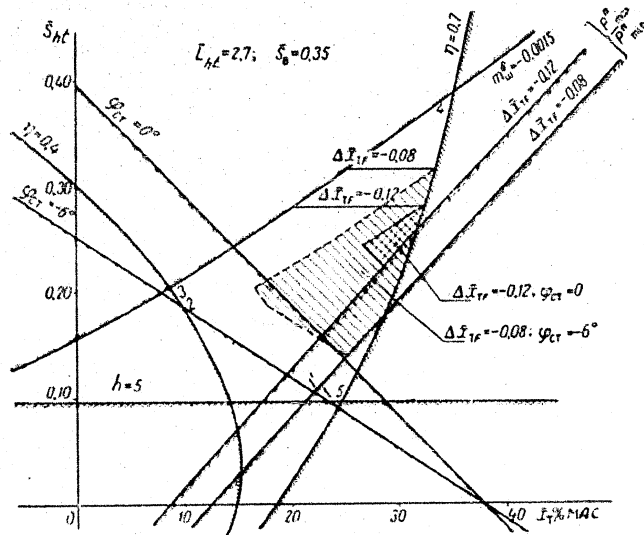


Fig. 10.18 - Diagram of Boundary Lines for Selecting the Area of the Horizontal Tail Surface and Centering of the Aircraft

As shown in Fig. 10.18, the entire group of boundary conditions defines a region within which the designer may select any combination of values of $\bar{S}_{\text{h.t.}}$ and \bar{x}_{T} most acceptable from his point of view.

If the balance of the aircraft did not change with the fuel consumption and the position of the aircraft a.c. m_x^{CL} likewise did not change with the attitude of flight ($\Delta \bar{x}_{\text{PT}} = 0$), then the designer would have a large zone of permissible values of \bar{x}_{T} and $\bar{S}_{\text{h.t.}}$ at his disposal. For our example, this zone is defined by the angular

POOR ORIGINAL

points 1, 2, 3, 4, 5. At $\varphi_{\text{land}} = -6^\circ$ (on landing) and $x_{PT} = 0.08$, the zone of permissible values of $\bar{S}_{h.t.}$ and \bar{x}_T in Fig.10.18 is hatched with parallel fine lines. At a constant angle of stabilizer setting on landing ($\varphi = 0^\circ$) and a large value of Δx_{PT} ($\Delta x_{PT} = 0.12$), the zone of permissible values becomes very small. In our example, this zone is double-hatched.

Let us elucidate the causes for the narrowing of the zone of permissible values of \bar{x}_T and $\bar{S}_{h.t.}$ when the a.c. and balance of the aircraft are shifted. We agreed

above, in defining the boundary lines by the condition $\frac{p_{\text{max}}^n}{p_{\text{min}}^n}$, that we would take as

the initial values the most rearward centering of \bar{x}_T and the most forward position of the a.c. of a tailless aircraft. These conditions mean that, in this case, the static stability of the aircraft at overload will be minimum.

The maximum permissible rearward centering or the minimum degree of stability are limited by the maximum allowable value of the coefficient n or by the ratio of the allowable values of P_{max}^n and P_{min}^n . In flight at maximum rearward balance and maximum rearward position of the a.c., the maximum degree of static stability is limited by the condition of maximum permissible aerodynamic compensation of the elevator, the condition of adequate elevator reserve for landing, or by the condition of the minimum permissible value of n . For this reason, if we take the maximum rearward balance of the aircraft as the starting point, then on the diagram of Fig.10.18 we must advance from the line bounding the extreme rearward balance by a horizontal distance corresponding to the given value of Δx_{PT} .

In order to allow for the possibility of changes in the design parameter

$$L_{h.t.} = \frac{l_{h.t.}}{b_A},$$

when using this method of selecting the centering and area of the

horizontal tail surface, we must construct diagrams analogous to that shown in Fig.10.18, at other values of $\bar{L}_{h.t.}$. It will evidently be sufficient in practice to construct such diagrams for two or three values of $\bar{L}_{h.t.}$.

POOR ORIGINAL

By analogous procedure we may also allow for the variation of such parameters as the coefficient of transmission k_h or of the relative radius of inertia of the aircraft

The variation in relative elevator area \bar{S}_B usually has no practical effect on the selection of $\bar{S}_{h.t.}$ and \bar{x}_T since, as the dimensions of the elevator increase, its efficiency begins to decline at smaller angles of deflection, which is taken into account in the calculation by reducing the value of δ_{max} .

Determination of the Characteristics of Stability and Controllability

Let us briefly enumerate the sequence of operations in the final calculation of the characteristics of longitudinal stability and controllability of the aircraft, after the parameters \bar{x}_T , $\bar{S}_{h.t.}$, $\bar{l}_{h.t.}$ and k_h have been selected.

1. The value of the coefficient of static stability with respect to overload $m_z^L = m_{zcB}^L$ and the coefficient of elevator efficiency m_h^δ are determined from the respective formulas. Then, starting from some definite value of P^n , the coefficient m_h^δ is calculated.

In this case, the formula for m_{zcB}^w , the ratio $\frac{m_h^q}{m_h^\delta}$ is taken approximately, starting from the expected value of the aerodynamic compensation $\bar{S}_{h.t.}$.

2. The value of m_h^δ and formulas or graphs are used for determining $S_{ax.c.}$ and then for defining the value of m_h^q . On the basis of the values of m_h^δ and m_h^q so obtained, the values of m_{zcB}^w and P^n are made more precise.

3. Starting from the condition of equality of stick-free and stick-fixed degrees of stability, the stick force due to the weight is next determined:

$$P_s = -P^n m_{zcB}^w \frac{m_h^q}{m_h^\delta} \left(\frac{1}{s} - D \right).$$

The value of the coefficient of static stability of the aircraft with respect

POOR ORIGINAL

to speed is then determined, after which the stick force due to the spring is found in order to obtain the desired coefficient P^V .

4. The elevator reserve for landing, the characteristics of the short-period oscillations of the aircraft, and the parameters characterizing the ability of the aircraft to follow the stick (η) are then determined, both at the most forward and most rearward operating aircraft balance. It is useful to determine the characteristics of stability and controllability at attitudes that are of greatest importance for an aircraft of a given function.

52
51
50
49
48
47
46
45
44
43
42
41
40
39
38
37
36
35
34
33
32
31
30
29
28
27
26
25
24
23
22
21
20
19
18
17
16
15
14
13
12
11
10
9
8
7
6
5
4
3
2
1
0



STAT

POOR ORIGINAL

CHAPTER XI

INFLUENCE OF STRUCTURAL ELASTICITY ON STABILITY AND CONTROLLABILITY

Up to now we have considered the aircraft as an absolutely rigid body. In reality, the action of aerodynamic forces and moments causes a deformation of its structural elements. Under the action of aerodynamic forces, the wing is bent. In addition, the wing is twisted, since the center of pressure does not coincide with the elastic center in each section. The twisting of the wing changes the angle of attack of the wing sections and, consequently, also the value of C_L . For this reason the pilot, in his attempt to maintain a constant flying speed and the earlier value of C_L in the presence of deformation, will be compelled to change the angular position of the aircraft in space by deflecting the elevator.

The tail, like the wing, will be bent and twisted in flight, which will lead to a change in its lift coefficient. The equilibrium of the aerodynamic moments acting on the aircraft will thus also be impaired. The angle of attack of the tail will also change as a function of the fuselage bending. To counteract the moments due to elasticity, a corresponding deflection of the elevator and additional stick force or force applied to the control wheel are required.

At low structural rigidity and location of the centers of pressure at great distances behind the elastic axes of the wing and tail it may happen that when the angle of attack of the wing increases, or when the elevator is deflected, no increment in wing lift or tail lift will be obtained, because of the twisting. In other words, there may be complete loss of control of the aircraft, due to structural de-

POOR ORIGINAL

formation. Loss of controllability may also result from bending of the fuselage.

The skin of the wing and tail is deformed under the influence of local loads, thus distorting the original shape of the profile. As a result of the deformation of the control transmission, the stick displacements necessary for deflecting the elevator are increased by comparison with the stick displacements at an absolutely rigid transmission.

The structural deformations that change the geometric shape of the aircraft naturally affect its dynamics, stability, and controllability. The influence of deformations becomes particularly marked in flight at high speed, since the aerodynamic forces and moments increase with speed. Adding to this, the increase in structural loads at high Mach numbers may be due to the influence of the compressibility of air on the aerodynamic forces and moments.

The number of structural elements whose deformation affects the stability and controllability of the aircraft is rather large. Those of greatest importance in the analysis of longitudinal stability and controllability are the elastic deformations of the wing and tail, the bending of the fuselage, the deformation of the elevator tab, and the deformation of the wing and tail skins.

A detailed consideration of the influence of deformations would require too much space. Therefore, only a brief survey over the influence of deformation, will be given, including the physical picture of the phenomena and a listing of the major parameters that determine these phenomena. We will consider the influence of each deformation separately. The total result may be obtained by combining (algebraic sum) the effect of the individual deformations.

Twisting of the Wing

Let us consider first a simplified model of this phenomenon (Fig. 11.1). Let us assume the wing itself to be absolutely rigid; let its elasticity be represented by two springs located in such a way that the center of rigidity is at distance from the wing aerodynamic center.

POOR ORIGINAL

Assume the wing to be placed in an air stream at the angle of attack α . As a result of the elasticity of the wing, the angle of attack varies by the quantity

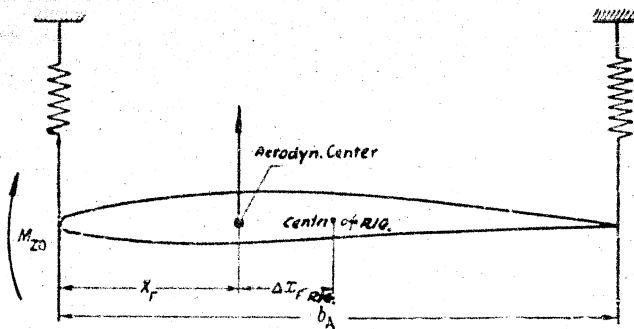


Fig.11.1 - Diagram of Elastic Wing and its Twisting Moments

under the action of the air stream. The aerodynamic forces and moments acting on the wing may be represented by the force Y_1 normal to the chord, by the tangential force X_1 , and by the moment M_z , the forces Y_1 and X_1 being applied at the wing aerodynamic center. We will assume that the force X_1 passes approximately through the elastic center. The force Y_1 may be considered equal to the lift Y .

The equation of equilibrium of the moments applied to the wing will be

$$M_{z0} + Y \Delta x_r - k_{\theta} \Delta \alpha = 0, \quad (11.1)$$

where k_{θ} is the coefficient of elasticity of the wing in torsion.

On substituting the value of Y in eq. (11.1) and using the expression $Y = \frac{dC_l}{d\alpha} (\alpha + \Delta \alpha)$, we get

$$\left[m_{z0} b_A + \frac{dC_l}{d\alpha} (s + \Delta s) \Delta x_r \right] - \frac{k_{\theta} \Delta \alpha}{s_{\theta}} = 0.$$

On determining the angle of wing twist from this equation, we obtain



POOR ORIGINAL

$$\Delta z = \frac{\left(a_{22} + \frac{d\epsilon_1}{ds} \Delta \bar{x}_{P_n} \right) S D_{2,0}}{k_{sp} - \frac{d\epsilon_1}{ds} \Delta \bar{x}_{P_n} S D_{2,0}} \quad (11.2)$$

where

$$\Delta \bar{x}_{P_n} = \frac{\Delta x_{P_n}}{b_s}$$

It is clear from this that, with increasing value of q , the torsion angle will increase, and that at

$$q_{crit} = \frac{k_{sp}}{\frac{d\epsilon_1}{ds} \Delta \bar{x}_{P_n} S D_{2,0}}$$

the torsion angle of such a wing will become infinite, leading to the phenomenon of the so-called divergence of the wing or aperiodic instability of the wing structure in torsion.

If the value of k_{sp} in the denominator of eq. (11.2) is taken out of the parentheses, we obtain the following expression for Δz :

$$\Delta z = \frac{\left(a_{22} + \frac{d\epsilon_1}{ds} \Delta \bar{x}_{P_n} \right) S D_{2,0}}{k_{sp} \left(1 - \frac{q}{q_{crit}} \right)} \quad (11.3)$$

Equation (11.3) readily shows that, as the value of q increases and approaches q_{crit} , the torsion angle increases with ever increasing intensity.

Let us analyze the influence of the twisting of the wing on the static stability of the aircraft.

Influence of the Torsion of a Rectangular Wing on the Static Stability

In order to evaluate the influence of the elastic torsion of a straight wing on

POOR ORIGINAL

the static stability of the aircraft, it is sufficient to compare the increment of longitudinal moment at a definite and constant variation in flying speed or load,

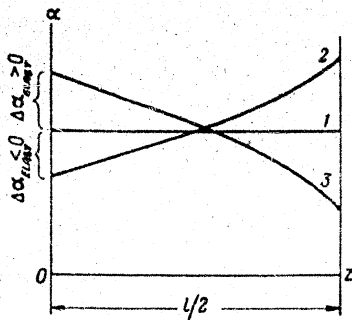


Fig.11.2 - Spanwise Variation in Angle of Attack of the Wing Sections, as a Result of Torsion at Constant Variation in Lift Coefficient ($C_L = \text{const}$) for Three Cases.

- 1- Absolutely rigid wing; 2- Sectional angles of attack increase toward wing tips (positive angles of torsion);
- 3- Sectional angles of attack decrease toward wing tips.

An increase in C_L will cause the sectional angles of attack to increase toward the wing tip. Curve 3 corresponds to an elastic wing in which the sectional angles of attack decrease toward the wing tip.

To obtain one and the same values of ΔC_L in Case 2, a smaller variation of the angle of attack of the wing $\Delta\alpha$ is required, and in Case 3 a larger variation (for

for an aircraft with a rigid wing and for one with an elastic wing. In considering this question, we will use a layout closer to reality than that shown in Fig.11.1. We will assume the center section to be undeformed, rigidly connected with the aircraft, and the torsion angle to increase in absolute value from the center section of the wing toward its tips.

The possible nature of the spanwise increment in angle of attack, in rigid and elastic wings, required for the same increment in the lift coefficient, is schematically shown in Fig.11.2, where for the sake of definiteness, we have assumed that $\Delta C_L = \text{const} > 0$. The straight line 1 in Fig.11.2 corresponds to an absolutely rigid wing. In this case, the angle of attack varies by the same value in all sections. Curve 2 corresponds to an elastic wing with elasticity characteristics such that an increase in C_L will cause the sectional angles of attack to increase toward the wing tip.

POOR ORIGINAL



which the angle of attack of a center section is used).

It may be considered, in first approximation (neglecting the contribution of the horizontal tail in producing the lift), that the lift of the entire aircraft is equal to the lift of the wing. For this reason the difference in the variation of the longitudinal moment of the whole aircraft with rigid and elastic straight wings at $\Delta C_L = \text{const}$ may be considered due only to the difference in variation of the angles of attack of the horizontal tail surfaces, i.e.,

$$\Delta M_x = M_{ELAST} - M_{RIG} = \Delta M_x \Delta \epsilon$$

or

$$\Delta M_x = -S_x \Delta \epsilon \Delta z_{HT} \quad (11.6)$$

where

$$\Delta z_{HT} = S_x \cdot e_{ELAST} - S_x \Delta \epsilon$$

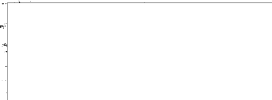
The angle of attack of the tail with an elastic wing will differ from the angle of attack of the tail with a rigid wing, because of the difference in the angles of attack of the aircraft (the angles of attack of the root section of the wing) and because of the difference in the angles of downwash.

According to the character of the curves in Fig. 11.2, the angle of attack of the tail in Case 2 will be lower (not allowing for the variation in downwash), and in Case 3 higher, than the angle of attack of the tail with a rigid wing. In addition, the angle of attack of the tail will vary in accordance with the variation in angles of downwash, because of the spanwise redistribution of the lift. With a certain degree of approximation, which is not reflected in the fundamental aspect of our further reasoning, we can consider the variation in angle of downwash to be proportional to the variation in angle of attack of the center wing section, i.e., proportional to the variation in angle of attack of the aircraft α .

Then,

$$\Delta \epsilon = \lambda \Delta \alpha_{ELAST}$$

where $\lambda = \frac{dz}{d\alpha} = D \frac{dC_L}{d\alpha}$ and $\Delta \epsilon$ is the difference between the variation in angle of



POOR ORIGINAL

downwash for a rigid and an elastic wing, respectively.

$$\text{Thus, } \Delta \alpha_{AC} = \lambda \alpha_{ELAST} - \Delta \alpha = (1 - \lambda) \Delta \alpha_{RIGID} \quad (11.5)$$

The quantity $\lambda = D \frac{dC_L}{d\alpha}$ is usually positive and less than unity. For this reason, the sign of $\Delta \alpha_{h.t.}$ may be considered to be the same as that of $\Delta \alpha_{yp}$.

To a wing twist of positive sign (cover 2, Fig. 11.2) corresponds $\Delta \alpha_{yp} < 0$. According to eqs. (11.5) and (11.4), the horizontal tail surface in this case will have a smaller angle of attack than in the case of the rigid wing ($\Delta \alpha < 0$), i.e., $m_z > 0$, which corresponds to an additional increment of climbing moment in an aircraft with an elastic wing. At $\Delta C_L > 0$, the existence of $m_z > 0$ indicates a decrease in the restoring moments, i.e., reduction of the static stability of the aircraft. On the other hand, the ratio of $\Delta \alpha_{yp} > 0$ and $\Delta m_z < 0$ at $\Delta C_L > 0$ determines an increase in the static stability.

Thus in order for the elastic torsional deformations of the straight wing to increase the static stability of the aircraft, it is a condition that the following inequality is satisfied:

$$\frac{d m_z}{d C_L} > 0. \quad (11.6)$$

It is therefore a condition for the increase in static stability of the aircraft by the nonrigidity of the wing that the wash-in or wash-out at the wing tips is negative, according to the type of curve 3, Fig. 11.2.

The twist of every actual wing depends on the variation of the zero moment, c_{m0} , of spanwise sections along the wing, and the variation of the distances between the line of rigidity and the line of foci in each section.

Let us return to the simplified diagram of Fig. 11.1. We will assume that the mean torsion angle of the wing depends linearly on the value of the zero moment m_{z0} and of the wing lift as a whole. Then eq. (11.1) can be used for determining the value of $\Delta \alpha_{yp}$. Bearing in mind that, in order to keep the lift constant, the pilot must vary the angle of attack of the wing by a quantity equal (and opposite) to that

POOR ORIGINAL

of the torsion angle $\Delta\alpha_{\text{land}} = -\Delta\alpha$

we obtain

$$\Delta\alpha_{\text{ELAST}} = \frac{M_0 + Y\Delta\bar{x}F_{PK}}{k_{kp}} \quad (11.7)$$

or, in a more developed form,

$$\Delta\alpha_{\text{ELAST}} = \frac{(m_0 + c_1 \Delta\bar{x}F_{PK}) S \Delta q}{k_{kp}} \quad (11.8)$$

To evaluate the influence of the elastic torsion of the wing on the static stability with respect to overload, we differentiate eq.(11.8) under the condition that $q = \text{const}$. Then,

$$\frac{\partial \Delta\alpha_{\text{ELAST}}}{\partial c_L} = - \frac{\Delta\bar{x}F_{PK} S \Delta}{k_{kp}} q \quad (11.9)$$

Since the quantities q and k_{kp} are positive, the sign of the derivative is opposite to the sign of the quantity \bar{x}_{PK} . When the elastic center is behind the wing a.c., the quantity \bar{x} is considered positive and, therefore $\frac{\partial \Delta\alpha_{\text{land}}}{\partial c_L}$ will correspond to it. On the basis of eq.(11.6) we reach the conclusion that the static stability with respect to the overload is decreased by the elasticity of the wing if the elastic axis of the wing is located rearward of the line of foci. It must be noted that, as will be seen from eq.(11.9), the influence of the elastic torsion of the wing on the static stability of the aircraft with respect to the overload does not depend on the coefficient of zero wing moment, m_{z0} .

To evaluate the influence of the elastic torsion of the wing on the static stability with respect to flying speed, we must find the derivative $\frac{d\Delta\alpha_{\text{land}}}{dc_L}$ under the condition of a constant load factor n , in other words, when c_L varies under the conditions of rectilinear flight.

Bearing in mind that, in rectilinear flight $Y = CLS_q \approx G = \text{const}$, let us rewrite eq.(11.8) in the form:

$$\Delta\alpha_{\text{ELAST}} = \frac{m_0 S q \cdot \Delta\bar{x} F_{PK}}{k_{kp}}$$

POOR ORIGINAL

By differentiating this equation, we get

$$\frac{d\Delta_{\text{elastic}}}{dc_L} = \frac{m_{sp} S b_A}{h_{sp}} \left(\frac{dq}{dc_L} \right)_{n-1} - \frac{S b_A q}{h_{sp}} \frac{\partial m_{sp}}{\partial M} \left(\frac{dM}{dc_L} \right)_{n-1} - \frac{G b_A}{h_{sp}} \frac{\partial \Delta_{\text{elastic}}}{\partial M} \left(\frac{dM}{dc_L} \right)_{n-1}$$

From the condition of rectilinear steady flight $C_L S q = G$, we get

$$\frac{dq}{dc_L} = -\frac{q}{c_L}$$

Further, representing the preceding equation in the form $C_L S \times \frac{\rho a^2 M^2}{2} = G$, and differentiating it, we obtain

$$\left(\frac{dM}{dc_L} \right)_{n-1} = -\frac{M}{2c_L}$$

On the other hand, $\Delta \bar{x}_{pt} = \bar{x}_t - \bar{x}_p$, where $\bar{x} = \frac{x_i}{b_A}$ is the dimensionless distance between the leading edge of the wing and the elastic axis. Then,

$$\frac{d\Delta_{\text{elastic}}}{dc_L} = \frac{m_{sp} S b_A}{h_{sp}} \frac{q}{c_L} + \frac{S b_A q}{h_{sp}} \frac{M}{2c_L} \frac{\partial m_{sp}}{\partial M} - \frac{G b_A}{h_{sp}} \frac{M}{2c_L} \frac{\partial \Delta_{\text{elastic}}}{\partial M} \quad (11.10)$$

Usually the coefficients $\frac{\partial m_{zo}}{\partial M}$, $-\frac{\partial x_F}{\partial M}$ are negative. The quantity $\frac{d\Delta_{\text{elastic}}}{dc_L}$ is likewise usually negative. In accordance with the condition (11.6) it follows from this that usually the elastic torsion of a straight wing decreases the static stability of the aircraft with respect to speed. An exception to this rule might be a flight at high Mach numbers, where the derivative $\frac{\partial m_{zo}}{\partial M}$ might also be positive.

As indicated by eq. (11.10), the variation in stability with respect to speed, on twisting of the wing, does not depend on the mutual position of the elastic axis and the wing aerodynamic center.

Bending of the Rectangular Wing

Bending of a rectangular wing does not cause the angles of attack of the sec-



POOR ORIGINAL

tions to vary. For this reason, in order to obtain the same increments ΔC_L , the aircraft (and the center section of the wing) must be rotated through one and the same angle $\Delta\alpha$, both in the case of a rigid wing and an elastic one. It follows from this that, in both cases, the longitudinal moments due to the normal force of the wing and to the horizontal tail will be the same, i.e., there will be no change in stability due to this factor. The change in stability will be connected only with the

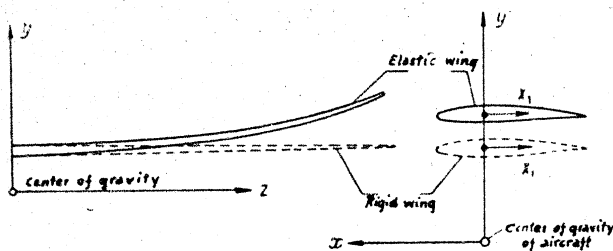


Fig.11.3 - Bending of Rectangular Wing and Variation of the Arm of the Tangential Force Leading to a Variation in the Magnitude of the Longitudinal Moment, for Rigid or Elastic Wings

change in the moment of the tangential forces acting on the rigid and on the elastic wing (Fig.11.3). The sign of this moment, and consequently also the variation in the stability, will depend both on the position of the wing in elevation with respect to the center of gravity of the aircraft and to the direction of the tangential force. The magnitude of the variation of the moments and of the stability due to the bending of a rectangular wing will be negligibly small, however, so that we can omit a detailed consideration of these variations.

Deformation of a Sweptback Wing

The analysis of the influence of the elastic deformations of the sweptback wing on the longitudinal stability is considerably more complex than in the case of the

POOR ORIGINAL

rectangular wing. The variation in angle of attack and lift along the wing span in this case is correlated with the torsion of the wing with respect to the elastic axis and with the bending of the elastic axis of the wing itself, leading to an additional variation in the angle of attack of the wing, due to its sweepback.

Thus the variation in angle of attack $\Delta\alpha_{\text{elast}}$ of any wing section with respect to the root section may be represented by the algebraic sum of two summands:

$$\Delta\alpha_{\text{elast}} = \Delta\alpha'_{\text{elast}} + \Delta\alpha''_{\text{elast}}$$

where $\Delta\alpha'_{\text{elast}}$ represents the variation in angle of attack due to the torsion of the wing with respect to the line of rigidity, as in the case of a rectangular wing. The sign of $\Delta\alpha'_{\text{elast}}$, as in the case of the rectangular wing, will depend on the sign and values of m_{z_0} and ΔX_{ep} taken for each wing.

The value of $\Delta\alpha''_{\text{elast}}$ represents the change in angles of attack due to the bending of the elastic axis of the wing in a direction perpendicular to its plane. Since the elastic axis of the wing is being bent, the angles of attack of the wing section perpendicular to the elastic axis remain unchanged. If, however, sections parallel to the plane of symmetry are taken, then, the angles of attack of these sections will vary on bending. At a positive (direct) sweepback, of the wings, the angles of the sections, due to the bending, will decrease.

The change in the angles of attack of the wing section in this case will be due to the fact that the sweepback causes the elementary lift of the individual wing areas to create a torsional moment with respect to the elastic center of the root section of the wing. At a positive lift and a positive sweepback, this moment will decrease the angles of attack of the wing sections more, the closer the given section is located to the wing tip.

In this way the curve of spanwise distribution of the angles of attack with any variation in C_L of the elastic sweptback wing will be compounded of two partial deformations, so that no general conclusions as to the variations in $\Delta\alpha_{\text{elast}}$ of the sweptback wing can be drawn.

POOR ORIGINAL

Let us consider the variation of the longitudinal moment and the stability in two cases of the spanwise distribution of the angles of attack along a sweptback wing, which is schematically represented in Curves 2 and 3 of Fig. 11.2. For the sake of definiteness we assume, as before, that these curves correspond to a definite and constant lift increment ($\Delta C_L = \text{const}$). The variation of the moment Δm_z consists of two parts: one component connected with the variation in angles of attack of the horizontal tail for an aircraft with an elastic or rigid wing, as the case may be; a second component connected with the spanwise redistribution of the lift and with the resultant appearance of additional moments in the elastic wing by comparison with the case of the rigid wing.

The variation in torsion for moments due to the horizontal tail, has already been considered in the case of the rectangular wing. With a sweptback wing, there is no fundamental modification in the situation, i.e., when the condition

$$\frac{d\alpha_{\text{elast}}}{dC_L} > 0 \quad (11.6)$$

is satisfied, the horizontal tail of an aircraft with an elastic sweptback wing will increase the longitudinal static stability.

As already pointed out, the condition (11.6) corresponds to Curve 3 of Fig. 11.2, i.e., a wing twist of negative sign. In the case of a twist of negative sign, the center section of an elastic wing will have a higher value of C_L than that of a rigid wing, while the wing tips will have lower values of C_L . For this reason, in such a sweptback elastic wing, there will be an additional climbing moment exerted directly by the wing as C_L increases. Therefore destabilizing moments will arise directly on the wing, causing the stability to decrease.

Thus, with an elastic sweptback wing, the variation in stability due to the moments arising on the wing and on the tail will be of opposite sign, i.e., the wing and tail have a mutually weakening effect.

POOR ORIGINALThe Torsional Deformations of the Tail

All statements on the torsion of the wing also are applicable to an analysis of the torsion of the tail. For the aerodynamic moment with respect to the center of gravity of the horizontal wing we obtain the expression

$$M_{h.t.} = Y_{h.t.} \Delta x_{h.t.} + M_{z0 h.t.}$$

or, in developed form,

$$M_{h.t.} = c_{L h.t.} S_{h.t.} \Delta \bar{x}_{h.t.} b_{h.t.} kq + m_{z0 h.t.} S_{h.t.} b_{h.t.} kq. \quad (11.11)$$

It is to this moment that the torsion angle of the tail will be proportional.

Here $\Delta \bar{x}_{h.t.} = \frac{\Delta x_{h.t.}}{b_{h.t.}}$ is the distance between the line of foci and the line of rigidity of the tail, related to the chord of the horizontal tail surface; $m_{z0 h.t.}$ is the coefficient of zero moment of the horizontal tail surface.

By differentiating eq. (11.11) with respect to C_L under the condition of a constant velocity head, $q = \text{const}$, we get

$$\frac{\partial M_{h.t.}}{\partial C_L} = \frac{\partial c_{L h.t.}}{\partial C_L} S_{h.t.} \Delta \bar{x}_{h.t.} b_{h.t.} kq. \quad (11.12)$$

If $\frac{\partial M_{h.t.}}{\partial C_L} > 0$, then with increasing C_L of the aircraft, a climbing moment will be produced on the horizontal tail surface with respect to its elastic axis; this moment will increase as a result of the elastic deformation of the angle of attack of the horizontal tail surface (Fig. 11.4). A larger angle of attack of the tail will result in a greater diving moment with respect to the center of gravity of the aircraft. It follows from this that, at $\frac{\partial M_{h.t.}}{\partial C_L} > 0$, the stability with respect to the overload will increase with respect to the stability of an aircraft with an absolutely rigid tail. Let us determine the change in the coefficient of stability with respect to the overload.

The change in the coefficient m_z (with respect to the center of gravity of the aircraft) with any variation in the angle of attack of the horizontal tail surface, due to its elasticity, will be

POOR ORIGINAL

$$\Delta m_{x, \text{ elast}} = - a_{h.t.} A k \Delta \alpha_{h.t. \text{ elast}} \quad (11.13)$$

The value of $\Delta \alpha_{h.t. \text{ elast}}$ will be equal to

$$\Delta \alpha_{h.t. \text{ elast}} = \frac{M_{ht}}{k_t}$$

where k_t is the coefficient of rigidity of the tail with respect to torsion.

On the basis of eq. (11.13), we obtain the following expression for the variation in the coefficient of static stability with respect to overload due to elastic torsion of the tail

$$\Delta m_{x, \text{ elast}}^c = - a_{ht} A k \frac{\partial \alpha_{h.t. \text{ elast}}}{\partial c_L}$$

Since

$$\frac{\partial \alpha_{h.t. \text{ elast}}}{\partial c_L} = \frac{1}{k_t} \frac{\partial M_{ht}}{\partial c_L}$$

then, making use of eq. (11.12), we obtain

$$\Delta m_{x, \text{ elast}}^c = - \frac{M}{k_t} a_{ht} A S_{ht} \Delta \bar{x}_{ht} b_{ht} \theta \frac{\partial c_L}{\partial c_L} \quad (11.14)$$

The quantity $\frac{\partial C_{L, h.t.}}{\partial C_L}$ is always positive, since, when the C_L of the aircraft increases, the angle of attack of the wing and tail also increase, causing the lift coefficient of the tail to increase.

It will be seen from eq. (11.14) that, if the elastic center of the tail is located behind the aerodynamic center, the static stability of the aircraft with respect to overload will increase, because of the elastic torsion of the tail. The absolute value of the variation in the coefficient of stability in this case will be proportional to the velocity head, which indicates the rapid increase of the elasticity of the structure with increasing speeds.

POOR ORIGINAL

It is obvious that, when the elastic center is located behind the a.c., the static stability with respect to overload, due to the elastic torsion of the tail, will increase, if we start from simple physical considerations. For example, let the angles of attack of an aircraft increase due to an external disturbance such as a vertical gust. In this case, the angle of attack of the tail will increase, and the lift of the tail will be augmented. At $q = \text{const}$ and $\delta = \text{const}$, the value of

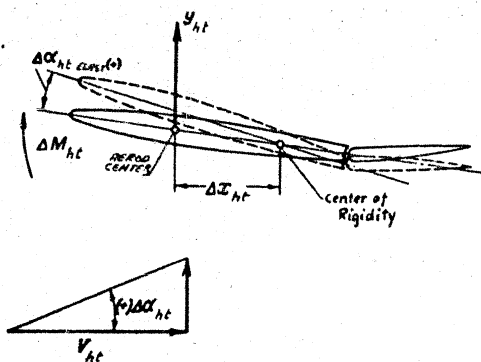


Fig.11.4 - Increase of the Angle of Attack of the Horizontal Tail Surface

Due to Twisting, at $\Delta x_{h.t.} > 0$

the coefficient of zero moment of the tail, $m_{z0 \text{ h.t.}}$, will remain constant. If the aerodynamic center of the tail is located forward of the elastic axis, then the tail due to its elasticity will increase its angle of attack by $\Delta\alpha_{h.t. \text{ elast}}$ which will in turn produce an additional increment of the aerodynamic moment of the tail with respect to the center of gravity of the aircraft in the direction of a dive. Therefore, the restoring moment of the aircraft will be increased, i.e., its static stability with respect to overload will improve.

The influence of the elastic torsion of the tail on the static stability with respect to speed is obtained by differentiating the following expression for Δm_z ,

POOR ORIGINAL

which is easily obtained from eqs. (11.11) and (11.13):

$$\Delta m_z = -a_{ht} A h^2 \frac{S_{ht} \theta_{ht}}{b_c} (c_{y_{ht}} \Delta \bar{x}_{ht} + m_{a_{ht}}) \quad (11.15)$$

Bearing in mind the above expressions for $\frac{dm_z}{dC_L}$ and $\frac{dq}{dC_L}$, we obtain, after simplifications,

$$\Delta \frac{dm_z}{dC_L} = Nq \left\{ -\frac{M}{2} \frac{c_{l_{ht}}}{c_l} \frac{\partial \bar{x}_{p_{ht}}}{\partial M} + \frac{M}{2c_l} \frac{\partial m_{a_{ht}}}{\partial M} + \left(\frac{c_{l_{ht}}}{c_l} - \frac{c_{l_{ht}}}{c_l} \right) \Delta \bar{x}_{ht} + \frac{m_{a_{ht}}}{c_l} + (c_{l_{ht}} \Delta \bar{x}_{ht} + m_{a_{ht}}) \frac{1}{a_{ht}} \frac{M}{2c_l} \frac{\partial a_{ht}}{\partial M} \right\}.$$

where

$$N = a_{ht} A h^2 \frac{S_{ht} \theta_{ht}}{b_c}.$$

The complex form of this expression for $\Delta \frac{dm_z}{dC_L}$ does not permit general conclusions, valid for all types of aircraft and for various states of flight, as to the influence of elastic torsion of the tail under static stability with respect to speed. This influence depends on the combination of a relatively large number of parameters.

The designer can exert an influence on the magnitude of the stability variations with respect to speed, mainly by the following measures:

- a. by changing the distance between the center of gravity and the aerodynamic center of the tail;
- b. by changing the value of the $C_{L_{ht}}$; this change is in turn determined by the value of the moment of the aircraft without horizontal tail surface depending on the moment characteristics of the wing and the fuselage, and on the centering of the aircraft;

POOR ORIGINAL

c. by changing $m_{zoh.t.}$. Besides the characteristics of the original wing profile, the value of $m_{zoh.t.}$ depends to a great extent on the elevator deflection which, in turn, depends on the angle of stabilizer setting and on the initial state of flight. To each value of φ_0 there must correspond a definite elevator deflection necessary to produce one and the same tail lift, starting from the conditions of balancing the aircraft in the given attitude.

Bending Deformations of the Fuselage

In any steady state of flight, the aerodynamic forces on the horizontal tail surface must balance the moment of the aircraft without horizontal tail surface, with respect to the center of gravity of the aircraft.

In Chapter III we established that the moment coefficient of the horizontal tail surface, $m_{zh.t.}$, is determined by the formula

$$m_{zh.t.} = -a_{ht} Ak(a_{ht} + \alpha^2) \quad (11.16)$$

When the fuselage is bent, the angle of attack of the tail will differ by the quantity $\Delta\alpha_{h.t.elast}$ from the angle of attack of the tail with a rigid fuselage, in the very same initial flight condition, i.e.,

$$\Delta\alpha_{h.t.elast} = \alpha_{ht} - \alpha_{ht.elast}$$

The value of $\Delta\alpha_{h.t.elast}$ may be considered proportional to the lift of the horizontal tail surface, namely

$$\Delta\alpha_{h.t.elast} = -(\gamma_{ht} = -C_{a_{ht}} S_{ht} k(a_{ht} + \alpha^2) q)$$

On substituting this expression in the preceding formula, we obtain

$$(1 + C_{a_{ht}} S_{ht} k) \alpha_{ht.elast} = \alpha_{ht} - C_{a_{ht}} S_{ht} k \alpha_{ht}$$

* Translator's note: This and many other subscripts illegible in document.

POOR ORIGINAL

From this we find the angle of attack of the horizontal tail surface, taking the fuselage into consideration,

$$a_{ht}^{ELAST} = \frac{a_{ht}^{RIG}}{1 + C_{a_{ht}} S_{ht} A_q} - \frac{C_{a_{ht}} S_{ht} A_q}{1 + C_{a_{ht}} S_{ht} A_q} \quad (11.17)$$

The moment without a horizontal tail surface, under the conditions of one and the same initial flight condition, may be considered the same in an aircraft with rigid fuselage as one with elastic fuselage, within the limits of the conventional fuselage (if we neglect the slight moment generated by the camber of the fuselage).

It follows that the difference in the coefficients of stability with a rigid fuselage and with an elastic one will be determined by the variations in the moment coefficient of the horizontal tail surface.

Let us find, for example, the variation in the coefficient of static stability with respect to overload. By differentiating eq. (11.17) with respect to C_L under the condition $q = \text{const}$, and on substituting the result in the expression for $m_{z_{h.t.}}^{C_L}$ as defined by eq. (11.16), we obtain

$$m_{z_{h.t.}}^{C_L} = -a_{ht} A \frac{\partial a_{ht}^{RIG}}{\partial C_L} \frac{1}{1 + C_{a_{ht}} S_{ht} A_q} \quad (11.18)$$

Consequently,

$$\Delta m_z^{C_L} = m_{z_{h.t.}}^{C_L} - m_{z_{h.t.}}^{C_L} = -a_{ht} A \frac{\partial a_{ht}^{RIG}}{\partial C_L} \frac{1}{1 + \frac{1}{C_{a_{ht}} S_{ht} A_q}} \quad (11.19)$$

Since the quantity $\frac{\partial a_{ht}^{RIG}}{\partial C_L}$ is always positive, it follows from eq. (11.19) that $\Delta m_z^{C_L}$ will always be greater than zero. In other words, the static longitudinal stability with respect to overload, due to the elasticity of the fuselage, will always decrease. It is not difficult to prove the accuracy of this on the basis of simple physical considerations.

POOR ORIGINAL

Let us assume, for example, that for some reason the angle of attack of an aircraft increases. In this case, the increased angle of attack of the horizontal tail surface will cause its lift to increase. In consequence of this, the rear section of the fuselage is bent upward as shown in Fig.11.5. In this way the total angle of

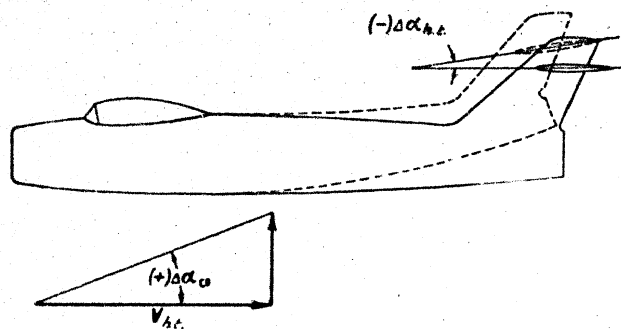


Fig.11.5 - Reduction of the Angle of Attack of the Horizontal Tail Surface Due to Elasticity of the Fuselage

attack of the horizontal tail surface in the elastic aircraft, other conditions being equal, will be less than in a rigid aircraft. Therefore, the elastic aircraft, with increasing angle of attack, will have a smaller restoring moment for diving than a rigid aircraft. This means that, due to the elasticity of the fuselage, the static stability of the aircraft with respect to overload will decrease.

In a similar manner, the expression for the change in the coefficient of static stability with respect to speed, as related to the elasticity of the fuselage, can be obtained. This expression, just as in considering the influence of the elastic torsion of the tail on the stability with respect to speed, is obtained in a rather complex form. It is impossible to draw any general conclusions valid for any aircraft and any state of flight as to the influence of the elasticity of the fuselage

POOR ORIGINAL

on static stability with respect to speed. In each specific instance, this influence, however, may be found by means of suitable calculations.

Effect of Deformations of the Fuselage and Tail on the Elevator

Efficiency

The elastic deformations of the fuselage, tail, and of the elevator itself diminish the elevator efficiency, i.e., they diminish the value of the aerodynamic moment with respect to the center of gravity of the aircraft due to a definite deflection of the elevator. Indeed, a deflection of the elevator changes the lifting power of the horizontal tail surface and creates an additional torsional moment, of a sign such that the effect of the deflection of the elevator itself is reduced. (Fig.11.6). For example, an upward deflection of the elevator leads to an increase

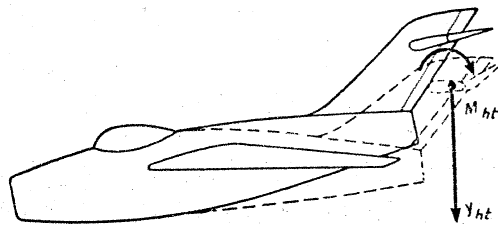


Fig.11.6 - Variation in the Angle of Attack of the Horizontal Tail Surface on Deflection of the Elevator, Due to Elasticity of the Fuselage and Tail

of the lift on the tail by the quantity $\Delta Y_{h.t.}$ in a downward direction, and an additional clockwise torsional moment. The generated $\Delta Y_{h.t.}$ and $\Delta M_{h.t.}$ increase the angle of attack of the horizontal tail surface, i.e., they give an effect opposite to the direct action of the elevator on the lift of the horizontal tail surface.

The extreme section of the elevator is deflected through a smaller angle than the center section of the elevator. This deflection is primarily due to the torsion

POOR ORIGINAL

produced in the elevator itself*. In evaluating the effect of the deformation on bending of the fuselage and twisting of the wing, we will take the effective angle of elevator deflection corresponding to a certain mean elevator section.

In Chapter III we established that the coefficients of elevator efficiency, in absence of elastic deformations, may be represented by the formula

$$m_{z, hc}^i = -a_{hc} A h \alpha,$$

obtained by differentiating the moment coefficient of the horizontal tail surface with respect to the center of gravity of the aircraft

$$m_{z, hc}^i = -a_{hc} A h \alpha (z_{hc} + n^i).$$

In the presence of elastic deformations, we have

$$m_{z, ELAST}^i = \frac{\partial m_{z, hc}^i}{\partial \alpha} = -a_{hc} A h \left(\frac{\partial z_{hc}}{\partial \alpha} + n^i \right). \quad (11.20)$$

Let us find the value of

$$\frac{\partial z_{hc}}{\partial \delta} = \left(\frac{\partial z_{hc}}{\partial \alpha} \right)_{\alpha} + \left(\frac{\partial \alpha}{\partial \delta} \right)_{\alpha}.$$

where $\left(\frac{\partial z_{hc}}{\partial \alpha} \right)_{\alpha}$ is connected with the bending of the fuselage, while the ex-

* What has been said of the sign of $\Delta M_{h.t.}^i$ will always be valid at $\Delta x_{h.t.} > 0$. At $\Delta x_{h.t.} < 0$, this will be true only on condition that

$$|Y_{hc}^i \Delta x_{hc} b_{hc}| < |M_{z0, hc}^i|.$$

where $Y_{h.t.}^i$ and $M_{z0, h.t.}^i$ are derivatives respectively of the lift and the zero moment with respect to the angle of elevator deflection. This condition is usually satisfied in practice.

POOR ORIGINAL

pression $\left(\frac{\partial a_{h.t. elast}}{\partial \delta}\right)_c$ is connected with the twisting of the stabilizer. Starting from the law that the deformation is proportional to the forces or moments causing them, we have

$$(\Delta a_{h.t. elast})_f = -\frac{c_{h.t.}^i \Delta h}{h_1};$$

$$(\Delta a_{h.t. elast})_c = \frac{m_{h.t.}^i \Delta h}{h_1}.$$

Whence

$$\left(\frac{\partial a_{h.t. elast}}{\partial \delta}\right)_f = -\frac{c_{h.t.}^i S_{h.t.} h q}{h_1} = -\frac{a_{h.t.} S_{h.t.} m h q}{h_1},$$

$$\left(\frac{\partial a_{h.t. elast}}{\partial \delta}\right)_c = \frac{m_{h.t.}^i S_{h.t.} h q}{h_1}.$$

in this case $c_{h.t.}^i > 0$, and $m_{h.t.}^i < 0$.

The difference in the coefficient of elevator efficiency, for a rigid and an elastic aircraft, will be

$$\Delta m'_1 = m'_{1, elast} - m'_{1, r} = a_{h.t.} A h \left(\frac{a_{h.t.} S_{h.t.} h q}{h_1} - \frac{m_{h.t.}^i S_{h.t.} h q}{h_1} \right)$$

or

$$\Delta m'_1 = a_{h.t.} A S_{h.t.} h^2 \left(\frac{a_{h.t.}^2}{h_1} - \frac{m_{h.t.}^i}{h_1} \right) q.$$

We see from this that $\Delta m'_1 > 0$, i.e., that the elevator efficiency is lowered and that the loss of elevator efficiency is proportional to the velocity head.

On the basis of the above equations it is not hard to determine the critical velocity head corresponding to the so-called reversed elevator, i.e., the total loss of the elevator efficiency due to elastic deformations. The reverse sets in when

$$m_{h.t.}^i = 0.$$

STAT

POOR ORIGINAL

On turning to eq. (11.20), we find that the equation corresponds to this condition:

$$n + \frac{\partial a_{h.c. elast}}{\partial \delta} = 0.$$

On replacing $\frac{\partial a_{h.c. elast}}{\partial \delta}$ by the above two summands, we obtain

$$n - S_{h.c.} k \left(\frac{a_{h.c.}}{k_2} - \frac{m_{h.c.}^i}{k_1} \right) q_{REV} = 0,$$

where q_{REV} denotes the velocity head at which the elevator reverse begins.

By solving this equation, we find that

$$q_{REV} = \frac{n}{k S_{h.c.}} \frac{k_1 k_2}{a_{h.c.} n k_1 - m_{h.c.}^i k_2}. \quad (11.22)$$

Deformation of the Elevator Tab

The elastic deformations of the tab exert a very substantial influence on the longitudinal stability of the aircraft and on the force from the elevator on the stick of the control wheel. At the beginning, let us consider only the qualitative aspect of the phenomenon of the influence of deformation of the tab.

The position of the tab on the elevators, necessary to ensure balancing of the aircraft on exerting a force (at stick force $P = 0$) in any assigned state of flight depends on a rather large number of design and geometric parameters: centering of the aircraft, moment characteristics of the wing and fuselage, angle of stabilizer setting, existence of springs and balances in the control transmission, and elasticity of the tail.

Let us consider the various states of steady rectilinear flight. Let us assume that the tab position $\tau_1 < 0$ as shown in Fig. 11.7a corresponds to the balancing of the aircraft by stick force at a velocity V_1 . When the speed of flight increases, the aerodynamic hinge moment with respect to the axis of rotation of the tab also increases, and in the presence of elasticity of the tab, the angle of its deflection decreases (in absolute value) to τ_2 . Such a change in the position of

POOR ORIGINAL

the tab with increasing flying speed, as shown in Fig. 11.7a, will produce an additional hinge moment of the elevator, tending to rotate the elevator upward more than a rigid tab would do. In order to establish a state of flight at high speed, the pilot must apply an additional force to the stick in the direction "away from him". When he releases the stick, in this case, the elevator will begin to rotate more toward the equilibrium angle of deflections than it would if the tab were rigid. It

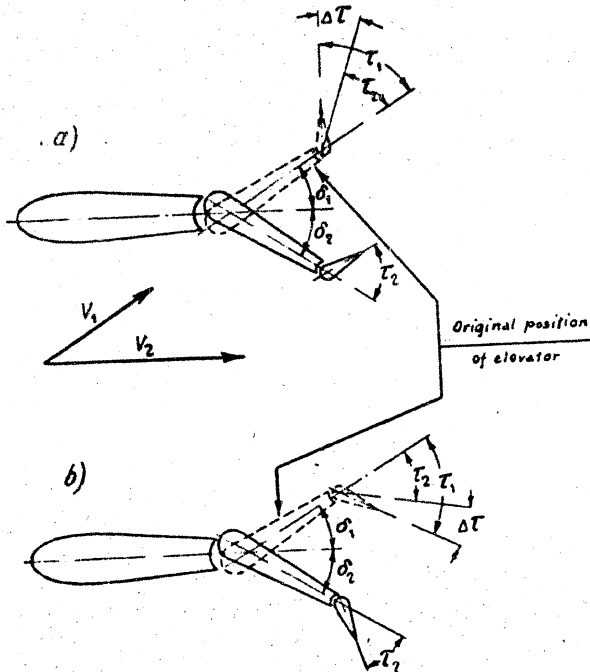


Fig. 11.7 - Elastic Deformations of the Elevator Tab
on Variation of the Flying Speed

is obvious that the static stability of the aircraft with respect to speed also increases in this case.

On the other hand, at an initial positive angle of the tab in the state of bal-



POOR ORIGINAL

ancing, i.e., at $v_1 > 0$, as shown in Fig. 11.7b, with increasing flying speed an elastic tab will lead to the appearance of a positive elevator hinge moment. In this case, the pilot, with increasing speed, will have to exert less pressure on the stick than with a rigid tab. On releasing the stick, the elevator will not return so violently to its equilibrium position so that the static stability of the aircraft will decrease with increasing speed. As we see, the effect of the elasticity of the tab on the stick force and stability with changing speed depends on the angle of deflection of the tab at the original state of balancing. This angle itself, however, depends on the factor indicated above (centering, angle of stabilizer setting, etc.) and on the original velocity V_1 at which the aircraft was balanced.

In these arguments it has been assumed that the elastic deformations of the tab are connected only with its angle of deflection and with the flying speed. In reality, however, the hinge moment is affected by both the angle of elevator deflection δ and the angle of attack of the horizontal tail $\alpha_{h.t.}$, although this influence is obviously considerably weaker than the influence of v and V .

The influence of δ and $\alpha_{h.t.}$ on the hinge moment of an elastic tab will lead to a change in the stability and stick force when the overload varies. However, in view of the smaller importance of the influence of these quantities by comparison with the initial angle of tab setting, we will not consider this problem in detail here.

Let us derive the analytic expressions for allowing for the influence of the elastic deformation of the tab on the stick force and on the stability. We will make certain assumptions to simplify the calculation.

Let the coefficient of elasticity of the trim tab be equal to

$$\zeta = \frac{\Delta \tau}{\Delta M_{HT}}$$

a constant quantity independent of the value of ΔM_{HT} , the variation in the hinge moment about the axis of the trim tab or the value of $\Delta \tau$, the angular displacement of the tab. The angular deformation of the tab at a given value of M_{HT} is deter-

POOR ORIGINAL

mined by the formula

$$\Delta\tau = CM_{ht}$$

where

$$\Delta\tau = \tau_{ELAST} - \tau_{rig}$$

where τ_{elast} denotes the actual angle of tab deflection, while τ_{rig} is the angle of tab deflection in the same position of the tab control wheel, but in the absence of load ($M_{ht} = 0$), or with an absolutely rigid tab.

The aerodynamic hinge moment M_{ht} of the tab may be represented in the form

$$M_{ht} = m_{ht} S_T b_T k q \quad (11.23)$$

where m_{ht} is the coefficient of hinge moment;

S_T is the area of the tab;

b_T is the tab chord;

k is the coefficient of loss of velocity of the flow about the tail.

On considering the influence of the elasticity of the tab on the stability and stick force during any variation in flying speed, the quantity m_{ht} will be used as a function of the angle of deflection of the tab.

Then,

$$\tau_{ELAST} - \tau_{rig} = C m_{ht} S_T b_T \tau_{ELAST}$$

Whence

$$\tau_{ELAST} = \frac{\tau_{rig}}{1 + C} \quad (11.24)$$

where

$$C = -m_{ht} S_T b_T \quad (11.25)$$

We note that C is a positive quantity, since the quantity m_{ht} is negative.

Let the aircraft be balanced by stick force and be in a stick-free steady state of rectilinear flight at $C_L = C_{L0}$. We assume further that the aircraft has been brought into an attitude corresponding to the value of $C_L \neq C_{L0}$. In the case of an

POOR ORIGINAL

absolutely rigid tab, the aerodynamic moment $m_{z_{cB}}$ arises with respect to the center of gravity of the aircraft, and in the case of an elastic tab, the moment $m_{z_{cB}} = m_{z_{cB}} + m_{z_{cB}}$. On transition from one state of flight at $q = q_0$ to a state at $q = q_0 + \Delta q$, where Δq is a small quantity, the tab, owing to its elasticity, will change its position, as follows from eq. (11.24), by the quantity

$$\Delta \tau = -\frac{K C_{\tau} \Delta q}{(1 + C_{\tau})^2} \quad (11.25)$$

In order to have the released elevator in equilibrium, it must vary its position, when using an elastic tab, by the quantity $\Delta \delta$, relative to the angle of deflection with a rigid tab. The value of $\Delta \delta$ is found from the equation of the coefficients of elevator hinge moments:

$$m_h^i \Delta \delta_i + m_h^r \Delta \tau = 0.$$

Whence

$$\Delta \delta_i = -\frac{m_h^r}{m_h^i} \Delta \tau. \quad (11.27)$$

The variation in the coefficient of moment with respect to the center of gravity of the aircraft, due to the elasticity of the tab, is found from the formula

$$\Delta m_{z_{cB}} = m_z^i \Delta \delta_i = -m_z^i \frac{m_h^r}{m_h^i} \Delta \tau.$$

By substituting, in this equation, the value of $\Delta \tau$, from eq. (11.26), we obtain

$$\Delta m_{z_{cB}} = \frac{C_{\tau} m_z^i}{(1 + C_{\tau})^2} \frac{m_h^r}{m_h^i} \Delta q.$$

It is not difficult to determine from this the variation in the coefficient of static stability with respect to velocity, $\frac{dm_{z_{cB}}}{dC_L}$ which is due to the elasticity of the tab:

$$\Delta \frac{dm_{z_{cB}}}{dC_L} = \frac{C_{\tau} m_z^i}{(1 + C_{\tau})^2} \frac{m_h^r}{m_h^i} \frac{dq}{dC_L}.$$

As seen above, the derivative $\frac{dq}{dC_L}$ is equal to

134

STAT

POOR ORIGINAL

$$\frac{dq}{d\epsilon} = -\frac{C_1}{C_2 \epsilon} \quad (11.28)$$

Rejecting the index 0, we obtain an expression for the variation of the coefficient of stability:

$$\Delta \frac{dm_{z, \text{stab}}}{d\epsilon} = -\frac{C_{z, \text{stab}}^0 m_h^0 m_2^0}{m_h^0} \frac{q}{(1 + Cq)^2 \epsilon} \quad (11.29)$$

On expressing C_1 in terms of q from the condition $G = C_1 S q$, and substituting in eq. (11.29), we obtain

$$\Delta \frac{dm_{z, \text{stab}}}{d\epsilon} = -\frac{C_{z, \text{stab}}^0 m_h^0 m_2^0}{\frac{q}{S} m_h^0} \frac{1}{\left(C + \frac{1}{q}\right)^2} \quad (11.30)$$

Equation (11.30) shows that the variation in the coefficient of stability with respect to flying speed, due to the elasticity of the tab, will be greater at higher initial angles of setting of the tab τ_{rig} , higher flying speed, and lower relative wing loading.

Since the signs of the coefficients m_h , m_h^0 , and m_2 are negative in the aircraft while the quantity C is positive, we may write

$$\Delta \frac{dm_{z, \text{stab}}}{d\epsilon} = B \frac{1}{\left(C + \frac{1}{q}\right)^2} \quad (11.31)$$

where B is a constant quantity of positive sign. It is clear from this that, at a negative angle of tab setting $\tau_{\text{rig}} < 0$, the stability of the stick-free aircraft will increase with an elastic tab, but will decrease with $\tau_{\text{rig}} > 0$.

Let us then determine the variation in the force on the stick or control wheel from the elevator, due to the elasticity of the tab, under the condition that the aircraft is balanced by a stick force ($P = 0$) both with a rigid and an elastic tab at one and the same attitude of flight. Then, depending on the sign of the angle of tab deflection τ_{rig} , the balancing curves of the stick force P will vary as a function of the flying speed. The difference in the stick force with a rigid and an e-

POOR ORIGINAL

lastic tab may be found from the formula

$$\Delta P = -k_h m_h^2 S_h b_h A q \Delta \tau, \quad (11.32)$$

where

$$\Delta P = P_{acc} - P_{rec}; \quad \Delta \tau = \tau_{rec} - \tau_{acc}.$$

Making use of eq. (11.24), we find

$$\Delta \tau = \frac{\tau_{rec}}{1+Cq} - \frac{\tau_{acc}}{1+Cq_0} = -\frac{C(q - q_0)\tau_{acc}}{(1+Cq)(1+Cq_0)}.$$

On substituting this value of $\Delta \tau$ in eq. (11.32), we obtain

$$\Delta P = \frac{k_h m_h^2 C S_h b_h A \tau_{acc} (q - q_0) q}{(1+Cq)(1+Cq_0)}$$

Dividing the numerator and denominator in this expression by q^2 , we finally obtain

$$\Delta P = \frac{k_h m_h^2 C S_h b_h A \tau_{acc} \left(1 - \frac{q_0}{q}\right)}{\left(C + \frac{1}{q}\right) \left(C \frac{q_0}{q} + \frac{1}{q}\right)} \quad (11.33)$$

To evaluate the order of the variation of the stability and stick force due to the elasticity of the tab, we present a numerical example. Let us take an aircraft with the following data

$$\begin{aligned} \frac{G}{S} &= 200 \text{ kg/m}^2; \quad S_h = 1.5 \text{ m}^2; \quad b_h = 0.45 \text{ m}; \quad k = 0.9; \\ S_v &= 0.06 \text{ m}^2; \quad b_v = 0.07 \text{ m}; \quad k_h = 2.5; \quad m_h^1 = -0.015; \\ m_h^2 &= -0.01; \quad m_h^3 = -0.004; \quad m_h^4 = -0.006; \quad \tau_{rec} = -4^\circ; \\ \zeta &= 3.5 \text{ degree/kg-m.} \end{aligned}$$

Let us now calculate the value of the coefficients C:

$$C = 3.5 \times 0.01 \times 0.06 \times 0.07 \times 0.9 = 0.000133$$

Let the aircraft be balanced by the tab at a flying speed of 500 km/hr which, under condition of sea-level flight, corresponds to the velocity head

$$q = 1200 \text{ kg/m}^2$$

Let us then calculate the variation in the coefficient of stability from

POOR ORIGINAL

eq. (11.30):

$$\Delta \frac{dm_{z, \text{el}}}{dc_L} = \frac{0,000133 \cdot 4 - 0,004 \cdot 0,018}{200 - 0,06} \frac{1}{\left(C + \frac{1}{q}\right)^2} = \frac{2,65 \cdot 10^{-6}}{\left(C + \frac{1}{q}\right)^2}$$

At $q = 1200 \text{ kg/m}^2$, we have

$$\Delta \frac{dm_{z, \text{el}}}{dc_L} = -0,0284,$$

i. e., we obtain an increase in stability by about 3% MAC.

At $q = 3000 \text{ kg/m}^2$, which corresponds to a flying speed of 390 km/hr (at sea level) we get

$$\Delta \frac{dm_{z, \text{el}}}{dc_L} = -0,123,$$

i. e., an increase in stability by 12.3% MAC.

If the aircraft is balanced at $q_0 = 1200 \text{ kg/m}^2$, then at $q = 3000 \text{ kg/m}^2$ in the given example we obtain a variation of the force on the stick P due to elasticity of the tab, equal to

$$\Delta P = \frac{2,5 \cdot 0,004 - 0,000133 \cdot 1,5 - 0,45 - 0,9 \cdot 4(1 - 0,4)}{(0,000133 + 0,000339)(0,000133 - 0,4 + 0,000333)} = 10,8 \text{ kg}$$

As confirmed by this example, the effect of the elasticity of the tab is very substantial.

Measures for Reducing the Influence of Deformation on the Stability

It follows from the above analysis that, to reduce the influence of the elastic deformation of an aircraft on its stability and controllability, the following measures will be useful in addition to increasing the structural rigidity. First, reduction of the distance between the axis of the foci and elastic axis both in the wing and the horizontal tail; second, use of profiles with a small or zero moment coefficient c_m (the so-called momentless profiles); third, with the object of re-

* Illegible

POOR ORIGINAL

relieving the load and the horizontal wing at high speeds, all possible means must be used for ensuring the minimum value of the moment of an aircraft without horizontal tail surface ($m_{zbh.t.}$). In this case, the deformation of the fuselage will be reduced to a minimum. The angle of dihedral of the horizontal tail surface must be selected by calculating an angle of rudder or elevator deflection close to zero at high flying speeds.

With a correct selection of all the parameters affecting the stability and controllability of the aircraft, the influence of the deformation will be relatively small, so that all basic calculations can be made under the assumption of an absolutely rigid aircraft. After these calculations have been performed, a supplementary and verifying calculation must be made to evaluate the influence of the structural nonrigidity of the aircraft on its stability and controllability.

BIBLIOGRAPHY

1. - Description of A.F. Mozhayskiy's aircraft TSOVIAL, 749, page 175 (1978)
2. Adamovich, M.V. - Controllability of Modern Aircraft OBOZONGIZ, (1946)
3. Ostostavskiy, I.V. and Titov, V.M. - Aerodynamic Calculation of Aircraft OBOZONGIZ, Moscow (1947)
4. Lebedev, A.A. - Some Questions on the Aerodynamics of the Airfoil in Supersonic Flow, Dissertation for master's degree, Moscow Aviation Institute
5. Kolosov, Ye.I. - Propeller Downwash behind the Wing. Trudy TsAGI, p.315
6. Clauert, H. - Lift and Pitching Moment of an Airfoil Due to a Uniform Angular
7. Vedrova, V.S. - Dynamic Stability of the Airplane OBOZONGIZ (1938)
8. e.g. Ol'man, Ye.V., Solov'yev, Ya.I., and Tokarev, V.P. - Automatic Pilots OBOZONGIZ (1946)
9. Kotel'nikov, V.A. - Longitudinal Stability of an Aircraft with an Automatic Pilot, Trudy LII, No.3, (1941)
10. Kalachev, G.S. - On the Longitudinal Dynamic Stability of Aircraft, Trudy TsAGI

POOR ORIGINAL

No.235, (1935)

11. Kalachev, G.S. -- The Measure of the Longitudinal Dynamic Stability of Aircraft,

Trudy TsAGI, No.365, (1938)

0
1
2
3
4
5
6
7
8
9
10
11
12
13
14
15
16
17
18
19
20
21
22
23
24
25
26
27
28
29
30
31
32
33
34
35
36
37
38
39
40
41
42
43
44
45
46
47
48
49
50
51
52
53
54
55
56



439

32

STAT

POOR ORIGINAL



TABLE OF CONTENTS		Page
	Preface	ii
	Symbols Used	v
	Introduction	1
CHAPTER I		
CONCEPT OF THE STABILITY AND CONTROLLABILITY OF THE AIRCRAFT		
	Piloting and Motion of the Aircraft	15
	Motions of Aircraft with Long and Short Periods	22
	Maneuverability	23
	Indexes of Maneuverability	24
	Controllability of an Aircraft	26
	Stability	31
	Role of Static Stability	34
	Stability, Controllability, and Safety of Flight	39
CHAPTER II		
FORCES AND MOMENTS ACTING ON AN AIRCRAFT WITHOUT TAIL SURFACES IN STEADY RECTILINEAR FLIGHT		
	Moment of Wing with Constant Chord	41
	Aerodynamic Center	45
	The Influence of the Position of the Center of Gravity of the Aircraft on the Wing Moment	46
	The Moment of a Wing of Arbitrary Horizontal Contour	49
	The Influence of Sweepback on the Wing Moment	52
	The Mean Aerodynamic Wing Chord	54
	Wing Moment at High Angles of Attack	65



POOR ORIGINAL

	Page
0	
1	
2	
3	
4	
5	
6	
7	
8	
9	
10	
11	
12	
13	
14	
15	
16	
17	
18	
19	
20	
21	
22	
23	
24	
25	
26	
27	
28	
29	
30	
31	
32	
33	
34	
35	
36	
37	
38	
39	
40	
41	
42	
43	
44	
45	
46	
47	
48	
49	
50	
51	
52	
53	
54	
55	
56	

CHAPTER III	
MOMENT OF HORIZONTAL TAIL SURFACES IN STEADY FLIGHT	
Purpose of the Horizontal Tail Surfaces	105
The Possibility of Realizing a Tailless Aircraft	106
The Moment of the Horizontal Tail Surfaces	108
Operating Conditions of the Horizontal Tail Surface	111
Downwash at the Tail	114
Influence of the Propeller and Fuselage on the Downwash at the Tail Surface	121
Influence of the Compressibility of Air on the Downwash	125
The Downwash at Supersonic Flying Speeds	127
The Actual Angle of Attack of the Horizontal Tail Surface	129
Influence of the Proximity of the Ground and of the Deflection of the Flaps on the Downwash at the Tail Surface	130
Deceleration of Velocity in the Region of the Tail Assembly	134
Influence of the Operating Propeller on the Flow Velocity at the Tail Surface	138
Influence of Elevator Deflection on the Tail Moment	140
Influence of the Compressibility of Air on the Elevator Efficiency	141

POOR ORIGINAL

	Page
0	
2	143
4	
6	
8	
10	
12	
14	
16	
18	
20	
22	
24	
26	
28	
30	
32	
34	
36	
38	
40	
42	
44	
46	
48	
50	
52	
54	
56	

General Expression for the Moment of the Horizontal Tail Surfaces 143

CHAPTER IV

TOTAL MOMENT OF AIRCRAFT IN STEADY RECTILINEAR FLIGHT

Moment Coefficient Acting on the Aircraft	148
Equivalents of Elevator Deflection and Variation in Tail Dihedral	149
Aerodynamic Center of Aircraft, Neutral Centering	150
Balancing of Aircraft with Respect to Moment	154
The Balancing Curve	155
Maximum Permissible Forward Centering	157
Aircraft Moment at High Flying Speeds	159
Influence of Horizontal Tail Surface on the Aircraft Lift	163

CHAPTER V

THE ELEVATOR HINGE MOMENT AND THE STICK FORCE

The Elevator Hinge Moment	167
Aerodynamic Balance of the Elevator	170
The Coefficient of Elevator Hinge Moment	174
Influence of the Compressibility of Air on the Hinge Moment	177
Forces at the Elevator Control Stick	183
Relation of the Stick Force and the Velocity of Horizontal Flight	186
Influence of Balancers and Springs on Force on Stick	191
Hydraulic Boosters and Automatic Rudder Control	201
Influence of Friction in the Control Transmission on the Stick Force	203

POOR ORIGINAL

CHAPTER VI	
ADDITIONAL MOMENTS ACTING ON THE AIRCRAFT IN UNSTEADY MOTION	
	Page
Influence of the Unsteady Character of Motion on the Longitudinal Moment	205
Hypothesis of the Stationary State	206
Influence of Angular Velocity on the Moment of the Wing, Fuselage, and Tail	208
The Damping Moment of the Horizontal Tail Surface	209
Damping Moment of the Wings	214
Influence of Sweepback on Damping Moment of Wings	217
Damping of Fuselage. Resultant Damping Moment	220
Lag of the Downwash at the Tail	220
Influence of the Compressibility of Air on the Moment of Damping	223
CHAPTER VII	
LONGITUDINAL MOTION OF THE AIRCRAFT AND ITS STABILITY	
Resolution of the Aircraft Motion into Longitudinal and Lateral Components	225
Forces and Moments Acting on the Aircraft	229
General Equation of the Longitudinal Motion of an Aircraft	230
Integration of the Equations of Motion	234
Numerical Integration of the Equation of Motion	235
The Method of Small Disturbances	237
The Dimensionless Forms of the Equations of Motion	243
Solution of the Equations of Motion. Characteristic Equation	249
Correlation of the Roots and Coefficients of the Characteristic Equation	253
The Character of Disturbed Motion	255
Conditions of Stability	259

POOR ORIGINAL

0		Page
	Stability of Aircraft with Automatic Pilot	261
	The Stability of a Stick-Free Aircraft	266
	CHAPTER VIII	
	ANALYSIS OF THE DISTURBED MOTION OF AN AIRCRAFT	
	Practical Method of Calculation and Analysis of Disturbed Aircraft Motion	267
	Examination of the Coefficients of the Characteristic Equations	270
	Approximate Formulas for Determining the Coefficients of the Characteristic Equation	278
	Finding the Root of the Characteristic Equation	282
	Determination of the Period and Coefficient of Damping	285
	The Two Types of Disturbed Motion of the Aircraft	287
	A Characteristic Example of Disturbed Motion	289
	Physical Causes Responsible for the Resolution of Disturbed Motion into Two Types	293
	Practical Significance of the Two Types of the Disturbed Motions	296
	Simplified Theory of the Short-Period Motions of an Aircraft	299
	Influence of the Compressibility of Air on the Longitudinal Moment	303
	Static Stability with Respect to Overload and with Respect to Flying Speed	304
	The Role and Place of Static Stability in the Dynamic Stability of the Aircraft	308
	CHAPTER IX	
	STABILITY, CONTROLLABILITY, AND MANEUVERABILITY OF AIRCRAFT	
	Elements of Maneuvers Performed in Flight	321
50		
51		
52		
53		
54		
55		



POOR ORIGINAL

	Page
0	
2	
4	
6	
8	
10	
12	
14	
16	
18	
20	
22	
24	
26	
28	
30	
32	
34	
36	
38	
40	
42	
44	
46	
48	
50	
52	
54	
56	
	326
Angle of Elevator Deflection during Maneuver	
Relation between the Variation in Angle of Attack, Angular Velocity, and Angular Acceleration of the Aircraft, with any Variation in Speed and Overload	327
Deflection of Stick during Maneuver	331
Force on the Stick During Maneuver	333
Relation between Stick Force during a Maneuver and Stick Displacement	342
Selection of Weights and Springs Installed in the System of Longitudinal Control	343
Bringing the Aircraft to Assigned Overload	345
Rapid Variation in Overload	349
Stability and Controllability at High Flying Speeds	350
Pulling the Aircraft into a Dive	353
The Possibility of Obtaining High Overloads	357
CHAPTER X	
METHODS OF SELECTING THE DEGREE OF STABILITY OF AN AIRCRAFT	
	361
General Remarks	
Behavior of the Aircraft in Bumpy Flight	361
Controllability of the Aircraft during a Maneuver	365
General Considerations	367
The Initial Equations	371
General Analysis of the Aircraft's Ability to "Follow" the Stick	378
Symbols of "Following" the Stick	383
Controllability and Degree of Longitudinal Static Stability	389
Influence of Flying Speed on Controllability	389
Influence of the Dimensions of the Aircraft on its Controllability	389

POOR ORIGINAL

	Page
Method of Selecting Design Parameters for an Aircraft during the Design	391
Control Surface Reserve for Landing	394
Damping of the Short-Period Disturbed Motion	396
"Following" the Stick	398
Maximum Allowable Aerodynamic Elevator Balance	399
Permissible Limits of Variation of the Stick Force	401
Equal Degree of Stability, Stick-Fixed and Stick-Free	402
The Derivative of Stick Force with Respect to Speed	403
Selection of Horizontal Wing Area and of Aircraft Centering	403
Determination of the Characteristics of Stability and Controllability	406
CHAPTER XI	
INFLUENCE OF STRUCTURAL ELASTICITY ON STABILITY AND CONTROLLABILITY	
Twisting of the Wing	409
Influence of the Torsion of a Rectangular Wing on the Static Stability	411
Bending of the Rectangular Wing	416
Deformation of a Sweptback Wing	417
The Torsional Deformations of the Tail	420
Bending Deformations of the Fuselage	424
Effect of Deformations of the Fuselage and Tail on the Elevator Efficiency	427
Deformation of the Elevator Tab	430
Measures for Reducing the Influence of Deformation on the Stability	437
Bibliography	438